



ISF 弘立

# BAUHINIA 紫荊花



The Student Research Journal of The ISF Academy  
弘立書院學生研究期刊

Volume IX  
Issue 2, 2024

Editors: *Ms. C. Brillaux, Mr. B. Coronado-Guerra, Ms. Y. De Soto Gallegos,*  
*Ms. E. G. Dixon, Ms. B. Genzlinger, Dr. S. D. J. Griffin, Ms. S. Q. Huang,*  
*Ms. D. Ibarra, Ms. H. D. Johnson, Mr. K. Kampen, Mr. C. P. O'Neill, Dr. R. Oser,*  
*Dr. M. Pritchard, Ms. S. H. Ratzlaff, Mr. R. L. K. Richardson, Dr. L. Worth, Dr. Y. L. Zhang, Dr. J. Zhao*

ISSN 2409-4064



## Table of Contents

<b>The Evolutionary Roots of Depression</b> <i>Eric Jiang</i>	1
<b>Chinese Hydraulics through the Great Flood, Dujiangyan and Sponge Cities</b> <i>Abby Y.F. Wong</i>	8
<b>Redesigning a Child-Friendly Ambidextrous Utility Knife</b> <i>Troy Bacchus</i>	14
<b>Antibacterial Activity of Metallic Silver Nanoparticles against <i>Bacillus subtilis</i></b> <i>Cherry L.Y. Li</i>	35
<b>Modeling the Concentration of Morphine across the Blood-Brain Barrier: A Diffusion-Absorption Differential Equation Approach</b> <i>Bryan H.L. Wong</i>	54
<b>Hua Tuo's Development on the Idea of <i>Daoyin</i> in Traditional Medicine: the Five Animal Frolics</b> <i>Giselle Wong</i>	66
<b>How do Anti-reflective Coatings affect the Power Generation of Solar Panels?</b> <i>Skylar Rach</i>	71
<b>Connections and Comparisons: a Study of Science, Societal Psychology, and Geopolitics in the Manchurian Plague</b> <i>Katrina Chan</i>	75
<b>An Investigation on the Antioxidants and Antioxidant Capacity of <i>Polygoni cuspidati</i> Roots</b> <i>Ashley H.K. Wong</i>	81
<b>EnviroDroid: A Trash-Picking Robot</b> <i>Harry Wang</i>	92
<b>Investigating the Gut Microbiota of Domestic Dogs in Hong Kong by 16S Sequencing</b> <i>James A. Schrantz</i>	102
<b>The Application of Don Norman's Principles in Designing and Shaping the User Experience of Digital Products</b> <i>Jasmine J. L. Leung</i>	105
<b>The Effect of Framing Information on Decision-Making about Vaccines</b> <i>Ava Osann</i>	121

The Bauhinia flower represents Hong Kong's essence. The different stages of its blooming mirror the journey of curiosity, exploration, and ultimately the culmination of tireless efforts. As such, the Bauhinia is a metaphor for the endless depths of knowledge continuously expanded upon by countless researchers. Like butterflies drawn to the flower, these research papers possess the potential to enthrall and inspire those who read them. The illustration, paying homage to Chinese culture with its traditional *GongBi* style, bestows a unique touch to this cover. It serves as a celebration honoring the remarkable achievements of researchers and their profound contributions to the advancement of knowledge.

Artwork for cover by: JI, Sze Nga (Queena), G11 Student



## Editor's Note

Dear Readers,

We are delighted to introduce the ninth volume of our annual student research journal, *Bauhinia*! At The ISF Academy, we firmly believe in the power of student-led research and its potential to shape the future; this journal allows us to continue nurturing the intellectual curiosity and academic prowess of our young scholars.

In an age where Artificial Intelligence (AI) technology continues to evolve and augment the research landscape, it is crucial to celebrate the rigor and intellectual pursuits of students. *Bauhinia* strives to emphasize the indispensable role of the human intellect amidst an AI revolution. Authentic research goes beyond mere data analysis and algorithmic outputs. It encompasses the cultivation of critical thinking skills, the pursuit of knowledge, and the relentless exploration of unanswered questions. While AI technology has undoubtedly enhanced the efficiency and precision of certain research tasks, it is human ingenuity and creativity that remain at the heart of genuine research; moving forward, *Bauhinia* will need to delve deeper into this consideration.

We extend our sincere gratitude to the passionate educators, mentors, and the *Shuyuan* editorial team that have supported student research and have made this journal possible.

Please join us in celebrating the exceptional research endeavors of our students. From articles comparing Chinese and Western sources about the element of water, tea, ideal societies, virtues, entertainment, war, and death, to technologies such as hydraulics, utility knives, medicine, antibacterial nanoparticles, solar panels, and a trash-picking robot, there's content to please every palette.

Thank you for your support; we look forward to your contributions, readership, and engagement with *Bauhinia*. Feel free to reach out at [sy\\_team@isf.edu.hk](mailto:sy_team@isf.edu.hk).

Rachel Oser, Simon Griffin, Yulong Zhang, Diana Ibarra  
Editors-in-Chief

## 編者的話

親愛的讀者們,

我們非常高興地向您介紹學生研究年刊《紫荊花》的第九卷!在弘立書院,我們堅信學生主導的研究的力量以及它塑造未來的潛能。這本期刊的存在,使我們得以持續培養年輕學者的智識好奇心和學術實力。

在人工智能(AI)技術不斷演進並增強研究領域的時代,表彰學生的嚴謹態度和求知之心變得至關重要。《紫荊花》致力於強調人類智慧在人工智能革命中不可或缺的作用。真正的研究不僅僅是數據分析和算法輸出,它涵蓋了批判性思維技巧的培養、對知識和未解之謎的不懈探索。儘管人工智能技術無疑提高了某些研究任務的效率和精確性,但真正的研究核心仍然是人類的獨創性和創造力。展望未來,《紫荊花》需要進一步將這一點考慮在內。

我們要向那些對學生研究充滿熱情的教育者、導師以及書院編輯團隊表示衷心的感謝,正是他們的支持使這本期刊成為可能。

請與我們一同慶祝我們學生的傑出研究成就。從比較中西方關於水元素的看法,到茶、理想社會、美德、娛樂、戰爭和死亡,再到關於液壓技術、多用途刀具、醫藥、抗菌納米顆粒、太陽能面板和撿垃圾機器人等技術的內容,應有盡有,每位讀者都能找到喜愛的內容。

感謝您的支持;我們期待著您投稿、閱讀和參與《紫荊花》。如果您有任何疑問,歡迎通過 [sy\\_team@isf.edu.hk](mailto:sy_team@isf.edu.hk) 與我們聯繫。

歐睿秋, Simon Griffin, 張玉龍, Diana Ibarra



**Artist:** Sunny Jiang

**Title:** *Serenity*

**Medium:** Acrylic on canvas, 81cm x 61cm

**Description:** The painting creates a sense of calmness in our hectic world, using soft, muted colors, soft lines, and a simple composition. The mountains are a visual metaphor for the untapped depths of our identity, urging us to escape our routines and discover boundless possibilities. Stepping away from day-to-day routines is essential to uncover our true selves. It encourages introspection and reminds us of the importance of embracing the world's endless possibilities.

## A Note about Style

Articles included in this publication are written for many different purposes. Any differences in style are due to the need to adhere to the format required for that purpose. Generally, the Harvard Referencing style is used for articles written in English and Chinese. However, articles that were originally submitted as partial fulfillment of the International Baccalaureate (IB) programmes, such as the Diploma Programme's (DP) Extended Essay (EE) or Theory of Knowledge (TOK) course, have followed the specific requirements as outlined by the student's supervisor at the time of assignment, and they are published in this journal as they were originally submitted. A footnote under each article indicates the program from which each piece of work was culled.

## 關於文體的說明

本出版物中的文章是為許多不同目的而寫的。任何風格上的差異都是由於需要遵守該目的所需的格式。一般來說，文章如果是用英文或中文撰寫的，會使用哈佛引用風格。然而，原先作為國際文憑(IB)計劃部分學業完成要求而提交的文章，例如文憑課程的延伸論文(EE)或知識論(TOK)課程，則遵循了學生在作業指派時的指導老師的具體要求，它們被原樣發表在這本期刊上。每篇文章下的腳注都注明了文章入選前所屬的項目。

---

# The Evolutionary Roots of Depression

*Eric Jiang*

---

## Introduction

Depression is a deeply impactful yet paradoxical medical epidemic. Its severe symptoms and heavy human toll seem to clearly characterise it as a pathological dysfunction, while its heritability (Kendler *et al.*, 2006; Fernandez-Pujals *et al.*, 2015) and widespread cross-cultural prevalence (Kessler and Bromet, 2014) point to it being a genetically inherited trait, begging the question why, if detrimental to fitness, it has not been eradicated from human society simply through natural selection.

Depression, for the purposes of this essay, refers to major depressive disorder (MDD), a mental disorder characterised by nearly daily depressed mood and significant loss of interest or pleasure in one's usual activities (anhedonia). Specifically, this essay will use the American Psychiatric Association's DSM-5 definition of depression: at least one between depressed mood and anhedonia, plus four or more symptoms among significant weight or appetite change, near daily insomnia or hypersomnia, psychomotor agitation or retardation, fatigue, feelings of worthlessness, diminished ability to concentrate, and suicidal ideation (APA, 2013). Thus, to facilitate rigorous scientific analysis, depression will be treated in this essay as this 'package' of behavioural phenotypes, distinguished from less medically significant periods of sadness. Furthermore, this essay will focus on the evolutionary roots of MDD specifically, as opposed to that of other types of depression (e.g. grief, postpartum depression).

The societal burden of depression is profound. It is estimated that in 2019, 5% of adults worldwide were afflicted with depression — approximately 280 million people (IHME, 2019). Depression causes immense distress and interferes significantly with one's ability to continue daily life. MDD-afflicted individuals also have an increased risk of suicide; by one estimate, nearly 60% of all suicides are linked with depression (Holmes, 2021). Should we find an adaptive purpose for depression, we would be better able to treat depression's underlying causes instead of just its symptoms, leading to more effective treatment for countless people.

With this in mind, to what extent has depression served an evolutionary purpose in humans' ancestral past? This essay considers three competing perspectives.

The traditional wisdom is that depression is a standalone pathological dysfunction independent of any adaptive function. This is analysed with supporting evidence from McLeod *et al.* (2016) and a counter-argument from Nesse (2000).

The competing argument that depression evolved as an adaptation is presented by Watson and Andrews (2002), Hagen (2011), and Price *et al.* (1994), proposing variously for its adaptive function to be bargaining, social rumination, energy conservation, or yielding. Evidence from Gariépy *et al.* (2018), Segrin and Dillard (1992), Golin *et al.* (1979), Kardum *et al.* (2021), Raleigh *et al.* (1984), and Moncrieff *et al.* (2022) are used to analyse this perspective.

Furthermore, the argument that depression evolved as a spandrel — a byproduct of another adaptation — is presented by Nettle (2004) and supplemented by arguments from Huron (2018).

This essay will demonstrate that depression likely did evolve as a spandrel of the emotion of sadness, which may plausibly have served an adaptive purpose, but that due to general limitations on research in evolutionary psychology, the precise extent to which depression has served an evolutionary purpose cannot currently be ascertained.

## 1. The Dysfunction Explanation and its Limitations

As aforementioned, depression is popularly viewed today as a pathological dysfunction of normal psychological functioning, serving no evolutionary purpose. Indeed, much empirical research, such as the study McLeod *et al.* (2016), does indicate that depression is largely detrimental to adaptive fitness.

McLeod *et al.* conducted surveys with a sample of participants aged 30-35 about their quality of life, and

---

The above article was written as an Extended Essay in Psychology, in partial fulfillment of the IB Diploma Programme, 2023.

compared it to longitudinal data of their depressive symptoms at age 15-16. Quality of life was assessed by factors including mental health, suicidality, substance abuse, income, educational attainment, and domestic violence. Statistically significant correlations were found between adolescent depression and many of the above factors, especially subsequent mental health problems later in life and victimisation in domestic violence. McLeod *et al.* showed that the severity of adolescent depressive symptoms is correlated with worse outcomes of well-being in adulthood and thus lower fitness. Objections can be made to the operationalisation of adaptive fitness — income and educational attainment, for example, are not necessarily reliable predictors of life satisfaction as much as they are culturally normative standards; nevertheless, with a large sample size and high validity of the other measures of adaptive fitness used (e.g., suicidality), McLeod's findings carry reasonable confidence.

However, there are shortcomings in the explanation of depression as always having been dysfunctional. Depression is known to be partially heritable: twin studies such as Kendler *et al.* (2006) consistently find higher concordance in depressive symptoms between identical twins (with 100% genetic similarity) than between fraternal twins, (with 50% genetic similarity), affirming that depression can, to some degree, be inherited through genes. Given this, Nesse (2000) and others argue that many aspects of depression are uncharacteristic of a heritable dysfunction.

First, depression affects a large number of people worldwide — 5% of adults worldwide, as cited earlier — while other heritable dysfunctions occur much more rarely because they are naturally selected against. Schizophrenia, for example, only affects 0.45% of adults worldwide (IHME, 2019).

Second, depressive symptoms are especially common during young adulthood, the age of humans' reproductive prime, unlike the majority of other high-prevalence heritable dysfunctions (e.g. Alzheimer's) whose symptoms typically arise during old age and thus have less effect on reproductive fitness. Those dysfunctions that do affect individuals during their reproductive ages (e.g. cystic fibrosis) are largely inherited through recessive genes and are thereby less affected by evolutionary forces thanks to healthy carriers not bearing the associated fitness loss. No research thus far has shown the same for depression — Caspi *et al.* (2003), for example, found that the depression-linked 5-HTT gene instead exhibits codominant characteristics.

Third, the severity of depressive symptoms in the general population exhibits not a dichotomous but a continuous distribution. In other words, there are not distinct categories of depressed and nondepressed people, but rather a large number of people who fall in the middle, experiencing sub-clinical depressive symptoms but not meeting the requirements for a diagnosis — 13.8% of U.S. seniors, by one study (Laborde-Lahoz *et al.*, 2015). The blurred line between depression and normal low mood makes it difficult to argue that depression is fundamentally pathological.

## 2. Adaptationist Theories

In the past several decades, a number of hypothesised adaptive functions of depression have been proposed. These theories can be generalised into several categories based on the adaptive function they propose: the bargaining, social ruminative, energy conservation, and yielding functions.

The first is the bargaining function: that in the ancestral environment, depression motivates reluctant social partners to provide help or make concessions when the individual is experiencing negative life events. Watson and Andrews (2002), in their Social Navigation Hypothesis, argue that the symptoms of depressed mood, anhedonia, psychomotor retardation, and diminished ability to concentrate all served to decrease the individual's productivity, incurring fitness costs on close social partners and thus incentivising them to provide support that they might otherwise be unwilling to give. In this way, the benefit of depression to the individual in ancestral environments of eliciting social support in response to negative life events is hypothesised to have outweighed the direct cost of depressive symptoms, resulting in predisposition to depression being selected for.

It should be noted, before any analysis, that adaptationist theories of depression inherently possess low falsifiability due to the difficulty of validating speculations about the ancestral environment. With this in mind, though, the bargaining function accounts well for the commonly observed correlation between social support and decreased risk for depression. One meta-analysis by Gariépy *et al.* (2018) examined 100 studies from published research, finding that 90% showed a significant negative correlation between risk for depression and social support, especially from spouses, family, and friends. These findings provide strong evidence for the bargaining function under the logic that depression would tend to occur in situations

of low social support precisely to elicit such support through bargaining. A limitation exists in that the data is correlational in nature, so a causal relationship between social support and depression cannot be determined — the explanation that depression leads to low social support explains the correlation equally as well. This bidirectional ambiguity limits the support from Gariépy *et al.* for the bargaining function.

In fact, another meta-analysis by Segrin and Dillard (1992) strongly suggests that depressive symptoms, rather than eliciting social support, instead lead to rejection from social partners. Segrin and Dillard examined 46 studies, testing the hypothesis that depressed individuals induce more negative mood in others and elicit more social rejection than nondepressed individuals. In the studies examined, participants were led to interact with either friends or strangers, and their negative mood and rejection were assessed using various inventories. Analysis of the synthesised data found mixed support for depression inducing negative mood in others, but strong support for depression eliciting social rejection, thus disputing the bargaining function.

Furthermore, the bargaining function is also unable to account for other depressive symptoms such as rumination and feelings of worthlessness, which, if depression served simply to induce support from social partners, would be an unnecessary waste of mental resources. To explain these symptoms, Watson and Andrews proposed another adaptive function of depression in parallel with the bargaining function.

This second proposed function is the social ruminative function: that depression focuses an individual's mental resources to solving a troubling social issue at hand. In the ancestral environment where many dangers were present and humans lived in tribal communities to survive, social ostracism was likely tantamount to death; problems with one's social relationships would inferrably have been of the utmost priority. Forming the other half of Watson and Andrews' Social Navigation Hypothesis, the social ruminative function accounts for the depressive symptoms of rumination, anhedonia, fatigue, and psychomotor retardation — in the ancestral environment with scarce resources available, it would have been in the socially troubled individual's best interest to devote the bulk of their energy to solving their social issues through analytical rumination, reducing energy consumption in unrelated activities.

One piece of evidence that provides support for the social ruminative function is the 'depressive realism effect', an observed phenomenon where depressed

individuals' self-assessments of likelihood of success in certain situations are more accurate than those of nondepressed individuals. This was demonstrated in a quasiexperiment by Golin *et al.* (1979). Depressed and nondepressed participants were led to play a dice game where poker chips were bet around a dice table, and dice throws of certain numbers would win. The participants played the game under two conditions: either they themselves threw the dice, or a confederate did. Before each game, the participants were asked to rate their confidence of winning. Significantly, Golin *et al.* found that the nondepressed participants gave much higher ratings of confidence when they threw the dice compared to when a confederate threw it, while depressed participants' ratings had no significant difference between the two conditions. This is evidence that nondepressed individuals experience an optimism bias in their self-assessments when under an "illusion of control" while depressed individuals do not, supporting the depressive realism effect. The implication is that depressed individuals are more accurate in their self-assessments and thus better equipped to solve their social issues realistically, substantiating the social ruminative function.

However, many aspects of the study are highly artificial. First, it lacks mundane realism: the environment of an artificial dice game is substantially different from the natural environment in which depressed individuals usually ruminate, making it difficult to generalise findings from the experimental scenario to real life. Second, the operationalisation of optimism bias using participants' estimates of success at a dice game is questionable — numerous factors affect judgement when assessing one's life circumstances during depressive rumination compared to simply predicting success at a dice game. For example, the former usually triggers or aggravates depressed mood, while the latter does not. Hence, the findings' support for the depressive realism effect may be true for dice games, but not necessarily in our natural environment. This low ecological validity limits the strength of the study's support for the purported adaptive function of depressive rumination.

In fact, there is little empirical evidence supporting depressive rumination being effective at all in absolving social issues. Rather, much modern research demonstrates that rumination is counterproductive by causing individuals to fixate and brood on their negative feelings without any constructive planning to overcome their issues (Lyubomirsky and Tkach, 2004). It is difficult for the proposed social ruminative function of depression to hold in spite of this contravening evidence.



The third proposed function is the energy conservation function: that depression prompts individuals to withdraw from unsuccessful enterprises that waste more energy and resources than they provide rewards (e.g. foraging in a barren area). This is often termed the Psychic Pain Hypothesis (Hagen, 2011) — analogous to physical pain’s adaptive function against bodily harm, depression serves to induce withdrawal from other sources of fitness loss. This energy conservation function accounts well for the depressive symptom of anhedonia, and postulates for the other depressive symptoms that their aversiveness serves to condition the individual to avoid similar adverse enterprises in the future. However, this latter postulation, on top of being hypothetical and lacking empirical support, faces the counterargument that depressive symptoms impose a direct fitness cost upon the individual whereas pain itself imposes no such cost (excluding pathological chronic pain), voiding the analogy. It is questionable whether this hypothetical conditioning function of aversive depressive symptoms, in the ancestral environment, provided a net fitness benefit that outweighed the fitness cost of enduring the symptoms themselves. Suicidality is particularly difficult to explain — it is rather implausible that the fitness cost of an increased predisposition to ending one’s own life may have been outweighed by the fitness benefit of a conditioning function, and to substantiate such a proposition requires compelling evidence that currently does not exist.

Support for the energy conservation function does exist, though, from a study by Kardum *et al.* (2021) on the relationship between postpartum depression and the maternal circumstances of infant quality and perceived family support. Kardum *et al.* conducted a correlational study of 150 pregnant women, in which participants’ mood before and after delivery were measured, alongside perceived family support (by the

mother) and infant viability (using the Apgar score, a method for assessing newborn health). The study found significant negative correlations of both perceived family support and Apgar score with depressed mood of the mother. This supports the psychic pain hypothesis for postpartum depression by the explanation that lower perceived family support and infant viability reduce the infant’s chances of survival, inducing the adaptive response of the mother to experience postpartum depression and less desire for the child — reducing their investment in an “enterprise” with a high risk of failure. However, MDD and postpartum depression are classified (by the APA) as distinct mental disorders, limiting the transferability of this study’s findings to MDD.

Overall, there lacks empirical support for an energy conservation function in MDD.

The fourth proposed function is the yielding function: that, when on the losing side of a social conflict, depression encourages acceptance, inhibits aggressive behaviour toward superior foes, and signals ‘no threat’ to reduce further fitness loss through futile hostilities. This function was proposed by Price *et al.* (1994) in their Social Competition Hypothesis. It accounts well for the depressive symptoms of anhedonia, fatigue, and psychomotor retardation, which induce submissiveness and decrease aggression in the individual. However, it is much less able to account for the other depressive symptoms of suicidality, difficulty concentrating, insomnia or hypersomnia, and abrupt weight change. These symptoms serve no conceivable purpose in the yielding function of depression, and only represent unnecessary fitness costs. There does exist the defense that suicidality serves to communicate to hostile aggressors the genuineness of the yielding signal by inflicting a cost to the individual (since a signal that is costly to send is less likely to be insincere); however, this explanation is still implausible without compelling evidence, again (as with the energy conservation function) due to the disproportionately high fitness cost of risking one’s own death.

Evidence does exist for the yielding function of depression from animal research. Raleigh *et al.* (1984), for example, observed groups of adult male vervet monkeys in enclosure-based habitats and found that manipulating their social statuses led to changes in their blood serotonin levels. In the naturally formed dominance hierarchies, the researchers categorised individual monkeys as dominant and submissive using an observation schedule measuring behaviour such as threatening, contact aggression, and avoidance. In some groups, natural changes in the dominance hierarchy were observed in which the dominant monkey became submissive and a submissive monkey became dominant; in other groups, hierarchal changes were artificially induced via removing the dominant monkey, allowing a submissive monkey to become dominant. Through measurements taken before and after the hierarchal changes, Raleigh *et al.* found that not only were blood serotonin levels significantly higher in dominant monkeys, but both natural and artificial shifts up and down the dominance hierarchy were accompanied by substantial increases and reductions in blood serotonin levels respectively. Under the assumption that serotonin levels are a biochemical marker of depression, these findings would be significant in

showing a correlation between social submission and depression in monkeys.

Therein lies a limitation of this study: it assumes that serotonin levels are linked with depression. Once highly influential, this assumption has been challenged by recent research. A broad systematic review of the correlation between serotonin levels and depression conducted by Moncrieff *et al.* (2022) sampled previous systematic reviews, meta-analyses, and large dataset studies of human subjects, finding very little support for depressed individuals having lower serotonin levels than non-depressed individuals. Moreover, no significant evidence was found for depression being linked with various other biochemical mechanisms that have an effect on serotonin in the brain, including serotonin receptors, the serotonin transporter protein, and serotonin-related genes.

Another limitation of Raleigh *et al.*'s findings, alongside other animal research supporting the yielding function, is the limited generalisability of findings from animal research to humans. Both brain physiology and social behaviour of monkeys are significantly different from that in humans. Even if depression is indeed related to social rank in monkeys, it hardly means that the same is true for humans in their far more complex social environments.

As discussed above, while several adaptive functions of depression have been proposed in recent research, none are strongly empirically supported.

Rather, research has been generally inconclusive due to the difficulty of studying the ancestral environment and consequential low falsifiability of adaptationist theories. Indirect evidence based on depression in the modern environment requires interpretation, leaving researchers susceptible to confirmation bias — to first draw conclusions and then alter their interpretations of the evidence to fit, undermining objectivity of the adaptationist theories.

Moreover, depression lacks reliability of elicitation. According to Nettle (2004), adaptations are “reliably elicited” by the “triggers” that they evolved to respond against: for example, disgust is reliably elicited by disease-salient stimuli. As we have seen, however, depression is hardly a consistent, predictable reaction to negative life events, asymmetrically observed in people with genetic predispositions. This significant individual variation in depressive reactions challenges the central adaptationist premise of depression being an evolved behavioural trait.

### 3. The Spandrel Explanation

In light of the limitations of both the dysfunctional and adaptationist accounts, another perspective has emerged in recent research: that depression is not adaptive in its own right, but arose as a spandrel — an unavoidable byproduct of another adaptation. Specifically, some researchers argue that it is the emotion of sadness that evolved with an adaptive function, and that depression came about as a byproduct of the natural population distribution of affective reactivity.

Immediately, an issue that must be addressed is the distinction between the constructs of sadness and depression: although the two are proposed to be related, they remain separate, distinct behavioural phenomena. Depression's persistent recurrence over long periods of time is not associated with non-depressive sadness; nor are depressive symptoms such as suicidal ideation and sudden weight change. It is thus implausible that the two share underlying mechanisms without differences. Nettle (2004), a representative paper for the spandrel explanation, proposes that depression is caused by “the tendency of the affect system, in extreme deviations from center, to go into a self-reinforcing cycle, at both the neurobiological and psychological level”, explaining the relative pathological severity of depression as the product of a runaway positive feedback loop. If depression is a malfunction of the affect system for sadness, then, what might be the adaptive function of that affect system to begin with?

Researchers generally agree that the emotion of sadness is adaptive — it is universal across all cultures, is elicited reliably by specific types of stimuli, and, unlike depression, does not usually induce a fitness loss. Huron (2018), for example, proposes that sadness evolved partly as an immune response and partly to induce cognitive reflection. As Huron outlines, key features of sadness include fatigue, anhedonia, slowing of movement and speech, and sustained self-reflection, in addition to negative mood. Huron cites the usefulness of sadness-characteristic behaviour to immunity: limiting unnecessary muscle movement and reducing participation in one's usual energy-consuming activities during infection helps conserve metabolic resources for an effective immune response. Indeed, Huron cites a number of psychobiological studies associating pro-inflammatory cytokines, proteins in the bloodstream involved in producing an inflammatory immune response, with sadness-characteristic behaviour such as anhedonia and

fatigue. It stands to reason that an immune response that also induces sadness-characteristic behaviour would be more likely to succeed and thus would be evolutionarily selected for.

Importantly, though, the immunity explanation explains neither the reliable elicitation of sadness by cognitive and social stressors such as loss, nor the utility of low mood and sustained self-reflection. Huron (2018) attempts to account for this by proposing that sadness, although incorporating the immune response to some extent, also evolved to serve the function of cognitive self-reassessment — that a sad mood brought about by cognitive or social stressors induces the individual to analyse and re-optimize their behavioural patterns to prevent future fitness loss. Note the distinction between this hypothesis and the earlier proposed social ruminative function of depression: while Watson and Andrews (2002) propose that the adaptive trait in question is depression, Huron proposes for it to be sadness. Research has shown distinct differences between depressive rumination and the more beneficial cognitive reflection common in sadness (Trapnell and Campbell, 1999). Hence, the latter does not face a major limitation of the former.

A strength of the spandrel explanation is that it provides a sound explanation for the relationship between sadness and depression. Affective reactivity is distributed in a population along a polygenic continuum (it can reasonably be inferred that a large number of genes influence affective reactivity); at the upper end of this distribution, high affective reactivity can cause the overactivation of emotions such as sadness, making an originally adaptive mental process dysfunctional.

The main limitation of the spandrel explanation is a lack of supporting empirical evidence due to the recency of its introduction. The process by which sadness develops into depression, for example, requires further elucidation through research. Moreover, the construct validity of affective reactivity must also be reaffirmed — not enough is known of its biological mechanisms and genetic factors to conclusively assert the existence of a polygenic distribution.

## Conclusion

This essay has reviewed theories of depression as a dysfunction, an adaptation (with the bargaining, social rumination, energy conservation, and/or yielding functions), and a spandrel.

In summary, the spandrel explanation is the most plausible answer to this essay's research question of the extent to which depression served an evolutionary purpose in humans' ancestral past, because it is the only theoretical perspective out of those explored in this essay that does not possess significant argumentative flaws. Where the dysfunction explanation fails to address depression's widespread prevalence and proximity to healthy sadness, and the adaptationist explanations fail to account for the inconsistency of depression as a predictive response to negative life events, the spandrel explanation best accounts for all available evidence.

Throughout its analysis, however, this essay is only able to ascertain the likelihood of evolutionary theories for depression to be true. The spandrel explanation, while being the most plausible, is still limited by a lack of empirical support due to the recency of its introduction. As with much other current research on the evolutionary roots of depression, my findings remain inconclusive.

## References

- American Psychiatric Association (APA). (2013). *Diagnostic and statistical manual of mental disorders: DSM-5*. American Psychiatric Publishing.
- Fernandez-Pujals, A. M., Adams, M. J., Thomson, P., McKechnie, A. G., Blackwood, D. H., Smith, B. H., Dominiczak, A. F., Morris, A. D., Matthews, K., Campbell, A., Linksted, P., Haley, C. S., Deary, I. J., Porteous, D. J., MacIntyre, D. J., & McIntosh, A. M. (2015). Epidemiology and heritability of major depressive disorder, stratified by age of onset, sex, and illness course in generation scotland: Scottish Family Health Study (GS:SFHS). *PLoS One*, 10(11). <https://doi.org/10.1371/journal.pone.0142197>
- Gariépy, G., Honkaniemi, H., & Quesnel-Vallée, A. (2016). Social Support and protection from depression: Systematic review of current findings in western countries. *British Journal of Psychiatry*, 209(4), 284–293. <https://doi.org/10.1192/bjp.bp.115.169094>
- Golin, S., Terrell, F., Weitz, J., & Drost, P. L. (1979). The illusion of control among depressed patients. *Journal of Abnormal Psychology*, 88(4), 454–457. <https://doi.org/10.1037/h0077992>
- Hagen, E. H. (2011). Evolutionary theories of Depression: A critical review. *The Canadian Journal of Psychiatry*, 56(12), 716–726. <https://doi.org/10.1177/0706743711105601203>
- Holmes, L. (2021, June 24). *Rates and Statistics for Suicide in the United States*. Verywell Mind. Retrieved August 25, 2022, from <https://www.verywellmind.com/suicide-rates-overstated-in-people-withdepression-2330503>
- Huron, D. (2018). On the functions of sadness and grief. In H.C. Lench(ed.), *The Function of Emotions: When and Why Emotions Help Us*. Springer International Publishing, pp. 59-91.
- Institute for Health Metrics and Evaluation (IHME). (2019). *GBD Results*. Global Health Data Exchange (GHDX). Retrieved August 25, 2022, from <https://vizhub.healthdata.org/gbd-results>
- Kardum, I., Hudek-Knezevic, J., Kalebić Maglica, B., & Shackelford, T. K. (2022). Postnatal maternal mood provides evidence for the psychic pain hypothesis. *Evolutionary Behavioral Sciences*, 16(2), 116–127. <https://doi.org/10.1037/ebs0000256>
- Kendler, K. S., Gatz, M., Gardner, C. O., & Pedersen, N. L. (2006). A Swedish National Twin Study of Lifetime Major Depression. *American Journal of Psychiatry*, 163(1), 109–114. <https://doi.org/10.1176/appi.ajp.163.1.109>
- Kessler, R. C., & Bromet, E. J. (2013). The epidemiology of depression across cultures. *Annual Review of Public Health*, 34(1), 119–138. <https://doi.org/10.1146/annurevpublhealth-031912-114409>
- Laborde-Lahoz, P., El-Gabalawy, R., Kinley, J., Kirwin, P. D., Sareen, J., & Pietrzak, R. H. (2015). Subsyndromal depression among older adults in the USA: Prevalence, comorbidity, and risk for new-onset psychiatric disorders in late life. *International Journal of Geriatric Psychiatry*, 30(7), 677–685. <https://doi.org/10.1002/gps.4204>
- Lyubomirsky, S., & Tkach, C. (2003). The consequences of dysphoric rumination. In C. Papageorgiou & A. Wells (Eds.), *Rumination: Nature, theory, and treatment of negative thinking in depression* (pp. 21-41). Chichester, England: John Wiley & Sons.
- McLeod, G. F., Horwood, L. J., & Fergusson, D. M. (2016). Adolescent depression, adult mental health and psychosocial outcomes at 30 and 35 years. *Psychological Medicine*, 46(7), 1401–1412. <https://doi.org/10.1017/s0033291715002950>
- Moncrieff, J., Cooper, R. E., Stockmann, T., Amendola, S., Hengartner, M. P., & Horowitz, M. A. (2022). The serotonin theory of depression: a systematic umbrella review of the evidence. *Molecular Psychiatry*. <https://doi.org/10.1038/s41380-022-01661-0>
- Nettle, D. (2004). Evolutionary origins of depression: a review and reformulation. *Journal of Affective Disorders*, 81(2), 91–102. <https://doi.org/10.1016/j.jad.2003.08.009>
- Raleigh, M. J., McGuire, M. T., Brammer, G. L., & Yuwiler, A. (1984). Social and environmental influences on blood serotonin concentrations in monkeys. *Archives of General Psychiatry*, 41(4), 405. <https://doi.org/10.1001/archpsyc.1984.01790150095013>
- Segrin, C., & Dillard, J. P. (1992). The interactional theory of depression: A meta-analysis of the research literature. *Journal of Social and Clinical Psychology*, 11(1), 43–70. <https://doi.org/10.1521/jscp.1992.11.1.43>
- Trapnell, P. D., & Campbell, J. D. (1999). Private self-consciousness and the five-factor model of personality: Distinguishing rumination from reflection. *Journal of Personality and Social Psychology*, 76(2), 284–304. <https://doi.org/10.1037/0022-3514.76.2.284>

---

# Chinese Hydraulics through the Great Flood, Dujiangyan and Sponge Cities

Abby Y.F. Wong

---

## Introduction

In July of 2021, China's Henan province faced one of the most catastrophic floods ever recorded in history as a result of heavy rainfall at 201.9 milliliters of rainfall within an hour (BBC News 中文, 2021). With nearly 400 deaths and 12.7 billion USD of property damage, people turn their attention to water irrigation and flood prevention systems.

Up until today, people, especially the Chinese, are still learning to control floods in order for humankind to live in peace with nature. Sponge cities are one of the current solutions, in which urban planners and engineers aim to absorb rainwater through ecological landscapes, the perfect modern day example of living harmoniously with nature without harming the environment further in any way (Gies, 2022). This idea was indirectly inspired by Ancient Chinese hydraulic systems and the Chinese philosophical idea of harmony between humans and nature.

The paper aims to investigate the different hydraulic systems in Chinese history through the myth of the Great Flood, *Da yu zhi shui* (大禹治水), Dujiangyan (都江堰), and sponge cities. The systems show not only hydrology being a significant part of Chinese history, but also demonstrates the Chinese people's philosophy of having harmony with nature *Tian ren he yi* (天人合一).

Around 2000 years ago, methods of water management were already brought up through narratives provided by Chinese ancestors. A popular one that many may know would be the Great Flood, which through recent research, has been discovered to not be a myth but an actual event that happened even before the Xia (夏) dynasty (Normile, 2016). In the myth, the Great Yu created balance between nature and humankind by guiding the Yellow River waters so that people did not have to move every few months in fear of dying in floods. The story was told and passed on for many years. Through the myth, many ancient philosophers, including Confucius (孔子), were able to bring out the philosophy of the balance between human and nature.

A few thousand years later, during the Warring States Period (476-221 BC), the famous politician and hydraulics engineer Li Bing (李冰) led the construction of the Dujiangyan, one of the earliest irrigation systems in the history of civilization. The Dujiangyan was built with the intention of distributing the flood waters into the plains where people grew crops, demonstrating the Chinese philosophy of living harmoniously with nature.

The first section of the paper will focus on the myth of the Great Flood and recent research about the construction that Yu conducted. The following will be about the construction of Dujiangyan. The next section will be about the modern solution to floods, which was indirectly influenced by the ancient hydraulics in the way that they all aim to find balance between the well-being of humans and nature. Finally, the last section will address the philosophical idea of harmony between humans and nature.

## 1. The Great Flood 大禹治水

The earliest record of the Great Flood was found in the Classic of Mountain and Seas. The myth occurred up to 4000 years ago along the river banks of the Yellow River. According to modern day narratives, a catastrophic flooding disaster hit China more than 5000 years ago during the late primitive society. Life was extremely hard for the people, the floods damaged their land and took away their habitats. The people chose to move into the mountains, away from the river, but resources were scarce. The tribal alliance leader, Yao (堯), later emperor, recommended Gun (鯀) to settle the flooding issue. Gun used a blocking *Yin* (堙) and barrier *Zhang* (障) method with a mythical, self-expanding soil called *Xirang* (息壤) to barricade the river like a dam. This was mentioned in a chapter of The Book of Documents 《尚書》, the book says, “箕子乃言曰, 我聞在昔, 鯀鄆洪水, 汨陳其五行。” Though this method allowed the people to live in peace for 9 years, the blocked water began to overflow and came back as a flood bigger than before. When

---

The above article was written as a culminating essay for the *Shuyuan* NRI Scholar's Summer Retreat, 2022.

Shun (舜) became the next emperor, he made Gun responsible for the flooding and executed him. Gun's son, Yu, was then promoted to continue his father's work (Xiao, 2015).

In 《國語·魯語》, historian Qiuming Zuo said, “伯禹念前之非度, 釐改制量, 疏川導滯” meaning that Yu learned from his father's mistakes and overcame the challenges his father faced by realizing that he could dig out tributaries to guide the overflowing waters. According to the narratives, Yu was successful due to his methods of flood prevention, he used dredging *Shu* (疏) and guiding *Dao* (導) to create tributaries for the Yellow River. In the narratives about Yu in The Book of Documents, Yu claims, “予決九川距四海, 浚畎澮距川” meaning he dredged the tributaries and rivers that split the continent into nine realms, allowing the river water to flow into the ocean and prevent the water from overflowing onto the plains. “畎” and “澮” being the different types of gutters, describing how Yu excavated different sizes of gutters to allow for the water to pass through (朱慧琴, 1981). A chapter of the The Book of Documents 《尚書》, Tribute of Yu (禹貢) emphasized, “水過逢水, 台于大陸, 又播為九河, 曰為逆河, 入于海。” It was believed that the mainstream of the Yellow River diverges into tributaries through the excavation done by Yu (Xiao, 2015). This was Yu's first goal to stop floods from disrupting the people's lives. Diverting the water into tributaries allows the overflowing water to have more space to spread. The splitting of the tributaries also then created the nine provinces, leading into the new dynasty, Xia.

Mencius (孟子) once said, “禹之治水, 水之道也, 是故禹以四海為壑…….” Mencius commented on Yu's methods, believing that digging out tributaries and diverting the overflowing waters into the oceans conforms to the laws of nature as it doesn't disrupt the environment as much as other methods, like dams, may.

The myth resembles an idealized version of how humans should interact with nature based on the Taoist and Confucius philosophies, which will be brought up later in this paper.

## 2. Dujiangyan 都江堰

The Dujiangyan irrigation system dates back to more than 2000 years ago and is the oldest dam-free water diversion system in the world still standing today. The plan for the functions of Dujiangyan ranged beyond flood control, it also included other functions such as boating, drifting and irrigation. Dujiangyan was designed by Li Bing, an ancient politician and

one of the first hydraulics engineers in the world, to prevent floods and increase access to the river waters (en.chinaculture.org, n.d.). Based on old records, Dujiangyan's biggest goal was to eliminate the dangers of flooding. *Shiji: Hequ Book* by Sima Qian writes, “The governor of the Shu county chiseled away soil to prevent harm of the water 蜀守冰鑿離堆, 辟沫水之害.” The passage shows that the original intention of Dujiangyan was to excavate and remove the harm of floods in an attempt to allow humans and nature to live harmoniously together.

Though there are no clear records of the process of the construction, Sima Qian suggests in *Shiji: Hequ Book* that there could have been two methods: 1. The engineers built a diversion channel to guide the waters of the Minjiang river into the Chengdu plains; 2. The river branches of Minjiang were man-made according to geological surveys, meaning the ancient engineers took advantage of the geological conditions and dug thicker water inlets to increase the amount of water being let into the other river branches. Li Bing learnt to control the water levels of the river in order for the waters downstream to be better used (鄭肇經, 1993). Neither of these methods causes extreme harm to the environment and therefore proves that the goal of maintaining harmony between humans and nature was successfully achieved in the creation of Dujiangyan. On top of this, Dujiangyan makes use of the excess water in the river to support agricultural growth.

In many ways, the construction of Dujiangyan was also influenced by Yu's method of dealing with floods. For example, as mentioned earlier, the process of excavation through Dujiangyan was possible because of Yu's earlier works. According to the hydraulics researcher Feng Guanghong (馮廣宏) *et al.* (2013, p.743), Yu dredged open the upper streams of the Minjiang River, which then influenced Li Bing to do the same in the lower streams of the Minjiang River for Dujiangyan. Feng writes in his book 《都江堰文獻集成: 歷史文獻》: 「禹治水之後, 冰能因其舊跡, 而疏廣之。」 Many researchers up until today believe that Li Bing's excavation method was identical to Yu's, the only difference being their location and scale.

The following sections will be dedicated to discussions of the significant technical features of Dujiangyan.

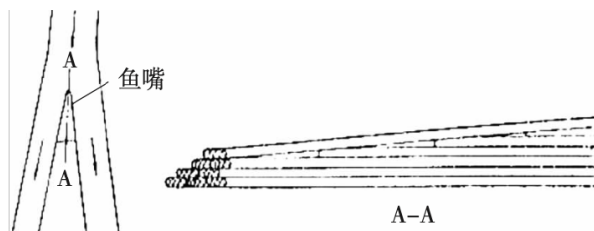
### 2.1 Fish Mouth Levee 魚嘴

The Fish Mouth Levee divides the Minjiang river into an inner and outer river and is based on the natural sandbar in the middle of the Minjiang River. The Levee is the first obstacle the waters of the Minjiang River face,

artificially built at the front end of the water diversion embankment. The Fish Mouth Levee also separates the sand of the Minjiang River. By doing so, the sand is kept at an equal level on both sides of the levee, preventing the water from overflowing and flooding onto the land where people grew their crops, allowing civilization to live harmoniously with nature. Keeping the sand at an equal level also prevents blockage in the river.

The earliest version of the Dujiangyan constructed by Li Bing was made specifically of bamboo cages and pebbles. The use of Omei Mountain Bamboos were most consistently seen throughout the construction of the bamboo cages. This type of bamboo is most commonly found in the Guizhou province of China and has a wide variety of functions including construction, paper making, and painting. These bamboos are stripped into pieces and weaved into cages with a circumference of approximately 3 feet. The length does not matter and depends on the person making it. Pebbles are stuffed into the cages to block the water as it forms the Fish Mouth Levee in the water. The bamboo cages are then stacked on top of each other and sunk to the bottom of the river to form the Fish Mouth Levee, as seen in Figure 1 (Wang and Hui, 2013).

The construction of the Fish Mouth Levee demonstrates balance between harmony and nature through the use of cheap and common materials, nature is not damaged in the process of collecting materials. Also, unlike modern day construction, the construction does not pollute the environment because of the simple materials used in the construction process (Price, 2019).



**Figure 1.** Bamboo cages stacked on top of each other and placed at the tip of the Dujiangyan to form the Fish Mouth Levee

## 2.2 Flying Sand Weir 飛沙堰

The Flying Sand Weir has a series of functions including flood discharge, sand discharge, and water regulation. The weir is 240 meters in length, 700 meters away from the Fish Mouth Levee, 200 meters away from the Bottleneck Channel and 2 meters above the inner riverbed. When the water level of the inner river reaches a maximum, excess water will be released from the Flying Sand Weir, which prevents the water from flooding the plains surrounding.

The weir is a significant contributor to flood discharge in the Dujiangyan. The water level of Minjiang peaks at the upper stream and the water moves at an extremely fast rate, the quick movement can lead to flooding and is more than what the irrigation system can sustain. Hence, as the water of the inner river flows towards the weir, it is forced to turn South at the Tiger Head Rock, a natural rock formation named for its resemblance to a tiger's head, and hit the other side of the riverbed, which slows down the flow of the water.

Though the Fish Mouth diverts most of the sand away, around 40% of the sand still crosses into the inner river. The Flying Sand Weir then continues the job and washes out 75% of the sand. Relocating the sand is especially important because it's one of the main contributors to the constant flooding in the Minjiang River, more sand means an increase in water level, which then leads to an overflow of water in the inner river.

The weir diverts the sand in two ways. The first being the use of bend circulation. When the water flows into the inner river, the mainstream follows the left of the riverbed and forms a curve at the Tiger Head Rock, which separates the stream into two, and through the use of centrifugal force, the water level in the lower side of the river will rise while the water level in the higher side will decrease. The second way being the use of lateral circulation. As the flow of the water enters the side of the weir, the curve in the waterway will cause a lateral circulation, allowing the sand and rocks to leave the weir (Zhang, 2000).

## 2.3 Bottleneck Channel 寶瓶口

A hole about 20 meters wide, 30 meters tall, and 100 meters long, is dug through the Yulei Mountain to form the Bottleneck Channel. The hole is not entirely artificial since there was originally already a gap in the mountain, but in order for the water in the inner river irrigation area to flow through the channel, hence the name Bottleneck, the gap was made wider.

The channel's first function is water diversion. More than 70% of the sand and soil has been rid of in the Fish Mouth Levee and Flying Sand Weir, the water is mostly purified and flows downstream through the channel. Clean water is provided for downstream irrigation, shipping and other domestic usage.

The second function of the channel is flood control. Though there are no gateways, the channel can still control the amount of water flowing in. This is done through the cooperation of the channel's own sectionings, excess water from the wasted soil and sand, and the water discharged from the Herringbone Embankment (人字堤).

The Bottleneck Channel relates to the philosophy of harmony between human and nature in the way that it uses what nature has provided to benefit the lives of humans instead of taking it away. The hole in the middle of the Yulei Mountain was mostly natural since there was already a spacing between the mountain originally. Chinese ancestors used that to their advantage and made the gap slightly wider to achieve their goal of creating the Bottleneck Channel (Liu, 2020).

### 3. Sponge Cities 海綿城市

The “sponge cities initiative” is a flood adaptive landscape project that aims to absorb rainwater and prevent flooding in urban areas through lakes and the growth of greeneries, the newest initiative also aims to release water from the greeneries and provide drinking water in response to water scarcity. This modern day construction demonstrates the same philosophical idea as other ancient Chinese irrigation systems.

#### 3.1 Science behind Sponge Cities

The current ideal sponge city cycle includes the process of absorption, storage, purification and drainage of water.

Rainwater is absorbed through different types of sponge city constructions like gardens, green roofs, plant edged sidewalks and permeable pavements. By increasing the surface area of greeneries, the carbon dioxide that pollutes the atmosphere will decrease through the process of photosynthesis in plants and floods can be prevented through the absorption of water. This process demonstrates the idea of harmony between human and nature by making use of nature, in this case being the greeneries and allowing humans to survive alongside with the floods (Zhou and Qiu, 2022).

The benefit of using plants and gardens to soak up rainwater is so that droughts can be easily prevented. With the increase in extreme weather conditions and global warming, many regions can suffer from extreme flooding and droughts all in the same year. Sponge cities do this by soaking up excess water from the rain and releasing the water slowly back into lakes and rivers. The traditional way of dealing with rainfall would be losing the water to evaporation, hence the common occurrence of droughts when there’s no rain for a long period of time.

To achieve the goal of reusing rainwater, an underground reservoir will be necessary to store and purify the rainwater absorbed and infiltrated from the sponge body. However, this part of the system is still being discussed in terms of its feasibility and sustainability.

The underground reservoir does not provide much value to the topic of discussion and hence will be overlooked in this paper.

The philosophy behind the idea of the sponge cities relates to the Taoist philosophy of harmony between human and nature. The famous Chinese landscape architect Kongjian Yu (俞孔堅) was one of the first people in modern society to suggest the idea of a flood and water adaptive landscape. He claimed that Chinese ancestors have used immense wisdom to live harmoniously with water instead of bending it to their will. Yet modern hydraulics implement the Western ways of blocking off water with dams, which damages the natural environment and goes against the ancient philosophy of living harmoniously with nature (Yu *et al.*, 2015). Sponge cities support this philosophy by making use of the excess water that is being provided by the rain instead of trying to prevent flooding in human living areas through the use of flood protection barriers and trap bags while putting other organisms in danger.



Figure 2. The use of flood protection barriers and trap bags while putting other organisms in danger.

### 4. The Harmony of Humans and Nature 天人合一

The idea of “harmony of human and nature” does not have a clear origin. The following passage will address the philosophical idea in terms of Taoism and Confucianism and its correlation with Chinese hydraulics.

In Taoism, humans and nature have an inseparable relationship. Zhuang Zi (莊子) thought that humans cannot exist independently without nature and he once said, 天地與我並生, 萬物與我為一(莊子)。The quote directly brings out the idea of how humans require



nature to live and humankind is a part of nature. Then, through cosmogony, Lao Tze (老子) said 道生一，一生二，二生三，三生萬物。萬物負陰而抱陽，沖氣以為和 (莊子) meaning that all beings were created equal and born from the same place, further emphasizing on the point that humans should not place themselves above nature and take them for granted (Wu, 2022) . As Mencius said, Yu from the Great Flood reflects the Taoist idea of “Unity between Human and Nature” in the way that he doesn’t artificially temper with nature when helping humankind survive from floods.

On the other hand, “unity between human and nature” in Confucianism starts from the perspective of the origin of human nature, believing that human nature is good and originates from the natural environment.

In Confucianism, a *Junzi* (君子) is someone who is respectable, follows social expectations, and meets traditional values. As Confucius said in 《論語·季氏》, 君子有三畏, 畏天命, 畏大人, 畏聖人之。 A Junzi is also someone who respects fate, or the will of nature, people of higher virtues, and the words of saints. According to Confucius (孔子) and Xunzi (荀子), Yu is a Junzi because of his morals and hardworking nature. In 《荀子·成相第二十五》, Xunzi says, 禹有功, 抑下鴻, 辟除民害逐共工。北決九河, 通十二渚, 疏三江。禹傳土, 平天下, 躬親為民行勞苦。得益、皋陶、橫革、直成、為輔。 Xunzi claims that Yu made meritorious deeds by cutting off rivers, dredging and connecting different tributaries. Yu worked hard for himself and his people, making him a respectable person worthy of the title Junzi. Yu was also a Junzi because of the way he dealt with floods through his respect for the environment and the laws of nature.

The construction of Dujiangyan demonstrates the Confucian notion that the natural environment should be respected during any form of human activity. As mentioned above, Dujiangyan was built with natural resources and materials that will not harm the environment. Confucianism believes in reasonable use of natural resources, this is a concept still applied in the plan for a more sustainable future currently (Liu and Su, 2021).

Sponge cities are a modern concept inspired by past hydraulic constructions and the Ancient Chinese philosophy of preserving nature. Not only does the construction of sponge cities support the growth of greeneries and environmental sustainability, but it also saves human beings from the current flood risks they face constantly. As mentioned earlier, sponge cities reuse water to solve water scarcity; an increase in greeneries will also solve carbon pollution in the atmosphere; and

finally, the water diversion and absorption system in sponge cities follow both the Taoist and Confucius idea of respecting the environment and providing harmony between humanity and nature.

Taoism focuses more on the environmental nature while Confucianism focuses more on human nature, both clearly demonstrated in the myth of the Great Flood, the construction of Dujiangyan and the idea of sponge cities.

## Conclusion

Looking back from the myth of the Great Flood to the invention of the Dujiangyan and now the development of sponge cities, the goal of controlling floods and living harmoniously with nature is shown to be extremely vital in Chinese culture. On top of this, the different methods demonstrated in the evolution of Chinese hydraulic systems reveal the importance of the Chinese philosophy about harmony between nature and humans. Ancient hydraulics reflect the idea and modern day hydraulic systems are directly inspired by this philosophy.

## References

BBC News 中文. (2021). “河南洪水：鄭州至少51人死亡 中國網民持續互助尋人” [online] Available at: <https://www.bbc.com/zhongwen/trad/chinese-news-57928517> [Accessed 10 Apr. 2023].

en.chinaculture.org. (n.d.). *Li Bing*. [online] Available at: [http://en.chinaculture.org/library/2008-02/01/content\\_26324.htm](http://en.chinaculture.org/library/2008-02/01/content_26324.htm).

馮廣宏, 曠良波, 李釗 and 鮮喬瑩 (2013). “都江堰文獻集成：歷史文獻卷”,《巴蜀書》, p.743.

Gies, E. (2022). *Slow water: can we tame urban floods by going with the flow?* [online] the Guardian. Available at: <https://www.theguardian.com/environment/2022/jun/07/slow-water-urban-floods-drought-chinasponge-cities>.

Liu, C. (2020). “都江堰水利工程”,《悅讀新視》

Liu, X. and Su, B. (2021). 儒家‘天人合一’思想中的生態智慧. *Journal of Qingdao Agricultural University (Social Sciences)*, 33(2).

Normile, D. (2016). *Massive flood may have led to China's earliest empire*. [online] www.science.org. Available at: <https://www.science.org/content/article/massive-flood-may-have-led-chinas-earliest-empire>.

Price, N. (2019). *Dujiangyan Irrigation System – Environmental China*. [online] Environmental China. Available at: <https://environmentalchina.history.lmu.build/group-page-theme-2-water-control/dujiangyan-irrigation-system/>.

Wang, S. and Hui, F. (2013). “都江堰內外江分水魚嘴工程變遷考述”. 南京農業大學中華農業文明研究院.

Wu, D. (2022). 中國傳統文化‘天人合一’的思想內涵與生態智慧. *Journal of Shaanxi Youth Vocational College*, (4).

Xiao, B. (2015). “大禹治水”. China Academic Journal Electronic Publishing House.

Yu, K., Li, D., Yuan, H., Fu, W., Qiao, Q. and Wang, S. (2015). ‘Sponge City’: Theory and Practice. *City Planning Review*, 39(6), pp.26–33.

Zhang, F. (2000). “古代大型的系統工程——都江堰”. China Academic Journal Electronic Publishing House, pp.4–6.

鄭肇經 (1993). “中國水利史”. 台灣商務.

Zhou, Y. and Qiu, X. (2022). 海綿城市建設在城市防洪排澇中的應. *Yunnan Water Power*, 38(1).

朱慧琴 (1981). “略論大禹治水和《禹貢》的治水思想”. China Academic Journal Electronic Publishing House.

莊子.《莊子·內篇·齊物論》

老子.《道德論(第四十二章)》

# Redesigning a Child-Friendly Ambidextrous Utility Knife

Troy Bacchus

## 1. Design Opportunity

### 1.1 Description of the Problem

“Lacerations are the most common injuries sustained in the workplace” (Bajaj) at 1.56 per 1000 children every year (Smith 2013), where utility knives were associated with 47% of the cases (AAEM) (Figure 1). While examining the design curriculum, I discovered that most projects for younger grades exclude utility knives. Currently, design teachers prohibit grade 6 students from using utility knives without one-to-one supervision due to safety concerns. Additionally, left-handed peers complained about how uncomfortable everyday right-hand bias products are. The physical world is built for right-handedness that comprises 90 percent of the population (Figure 2).

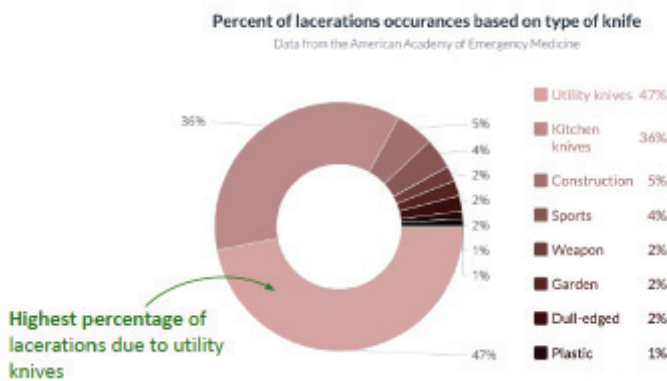


Figure 1. Percent of total lacerations incidents based on knife type

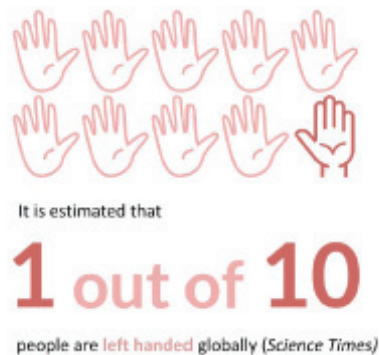


Figure 2. Estimated number of left-handed people globally

A brief preliminary survey identifies the suitability and relevance of this design opportunity. Results demonstrate a correlation between the comfort of utility knives and the user’s age. Overall, teachers found the knives more comfortable than the children. A distinction was found between right and left-handed surveyees for the comfortability of type 3 and 4 utility knives.

To improve the safety and inclusiveness of utility knives for left-handed grade 6 students, the new design will incorporate an ambidextrous mechanism that has increased comfortability for smaller hands and a more secure safety mechanism. With the aim of creating more design opportunities for grade 6 students.

### 1.2 Preliminary Data Collection

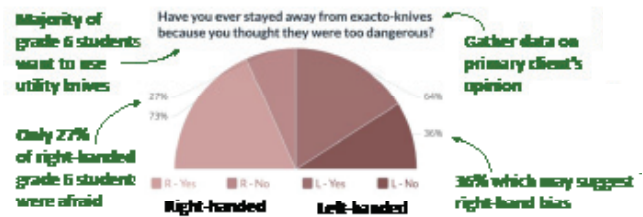


Figure 3. Pie chart comparing percentage of students with R/L dominant hand who stay away from utility knives because they are too dangerous

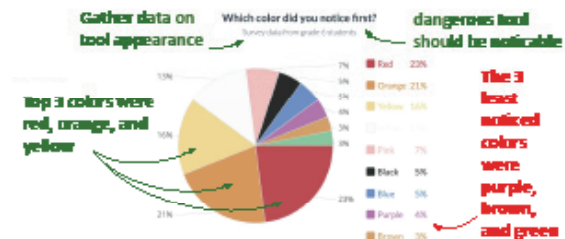


Figure 4. Pie chart comparing the first color grade 6 students noticed

The above article was written as an Internal Assessment (IA) for Design Technology, in partial fulfillment of the IB Diploma Programme, 2023.

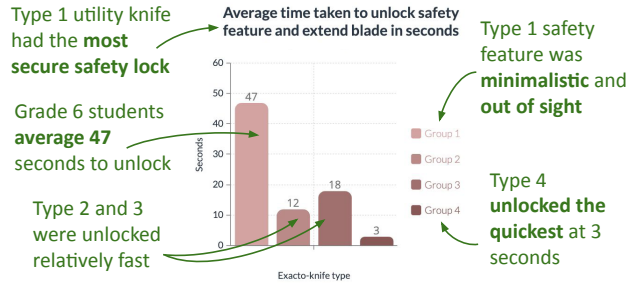


Figure 5. Bar chart of avg time taken to unlock safety feature

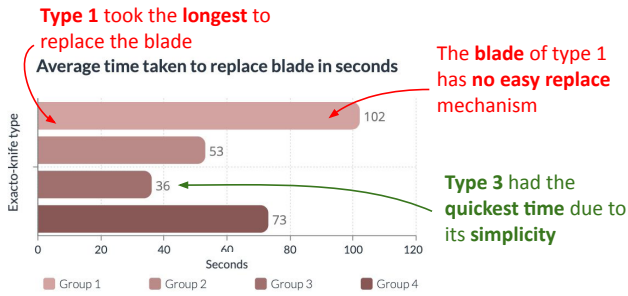


Figure 6. Bar chart of avg time taken to replace blade of each utility knife type

### 1.3 Primary and Secondary Client



Figure 7. Primary client with initials "TM" (left-handed grade 6 design student)

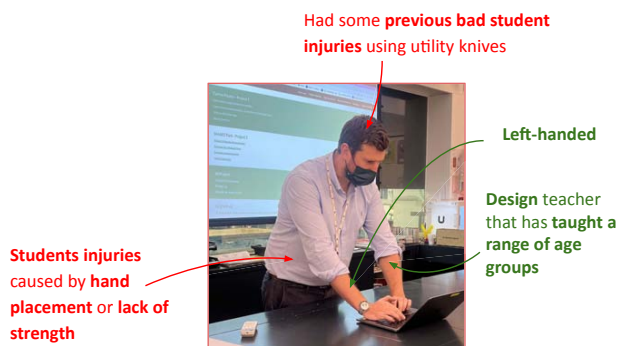


Figure 8. Secondary client named Mr. D (expert design teacher with 5 years of teaching experience with a range of students from G6 - G12)

### 1.4 Interview with Primary and Secondary Client to Identity Current Problem and Needs

I would give it a 2 out of 10, it is extremely uncomfortable and the knob of the sliding mechanism always rubs against my hand.

~ primary client

Figure 9. Quote from TM on tool comfort\*

All the design tools at this school are designed for the 50th percentile.

~ secondary client

Figure 10. Quote from Mr. D on tool design\*

\*Full interview and brief summary of interview found in Appendix 1 & Appendix 2

## 2. Design Brief

### 2.1 Incremental Solution

The injury rate for unintentional injuries of children using utility knives was 1.56 per 1000 people every year (Figure 1). I found the main reasons for lacerations injuries are incorrect hand placement, exposed blades, and lack of strength. Additionally, schools often purchase tools and supplies in bulk, where they are one-size-fits-all. These tools encounter the 50th percentile problem as they are handled by various hand sizes (Figure 10). Furthermore, studies have estimated that 1 out of 10 people are left-handed globally (Figure 2) and are constantly affected by right-hand bias in tools. Some industrial tools are uncomfortable and hard to use by left-handed people, which places them at risk. Therefore, this product will be a utility knife for left- and right-handed students above age 11. This product will increase inclusiveness for left-handed children and give teachers more confidence to allow their students to use utility knives.

## Parameters of the Problem

Safety	Client	Function	Ergonomics	Aesthetics	Size	Material	Packing
Prevents use for below 11 and safe use for 11 and up	<b>Primary:</b> left-handed G6 students <b>Secondary:</b> G6 design teachers	<b>Retractable</b> utility knife that is safe and precise	Size of left and right <b>hands</b> of <b>children</b> above age 11	<b>Bright neon</b> colors: red, orange, yellow	Handle diameter around <b>44 mm</b>	<b>Sturdy non-toxic</b> handle, metal blade	Stored with little to no <b>air pockets</b> or <b>blade exposure</b>

## Constraints

Constraint	Justification
<b>Limited time</b> to complete project	- Project must be <b>completed</b> before <b>April 2023</b> - <b>Final product</b> must be created within <b>30 hours</b> in given lessons
Access to only <b>a few</b> suitable clients	- There are only <b>a few left-handed young design students</b> which may <b>slightly restrict</b> the <b>opportunity</b> to receive <b>feedback</b> from clients - <b>Might</b> affect the user design cycle (eg. research, interviews, testing, feedback)

**Table 1.** Table of design constraints that may affect the quality of final product

## Manufacturing Process

Manufacturing techniques	Justification
<b>Early prototypes</b> created with <b>foam and clay modeling</b> and AutoCAD <b>Fusion 360</b>	- <b>Foam and clay modeling</b> can help test the <b>ergonomics</b> of the <b>handle's grip</b> - Fusion 360 models can help <b>visualize</b> how the design will be built
A <b>full scale mockup</b> created with Fusion 360	- Fusion 360 model will help test <b>inner mechanisms</b> and <b>overall aesthetic</b> - <b>Test Environment rendering and get feedback from client</b>
Full scale <b>3D printed ABS plastic</b> mock-up	- A 3D printed <b>mockup</b> will be used to help get <b>initial feedback</b> on form, <b>comfortability, ergonomics, angle of use.</b>
Fully functional <b>final</b> product to be determined	- Manufacturing technique to be determined with product development

**Table 2.** Table of manufacturing processes that will be used throughout the design cycle for this product

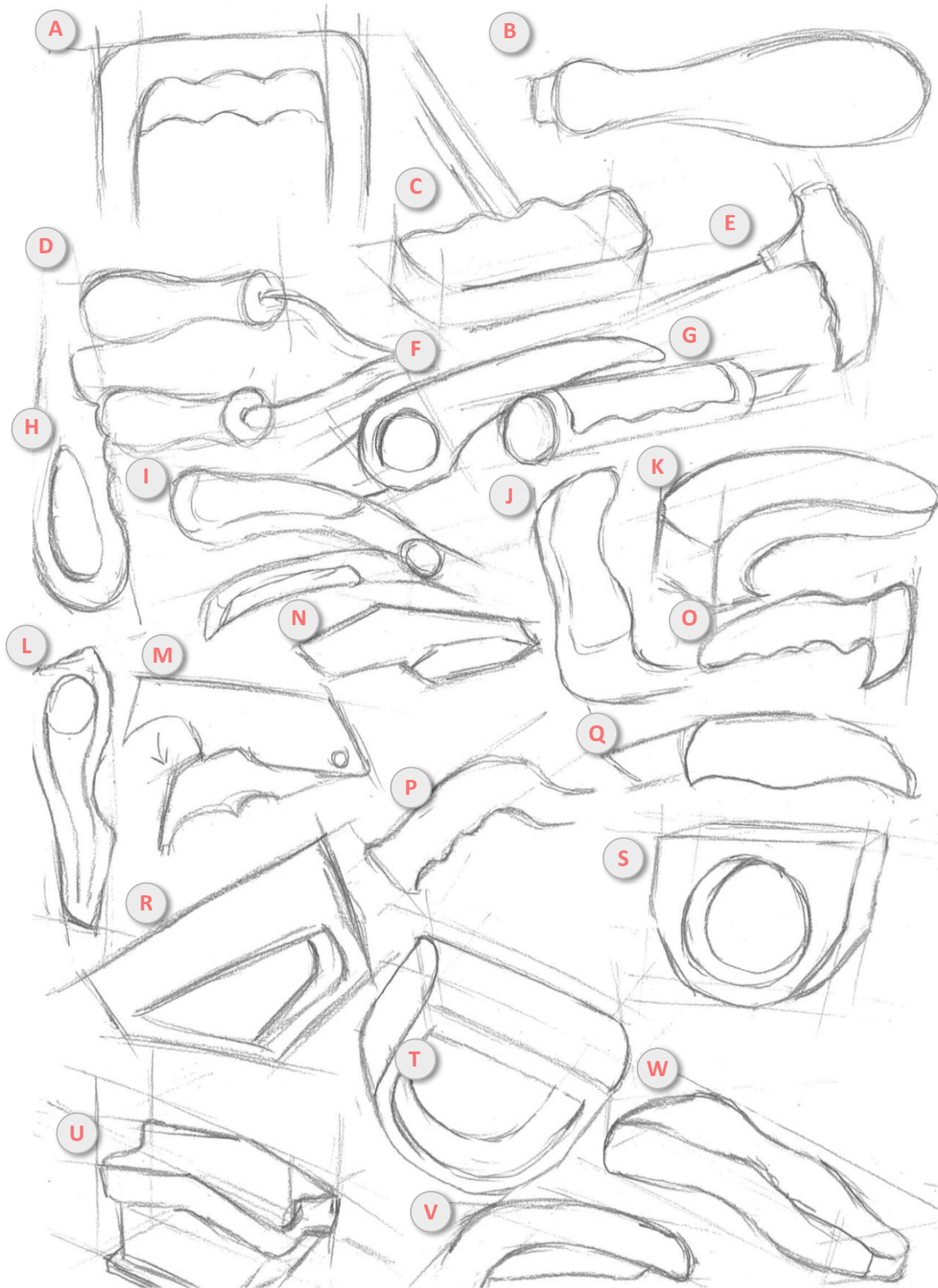
## Persona Mapping

Client	User	Role	Purpose
Primary client	Grade <b>6</b> design <b>students</b>	Students gaining <b>design experience</b>	Become more <b>immersed in design</b> and able to use all tools <b>safely</b> and <b>effectively.</b>
Secondary client	Grade <b>6</b> design <b>teachers</b>	<b>Teaching</b> students on design	

**Table 3.** Table of identifying my clients and what they want to achieve

### 3. Design Development

#### 3.1 Napkin Sketches



### 3.2 Initial Sketches

Client feedback

Represents top 5 specifications



1M



SELECT

Very compact design that folds itself close

Orange pivot point which is noticeable (5.1-5.2)

Swing mechanism that hides the blade while not in use (3.2)

Iteration 4

Crescent shaped object which stops blade from sliding too far

Short blade (1.4)

Suitable for left and right handed people (2.1)

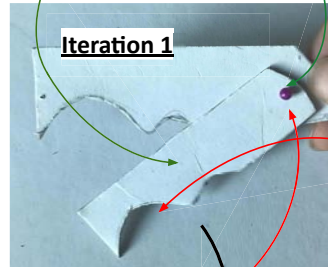
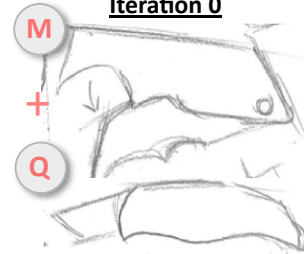
Nothing stopping blade from swinging out

Easier access to pull and swing the component out

Inner component that can be stored and swung out

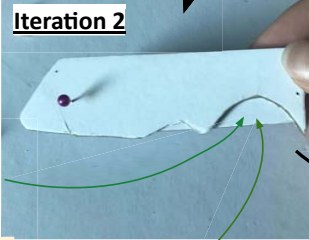
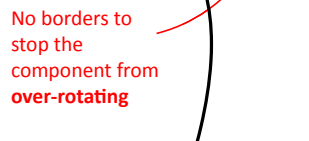
Pin needle which acts as pivot point

Iteration 0



Iteration 1

while stacked together you cannot access inner component

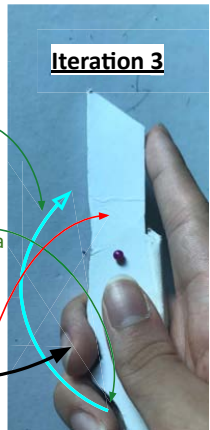


Iteration 2

Removed the dips in the inner component

Pivot motion

Storage mechanism doubles as a handle



Iteration 3

dangerous exposed blade (1.3)

2I



SELECT

Orange colored handle and neutral case (5.1-5.2)

Spring which pushes mechanism back into place (3.1)

Irregular shaped components sticking out

Short blade (1.4)

Mechanism pulls up to base instead of down

No safety mechanism (1.2)

Symmetrical design (2.1)

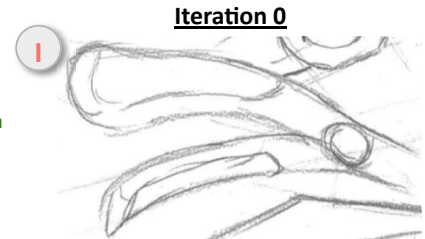
Mechanism is an improvement over cardboard model

Theoretical paper line

Suitable for left and right handed people (2.1)

Ergonomic wave design for finger grooves to increase comfort (4.1-4.2)

Spring mechanism which springs top section after pushing it down

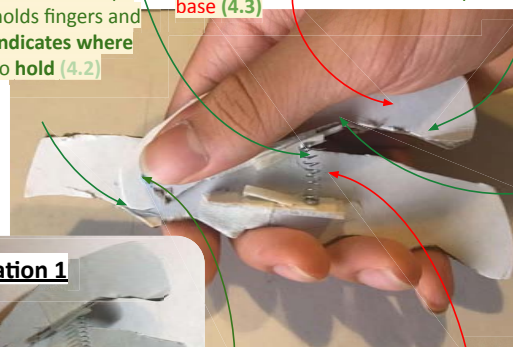


Iteration 0

Uncomfortable having to pushing palm down towards base (4.3)

Cardboard model held together with tape

Wave-like shape holds fingers and indicates where to hold (4.2)



Cardboard model front view

Blade is extended while both handles are gripped together (3.1-3.4)

Spring puts structure under lots of pressure (7.1)

Would be more intuitive to bring fingers to palm

### 3.3 Developed Designs

**D2** **SELECT**

Orange colored mech and neutral colored base (5.1-5.2)

Blade extends when mech is pulled upwards (3.1-3.4)

**Iteration 4**

Spring which pushes mechanism back into place (3.1)

Base material in PLA plastic (7.1)

Push joints and hexagonal screw to hold product together

Inspired by 2I mechanism and 3K shape

Safety pin safety mechanism is awkward and difficult to use

New proposed safety mechanism integrated into the end of base

Symmetrical design (2.1)

Length of handle 80 mm (6.1)

Ergonomic wave design for finger grooves to increase comfort (4.1-4.2)

Sliding mechanism: Locked (orange position), unlocked (red position)

Smaller than 165 x 60 x 50 mm (6.3)

**Iteration 5**

Suitable for left and right handed people (2.1)

Simple safety mechanism (1.2)

Large round handle for increased grip (3.1)

Handle diameter 45 mm (6.2)

Mechanism must be scaled up to fit stanley sized blade

Mechanism which holds the blade into place

Large rounded handle with grooves for finger placement (3.1) (6.1)

Custom blade needs to be specially produced

Tool blade made out of carbon steel (7.3)

Flush with surface increases safety and usability for children (2.1-2.2)

Short hidden blade out of sight (1.4) (3.2)

Most pressure on point where mechanism pushes against base walls

Natural hand position helps reduce strain on wrist (4.3)

Proposed spring implementation method

**Iteration 6**

**Iteration 7**

FEA static stimulation safety factor when applying pressure

Maximum pressure point

Blue and green highlighted pressure points need to be thickened

Blade retracts while not in use (3.4)

Natural shape that prevents fingers from slipping into blade (1.3) (4.2)

Difficult to make slight adjustments while cutting (3.3) (4.3)



### 3.4 Final Iterative Designs

**FD1** **Iteration 9**

Textured grip to increase friction and control (7.3)

Safety mechanism slightly uncomfortable against fingers (4.1)

Implemented red colored safety lock mechanism (unlocked position) (1.2)

Range of motion

Guard prevents fingers from slipping into exposed blade (1.1)

Spring pushes the mechanism back into enclosed area (3.2)

Designed for stanley knife blade

Theoretical paper line

Blade at a 10 degree angle for efficient cuts (3.3)

**FD1 Client feedback**

- The handle on this design is the **most comfortable**
- What **material** is the textured grip?
- Is the spring **attached** to the mechanism?
- How does the **spring** work?

**FD2** **Iteration 8**

Textured grip to increase friction and control (7.3)

Old safety mechanism should be removed (1.2)

Made the front thinner for increased control while turning (3.3)

Theoretical paper line

Blade at a 10 degree angle for efficient cuts (3.3)

Thinner handle will fit more comfortably around children's fingers (3.3)

Implemented red colored safety lock mechanism (unlocked position) (1.2)

Range of motion

Spring pushes mechanism out and blade into enclosed area (3.2)

**FD2 Client feedback**

- I love the **thinner front design**
- What will the **tracks** on the safety mechanism look like?
- I like the **blade mechanism** on this design
- Design feels **smart, safe** and really **comfortable** to use

**FD3** **Iteration 6**

Textured grip on mechanism increases friction and control (7.3)

Theoretical paper line

Implemented red colored safety lock mechanism (unlocked position) (1.2)

Reduced angle from 90 to 70 degrees to reduce gap

Added red colored mesh wall to reduce exposed blade (1.1, 1.3)

Range of motion

No automatic retraction system

Requires custom blade

Blade at a 10 degree angle for efficient cuts (3.3)

**FD3 Client feedback**

- I like the creativity of this design
- How will the **safety mechanism** lock in place?
- Could you add a **spring** to automatically retract the blade?

**FD4** **Iteration 7**

Textured grip on mechanism increases friction and control (7.3)

Flipped handle then rotated by 30 degrees (4.3)

Implemented safety lock system (currently in locked position) (1.2)

Range of motion

Theoretical paper line

Designed for stanley knife blade

Blade at a 10 degree angle for efficient cuts (3.3)

Ergonomic wave design for finger grooves to increase comfort (4.1-4.2)

No automatic retraction system

**FD4 Client feedback**

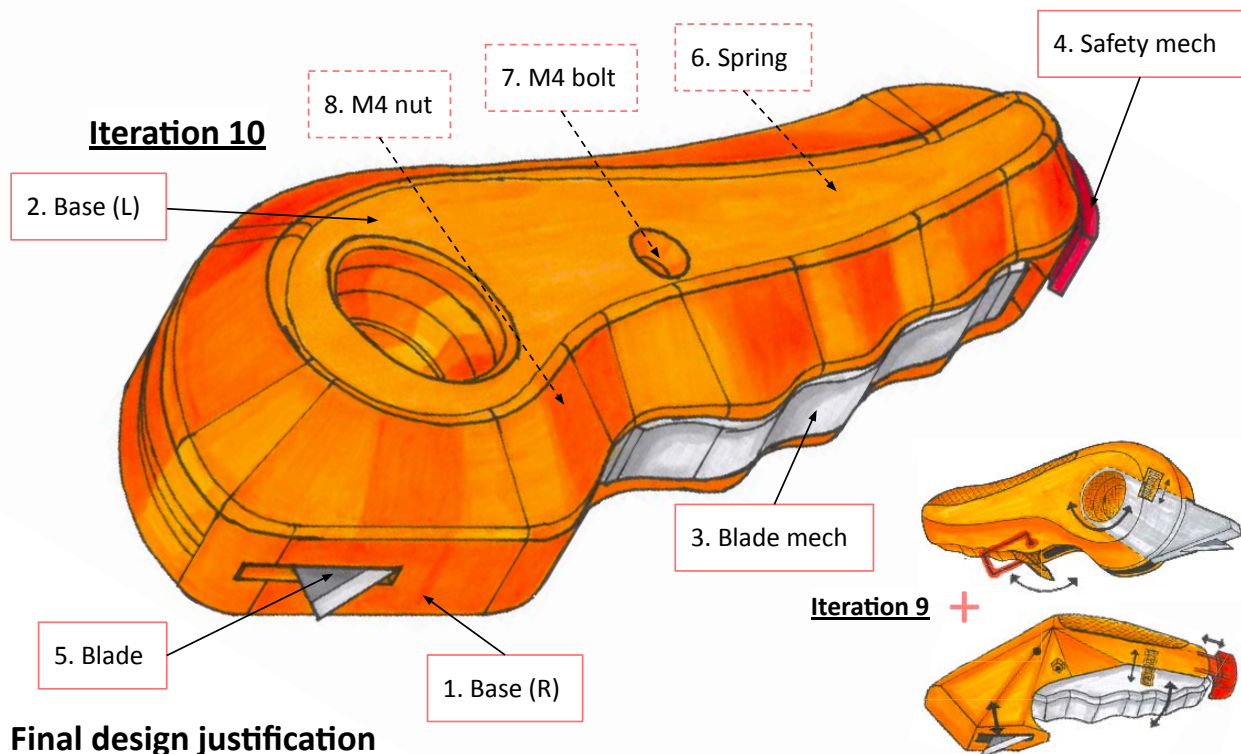
- I love the **organic** and ergonomic feel of the handle
- How does the safety mechanism **connect** to the base?
- I like the **finger grooves** because it clarifies the design

### 3.5 Evaluate against Specifications

Relevant specification points (maximum 5 points per point)	Final Iterative designs			
	FD1	FD2	FD3	FD4
1.1 Product <b>must</b> be safe for both <b>left and right handed</b> users above <b>age 11</b>	4	5	3	4
1.2 Product <b>must</b> have a <b>safety lock system</b>	4	5	3	3
1.3 <b>must</b> have <b>protection guard</b> to prevent hands from <b>slipping</b> into <b>exposed blade</b>	5	5	3	4
1.4 Blade <b>should</b> not extend beyond <b>50 mm</b> beyond opening	5	5	5	5
1.5 <b>Should</b> be able to <b>replace</b> the <b>blade</b> with limited contact within <b>30 seconds</b>	4	4	3	3
2.1 Product <b>must</b> be symmetrical to appeal to <b>left-handed users</b> to increase <b>usability</b>	5	5	5	5
2.2 Product <b>must</b> appeal to <b>younger design</b> students ( <b>Grade 6</b> )	5	5	4	4
3.1 Product <b>must</b> have a large (found in size specs) <b>rounded handle</b>	5	4	3	5
3.2 The blade of product <b>must</b> be <b>retractable</b> into an <b>enclosed area</b>	5	5	4	2
3.3 Product <b>must</b> be able to <b>precisely cut</b> in a <b>straight line</b>	5	4	5	4
3.4 Product <b>might</b> have an <b>automatic blade retraction mechanism</b>	4	5	3	2
4.1 Product <b>should</b> fit <b>comfortably</b> in the left or right <b>hand</b> of an <b>11 year old</b>	5	4	4	5
4.2 Product <b>should</b> <b>have grooves</b> on the <b>handle</b> to show children how to <b>hold</b> product	5	5	3	5
4.3 Product <b>should</b> reduce <b>strain</b> on wrist	5	5	5	5
5.1 <b>Base color</b> of product <b>must</b> be <b>bright red, orange, or yellow</b>	5	5	5	5
5.2 <b>Grip/mechanism color</b> of product <b>should</b> be <b>white or black</b>	5	5	5	0
6.1 <b>Length</b> of the handle <b>must</b> be between <b>51 and 79 mm (5th to 95th percentile)</b>	5	5	0	5
6.2 <b>Diameter</b> of the handle <b>must</b> be <b>44 mm (50th percentile)</b>	5	5	0	4
6.3 Product <b>should</b> be <b>smaller</b> than <b>165 x 60 x 50 mm (length, width, height)</b>	5	5	5	5
7.1 <b>Base material</b> for product <b>must</b> be <b>sturdy</b> and <b>non-toxic</b>	5	5	5	5
7.2 <b>Material</b> for blade <b>should</b> be <b>carbon steel</b>	5	5	5	5
7.3 <b>Material</b> for <b>handle</b> to increase friction between user and the tool	4	4	3	4
<b>Total score for <i>iteration 2 - 4 (initial)</i> developed design (Appendix 3) (out of /110)</b>	91	97	68	80
<b>Total score for <i>iteration 6 - 9 (final)</i> design (out of /110)</b>	105	105	81	89

\*As seen above, moving forward my final design will incorporate elements mostly from FD1 and FD2

### 3.6 Final Design Isometric View



#### Final design justification

##### Iteration:

The final design incorporates the **positive specification** qualities from **each** developed design to synthesize a refined utility knife. First of all, the **base** of the design originates from **D1 (score of 105)** because my client loved the ergonomic feel and **30 degree angle** of the handle. However, the blade mechanism of this design was **unsafe**. Thus, the **pivot-spring mechanism** of **D2 (score of 105)** was integrated with the **handle** of **D1**. For the **safety** mechanism, I needed something that would **slide** and **prevent** the pivot-spring mechanism from **retracting**. Hence, I utilized the sliding mechanism in **D3 (score of 81)** to **lock** the pivot-spring mechanism from **exposing** the razor blade. I redesigned the **inner pivot-spring** mechanism to be **flush** with the bottom of the base. In addition, the redesigned base will help the user get the **correct cutting angle** for more **clean** and efficient cuts.

##### Evaluation against specification:

The final design was **re-evaluated** against the same **specifications** used in **initial** and **final iteration** developed designs. As seen in **Appendix 4**, the **final design** achieved an evaluation score of **109 / 110**. This is a really impressive score considering the only point loss was due **lack of testing textured materials**.

##### Client feedback:

I held a **final discussion** with **my client** after showing him the **final designs**. Through this **conversation**, I learned that he **loved** this design and couldn't wait to test the **3D printed prototype**. However, there was some **feedback** where he pointed out that the **safety mechanism** might not stay up against **gravity** unless there was a lot of **friction**. Another point he raised was "what is the **purpose** of the **"hole"** at the front of the **knife**" to which I responded with "It creates an **alternative way** to hold the knife in a **pen hold** or a place to rest your **index finger**".

### 3.7 Rendered Design

#### Iteration 11



Final design iteration 11 render illustrating the blade mechanism range of motion



#### Iteration 12

Final design iteration 12 realistic environment renders in workplace / while in use

## 4. Manufacturing

### 4.1 Material Testing

Highly experienced  
Intermediate  
Beginner

Chosen material  
Advantages  
Disadvantages

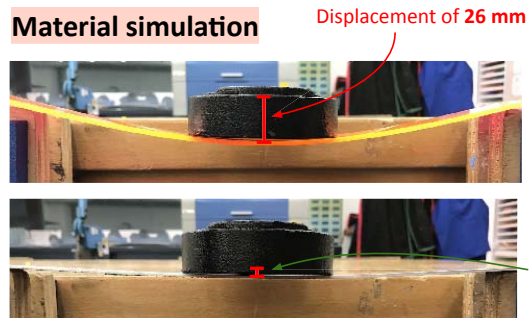


Figure 11. Test comparing strength of PLA plastic and stainless steel with a 2 KG weight

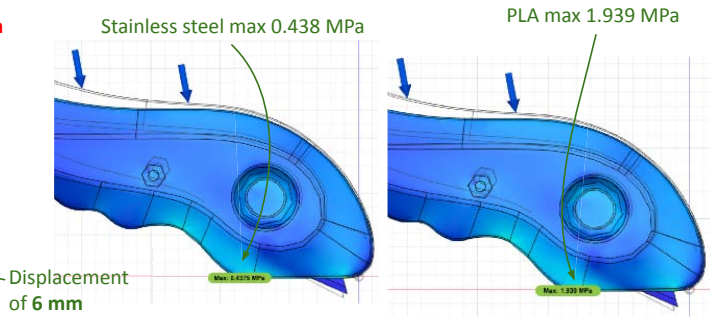
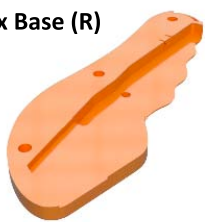





Figure 12. FEA shows PLA and stainless both have high strength - however the product's design does not require high levels of strength

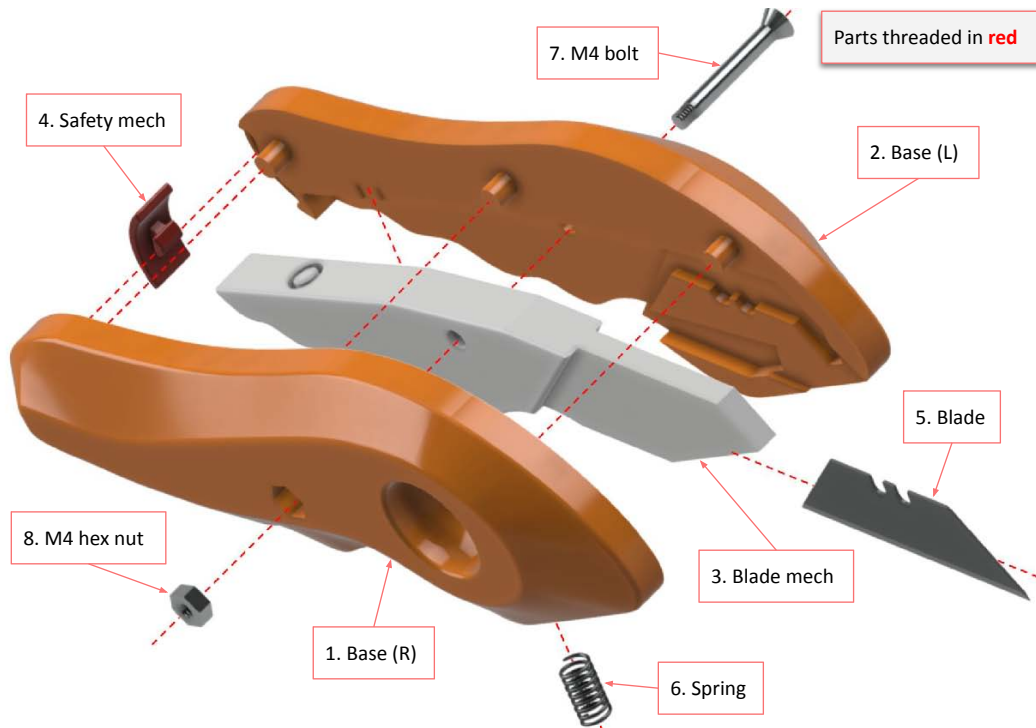
Component	Material	Material properties	Manufacturing process/justification
1x Base (R)  1x Base (L)  1x Blade mech  1x Safety mech 	<b>PLA plastic</b>	<ul style="list-style-type: none"> <li>- Tensile strength <b>33 MPa</b></li> <li>- Yield strength <b>26 MPa</b> (AIP)</li> <li>- Elongation at break <b>6%</b></li> <li>- Flexural modulus <b>4 GPa</b></li> <li>- density <b>1.24 g/cm<sup>3</sup></b> (National Library of Medicine)</li> <li>- highly suitable for <b>recycling</b> (Adreco plastics)</li> <li>- PLA is <b>versatile</b> in the range of <b>colour</b></li> <li>- PLA objects will usually have a <b>glossier</b> look &amp; feel (Vexma)</li> </ul>	<b>3D printing</b> <ul style="list-style-type: none"> <li>- <b>minimal</b> upfront costs</li> <li>- <b>additive process takes up to 24 hours</b></li> <li>- Better for <b>prototyping</b> as no limits to how complex each component is</li> <li>- Cost of around <b>\$170 HKD per kg</b></li> <li>- There are at least 20 3D printers <b>available</b> at my school</li> </ul> <b>Injection molding</b> <ul style="list-style-type: none"> <li>- high volume production with <b>minimal material wastage</b></li> <li>- Enhanced strength of materials (Premier Engineered products)</li> <li>- Cost per part of around <b>\$31 HKD</b></li> <li>- There is <b>no injection molding equipment</b> at my school</li> </ul>
	<b>Stainless steel grade 304</b>	<ul style="list-style-type: none"> <li>- Tensile strength <b>621 MPa</b></li> <li>- Yield strength <b>215 MPa</b></li> <li>- Elongation at break <b>70%</b></li> <li>- Flexural modulus <b>193 GPa</b></li> <li>- density <b>8.03 g/cm<sup>3</sup></b> (ASM)</li> <li>- infinitely <b>recyclable</b> (Aluminum Association)</li> <li>- <b>Stainless steel only comes in colors of gray, gold and copper.</b></li> </ul>	<b>Die casting</b> <ul style="list-style-type: none"> <li>- <b>significant upfront investment</b></li> <li>- faster manufacturing (<b>30-45 seconds</b>)</li> <li>- creates waste from <b>unused molding material</b></li> <li>- For products of the same type out of the same material, die casting is much faster, so <b>high volumes</b> are often more <b>cost-effective</b>. (Premier Engineered products)</li> <li>- material is extracted and reused with no degradation in performance from product to product</li> <li>- Cost per part of around <b>\$20 to \$40</b></li> <li>- There is <b>no die casting equipment</b> at my school</li> </ul>

In conclusion, **3D printing** will be used for **manufacturing prototypes** throughout the **iterative process**. Once a final design is created, **injection molding** will be used to **mass produce** the product for the target market.

## 4.2 Orthographic Drawings



## 4.3 Assembly Drawings and Bill of Materials



\*measurements rounded to whole numbers \*cost rounded to 2 decimal places

Part #	Part name	Qty	Material	L (mm)	W (mm)	H (mm)	Making / Buying	Total grams / Cost
1	Base (R)	1	PLA plastic	167	58	15	Making	42 grams
2	Base (L)	1	PLA plastic	167	58	20	Making	48 grams
3	Blade mech	1	PLA plastic	143	32	11	Making	17 grams
4	Safety mech	1	PLA plastic	14	10	10	Making	1 gram
5	Blade	1	Carbon steel	61	19	1	Buying	\$3.93 each in 10 pack
6	Spring	1	Stainless steel	14	7	7	Buying	\$7.85 each in 10 pack
7	M4 bolt	1	PLA plastic	7	7	30	Making	0.5 grams
8	M4 hex nut	1	PLA plastic	9	7	3.3	Making	0.5 grams
Total filament needed - 109 grams (Average \$170 HKD per 1000 grams of PLA filament)								\$18.53
Total cost in HKD								\$30.31

## 4.4 Production Plan

#	Process	Equipment	Scheduling	Quality control	Risk assessment
<b>Preparing for manufacturing</b>					
1	Create CAD model of <b>final design</b>	Computer with Fusion 360	8 hours	At least <b>0.5 mm</b> tolerance between each fitted joint	Take breaks away from computer to <b>prevent eye fatigue</b>
2	Export each individual component as a <b>STL file</b>	Computer with Fusion 360	1 hour	Ensure the exported files are <b>grouped</b> and <b>named</b> correctly	Correct file <b>conventions</b> ensure parts are printed in <b>correct color</b> and materials are not wasted
3	Convert STL files into <b>gcode</b> through <b>Ultimaker Cura</b>	STL files, Ultimaker Cura	30 minutes	Check slicing settings and support structure is set to <b>default</b>	If support structure is <b>turned off</b> the print will <b>fail</b> and <b>waste materials</b>
4	Upload gcode files to USB <b>grouped</b> by <b>color</b> of filament	Computer with gcode files, USB sticks	15 minutes	gcode files are <b>grouped</b> by the correct color	<b>Eject</b> USB properly before removing it from computer
<b>Manufacturing</b>					
5	Insert each USB into correctly <b>colored 3D printers</b>	USB, 3D printers	15 minutes	Check <b>level</b> of bed; Calibrate nozzle <b>height</b> ; Confirm file <b>name</b>	Make sure bed is <b>empty</b> ; Don't place hands <b>inside</b> printer
6	Start 3D prints and wait for them to finish	3D printers	Up to 18 hours	There is enough <b>filament</b> ; Wait for first layer to <b>print</b>	Stay away from <b>heated</b> PLA plastic
7	Use a <b>scraper</b> to remove 3D prints	Scraper, 3D printers	15 minutes	<b>Delicate</b> removal, 3D printed parts stay <b>intact</b>	Point the scraper face <b>down</b> while moving around
8	Use <b>pliers</b> to remove large chunks of structure material	Pliers, 3D printed parts	30 minutes	Don't <b>remove chunks</b> of the actual part	Keep fingers away from the head of the <b>pliers</b>
9	Use <b>small cutting</b> pliers to remove intricate sections of structure	Cutter pliers, 3D printed parts	15 minutes	Don't <b>remove chunks</b> of the actual part	Keep fingers away from the head of the <b>cutter pliers</b>
10	Use a stanley knife to shave off the brim edge	Stanley knife, 3D printed parts, cut resistant glove	5 minutes	Don't remove any <b>material</b> from the base part	Wear a <b>cut resistant glove</b> , cut <b>away</b> from the fingers

#	Process	Equipment	Scheduling	Quality control	Risk assessment
<b>Assembly</b>					
11	Sandwich safety mech <b>between</b> base (R) and base (L)	3D printed parts	1 minute	Make sure the push joints have <b>enough tolerance</b>	Not <b>enough tolerance risks</b> components get <b>jammed stuck</b> together
12	Place <b>spring</b> into <b>circular slot</b> on base	Spring, 3D printed parts	1 minute	Check if spring fully <b>fits inside</b> the <b>circular base hole</b>	Wear <b>goggles</b> in case the spring <b>shoots</b> towards face
13	Place stanley <b>blade</b> into blade mech at <b>30 degree</b> angle	Stanley blade, 3D printed parts, Cut resistant glove	1 minute	Shake the <b>blade mech</b> slightly to ensure no blade <b>movement</b>	Wear a <b>cut resistant glove</b> ; Wear <b>safety goggles</b> if blade <b>chips</b>
14	Slot <b>blade</b> mech into base and fit spring inside <b>hole</b>	3D printed parts	1 minute	Check if the <b>inner bolt hole lines up</b>	Attempting to <b>compress</b> an <b>unaligned spring</b> may cause <b>spring</b> to <b>strike eye</b>
15	Place M4 hex nut and <b>screw in</b> M4 bolt	M4 hex nut, M4 bolt, 3D printed parts, phillips screwdriver	1 minute	Ensure <b>negative space</b> on base fits both <b>nut and bolt</b>	If base isn't <b>screwed properly</b> then <b>spring</b> may <b>strike eye</b> or <b>blade</b> may fall out and <b>cut hand</b>
16	Check if <b>spring</b> and <b>safety mechanism</b> work	Utility knife product	5 minutes	Check if the blade comes out <b>at least 5 mm</b>	Wear <b>cut resistant gloves</b> ; Wear <b>safety goggles</b> if product snaps



# 5. Evaluation

## 5.1 Evidence of Testing

Fully meets spec  
Partially meets spec  
Does not meet spec

**Has a safety lock mechanism**

**UT1**

Safety lock mechanism

**Is symmetrical across the z-axis**

**UT2**

There is a line of symmetry

**Has grooves on the handle**

**UT3**

There are no grooves

**Blade can retract into an enclosed area**

**UT4**

Enclosed area

**Blade automatically retracts into an enclosed area**

**UT5**

**Correct color of base and blade/safety mechanisms**

**UT6**

**Suitable material of product and blade**

**UT7**

**Ease of understanding utility knife**

**FT1**

Age 12	- It was hard to use the knife with a ruler
Age 17	- I wish the safety mechanism worked properly
Age 34	- If I open the knife too fast everything falls out

**Client testing feel of handle**

**Cutting paper and cardboard**

**FT2**

Client cutting cardboard with a ruler

**Survey range of users after using knife**

**FT3**

My product ranked second best

Type*	1	2	3	4	Mine
Rank	1	3	4	5	2

\*Knife 1,2,3,4 taken from A1

**My product compared to current market**

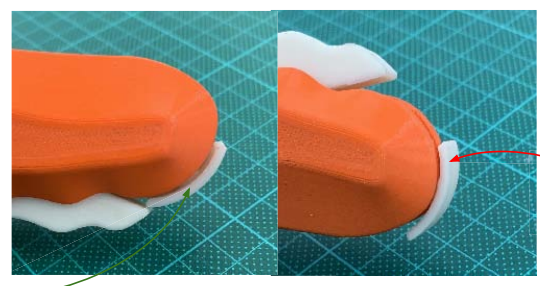
**FT4**

Fully meets spec  
Partially meets spec  
Does not meet spec

Safety mechanism locks while in different positions

PT1

Safety mechanism stays in place while right side up



Safety mechanism withstands grip force

PT2

Client applying grip force to blade mechanism



Users can replace blade within 30 seconds

PT4

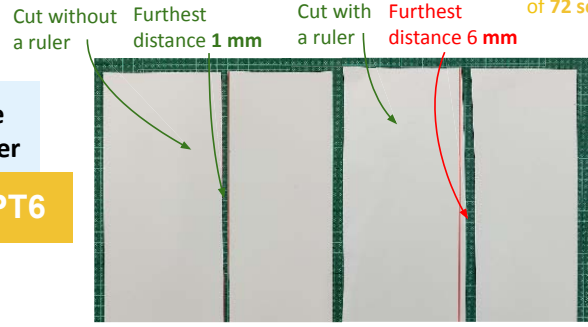
Time taken to replace	User 1	User 2	User 3	User 4	Avg
	54 secs	84 secs	73 secs	77 secs	72

Average time of 72 seconds

% force applied	Locks?
0%	No
25%	No
50%	Yes
75%	Yes
100%	Yes

Cut in a straight line with and without ruler

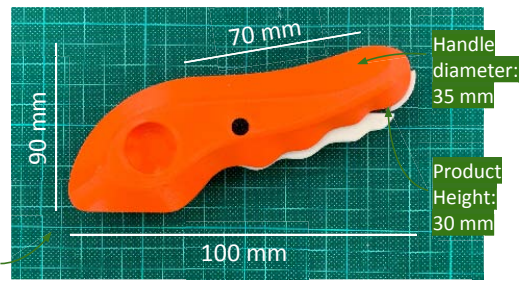
PT5 & PT6



Product should fit within dimension constraints

PT7

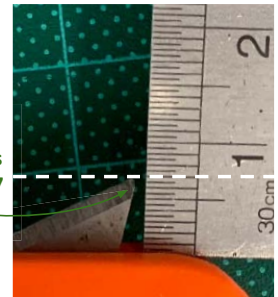
All dimensions are within constraints



Blade doesn't extend beyond 50 mm

PT3

Blade extends out by 7 mm



Compare price against existing products

C1

Type*	1	2	3	4	Mine
Price (HKD)	68	47	12	40	30

Compare advantages against existing products

C2

Type*	1	2	3	4	Mine
Advantage	Auto retract blade	Heavy, sturdy feel	Cheap blades	More precise wrist control	Safe and inclusive

\*Knife 1,2,3,4 taken from A1

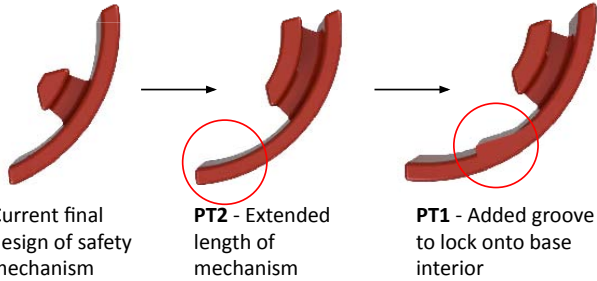
## 5.2 Improvements

### Safety mechanism

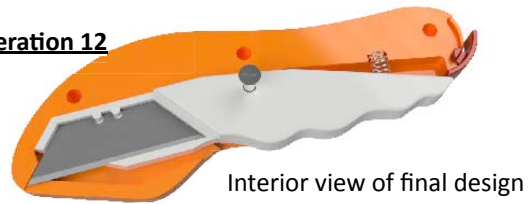
**FT3** > Safety mechanism felt too slippery, slid around too much, and was hard to grip

**PT1** > Safety mechanism was fairly loose and become unlocked while flipped upside down and straight up

**PT2** > Safety mechanism was way too short and didn't have any enough surface area to hold the mechanism



### Iteration 12



Interior view of final design

### Exterior base shell

**UT3** > The product does not have any grooves

**UT7** > Can combine hex nut threads onto base shell

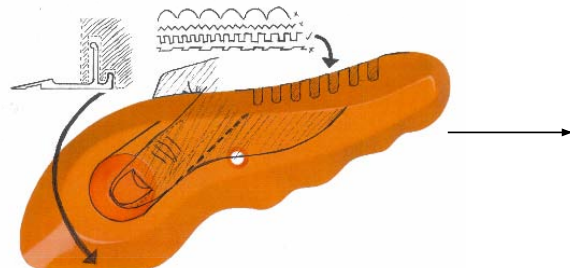
**FT2** > The hole shape for the finger was too rigid and steep

**FT2** > The knife was a bit on the heavier side

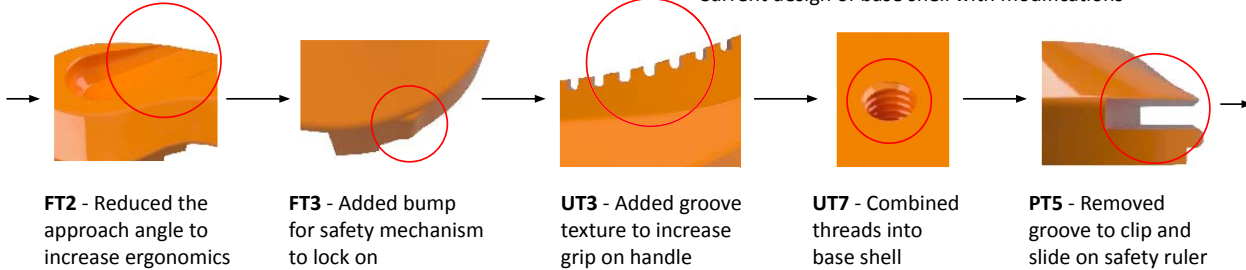
**PT4** > Add a blade storage area for quicker access to blades

**PT4** > Add a circular ring for the blade mechanism to stay in place

**PT5** > Awkward to press shape of the knife against the safety ruler



Current design of base shell with modifications



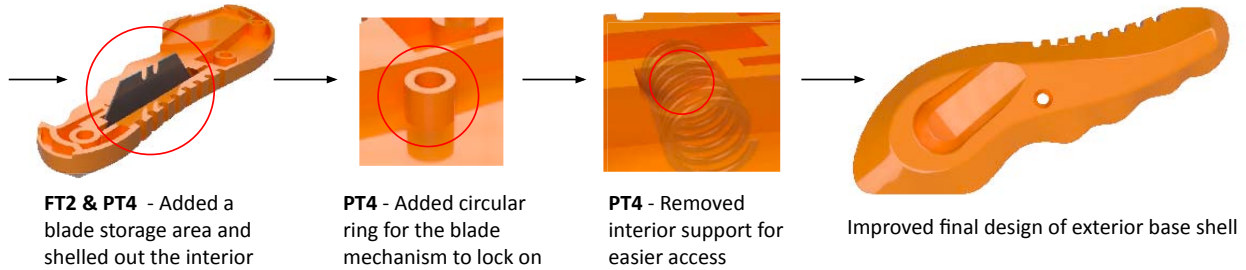
**FT2** - Reduced the approach angle to increase ergonomics

**FT3** - Added bump for safety mechanism to lock on

**UT3** - Added groove texture to increase grip on handle

**UT7** - Combined threads into base shell

**PT5** - Removed groove to clip and slide on safety ruler



**FT2 & PT4** - Added a blade storage area and shelled out the interior

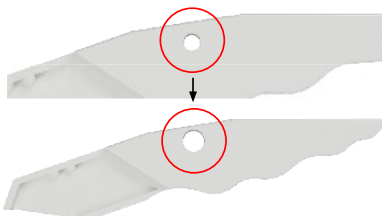
**PT4** - Added circular ring for the blade mechanism to lock on

**PT4** - Removed interior support for easier access

Improved final design of exterior base shell

### Blade mechanism

**PT4** > Increase opening to fit around circular ring



**PT4** - Increased opening to account for new tunnel modification

### Iteration 13

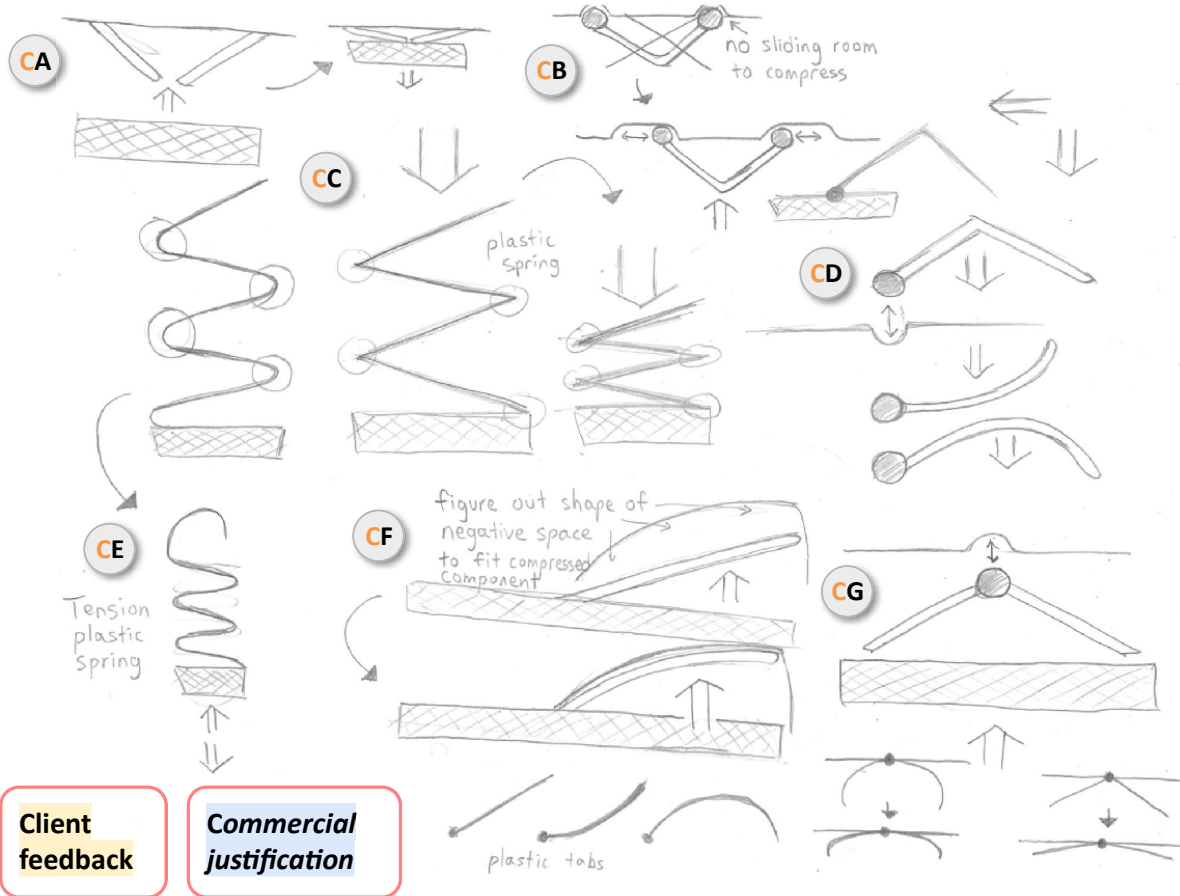


Interior view of improved final design

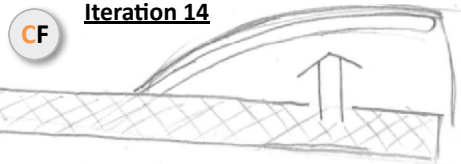
# 6. Commercial Considerations

## 6.1 Commercial Initial Design

**C = commercialized redesign**



**1C** ✓ ✓ ✓ **SELECT**



**Iteration 16**

Blade mechanism in neutral resting position

Reduces total number of parts, reduces inventory and costs (9.3)

Fillet on inner and outer edge to increase stability

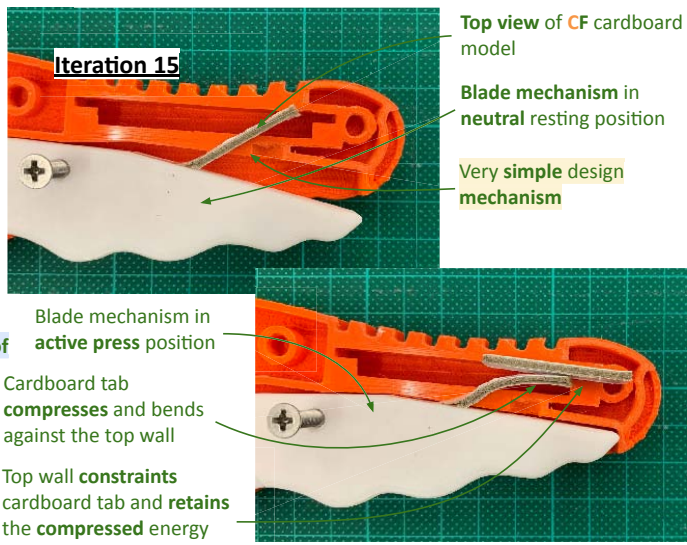
Adjusted wall to be thick enough for injection molding (9.2)

Angle may be too shallow to generate enough potential energy

Design for ease of fabrication (9.3) (10.1)

Implementation of mechanism will not inhibit blade storage space (8.2)

Mechanism requires limited additional materials (7)



## 7. Industrial Production

### 7.1 Justify Scale and Volume

Globally, it is estimated there are 110,000 laceration cases for children age 11. However, my product will initially be specifically aimed for parents or schools that have kids/students in secondary school whom are interested in design or left handed people in general in Hong Kong.

As seen in the graph (Figure 13), there are around 344,600 secondary students across all public and private schools in Hong Kong. However, out of all 510 secondary schools, only 60 offer design-related subjects. If one-third of the schools purchase 50 utility knives, I will need to produce 1000 units.

Additionally, parents of children may want to purchase a personal utility knife for home use. If 1 out of every 1,000 potential student families purchased the utility knife, I would need to produce 344 units.

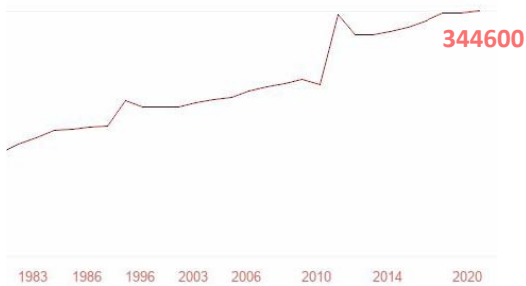


Figure 13. Graph trend for number of secondary students in Hong Kong since 1983

Lastly, according to BMC Psychology, left-handedness prevalence has been consistently reported at around 10% using a Hong Kong sample. With a population of 7.413 million (Figure 14), calculations show there are roughly 741,300 left-handed people in Hong Kong. If 1 out of every 1,000 people purchased the utility knife, I would need to produce 741 units.

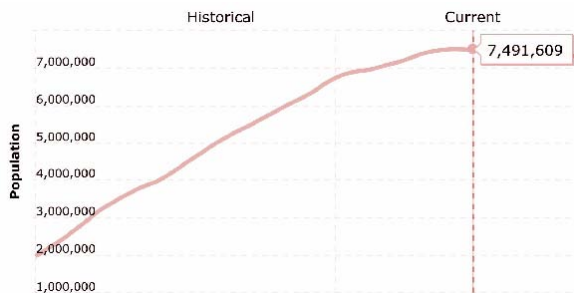


Figure 14. Graph trend for Hong Kong population since 1950

Mass production	Batch production
Purchased in <b>large</b> quantities	Purchased in <b>set</b> quantities
Taking advantage of <b>economies of scale</b> , materials are cheaper as they can be purchased in <b>larger</b> quantities	Since larger numbers of units are produced, the <b>unit cost is lower</b>
Cheaper <b>labor cost</b>	Cheaper <b>machinery</b>
Workers are <b>not motivated</b>	More <b>expensive</b> labor cost
Production lines are <b>inflexible</b> and hard to adapt	Products <b>stored</b> until sold, <b>expensive</b> inventory space
More <b>expensive</b> machinery to set up production lines	Can be a <b>repetitive process</b> which may <b>demotivate</b> crafters
<b>Justification</b>	<b>Batch production</b> is most effective when producing a <b>set number of products</b> where all the items are the <b>similar</b> . The process is <b>repeatable</b> , which ensures <b>consistency</b> and <b>quality</b> between products. My product is aimed specifically for <b>secondary students interested in design</b> or those with <b>left-handedness</b> . Therefore my product will be aimed towards a <b>set small quantity</b> of clients within a <b>target market</b> in a <b>market segment</b> . For these reasons, <b>batch production</b> is the most suitable <b>scale of production</b> for my product.

Table 4. Table comparing the pros and cons of mass production vs batch production

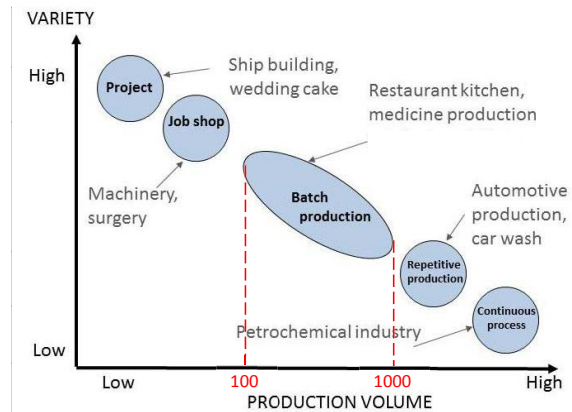


Figure 15. Different production types on the diagonal axis according to the amount of variants and the production volume

As seen in Figure 15, batch production is the most suitable production method as research shows I will be producing roughly 522 units quarter-yearly. This number fits the 100 - 1000 unit constraints of batch production volume.

To spread out unit production throughout the year, I will initially use injection molding to produce the utility knife in batches of 522 units quarter-yearly  $((1000 + 344 + 741) / 4 = 522)$ .

## References

- AdrecoPlastics. "ABS Plastic Properties | Great Advantages Of Acrylonitrile Butadiene Styrene." *Adreco Plastics*, 2022, <https://adrecoplastics.co.uk/abs-plastic-properties/>. Accessed 3 March 2023.
- ASM Handbook Committee. "Die Threading." *ASM HANDBOOKS ONLINE*, 1989, <https://doi.org/10.31399/asm.hb.v16.a0002143>. Accessed 3 March 2023.
- "ASM Material Data Sheet." *ASM Material Data Sheet*, <https://asm.matweb.com/search/SpecificMaterial.asp?bassnum=mq304a>. Accessed 4 October 2022.
- Bajaj, R. Slice cutting tools: Safer safety knives. (GSTDTP): Slice Cutting Tools: Safer Safety Knives. June 9, 2022, <http://resp.llas.ac.cn/C666/handle/2XK7JSWQ/113799>. Accessed 3 March 2023.
- Brown, Robert. "Wiss Safety Knife – Auto-Retracting Utility Knife." *YouTube*, 24 June 2015, <https://youtu.be/leiSWm7Czwo>. Accessed 25 May 2022.
- "Comparison between Stainless Steel Spring and Carbon Steel Spring - Dongguan Cailong Metal Spring Mfg.Co.,Ltd." Cailong, <https://www.kc1970.com/comparison-between-stainless-steel-spring-and-carbon-steel-spring.html>. Accessed 4 October 2022.
- Cornell Forge Co. "Differences Between Hot and Cold Forging Processes." *Cornell Forge*, 15 March 2021, <https://www.cornellforge.com/blog/differences-between-hot-and-cold-forging-processes/>. Accessed 3 March 2023.
- "Die Casting vs. 3D Printing | Premier Engineered Products." *Die Casting*, 20 April 2020, <https://diecasting.com/blog/die-casting-vs-3d-printing/>. Accessed 4 October 2022.
- Fuente, Javier de la. "19-Functional grip diameter (dominant hand) vs. age. Comparison between... | Download Scientific Diagram." ResearchGate, August 2006, [https://www.researchgate.net/figure/Functional-grip-diameter-dominant-hand-vs-age-Comparison-between-working-groups-and\\_fig31\\_220012972](https://www.researchgate.net/figure/Functional-grip-diameter-dominant-hand-vs-age-Comparison-between-working-groups-and_fig31_220012972). Accessed 25 May 2022.
- Geer, Katie Kerns. "Left-Handers and Health Risks: 12 Little-Known Facts." *Everyday Health*, 13 August 2015, <https://www.everydayhealth.com/healthy-living-pictures/little-known-facts-about-lefthanders.aspx>. Accessed 25 May 2022.
- Gharge, Pranav. "Printing with ABS – 6 Simple Tips to Succeed." *All3DP*, 19 January 2022, <https://all3dp.com/2/printing-with-abs-tips-tricks/>. Accessed 3 March 2023.
- Klein, Thomas R. "Folding Utility Knife - 44131." *Klein Tools*, 2017, <https://www.kleintools.com/catalog/utility-knives/folding-utility-knife>. Accessed 25 May 2022.
- Kyocera Professional Chef's Knife FK-200 WH-BK, blade length 20 cm. Accessed January 2020 at [https://europe.kyocera.com/products/kitchen\\_products/prd/ceramic\\_knives/fk\\_series.html](https://europe.kyocera.com/products/kitchen_products/prd/ceramic_knives/fk_series.html)
- Langnau, Leslie. "How tensile strength relates to 3D printing." *Make Parts Fast*, 4 September 2019, <https://www.makepartsfast.com/how-tensile-strength-relates-to-3d-printing/>. Accessed 4 October 2022.
- Lewin, Walter. "How-Its-Made-Utility-Knives." *YouTube*, 9 April 2017, <https://youtu.be/XVwCJA4fCn0>. Accessed 25 May 2022.
- Logistiikan Maailma. "Production types." *Logistiikan Maailma*, 2023, <https://www.logistiikanmaailma.fi/en/production/production-types/>. Accessed 3 March 2023.
- L.S, Starrett. "WKAR1 Wiss Auto-Retractable Utility Knife." *Manson Tool & Supply*, <https://www.mansontool.com/PROD/WKAR1.html>. Accessed 25 May 2022.
- Martor USA. "Ceramic Blades vs Steel Blades." *Martor USA*, 2022, <https://martorusa.com/blog/ceramic-blades-vs-steel-blades>. Accessed 4 October 2022.
- MasterClass. "How to Sharpen Ceramic Knives in 3 Ways - 2023." *MasterClass*, 3 December 2021, <https://www.masterclass.com/articles/how-to-sharpen-ceramic-knives>. Accessed 3 March 2023.
- McCarthy, Philip J. "Vital and Health Statistics; Series 11, No. 123 (1/73)." *CDC*, January 1973, [https://www.cdc.gov/nchs/data/series/sr\\_11/sr11\\_123acc.pdf](https://www.cdc.gov/nchs/data/series/sr_11/sr11_123acc.pdf). Accessed 25 May 2022.
- NexLand Outdoors Store. "UT1 Ceramic Utility Blade Razor Sharp 10pack." *Amazon*, 27 June 2022, <https://www.amazon.com>. Accessed 3 March 2023.
- Patel, Shaurin, and Shaurin Patel. "Pla 3d Printing Material Properties & Specifications." *Vexmatech*, 2022, <https://vexmatech.com/pla-material.html>. Accessed 4 October 2022.
- "Plastic vs metal fasteners: why plastic can be a better choice | Global Manufacturer & Distributor of Component Solutions — Essentra Components." *Essentra Components*, 13 February 2018, <https://www.essentracomponents.com/en-gb/news/product-resources/plastic-vs-metal-fasteners-why-plastic-can-be-a-better-choice>. Accessed 4 October 2022.
- Scimone, T.J. "Slice." The Self-Retracting Utility Knife: Is It For You? | *Slice*, 25 December 2017, <https://www.sliceproducts.com/self-retracting-utility-knife>. Accessed 25 May 2022.
- Shim, Jae Kun & Oliveira, Marcio & Hsu, Jeffrey & Huang, Junfeng & Park, Jaebum & Clark, Jane. (2007). Hand digit control in children: Age-related changes in hand digit force interactions during maximum flexion and extension force production tasks. *Experimental brain research. Experimentelle Hirnforschung. Expérimentation cérébrale*. 176. 374-86. 10.1007/s00221-006-0629-x.
- Smith, Gary A. "Knife-related injuries treated in United States emergency departments, 1990-2008." PubMed, 13 July 2013, <https://pubmed.ncbi.nlm.nih.gov/23849364/>. Accessed 25 May 2022.
- Subramaniam, S. R., et al. "Preliminary investigations of polylactic acid (PLA) properties: AIP Conference Proceedings: Vol 2059, No 1." *AIP Publishing*, 11 January 2019, <https://aip.scitation.org/doi/abs/10.1063/1.5085981>. Accessed 4 October 2022.
- Team Xometry. "ABS Injection Molding: Definition, Applications, Process, and Techniques." *Xometry*, 24 October 2022, <https://www.xometry.com/resources/injection-molding/abs-injection-molding/>. Accessed 3 March 2023.
- Team Xometry. "PLA vs. ABS: What is the difference?" *Xometry*, 3 October 2021, <https://www.xometry.com/resources/3d-printing/pla-vs-abs-difference/>. Accessed 3 March 2023.
- Travieso-Rodríguez, Antonio, et al. "Mechanical Properties of 3D-Printing Polylactic Acid Parts subjected to Bending Stress and Fatigue Testing." *NCBI*, 22 November 2019, <https://www.ncbi.nlm.nih.gov/pmc/articles/PMC6926899/>. Accessed 4 October 2022.

Vaughan, Jennifer. "Self-Retracting Blade Safety Knives." *YouTube*, 24 July 2013, <https://youtu.be/sqXpcXu1PIU>. Accessed 25 May 2022.

WU, SYLVIA. "Manufacturing at Different Magnitudes Part 2: From 100 - 1,000 Units." *Fictiv*, 19 October 2017, <https://www.fictiv.com/articles/manufacturing-at-different-magnitudes-part-2-best-practices-for-producing-100-10-000-units>. Accessed 3 March 2023.

Zheng, Mo. "Prevalence and heritability of handedness in a Hong Kong Chinese twin and singleton sample - BMC Psychology." *BMC Psychology*, 22 April 2020, <https://bmcp psychology.biomedcentral.com/articles/10.1186/s40359-020-00401-9>. Accessed 3 March 2023.

## Appendix



---

# Antibacterial Activity of Metallic Silver Nanoparticles against *Bacillus subtilis*

Cherry L.Y. Li

---

## 1. Background

The mounting of antibiotic resistance due to overconsumption of antibiotics has been a prevailing phenomenon in recent years. Silver (Ag), a xenobiotic metal (Hansson & Abedi-Valugerdi, 2003) possessing potent antibacterial properties has gained popularity as a possible alternative to treat bacterial infections. Specifically, Ag in the form of nanoparticles (“particulate dispersions within diameters of 1-100 nm”) (Horiba Scientific, 2020) has high prominence in the medical field. Currently, silver nanoparticles (AgNPs) are medically utilized in antimicrobial and anti-cancer therapy (Abass *et al.*, 2022), wound repair (Gunasekaran *et al.*, 2012) and bone healing (Zhang *et al.*, 2015). Particularly, AgNPs have been shown to enhance antibacterial activity of clinically approved drugs, including Cephadrine and Vildagliptin (Masri *et al.*, 2018). Aware of the current studies on utilizing AgNPs in antibiotics, I was interested to investigate the antibacterial effect of AgNPs themselves. This study focuses on the antibacterial activity (“killing or inhibiting bacterial growth”) (*NCI Dictionary of Cancer terms*) of AgNPs given their popularity among scientists (Ferdous and Nemmar, 2020) and high stability compared to organic nanoparticles (Paul and Sharma, 2014).

Ag is one of the least chemically reactive metals. It is unreactive with dry oxygen in the atmosphere, although reacts with sulfur (Ducksters, 2022). Historically used in wound dressing, Ag possesses strong antiseptic properties. Ag ionizes into silver ions (Ag<sup>+</sup>) in presence of moisture, namely in wound fluids and exudates (Lansdown, 2004). Ag<sup>+</sup> binds with proteins on cell surfaces, disrupting and causing cell death (Lansdown, 2004).

Published studies on the antibacterial effects of AgNPs against pathogenic bacteria are abundant. A study reported significant reduction in the growth in *Pseudomonas aeruginosa* using well diffusion

method (Kora and Arunachalam, 2010). Another study observed bactericidal effects using 10µg/mL AgNPs on *Escherichia coli* (Li *et al.* 2009). Although the increased use of AgNPs seems promising, its high toxicity against pathogenic bacteria also raises concern about their potential ability to inhibit the growth of non-pathogenic bacteria in a similar manner. I was thus inspired to investigate the potential antibacterial activities of AgNPs on non-pathogenic bacteria. Potential bactericidal effects of AgNPs on probiotics may challenge the suitability of their consumption, as most probiotics play important roles in maintaining a healthy human body (U.S. Department of Health and Human Services, 2019).

### 1.1 Differences between Gram-negative and Gram-positive Bacteria

To date, most recognized probiotics are gram-positive bacteria (GPB) (Behnsen *et al.*, 2013), whilst gram-negative bacteria (GNB) are the most common primary pathogens (Mayer & Donnelly, 2013). The differences in the membranes of GNB and GPB (Figure 1) may lead to AgNPs exhibiting different antibacterial properties.

GPB such as *Bacillus subtilis* lacks an outer membrane, distinguishable from GNB (Figure 1). However, the cell wall of GPB is composed of a significantly thicker peptidoglycan layer. Teichoic acids (TAs), are embedded in the inner membrane and attached to the peptidoglycan layers (Rajagopal & Walker, 2017), serving functions including 1) influence membrane permeability, 2) mediate extracellular interactions 3) provide additional stability to the plasma membrane (Swoboda *et al.*, 2010). GNB lacks TAs as their outer membrane is sufficient to perform essential functions for cell protection (Swoboda *et al.*, 2010).



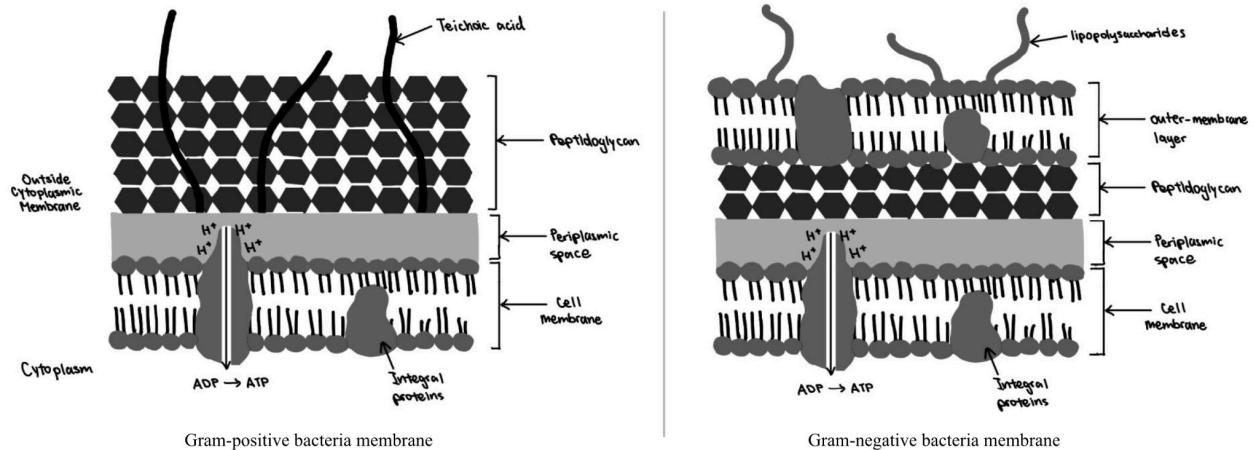


Figure 1. Cell wall of Gram-positive bacteria (GPB) and Gram-negative bacteria (GNB)

## 1.2 Probable Mechanisms for the Antibacterial Activity of AgNPs

### Adhesion towards Bacterial Membrane

AgNPs adhere to the bacterial membrane due to electrostatic attractions between positively charged  $\text{Ag}^+$  and the negatively charged membrane. As  $\text{Ag}^+$  have high affinity towards sulfur in membrane proteins,  $\text{Ag}^+$  can better adhere to the membrane, increasing membrane permeability, and damaging its integrity (Le Ouay & Stellacci, 2015).

### Penetration and Disruption of Biomolecules, DNA Replication and Expression of Proteins

Subsequently, the nanosize of AgNPs allows for easy penetration of the nanosize membrane.  $\text{Ag}^+$  binds and forms covalent bonds with bioactive molecules due to its high affinity, inactivating many biological pathways, and perturbing aspects of cell metabolism (Salleh *et al.*, 2020). Studies reported AgNPs inhibiting dehydrogenase in chemiosmosis, in *Staphylococcus aureus* (Salleh *et al.*, 2020), and AgNPs dissociating the double helix of DNA (Chatterjee *et al.*, 2016).

## Generation of Reactive Oxygen Species

Reactive oxygen species (ROS) are produced during mitochondrial oxidative metabolism (Ray *et al.*, 2012). Disruption of the electron transport chain due to AgNPs' high affinity may increase ROS production when the bacteria is exposed to AgNPs (Quinteros *et al.*, 2016). Overproduction of ROS causes cellular oxidative stress, possibly inducing membrane lipid damage, and subsequent leakages of cellular components, leading to cell apoptosis (Redza-Dutordoir and Averill-Bates, 2016).

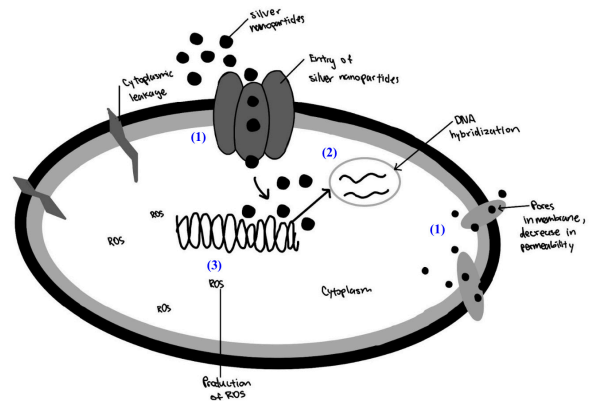


Figure 2. Schematic diagram of AgNPs inside bacterium membrane (Salleh *et al.*, 2020) - (1) Adhesion towards the surface membrane of bacteria. (2) Penetration and disruption of biomolecules, DNA replication and expression of proteins. (3) Generation of ROS. The mechanisms in Figure 2 were synthesized based on multiple studies conducted on GNB, although the mechanism should still be relevant for GPB as GPB still possesses a cell wall, cell membrane and naked DNA.

### 1.3 Justification for Choosing *B. subtilis* and its Growth Conditions

*B. subtilis*, the chosen bacterium for this investigation, is non-pathogenic and ubiquitous in the human gastrointestinal tract (GIT) (Hong *et al.*, 2009). Effective in strengthening gut barrier and preventing inflammatory responses, *B. subtilis* plays a key component of a healthy GIT. This study will focus on GPB given the extensive studies on AgNPs against GNB and the limited experimental time to conduct a comparison between GPB and GNB.

The pathogenic nature of most GNB possesses health risks. As such, the results of this study may reflect a possible limitation to the consumption of AgNPs, where its ability to treat bacterial infections may result in simultaneous bactericidal effects on probiotics naturally found in the human body. Subsequently, the results may indicate the maximal concentration of AgNPs that should be consumed to reduce possible toxicity. As all GPB possess a similar membrane (Salton and Kim, 2009), *B. subtilis* will give insights into how other GPB may be affected similarly.

The growth conditions of *B. subtilis* are warranted to maximize chances of successful cultivation and collect data that is statistically significant. *B. subtilis* is safe to use, has low risks of contamination, and grows optimally at 25-35 °C (*Bacillus subtilis*, 2015). To follow IB guidelines, all plates were incubated between 20-25 °C. *B. subtilis* is easy to cultivate as no special living conditions are required due to its highly adaptable metabolism (Su *et al.*, 2020), making it a suitable bacteria for this investigation.

### 1.4 Justification for Chosen Concentration Range

To have a comprehensive investigation of the antibacterial activity of AgNPs against *B. subtilis*, I wanted to test its effect on a range of concentrations. A study reported the minimum inhibitory concentration of AgNPs against *B. subtilis* at 40 µg.mL<sup>-1</sup>, and the maximum bactericidal concentration at 60 µg.mL<sup>-1</sup> using paper disc diffusion (Ruparelia *et al.*, 2008). However, pretests using paper disc diffusion did not show noticeable antibacterial activity at 40-60 µg.mL<sup>-1</sup> (Appendices - 11.2. Pretest using paper disc diffusion for concentrations 30, 40, 60, 70, and 80 µg.mL<sup>-1</sup>), possibly due to the small diameter (2-8 nm) of AgNPs in the study, relative to the AgNPs used in this investigation (~100 nm) (Appendices - 11.1. SEM of AgNPs). Additionally, a 0.2 µm membrane filter

was used in the study to further reduce aggregation after sonication, although 0.2µm membrane filters were not available in this investigation. Further pretests done by directly coating plates with AgNPs, *B. subtilis* and Luria-Bertani (LB) solutions without paper discs were tested with amplified concentrations. The concentrations: 0, 2000, 6000, 10000, 14000 µg.mL<sup>-1</sup> showed notable effects, hence, this method was chosen as a reliable way to obtain results through colony counting.

### 1.5 Justification for Counting Colonies

The antibacterial activity of AgNPs will be measured via colony counting. Measuring zones of inhibition was conducted in pre-tests with reference to previous studies. However, diffusion of AgNPs proved to be difficult due to aggregation, and the negligible formation of zones deemed this method unfeasible to show any statistical significance (Appendices - 11.2. Pretest using paper disc diffusion for concentrations 30, 40, 60, 70, and 80 µg.mL<sup>-1</sup>). An alternative method of counting colonies was tested and shown to be viable. First tested by manual counting, a trend was qualitatively visible, although biases involved meant significant random errors. Automated colony counting using digital application was chosen to minimize uncertainty and maximize the chances of answering the research question objectively.

To reduce chances of lawn formation, the bacterial solution will be diluted by a ratio of 1:100K via serial dilution. This ratio was determined through pretests using a range of dilution ratios and six incubation times of 24 and 48 hours. AgNPs will be mixed with the *B. subtilis* and LB broth solution (1:100K) before plating to mimic the nature of “ingesting” AgNPs and the GIT environment.

## 2. Hypotheses

### 2.1 Null Hypothesis (H<sub>0</sub>):

As the concentration of AgNPs increases, there will be no significant difference in the number of *B. subtilis* colonies formed.

### 2.2 Alternative Hypothesis (H<sub>1</sub>):

As the concentration of AgNPs increases, the number of *B. subtilis* colonies formed will decrease.

### 3. Variables

#### 3.1 Independent Variable

Concentration of AgNPs added to *B. subtilis* and LB broth.

- Range: 0, 2000, 6000, 10000, 14000  $\mu\text{g.mL}^{-1}$ . This will be achieved by preparing solutions of AgNPs with DI water, given that Ag is unreactive with water. (Table 1)

Mass of AgNPs (mg)	Volume of DI water ( $\text{cm}^3$ )	Concentration ( $\mu\text{g.mL}^{-1}$ )
0	5	0
10	5	2000
30	5	6000
50	5	10000
70	5	14000

**Table 1.** Concentration table of AgNPs and DI water

- 0  $\mu\text{g.mL}^{-1}$  will act as a negative control. Positive control using 70% ethanol and 0  $\mu\text{g.mL}^{-1}$  AgNP will be performed. 70% ethanol was chosen as most disinfectant products contain 70% ethanol due to its bactericidal activity (Sauerbrei, 2020). Thus, the effectiveness of AgNPs compared to existing antibacterial agents may reflect its relative toxicity and suitability for medical use.
- 5  $\text{cm}^3$  DI water was used to create the AgNPs concentrations. 5  $\text{cm}^3$  was calculated to keep the total volume of AgNPs and DI water solution constant for all concentrations.

#### 3.2 Dependent Variable:

Number of *B. subtilis* colonies formed on LB agar plates. The number of colonies (CFU) will be counted using ImageJ.

#### 3.3 Controlled Variables

Factor	Reason	Method of control
Growth condition		
Incubation temperature	Temperature affects bacterial growth. High temperatures increase enzyme activity, promoting bacterial growth, whilst lower temperatures decrease enzyme activity, decreasing bacterial growth (Wei, 2021).	Plates were incubated between 20-25 °C, following IB guidelines.  <i>See “Justification for methodology” for further details.</i>
Incubation time	Bacteria undergo the lag phase, log phase, stationary phase, and death phase when sufficient time is provided during incubation. Bacteria grow exponentially during lag phase, whilst depletion of nutrients minimizes reproduction during stationary phase. If incubation time isn't controlled, samples may be in different phases, reducing precision and reliability.	The incubation time will be kept constant at 48 hours.  <i>See “Justification for methodology” for further details.</i>

Factor	Reason	Method of control
Preparation of AgNPs, <i>B. subtilis</i> and LB solution		
Source of AgNPs	Different sources of AgNPs may have different diameters and percentage purities of Ag, affecting its toxicity. Nanoparticles with smaller diameters can penetrate cell membranes easier, increasing antibacterial activities (Dunning, 2020).	AgNPs were obtained from XFNANO, a company specialized in manufacturing nanoparticles. AgNPs were observed under SEM to ensure diameters of AgNPs are $\leq 100$ nm ( <i>Appendices - SEM of AgNPs</i> ).
Mixing technique of AgNPs	AgNPs aggregate in aqueous solutions. The degree of aggregation affects the surface area to volume ratio of AgNPs. Greater surface area to volume ratio allows for greater penetration and more potent antibacterial activity (Ferdous and Nemmar, 2020).	To reduce aggregation of AgNPs, AgNPs across all trials were sonicated twice, and manually mixed with a glass rod for 30 seconds to ensure heavy sediment was not sinking to the bottom.
Concentration of <i>B. subtilis</i>	Colony counting cannot quantify bacterial lawns. The maximum number of colonies reported to be accurately counted is $\leq 250$ , as any colonies above 250 may overlap, and be discounted, reducing precision (Microbiology writing guide: Presenting data. Writing Intensive Curriculum Program, 2017).	A serial dilution will be performed to control the concentration of <i>B. subtilis</i> .
Nutrient of agar	Different nutrient agars suit the growth of different organisms. For instance, blood agar is used to grow fastidious organisms (Blood agar plates and hemolysis, 2016). <i>B. subtilis</i> is non-fastidious, and grows on minimal media (Widner <i>et al.</i> , 2005). If the amount of nutrients in agars varies, bacterial growth will vary.	LB agar was chosen based on elimination. Plates specific for growing GNB, such as MacConkey agar, were eliminated. Similarly, plates targeting specific bacterium, such as Chapman agar for <i>Staphylococcus</i> were also eliminated. Furthermore, a study has reported notable growth of smooth, sticky and medium-sized <i>B. subtilis</i> colonies on TSA agar medium, whilst LB agar showed almost circular, flat and dry colonies (Lu <i>et al.</i> , 2018). Given that TSA agar medium was not available, LB agar was chosen.
Colonies counting		
Software for colony counting	Settings including circularity and size may affect colony counting on ImageJ.	See “Method used to count the number of <i>B. subtilis</i> colonies formed (CFU)” for details.

**Table 2.** Controlled variables

## 4. Methodology

### 4.1 Equipment and Materials List

<p>Handling of bacteria:</p> <ul style="list-style-type: none"> <li>• 3 ml <i>B. subtilis</i> stock solution</li> <li>• x1 vortex mixer</li> <li>• p1000, p200, p10 micropipette tips</li> <li>• x1 10-100 <math>\mu</math>l micropipette (<math>\pm 1\mu</math>l)</li> <li>• x1 100-1000 <math>\mu</math>l micropipette (<math>\pm 5\mu</math>l)</li> <li>• x1 2-20 <math>\mu</math>l micropipette (<math>\pm 0.1\mu</math>l)</li> <li>• x30 microcentrifuge tubes</li> <li>• x35 LB agar plates</li> <li>• x1 parafilm roll</li> <li>• 25 cm<sup>3</sup> DI water</li> <li>• 30 ml LB broth</li> <li>• x1 Ethanol bunsen burner</li> <li>• 1 ml 70% ethanol</li> <li>• x1 Heatproof mat</li> <li>• x1 Glass spreader</li> <li>• x1 Lighter</li> <li>• x1 permanent marker</li> </ul>	<p>Handling of AgNPs:</p> <ul style="list-style-type: none"> <li>• 1 g AgNPs</li> <li>• x1 Electronic weighing scale with windshield (<math>\pm 0.001</math>g)</li> <li>• x1 Weighing boat</li> <li>• x1 10 cm<sup>3</sup> volumetric pipette (<math>\pm 0.05</math> cm<sup>3</sup>)</li> <li>• x1 Forcep</li> <li>• x5 Test tubes</li> <li>• x1 Glass rod</li> <li>• x1 Sonicator bath</li> <li>• x1 Test tube rack</li> </ul> <p>Safety purposes:</p> <ul style="list-style-type: none"> <li>• Safety goggles</li> <li>• Disposable nitrile gloves</li> <li>• Disposable bin</li> <li>• Lab coat</li> </ul>
--	---

**Table 3.** Equipment and material list

### 4.2 Safety Considerations

\*There were no environmental or ethical considerations in this investigation.

1. Incubating at human-body temperature (above 30 °C) may risk culturing pathogenic bacteria. To reduce risks of contamination and growth of pathogenic microorganisms, plates will be incubated at room temperature.
2. Strains of *B. subtilis* may be left in laboratory areas and transferred to people, potentially causing infections. Gloves, laboratory coats and safety goggles were worn throughout the experiment. All equipment contracted with *B. subtilis* will be disposed of in disposal bins labeled with hazard-warning signs. Laboratory areas must be disinfected with alcohol before and after use.

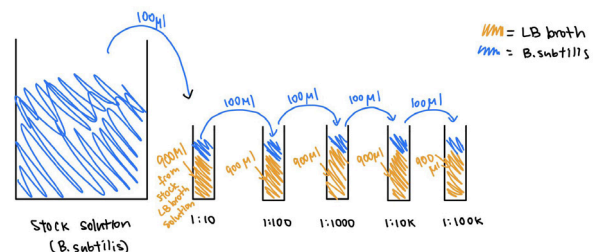
### 4.3 Procedure

#### Part I: Preparation of AgNPs solution

1. An electronic weighing scale with windshield was used to weigh 10 mg of AgNPs onto a weighing boat. The windshield was covered with a lid to reduce external influences.
2. 10 mg of AgNPs was transferred into a test tube.

3. 5 cm<sup>3</sup> DI water was pipetted into the test tube using a 10 cm<sup>3</sup> volumetric pipette.
4. The AgNPs and DI water solution in the test tube was sonicated using ultrasonic bath at 50 W for 2 minutes.
5. Steps 1-4 were repeated for the other concentrations with reference to Table 1 for the mass of AgNPs used.

#### Part II: Preparation of *B. subtilis* and LB broth solution via serial dilution (Figure 3)



**Figure 3.** Serial dilution: An aliquot of 100  $\mu$ l of *B. subtilis* was taken from the stock solution and mixed with 900  $\mu$ l of LB broth.

1. A bunsen burner was lit to reduce contamination of other microorganisms present in the air.
2. 100  $\mu$ l of *B. subtilis* was pipetted into a microcentrifuge tube using a 10-100  $\mu$ l micropipette.

3. 900  $\mu\text{l}$  of LB broth was pipetted into the same microcentrifuge tube from step 2 using a 100-1000  $\mu\text{l}$  micropipette. The *B. subtilis* and LB broth solution was pipetted up and down to mix the solution.
4. Steps 2-3 were repeated 4 times to obtain a stock solution of *B. subtilis*: LB broth, at a concentration of 1:100K.
5. As 5000  $\mu\text{l}$  stock solution was need, steps 2-4 were repeated 4 times
6. 7 new microcentrifuge tubes were labeled according to the concentration range and the positive and negative controls.
7. 500  $\mu\text{l}$  of *B. subtilis*: LB Broth (1:100K) solution was pipetted into each microcentrifuge tube using a 100-1000  $\mu\text{l}$  micropipette.

Part III: Creating stock solutions of AgNPs and *B. subtilis* in LB broth for 5 replicates of each concentration

1. AgNPs and DI water solutions from part I were manually mixed for 30 seconds using a glass rod
2. 50  $\mu\text{l}$  of the solution containing 10 mg of AgNPs from part I was pipetted into the microcentrifuge tube labeled with 2000  $\mu\text{g}\cdot\text{mL}^{-1}$  from part II, using a 10-100  $\mu\text{l}$  micropipette.
3. 500  $\mu\text{l}$  of *B. subtilis* and LB broth solution from part II was pipetted into the same microcentrifuge in step 2, using a 100-1000  $\mu\text{l}$  micropipette. This creates a ratio of 10:100  $\mu\text{l}$  (AgNPs : *B. subtilis* + LB broth), enough for 5 replicates at 2000  $\mu\text{g}\cdot\text{mL}^{-1}$ .
4. Steps 2-3 were repeated 3 more times for the other concentrations. The microcentrifuge tube labeled with 0mg does not contain any AgNPs.
5. 50  $\mu\text{l}$  of 70 % ethanol was pipetted into the microcentrifuge tube labeled with positive control using a 10-100  $\mu\text{l}$  micropipette.
6. 50 $\mu\text{l}$  of DI water was pipetted into the microcentrifuge tube labeled with negative control using a 10-100  $\mu\text{l}$  micropipette.

Part IV: Plating and incubation

1. A bunsen burner was lit close to the working environment for sterility purposes.
2. 35 agar plates were labeled: each concentration was labeled on 5 plates ; positive control was labeled on another 5 plates ; remaining 5 plates labeled for the negative control.

3. A vortex mixer was used to disperse the AgNPs inside the microcentrifuge tube labeled with 2000  $\mu\text{g}\cdot\text{mL}^{-1}$  from part III.
4. 100  $\mu\text{l}$  of solution from the microcentrifuge tube in step 3 was pipetted in the agar plate labeled 2000  $\mu\text{g}\cdot\text{mL}^{-1}$  using a 2-20  $\mu\text{l}$  micropipette.
5. Steps 2-4 were repeated 4 more times to obtain 5 trials.
6. Steps 2-5 were repeated 6 more times for each concentration and controls respectively.
7. Parafilm was used to partially seal the agar plates.
8. Plates were incubated for 48 hours at room temperature (20-25  $^{\circ}\text{C}$ ) to reduce risks of contamination.

#### 4.4 Justification for Methodology

Equipment:

1. A volumetric pipette was the most precise equipment available for a measurement of 5  $\text{cm}^3$ . Although using the upper limits of micropipettes may not be the most precise, the biggest micropipette available was 100-1000  $\mu\text{l}$ .
2. AgNPs and DI water solutions were sonicated and mixed using a vortex mixer to reduce aggregation of NPs.
3. AgNPs and DI water solutions were mixed with a glass rod before pipetting to avoid AgNPs from settling to the bottom of the test tube.

Procedures:

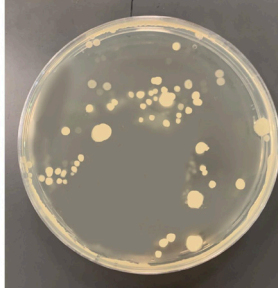
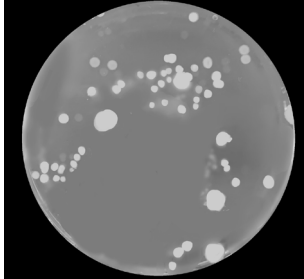
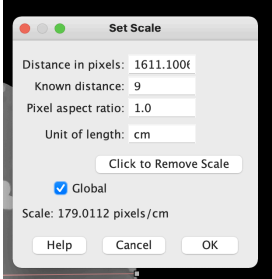

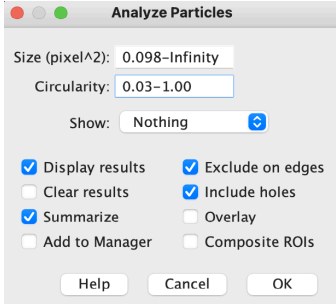
1. Two minutes of sonication was observed to have dispersed the AgNPs throughout the DI water solution in pretesting, hence was chosen.
2. A serial dilution was performed as pre-tests have shown that the concentration of the stock *B. subtilis* solution was too high to observe any antibacterial activity. The ratio, 1:100K (*B. subtilis*: LB broth) allowed formation of individual colonies.
3. Plates were partially sealed to allow an aerobic growth environment and avoid growth of pathogenic anaerobic bacteria. Additionally, Hsueh *et al* reported AgNPs leaching Ag<sup>+</sup> ions under aerobic conditions but not under anaerobic conditions (Hsueh *et al.*, 2015).
4. Plates were incubated for 48 hours as Arduino *et al* concluded that the optimum incubation time for the highest yield of bacteria was achieved between 32 to 48 hours (Arduino *et al.*, 1991). Due to time constraints, the incubation options were 24, 48 or 72 hours, in which 48 hours provided the clearest results in pretesting.

## 5. Data and Analysis:

### 5.1 Method Used to Count the Number of *B. subtilis* Colonies Formed (CFU)

Colonies were digitally counted using ImageJ. Manual colony counting is difficult given variations in the size of colonies and overwhelming number of colonies at lower concentrations. Automated cell counting significantly reduces random errors and subjectivity:

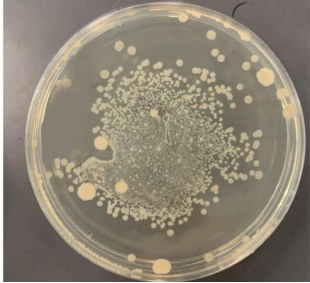
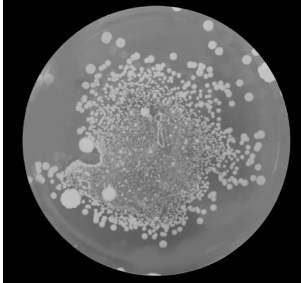
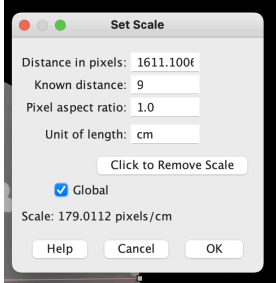
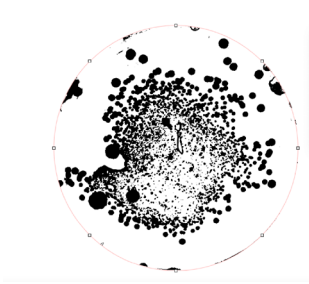
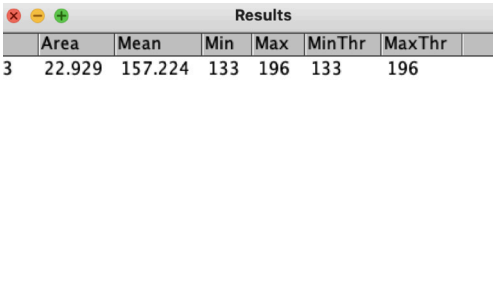
1. Size threshold of colonies set at 0.098 cm-infinity in diameter across all trials. The range was initially set from 0-infinity, although this led to unreasonably high CFU counts and lack of precision in pretests. 0.098 cm was chosen as the smallest colony formed at the highest concentration of AgNPs was 0.098 cm in diameter. (measured on ImageJ).
2. Overlapping and irregularly shaped colonies were discarded by setting the circularity to 0.03 across all trials, determined after testing a range of values. 0.03 showed the clearest trend.

 <p><b>Figure 4.</b> Sample agar plate</p>	 <p><b>Figure 5.</b> 8-bit scale</p>	 <p><b>Figure 6.</b> Scale setting</p>
<p>A photo of the agar plate was taken under a black background to reduce effects of lighting and shadows.</p>	<p>The photo was cropped, showing only the surface of the plate. It was converted to 8-bit grayscale.</p>	<p>The image was scaled by adjusting the number of pixels of the diameter of the plate to 9 cm (radius of plate = 4.5 cm).</p>
 <p><b>Figure 7.</b> Thresholded plate</p>	 <p><b>Figure 8.</b> Settings for the analysis of particles</p>	
<p>The image was thresholded and converted to binary image for analysis.</p>	<p>Finally, the image was analyzed for CFU counting. Figure 8 shows the settings used. The final CFU count is 41.</p>	

**Table 4.** Example of CFU counting at concentration 10000  $\mu\text{g}\cdot\text{mL}^{-1}$ , trial 5

## 5.2 Method Used to Calculate the Surface Area Covered by *B. subtilis* Colonies on Agar Plates

The surface area covered by *B. subtilis* on agar plates was calculated in addition to CFU count, as some trials, particularly 6000  $\mu\text{g}\cdot\text{mL}^{-1}$  trial 3 (Figure 9) showed overlapping of colonies and formation of loans. This set of data can verify and increase the reliability of correlations drawn from colony counting.

 <p><b>Figure 9.</b> Sample agar plate</p>	 <p><b>Figure 10.</b> 8-bit scale</p>	 <p><b>Figure 11.</b> Scale setting</p>
<p>Photos of agar plates taken previously for CFU counting were used.</p>	<p>The photo was cropped and converted to 8-bit grayscale.</p>	<p>The image was scaled by adjusting the number of pixels of the diameter of the plate to 9 cm.</p>
 <p><b>Figure 12.</b> Thresholded plate</p>	 <p><b>Figure 13.</b> Surface area calculation results table</p>	
<p>The image was thresholded and converted to binary image for analysis.</p>	<p>The image was analyzed and showed a total area of 22.929 <math>\approx</math> 23.00 cm.</p>	

**Table 5.** Example of calculating surface area using ImageJ for 6000  $\mu\text{g}\cdot\text{mL}^{-1}$  trial 3:

## 5.3 Raw Data and Sample Calculations

Concentration of AgNPs ( $\mu\text{g}\cdot\text{mL}^{-1}$ )	Number of colonies (CFU)				
	Trial 1	Trial 2	Trial 3	Trial 4	Trial 5*
0 (negative control)	248	211	214	221	267
2000	113	206	210	248	489
6000	79	64	105	61	77
10000	30	41	66	37	41
14000	24	13	15	12	12
positive control (70% ethanol, no AgNPs)	22	8	14	8	12

**Table 6.** Raw Data \*trial 5 for 2000  $\mu\text{g}\cdot\text{mL}^{-1}$  (489.00 CFU) was omitted as it is an anomaly. 5 replicates were conducted to increase precision and reliability



Example calculation of average number of colonies formed (CFU) at 6000  $\mu\text{g.mL}^{-1}$ :

$\frac{(79 + 64 + 105 + 61 + 77)}{5} = 77.2 \approx 77$  CFU (rounded to the nearest unit as colonies were counted as 1 unit). All values in table 5 were rounded to the nearest unit for the same reason.

Example calculation of standard deviation at 6000  $\mu\text{g.mL}^{-1}$ :

$$\sqrt{\frac{\sum(x_i - \mu)^2}{N}}, \text{ where}$$

$\mu$  = average number of colonies formed      SS = sum of squares  
 $N$  = number of trials       $x_i$  = sum of squares

Example calculation for the standard deviation at 6000  $\mu\text{g.mL}^{-1}$  trial:

Standard deviation	17.412639 $\approx$ 17.41 (2 d.p)	The standard deviation for concentration 2000 $\mu\text{g.mL}^{-1}$ was not calculated as the sample size was too small after trial 5.
$\mu$ (average)	77.20	
$x_i$	112.03	
SS	1212.80	
Variance	303.02	

## 5.4 Processed Data

Concentration of AgNPs ( $\mu\text{g.mL}^{-1}$ )	Average number of colonies	Standard deviation (STD)
0 (negative control)	232	24.32
2000	194	N/A
6000	77	17.41
10000	43	13.62
14000	15	5.07
positive control (70% ethanol)	13	5.76

**Table 7.** Standard Deviation for number of bacterial colonies appearing for each concentration of silver nanoparticles.

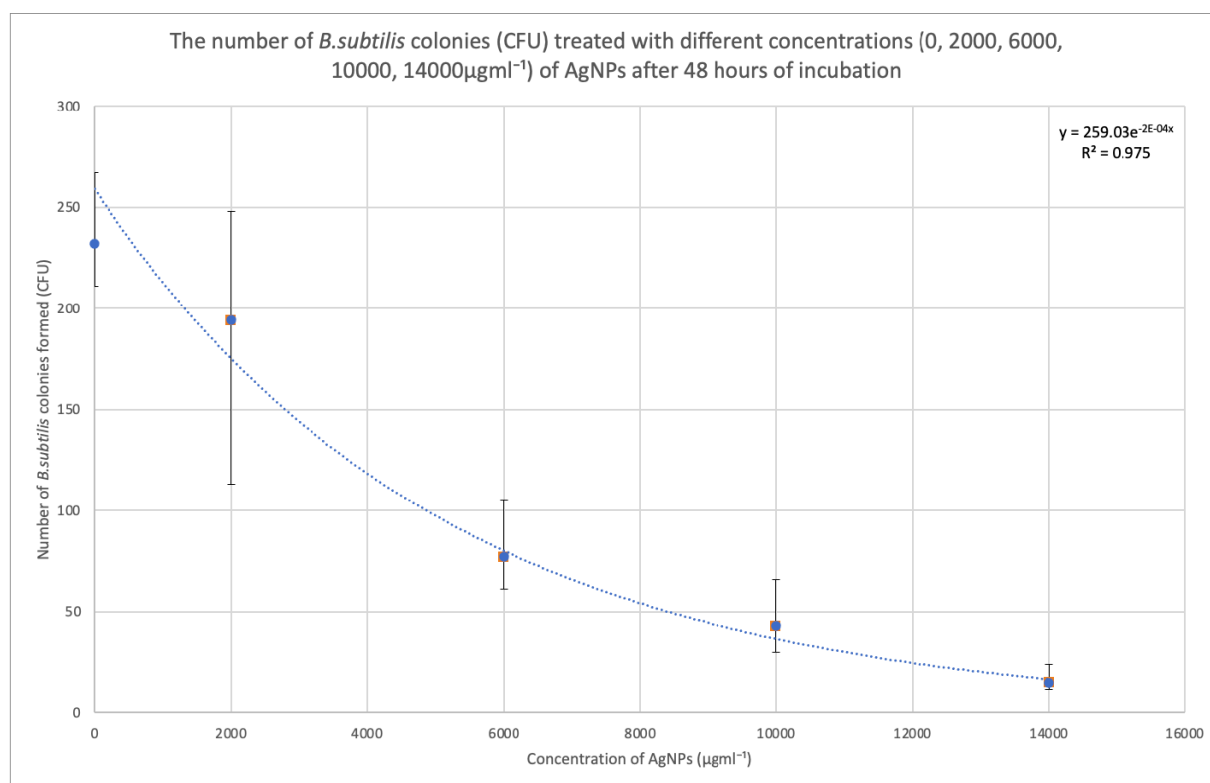
## 5.5 Statistical Tests - One-way ANOVA:

A one-way ANOVA test was conducted based on Table 7 to test for statistical differences across 5 concentrations of AgNPs and the positive and negative controls.

ANOVA						
Source of Variation	SS	df	MS	F	P-value	F crit
Between Groups	214050.878	5	42810.1755	68.2165337	5.0291E-13	2.63999943
Within Groups	14433.95	23	627.563043			
Total	228484.828	28				

**Table 8.** ANOVA test results

$H_0$  is rejected as  $p < 0.05$ .  $H_1$  is accepted. Increasing concentrations of AgNPs and the number of *B. subtilis* colonies formed shows statistical significance.



**Figure 14.** The number of *B. subtilis* colonies (CFU) treated with different concentrations (0, 2000, 6000, 10000, 14000 µg.mL<sup>-1</sup>) of AgNPs after 48 hours of incubation. (\*Asymmetric error bars were used instead of standard deviation to generate error bars due to the small sample size. The upper error bar is the largest data point and the lower error bar is the smallest data point for each concentration)

## 5.6 Statistical Tests - T-test

As overlaps in error bars in Figure 14 forms a discrepancy against the strength of the ANOVA test results and high R-squared value, t-tests between each increment of concentration were performed to further test for statistical significance.

Concentration intervals of AgNPs ( $\mu\text{g.mL}^{-1}$ )	P-value	Statistically significant?
2000-6000	0.01459253	Yes
6000-10000	0.00428822	Yes
10000-14000	0.00394139	Yes
14000 and positive control (70% ethanol)	0.25210462	No
2000 and negative control (0 mg)	0.37951455	No

**Table 9.** T-test results

Shown in Table 9,  $p < 0.05$  for concentration intervals: 2000-6000  $\mu\text{g.mL}^{-1}$ , 6000-10000  $\mu\text{g.mL}^{-1}$  and 10000-14000  $\mu\text{g.mL}^{-1}$ , whilst  $p > 0.05$  between 14000  $\mu\text{g.mL}^{-1}$  and the positive control, and 2000  $\mu\text{g.mL}^{-1}$  and the negative control.

## 5. Discussion

As the concentration of AgNPs increases, the average number of *B. subtilis* colonies formed decreases. This negative correlation is strongest between 2000  $\mu\text{g.mL}^{-1}$  and 6000  $\mu\text{g.mL}^{-1}$ , graphically shown by the steepest slope. However, the rate of decline in CFU count gradually decreases at 6000  $\mu\text{g.mL}^{-1}$  onwards, evident between 10000  $\mu\text{g.mL}^{-1}$  and 14000  $\mu\text{g.mL}^{-1}$ . As  $R^2 = 0.975$  ( $\approx 1$ ), the negative correlation is strong.

Overlapping in error bars is evident across 6000  $\mu\text{g.mL}^{-1}$ , 10000  $\mu\text{g.mL}^{-1}$  and 14000  $\mu\text{g.mL}^{-1}$ , forming a discrepancy against the high  $R^2$  value (0.975). However, the ANOVA and t-test results reinforce a statistical difference. Thus, while random errors are present, they may not have significantly impacted the data. Specifically,  $p < 0.05$  for 6000-14000  $\mu\text{g.mL}^{-1}$ , suggesting a stronger inhibitory effect at 14000  $\mu\text{g.mL}^{-1}$  compared to 6000  $\mu\text{g.mL}^{-1}$ . This aligns with the steep slope in Figure 14 between the two concentrations. However,  $p > 0.05$  between 2000  $\mu\text{g.mL}^{-1}$  and the negative control, indicating that they are statistically similar. At 2000  $\mu\text{g.mL}^{-1}$ , the proportion of smaller nanoparticles (<100 nm) (Appendices - SEM of AgNPs) was likely fewer at higher concentrations, thus less AgNPs could penetrate the membrane within 48 hours. This aligns with the significant error bar at 2000  $\mu\text{g.mL}^{-1}$  compared to the relatively trivial error bar at 14000  $\mu\text{g.mL}^{-1}$ . Thus, the lack of antibacterial activity may have resulted in similar CFU counts as when no AgNPs were added. Contrarily, the statistical similarity between 14000  $\mu\text{g.mL}^{-1}$  and the positive control ( $p > 0.05$ ) reflects comparable antibacterial activities of 14000  $\mu\text{g.mL}^{-1}$  against 70% ethanol. Given the various diameters of AgNPs, this investigation showed that minimum concentration of 6000  $\mu\text{g.mL}^{-1}$  may be required for AgNPs to exhibit antibacterial activity on *B. subtilis*, whereas 14000  $\mu\text{g.mL}^{-1}$  or above may be lethal. This indicates that consumption of medicine with 6000  $\mu\text{g.mL}^{-1}$  or above of AgNPs to treat infections may simultaneously kill probiotics ubiquitous in the human body.

Qualitative observations showed difficulty in distinguishing overlapping colonies nor were colony sizes taken into consideration (Appendices - Qualitative data). To further verify the correlation drawn, the surface area covered by *B. subtilis* colonies on agar plates was calculated (Table 10).

Concentration of AgNPs ( $\mu\text{g.mL}^{-1}$ )	Surface area cover by <i>B. subtilis</i> colonies ( $\text{cm}^2$ )					Average	Standard deviation
	Trial 1	Trial 2	Trial 3	Trial 4	Trial 5		
0 (negative control)	16.43	15.34	23.37	16.54	29.64	20.26	6.13
2000	37.00	19.25	31.46	11.32	7.37	21.28	12.72
6000	25.10	16.13	23.00	22.82	17.85	21.00	3.88
10000	5.57	8.03	4.12	5.53	4.56	5.56	1.51
14000	0.14	0.10	0.10	0.07	0.11	0.10	0.02
positive control (70% ethanol, no AgNPs)	0.71	0.11	1.03	4.90	1.51	1.65	0.02

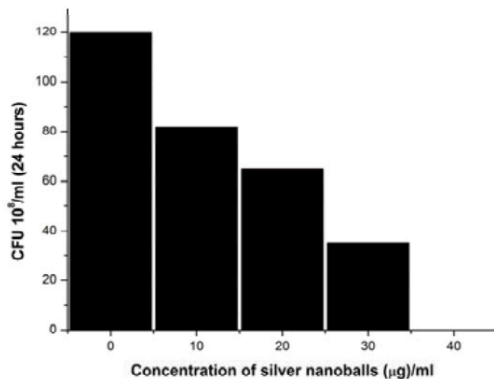
**Table 10.** Supporting data - Surface area cover by *B. subtilis* colonies ( $\text{cm}^2$ )

When no AgNPs were added, the average surface area was 20.26 cm<sup>2</sup>. It then reduced to 0.10 cm<sup>2</sup> at 14000 µg.mL<sup>-1</sup>. Based on the averages, the same correlation, where an increase in the concentration of AgNPs leads to a decrease in the growth of *B. subtilis* can be concluded.

It is notable that the standard deviation for concentrations 2000 µg.mL<sup>-1</sup> is significant. This is consistent with the significant error bar for 2000 µg.mL<sup>-1</sup> in Figure 14. Similarly, the standard deviation for the negative control is relatively large, further reinforcing the possibility that *B. subtilis* grew similarly with or without the presence of 2000 µg.mL<sup>-1</sup> AgNPs.

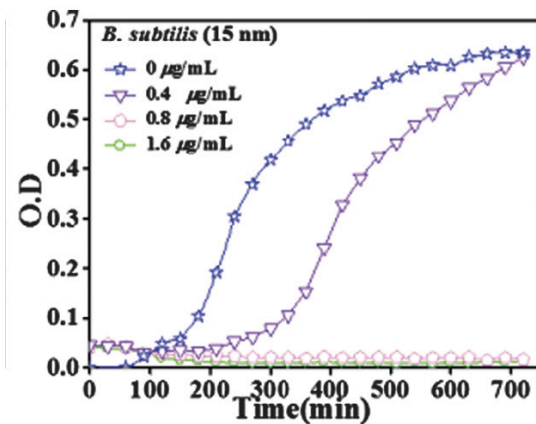
Nonetheless, despite the significant error bars in Figure 14, given that the surface area covered by *B. subtilis* colonies represents a similar correlation, random errors did not affect the overall trend. Thus, my dataset is informative and supports my hypothesis.

Published studies have reported similar conclusions: Hsueh *et al.* tested the antibacterial effect of AgNPs on *B. subtilis* via colony count, under 24 hours of incubation. Inhibition was notable at concentrations below 5ppm, and 10ppm or greater showed lethal effects (Hsueh *et al.*, 2015). Despite the significantly lower concentrations used, the correlation: increased concentrations of AgNPs results in greater antibacterial activities, can still be concluded. Another study investigated antibacterial activities of *B. subtilis* when treated with 0, 10, 20, 30 and 40 µg.mL<sup>-1</sup> of AgNPs, measured by colony counting (Tripathi *et al.*, 2010). Shown in Figure 15 an increase in concentration resulted in fewer colonies formed, and complete inhibition at 40 µg.mL<sup>-1</sup> (Tripathi *et al.*, 2010).



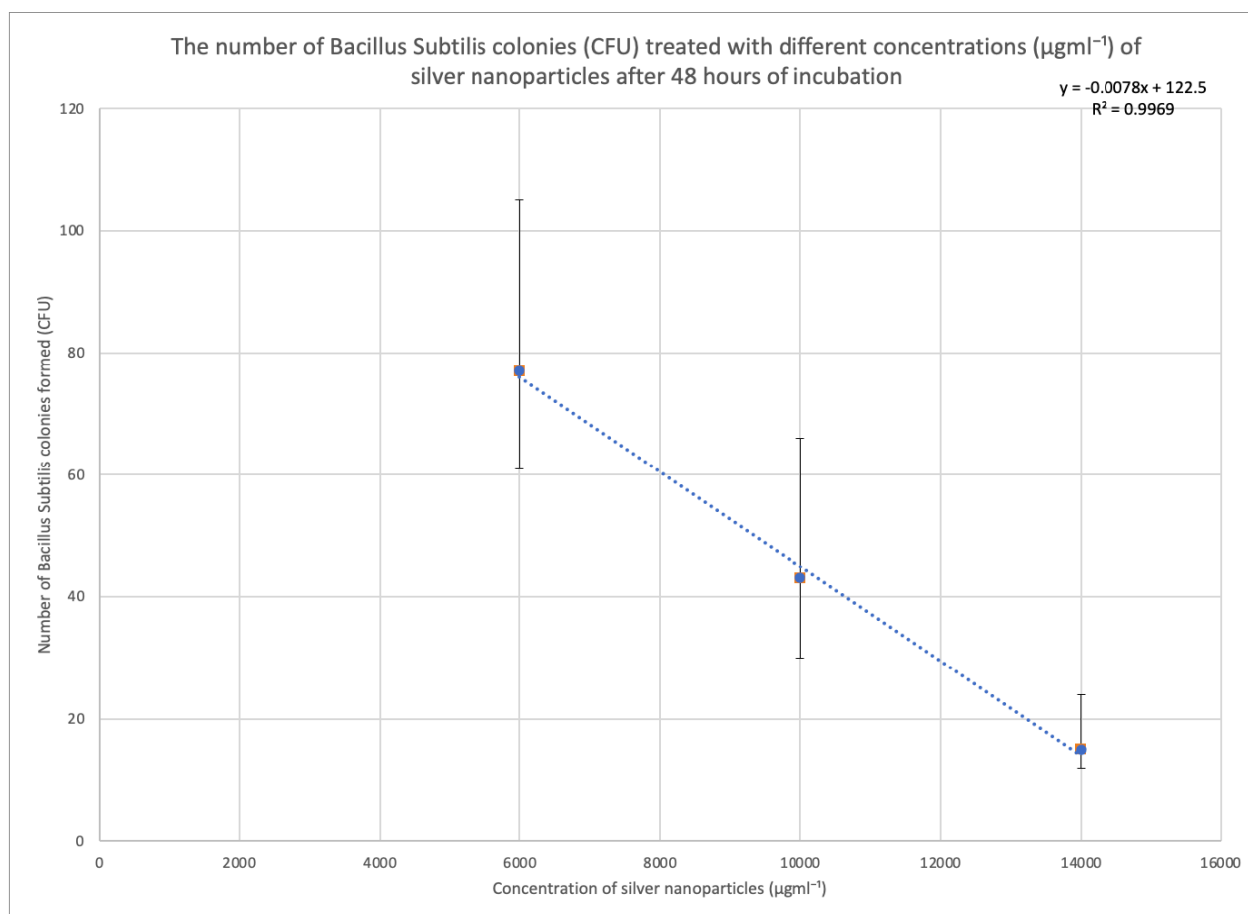
**Figure 15.** Antibacterial characterization by CFU as a function of silver nanoballs concentration on Bacillus subtilis MTCC 1133 after 24 hours incubation time on Macconky agar media (Tripathi *et al.*, 2010)

Specifically, Figure 15 shows an almost linear decrease in CFU count as concentrations increased, after 24 hours of incubation (Tripathi *et al.*, 2010). This forms a discrepancy against the negative exponential trend drawn in this investigation (Figure 14). Despite another study reporting AgNPs' ability to delay the exponential growth phase of *B. subtilis* (Figure 16) (Le Ouay & Stellacci, 2015), *B. subtilis* likely reached its stationary phase after 48 hours of incubation (incubation time in this investigation), given that Tripathi *et al.* showed *B. subtilis* reaching stationary phase after just 15 hours with 30-40 µg.mL<sup>-1</sup> of AgNPs, and 20 hours with 20 µg.mL<sup>-1</sup> of AgNPs (Tripathi *et al.*, 2010).



**Figure 16.** Antibacterial characterization by CFU as a function of silver nanoballs concentration on Bacillus subtilis MTCC 1133 after 24 hours incubation time on Macconky agar media (Le Ouay & Stellacci, 2015)

In this investigation, the datapoint representing 2000 µg.mL<sup>-1</sup> had the largest error bar despite eliminating an anomaly from Table 6, hence may not be reliable due to random errors. If this datapoint was factored out, the trendline models a linear relationship with R<sup>2</sup> = 0.9969 (Figure 17). This aligns with the negative correlation reported by Tripathi *et al.* (Figure 15), suggesting that potential antibacterial effects of AgNPs against *B. subtilis* may differ depending on the bacterium's growth phase, where further investigation is warranted.



**Figure 17.** The number of *B. subtilis* colonies (CFU) treated with different concentrations (6000, 10000, 14000  $\mu\text{g.mL}^{-1}$ ) of AgNPs after 48 hours of incubation.

## 6. Conclusion

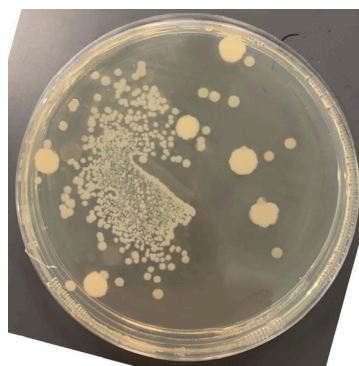
As the concentration (0, 2000, 6000, 10000, 14000  $\mu\text{g.mL}^{-1}$ ) of AgNPs increases, the number of *B. subtilis* colonies formed will decrease due to increased antibacterial activities. The statistical tests, high  $R^2$ -value, and supporting data on surface area (Table 10) reinforce the strength of this correlation. Thus,  $H_0$  is rejected and  $H_1$  is supported, suggesting that consumption of AgNPs, particularly at high concentrations (6000  $\mu\text{g.mL}^{-1}$  or above) may kill probiotics ubiquitous in the human body, answering my research question.

## 7. Evaluation

### 7.1 Methodology and Sources of Error

The transfer of AgNPs to *B. subtilis* and LB broth solutions was not exact as some remained on the weighing boat after weighing. This systematic error was more significant at lower concentrations, leading to a percentage error and greater error bar in Figure 14. To improve, AgNPs should be weighed directly into microcentrifuge tubes to minimize the transfer of them across different equipment.

Despite sonication, AgNPs likely aggregated in the *B. subtilis* and LB broth solution. The actual mass of AgNPs that was pipetted into agar plates may have differed across trials, leading to a lack of precision. This may have been more significant at lower concentrations as the likelihood of the micropipette picking up AgNPs decreases.



**Figure 18.** Agar plate treated with 6000  $\mu\text{g.mL}^{-1}$  AgNPs

Uneven coatings of AgNPs may have led to formation of lawns that were not counted. One example is a plate treated with 6000  $\mu\text{g}\cdot\text{mL}^{-1}$  of AgNPs (Figure 18). Clusters of bacterial colonies are evident, whilst the rest of the plate's surface remains relatively clear. This may possibly reflect an uneven spreading of *B. subtilis* given the dilution ratio of 1:100K. Similarly, AgNPs may not have fully coated the plates' surface, as plates treated with higher concentrations do not show clusters.

To minimize aggregation, a study directly autoclaved AgNPs in agar media at various concentrations (Tripathi *et al.*, 2010). Alternatively, measuring the surface area of bacterial growth was used as a supplementary set of data to verify correlations drawn, allowing for higher precision even if lawns form.

## 7.2 Evidence / Data

Strengths: Image J was used for CFU counting. Automated cell counting significantly lowers random error and subjectivity. Additionally, calculating the surface area offers another set of data to compare against. Figure 19 shows the plate treated with 1000  $\mu\text{g}\cdot\text{mL}^{-1}$  AgNPs for trial 1. Whilst the number of colonies counted was only 30 CFU, which is lower than the average of 43 CFU, the surface area was 5.57  $\text{cm}^2$ , which is close to 5.56  $\text{cm}^2$  (average).



**Figure 19.** Agar plate treated with 1000 $\mu\text{g}\cdot\text{mL}^{-1}$  AgNPs

Weaknesses: Colony counting does not take into consideration the formation of lawns, nor the various sizes and density of colonies. Similarly, the set circularity was based on trial and error which may involve bias. To improve, a cytometer would have offered more accurate results. Alternatively, measuring optical densities would have eliminated the limitations of colony counting.

Notably, concentrations found to be effective in this investigation are significantly higher than many published studies. AgNPs in this investigation had an approximate diameter of 100 nm whilst published studies used AgNPs with diameters ranging from 2-10 nm. AgNPs with smaller diameters would be able to penetrate the membrane easier, increasing toxicity. Thus, as the diameter of AgNPs used in this study is much greater than published studies, significantly higher concentrations were needed to show similar effects. This realistically isn't suitable for consumption as studies reported toxic effects of silver against human peripheral blood mononuclear cells with 12.5-50 ppm of AgNPs (Greulich *et al.*, 2012).

## 8. Further investigations

As this investigation suggested antibacterial activity of AgNPs against *B. subtilis*, a GPB, it is worthwhile to investigate the potential differences in the antibacterial activity of AgNPs against GNB compared to GPB. Currently, it is hypothesized that greater concentrations of AgNPs are needed to exhibit similar toxicities against GPB compared to GNB due to its thick peptidoglycan layer. Potential differences may highlight differences in the membrane of GNB and GPB that led to differing toxicities of AgNPs. This will allow a more comprehensive understanding of AgNPs toxicity against non-pathogenic bacteria.

## References

- Abass Sofi, M., Sunitha, S., Ashaq Sofi, M., Khadheer Pasha, S. K., & Choi, D. (2022). An overview of antimicrobial and anticancer potential of silver nanoparticles. *Journal of King Saud University - Science*, 34(2), 101791. <https://doi.org/10.1016/j.jksus.2021.101791>
- Behnsen, J., Deriu, E., Sassone-Corsi, M., & Raffatellu, M. (2013). Probiotics: Properties, examples, and specific applications. *Cold Spring Harbor Perspectives in Medicine*. Retrieved September 29, 2022, from <https://www.ncbi.nlm.nih.gov/>
- Blood agar plates and hemolysis. *ASM.org*. (2016). Retrieved August 25, 2022, from <https://asm.org/Protocols/Blood-Agar-Plates-and-Hemolysis-Protocols>
- Cataliotti, R. S., Aliotta, F., & Ponterio, R. (2009). Silver nanoparticles behave as hydrophobic solutes towards the liquid water structure in the interaction shell. A Raman study in the O–H stretching region. *Physical Chemistry Chemical Physics*. Retrieved August 25, 2022, from <https://pubs.rsc.org/en/content/articlelanding/2009/cp/b915317a>
- Pramanik, S., Chatterjee, S., Saha, A., Devi, P. S., & Suresh Kumar, G. (2016). Unraveling the Interaction of Silver Nanoparticles with Mammalian and Bacterial DNA. *The Journal of Physical Chemistry B*, 120(24), 5313–5324. <https://doi.org/10.1021/acs.jpcc.6b01586>
- Ducksters (2022) *Ducksters: Elements for kids, Ducksters* [italics]. Retrieved August 25, 2022, from <https://www.ducksters.com/science/chemistry/silver.php>
- Dunning, H. (2020). *Size determines how nanoparticles affect biological membranes*: Imperial News: Imperial College London. *Imperial News*. Retrieved August 25, 2022, from <https://www.imperial.ac.uk/news/204433/size-determines-nanoparticles-affect-biological-membranes/>
- Ferdous, Z., & Nemmar, A. (2020). Health impact of silver nanoparticles: A review of the biodistribution and toxicity following various routes of exposure. *International Journal of Molecular Sciences*. Retrieved August 25, 2022, from <https://www.ncbi.nlm.nih.gov/pmc/articles/PMC7177798/>
- Greulich, C., Braun, D., Peetsch, A., Diendorf, J., Siebers, B., Epple, M., & Köller, M. (2012). The toxic effect of silver ions and silver nanoparticles towards bacteria and human cells occurs in the same concentration range. *RSC Advances*, 2(17), 6981. <https://doi.org/10.1039/c2ra20684f>
- Gunasekaran, T., Nigusse, T., & Dhanaraju, M. D. (2012). Silver nanoparticles as real topical bullets for wound healing. *The Journal of the American College of Clinical Wound Specialists*. Retrieved August 25, 2022, from <https://www.ncbi.nlm.nih.gov/pmc/articles/>
- Hansson, M., & Abedi-Valugerdi, M. (2003). Xenobiotic metal-induced autoimmunity: Mercury and silver differentially induce antinucleolar autoantibody production in susceptible H-2s, H-2Q and H-2F mice. *Clinical and experimental immunology*. Retrieved August 25, 2022, from <https://www.ncbi.nlm.nih.gov/pmc/articles/PMC1808646/>
- Hong, H. A., Khaneja, R., Tam, N. M. K., Cazzato, A., Tan, S., Urdaci, M., Brisson, A., Gasbarrini, A., Barnes, I., & Cutting, S. M. (2009). *Bacillus subtilis* isolated from the human gastrointestinal tract. *Research in Microbiology*, 160(2), 134–143. <https://doi.org/10.1016/j.resmic.2008.11.002>
- Horiba Scientific (2020). What is a nanoparticle? Retrieved August 25, 2022, from <https://www.horiba.com/deu/scientific/products/particle-characterization/particle-education/what-is-a-nanoparticle/>
- Hsueh, Y.-H., Lin, K.-S., Ke, W.-J., Hsieh, C.-T., Chiang, C.-L., Tzou, D.-Y., & Liu, S.-T. (2015). The antimicrobial properties of silver nanoparticles in *Bacillus subtilis* are mediated by released AG+ ions. *PLOS ONE*. Retrieved August 25, 2022, from <https://journals.plos.org/plosone/article?id=10.1371/journal.pone.0144306>
- Huang, D., & Koshland, D. (1970). Chromosome integrity in *saccharomyces cerevisiae*: The interplay of DNA replication initiation factors, elongation factors, and origins. *Genes & Development*. Retrieved August 25, 2022, from <http://genesdev.cshlp.org/content/17/14/1741.short>
- Keenleyside, W. (2019). 8.3 cellular respiration. *Microbiology Canadian Edition*. Retrieved August 25, 2022, from <https://ecampusontario.pressbooks.pub/microbio/chapter/cellular-respiration/>
- Khan, R., Ray, S. (2019). Bacterial Cell Division Machinery: An Insight for Development of New Antibacterial Agent. In: Kumar, S., Egbuna, C. (eds) *Phytochemistry: An in-silico and in-vitro Update*. Springer, Singapore. [https://doi.org/10.1007/978-981-13-6920-9\\_7](https://doi.org/10.1007/978-981-13-6920-9_7)
- Kora, A. J., & Arunachalam, J. (2010). Assessment of antibacterial activity of silver nanoparticles on *Pseudomonas aeruginosa* and its mechanism of action. *World Journal of Microbiology and Biotechnology*, 27(5), 1209–1216. <https://doi.org/10.1007/s11274-010-0569-2>
- Lansdown, A. B. G. (2004). A review of the use of silver in wound care: Facts and fallacies. *British Journal of Nursing*, 13(Sup1). <https://doi.org/10.12968/bjon.2004.13.sup1.12535>
- Le Ouay, B., & Stellacci, F. (2015). Antibacterial activity of silver nanoparticles: A surface science insight. *NanoToday*, 10(3), 339–354. <https://doi.org/10.1016/j.nantod.2015.04.002>
- Li J;Rong K;Zhao H;Li F;Lu Z;Chen R; (n.d.). Highly selective antibacterial activities of silver nanoparticles against *bacillus subtilis*. *Journal of Nanoscience and Nanotechnology*. Retrieved August 25, 2022, from <https://pubmed.ncbi.nlm.nih.gov/24245147/>
- Li, W.-R., Xie, X.-B., Shi, Q.-S., Zeng, H.-Y., OU-Yang, Y.-S., & Chen, Y.-B. (2009). Antibacterial activity and mechanism of silver nanoparticles on *escherichia coli*. *Applied Microbiology and Biotechnology*, 85(4), 1115–1122. <https://doi.org/10.1007/s00253-009-2159-5>
- Liao, S., Zhang, Y., Pan, X., Zhu, F., Jiang, C., Liu, Q., Cheng, Z., Dai, G., Wu, G., Wang, L., & Chen, L. (2019). Antibacterial activity and mechanism of silver nanoparticles against multidrug-resistant *Pseudomonas aeruginosa*. *International Journal of Nanomedicine*. Retrieved August 25, 2022, from <https://www.ncbi.nlm.nih.gov/pmc/articles/PMC6396885/>
- Lu, Z., Guo, W., & Liu, C. (2018). Isolation, identification and characterization of novel *Bacillus subtilis*. *The Journal of Veterinary Medical Science*. Retrieved August 25, 2022, from <https://www.ncbi.nlm.nih.gov/pmc/articles>
- Masri, A., Anwar, A., Ahmed, D., Siddiqui, R. B., Raza Shah, M., & Khan, N. A. (2018). Silver nanoparticle conjugation-enhanced antibacterial efficacy of clinically approved drugs Cephadrine and Vildagliptin. *Antibiotics* (Basel, Switzerland). Retrieved September 28, 2022, from <https://www.ncbi.nlm.nih.gov/pmc/articles/PMC6316254/>

- Mayer, J., & Donnelly, T. M. (2013). *Clinical Veterinary Advisor: Birds and Exotic Pets*. Elsevier Health Sciences. <https://doi.org/10.1016/C2009-0-36486-7>
- MicrobeWiki (2015) *Bacillus subtilis*. Available at: [https://microbewiki.kenyon.edu/index.php/Bacillus\\_subtilis](https://microbewiki.kenyon.edu/index.php/Bacillus_subtilis) (Retrieved August 25, 2022)
- Microbiology writing guide: Presenting data. *Writing Intensive Curriculum Program*. (2017). Retrieved August 25, 2022, from <https://wic.oregonstate.edu/microbiology-writing-guide-presenting-data>
- Paul, W., & Sharma, C. (2010). Inorganic nanoparticles for targeted drug delivery. *Biointegration of Medical Implant Materials*, 204–235. <https://doi.org/10.1533/9781845699802.2.204>
- Qiu, Z., Zhang, Z., Roschke, A., Varga, T., & Aplan, P. D. (2017). Generation of gross chromosomal rearrangements by a single engineered DNA double strand break. *Nature News*. Retrieved August 25, 2022, from <https://www.nature.com/articles/>
- Quinteros, M. A., Aristizá, V. C., Dalmassod, P. R., Parajeae, M. G., & Páezbc, P. L. (2016). Oxidative stress generation of silver nanoparticles in three bacterial genera and its relationship with the antimicrobial activity. *ScienceDirect*. Retrieved August 25, 2022, from <https://doi.org/10.1016/j.tiv.2016.08.007>
- Rajagopal, M., & Walker, S. (2017). Envelope structures of Gram-positive bacteria. *Current Topics in Microbiology and Immunology*. Retrieved August 25, 2022, from <https://www.ncbi.nlm.nih.gov/pmc/articles/PMC5002265/>
- Ray, P. D., Huang, B.-W., & Tsuji, Y. (2012). Reactive oxygen species (ROS) homeostasis and redox regulation in cellular signaling. *Cellular Signalling*. Retrieved August 25, 2022, from <https://www.ncbi.nlm.nih.gov/pmc/articles/PMC3454471/>
- Redza-Dutordoir, M., & Averill-Bates, D. A. (2016). Activation of apoptosis signalling pathways by reactive oxygen species. *Biochimica et Biophysica Acta*. Retrieved August 25, 2022, from <https://pubmed.ncbi.nlm.nih.gov/27646922/>
- Ruparelia, J. P., Mukherji, S., Duttagupta, S. P., & Chatterjee, A.K. (2008). Strain specificity in antimicrobial activity of silver and copper nanoparticles. *Acta Biomaterialia*. Retrieved August 25, 2022, from <https://pubmed.ncbi.nlm.nih.gov/18248860/>
- Salleh, A., Naomi, R., Utami, N. D., Mohammad, A. W., Mahmoudi, E., Mustafa, N., & Fauzi, M.B. (2020). The potential of silver nanoparticles for antiviral and antibacterial applications: A mechanism of action. *MDPI*. Retrieved August 25, 2022, from <https://www.mdpi.com/2079-4991/10/8/1566/htm>
- Salton, M. R. J., & Kim, K.-S. (1996). *Structure - Medical Microbiology - NCBI Bookshelf*. Chapter 2 - Structure. Retrieved August 25, 2022, from <https://www.ncbi.nlm.nih.gov/books/NBK8477/>
- Sanyasi, S., Majhi, R. K., Kumar, S., Mishra, M., Ghosh, A., Suar, M., Satyam, P. V., Mohapatra, H., Goswami, C., & Goswami, L. (2016). Polysaccharide-capped silver nanoparticles inhibit biofilm formation and eliminate multi-drug-resistant bacteria by disrupting bacterial cytoskeleton with reduced cytotoxicity towards mammalian cells. *Scientific Reports*. Retrieved August 25, 2022, from <https://www.ncbi.nlm.nih.gov/pmc/articles/PMC4850392/>
- Sauerbrei, A. (2020). *Bactericidal and virucidal activity of ethanol and povidone-iodine*. *MicrobiologyOpen*. Retrieved August 25, 2022, from <https://www.ncbi.nlm.nih.gov/pmc/articles/>
- Silhavy, T. J., Kahne, D., & Walker, S. (2010, May). The bacterial cell envelope. *Cold Spring Harbor perspectives in biology*. Retrieved August 25, 2022, from <https://www.ncbi.nlm.nih.gov/pmc/articles/PMC2857177/#:~:text=Gram%2Dnegative%20bacteria%20are%20surrounded,found%20in%20the%20Gram%2Dnegatives.>
- Su, Y., Liu, C., Fang, H., & Zhang, D. (2020). *Bacillus subtilis: A universal cell factory for industry, agriculture, biomaterials and medicine - microbial cell factories*. *BioMed Central*. Retrieved August 25, 2022, from <https://microbialcellfactories.biomedcentral.com/articles/10.1186/s12934-020-01436-8>
- Sundararajan, K., Miguel, A., Desmarais, S. M., Meier, E. L., Casey Huang, K., & Goley, E. D. (2015). The bacterial tubulin ftzr requires its intrinsically disordered linker to direct robust cell wall construction. *Nature News*. Retrieved August 25, 2022, from <https://www.nature.com/articles/ncomms8281>
- Swoboda, J. G., Campbell, J., Meredith, T. C., & Walker, S. (2010, January 4). Wall teichoic acid function, biosynthesis, and inhibition. *ChemBiochem : a European Journal of Chemical Biology*. Retrieved August 25, 2022, from <https://www.ncbi.nlm.nih.gov/pmc/articles/PMC2798926/>
- Tripathi, R. M., Saxena, A., Gupta, N., & Kapoor, H. (2010). High antibacterial activity of silver nanoballs against E.coli MTCC 1302, S. typhimurium MTCC 1254, B. subtilis MTCC 1133 and P.aeruginosa MTCC 2295. *ResearchGate*. Retrieved August 25, 2022, from [https://www.researchgate.net/publication/279897395\\_High\\_antibacterial\\_activity\\_of\\_silver\\_nanoballs\\_against\\_Ecoli\\_MTCC\\_1302\\_s\\_typhimurium\\_MTCC\\_1254\\_b\\_subtilis\\_MTCC\\_1133\\_and\\_p\\_aeruginosa\\_MTCC\\_2295](https://www.researchgate.net/publication/279897395_High_antibacterial_activity_of_silver_nanoballs_against_Ecoli_MTCC_1302_s_typhimurium_MTCC_1254_b_subtilis_MTCC_1133_and_p_aeruginosa_MTCC_2295)
- U.S. Department of Health and Human Services. (2019). Probiotics: What you need to know. *National Center for Complementary and Integrative Health*. Retrieved August 25, 2022, from <https://www.nccih.nih.gov/health/probiotics-what-you-need-to-know>
- Wei, A. A. Q. (2021). The effect of temperature on microorganisms growth rate. *The Expedition*. Retrieved August 25, 2022, from <https://ojs.library.ubc.ca/index.php/expedition/article/view/195694>
- Widner, B., Behr, R., Von Dollen, S., Tang, M., Heu, T., Sloma, A., Sternberg, D., Deangelis, P. L., Weigel, P. H., & Brown, S. (2005). Hyaluronic acid production in bacillus subtilis. *Applied and Environmental Microbiology*. Retrieved August 25, 2022, from <https://www.ncbi.nlm.nih.gov/pmc/articles/PMC1168996/>
- Yin, I. X., Zhang, J., Zhao, I. S., Mei, M. L., Li, Q., & Chu, C. H. (2020, April 17). The antibacterial mechanism of silver nanoparticles and its application in dentistry. *International Journal of Nanomedicine*. Retrieved August 25, 2022, from <https://www.ncbi.nlm.nih.gov/pmc/articles/PMC7174845/>
- Zhang, R., Lee, P., Lui, V. C. H., Chen, Y., Liu, X., Lok, C. N., To, M., Yeung, K. W. K., & Wong, K. K. Y. (2015). Silver nanoparticles promote osteogenesis of mesenchymal stem cells and improve bone fracture healing in osteogenesis mechanism mouse model. *Nanomedicine : Nanotechnology, Biology, and Medicine*. Retrieved August 25, 2022, from <https://pubmed.ncbi.nlm.nih.gov>



## Appendices

### SEM of AgNPs

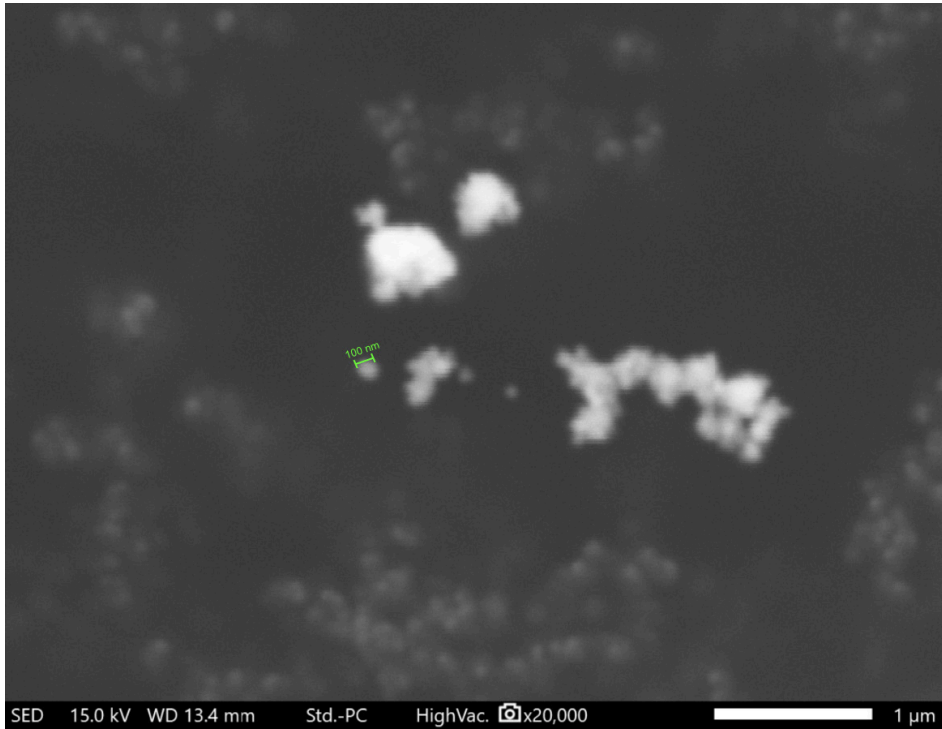
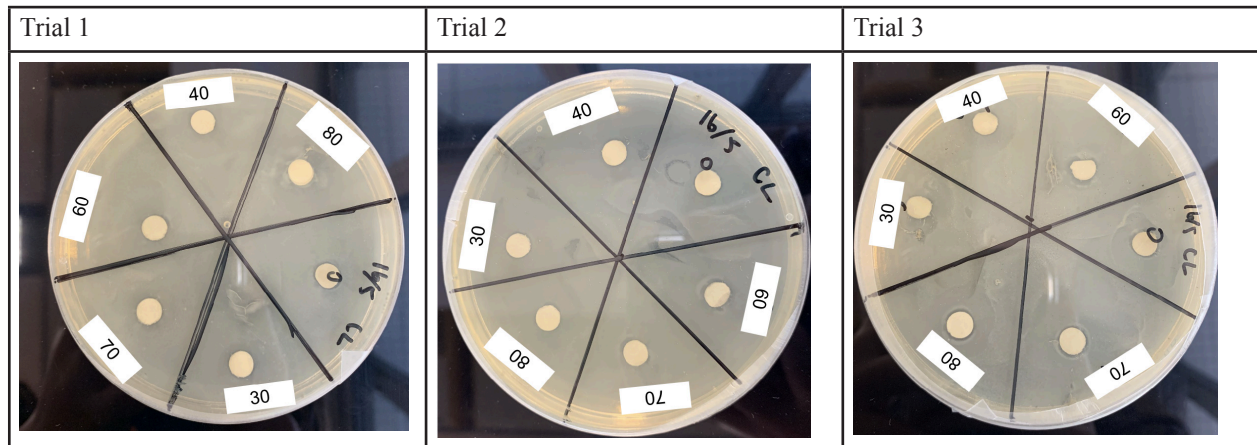


Figure 19. SEM of AgNPs used in this study - AgNPs measured to have an approximate diameter of 100 nm

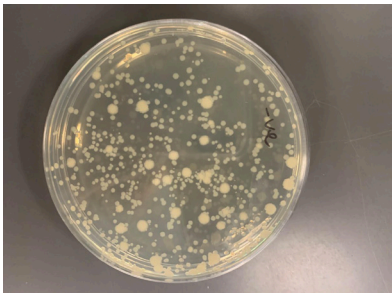
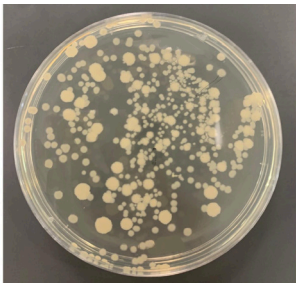
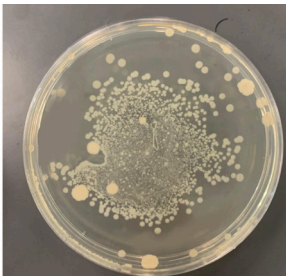
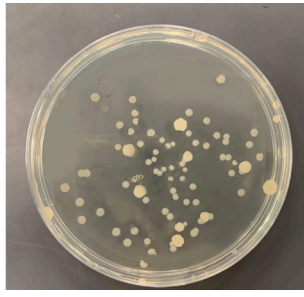
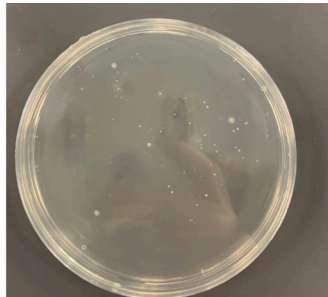
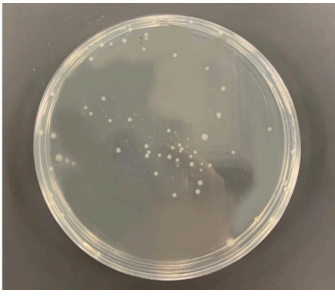
### Pretest Using Paper Disc Diffusion for Concentrations 30, 40, 60, 70, and 80 μg.ml<sup>-1</sup>:



#### Notes:

- Trivial zones of inhibitions
- Complete formation of lawn across all concentration

## Qualitative Data

Negative control (0 $\mu\text{g.ml}^{-1}$ )	2000 $\mu\text{g.ml}^{-1}$	6000 $\mu\text{g.ml}^{-1}$
 <p>248 CFU</p>	 <p>113 CFU</p>	 <p>79 CFU</p>
10000 $\mu\text{g.ml}^{-1}$	14000 $\mu\text{g.ml}^{-1}$	Positive control (70% ethanol)
 <p>30 CFU</p>	 <p>24 CFU</p>	 <p>22 CFU</p>

**Table 11.** Qualitative data and observations. Representative photographs of each treatment are shown with CFU counts.

### Notes:

- As the concentration of AgNPs increases, the formation of colonies qualitatively decreases.
- A bacterial cluster is evident in the plate treated with 6000  $\mu\text{g.ml}^{-1}$ , possibly due to uneven spreading of AgNPs. 6000  $\mu\text{g.ml}^{-1}$  may be insufficient to evenly coat the entire surface of the plate.
- The number of colonies visible on the plates at 14000  $\mu\text{g.ml}^{-1}$  and the positive control is similar, possibly reflecting similar antibacterial activities.

# Modeling the Concentration of Morphine across the Blood-Brain Barrier: A Diffusion-Absorption Differential Equation Approach

Bryan H.L. Wong

## Introduction

The blood-brain barrier is a major obstacle to current drug delivery into the brain due to its low permeability and tight junctions. This exploration will mathematically model how morphine, a common narcotic analgesic, may diffuse passively across this barrier through the concentration gradient and explore its implications. The main aim of this exploration is to find the exact equation for the concentration of drugs in the blood and brain as a function of time. It is assumed that the drugs always travel from a higher concentration region (bloodstream) to a lower concentration region (brain) passively, where it is then slowly absorbed by the body.

Section 2 considers how the drug diffuses across the concentration gradient until the concentration converges (steps 1 & 2). Section 3 further considers how the drug is absorbed simultaneously, inducing a new concentration gradient until all of the drugs are diffused and absorbed (steps 3 & 4). The peak concentration of the drug and its rate of convergence to equilibrium can then be determined, offering insight into how quickly a drug can deliver its effects and when it needs to be re-administered.

For simplification, the capillaries will be modeled as a cylinder. Therefore, the diagram from the scientific literature (Figure 2.1) is transformed into a geometric model (Figure 2.2) where all parameters can be specified.

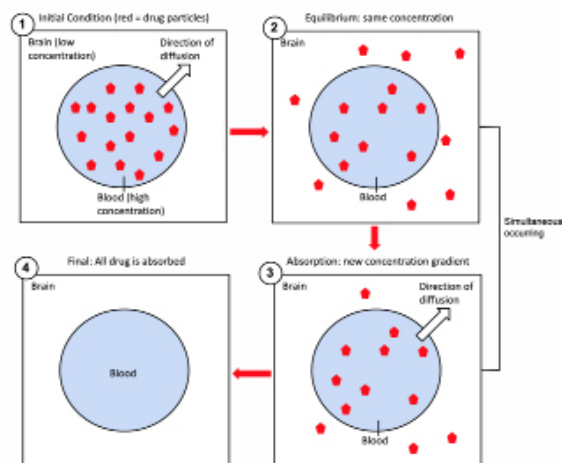


Figure 1. 4-step life cycle of a drug from the blood to the brain

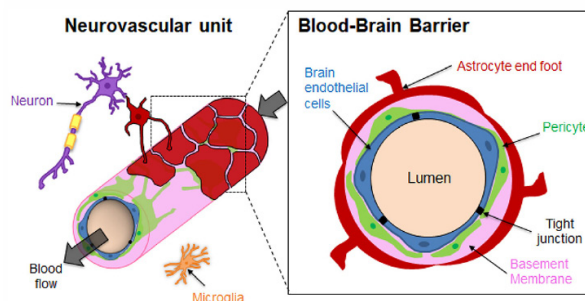


Figure 2.1 Diagram of blood-brain barrier (Piantino *et al.*, 2021)

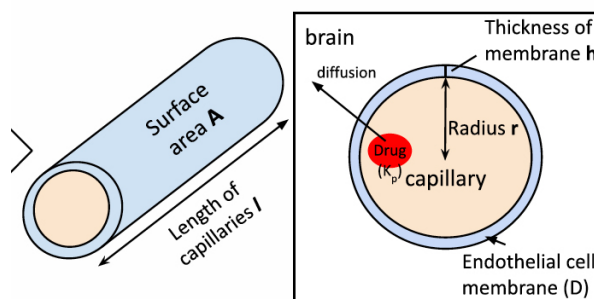


Figure 2.2. Simplified model

## 1. Defining the Model

According to Fick's first law, drug molecules will always diffuse from a higher concentration region to a lower concentration region based on the following differential equation (Bhosle *et al.*, 2017):

$$\frac{dQ}{dt} = \frac{D \cdot A \cdot K_p}{h} (c_{blood}(t) - c_{brain}(t)), \quad (1.1)$$

where  $c_{blood}(t)$  and  $c_{brain}(t)$  are the concentrations of the drug in the blood and brain respectively. Since  $dQ/dt$  is the rate of diffusion, its antiderivative,  $Q(t)$ , is thus the total amount diffused from the blood to the brain. The goal is, therefore, to derive the concentration gradient ( $c_{blood}(t) - c_{brain}(t)$ ) in terms of  $Q(t)$ , allowing equation (1.1) to be formulated as a differential equation of  $Q(t)$ .

Physically, this equation makes sense. The higher the concentration gradient, the greater the rate of diffusion. If the surface area  $A$  is higher, there is more space for molecules to diffuse across, increasing the rate of diffusion. Finally, if the membrane diffusivity  $D$  (ability to let drugs through) and the partition coefficient  $K_p$  of the drug (ability of drugs to diffuse through the membrane) are higher, it is easier for the drug to diffuse. However, if the thickness of the membrane  $h$  is higher, it takes longer for the drug to travel through, decreasing the rate of diffusion.

## 2. Coefficients

The physical parameters used to calibrate the model are based on scientific literature. The definition and values of the parameters are listed below:

### Volume and surface area of blood

- Total length of capillaries  $l = 400$  miles  
=  $6.44 \times 10^5$  m (Cipolla, 2009)
- Average radius of capillary  $r = 6.23$   $\mu$ m  
=  $6.23 \times 10^{-6}$  m (Smith *et al.*, 2019)

Therefore, the volume and surface area of the capillaries (blood) are given by

$$V_{blood} = \pi(6.23 \cdot 10^{-6})^2 \cdot 6.44 \cdot 10^5 \approx 7.85 \cdot 10^{-5} \text{ m}^3$$

$$A_{blood} = 2\pi(6.23 \cdot 10^{-6}) \cdot 6.44 \cdot 10^5 \approx 25.2 \text{ m}^2$$

### Volume of the brain

The volume of the brain used is based on the calculation of the average brain volume of an adult male from a study conducted with a sample size of 50 people

$$V_{br} = 1.51 \text{ dm}^3 = 1.51 \times 10^{-3} \text{ m}^3 \text{ (Lüders } et al., 2002)$$

### Diffusivity of the membrane

The diffusivity of the membrane  $D$  represents the capability of the membrane to allow chemical compounds to pass through diffusion. The greater the value of  $D$ , the faster the drug diffuses given the same concentration gradient.

$$D = 45.6 \text{ \AA}^2 / \text{ns} = 4.56 \times 10^{-10} \text{ m}^2/\text{s} \text{ (Shamloo } et al., 2016)$$

### Thickness of the membrane

The thickness of the cerebral endothelial membrane is around 0.3-0.5  $\mu$ m, so

$$h = 0.4 \text{ \mu m} = 4.0 \times 10^{-7} \text{ m} \text{ (Zlokovic, 2009)}$$

### Partition coefficient of the drug

The partition coefficient is a unitless measure of the lipophilicity of a drug. Since only lipophilic (lipid-loving) substances can diffuse through the blood-brain barrier (Duke University, 2022), it is also an indication of its ability to cross the cell membrane. For morphine, the partition coefficient

$$K_p = 0.78 \text{ (Ederoth } et al., 2004)$$

### Absorption rate constant of the drug

The half-life of a drug is the time taken for the amount of the drug in the brain to halve. The rate constant represents how quickly the drug is absorbed and is inversely proportional to the half-life. In particular, the rate constant

$$k = \frac{\ln(2)}{t_{1/2}}$$

Since the half-life of morphine in injured brain tissue is 161 seconds (Ederoth *et al.*, 2004),

$$k = \frac{\ln(2)}{161} = 4.31 \cdot 10^{-3} \text{ s}^{-1}$$

To summarize, the coefficients are listed below (values are rounded to 3 significant figures for clarity):

Parameter	Value	Parameter	Value
Diffusivity D	$4.56 \times 10^{-10} \text{ m}^2/\text{s}$	Volume of blood $V_{bl}$	$7.85 \times 10^{-5} \text{ m}^3$
Surface Area A	$25.2 \text{ m}^2$	Volume of brain $V_{br}$	$1.51 \times 10^{-3} \text{ m}^3$
Partition Coefficient $K_p$	0.78	Rate constant k	$4.31 \times 10^{-3} \text{ s}^{-1}$
Thickness h	$4.0 \times 10^{-7} \text{ m}$		

### 3. Passive Diffusion

I first want to solve for the concentration of the drug over time by considering the diffusion process of the drug alone (ie. assuming no drug is absorbed out of the system). The concentration of a substance in a solution is defined as the amount of a substance divided by the total volume of the solution.

$$c = \frac{m}{v}$$

Intuitively, the concentration of the drug remaining in the bloodstream should be equal to the initial concentration ( $c_0$ ) minus the concentration that has diffused away into the brain ( $Q(t)/V_{bl}$ ). Therefore,

$$c_{blood}(t) = c_0 - \frac{1}{V_{bl}}Q(t) \quad (3.1)$$

Similarly, because the initial concentration of the drug in the brain is zero, its cumulative concentration should just be the total concentration diffused in from the blood.

$$c_{brain}(t) = \frac{1}{V_{br}}Q(t) \quad (3.2)$$

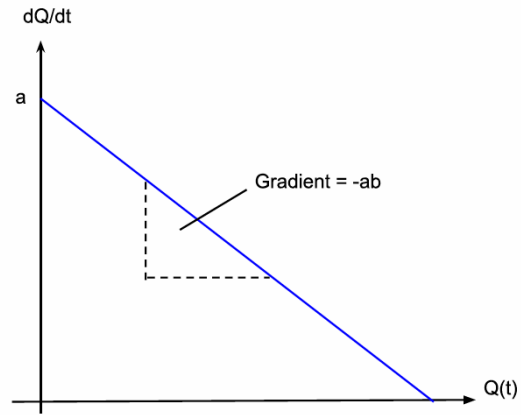
Therefore, by substituting the concentrations in equation (3.1) and (3.2) into equation (1.1),

$$\begin{aligned} \frac{dQ}{dt} &= \frac{D \cdot A \cdot K_p}{h} \left( c_0 - \frac{Q(t)}{V_{bl}} - \frac{Q(t)}{V_{br}} \right) \\ \therefore \frac{dQ}{dt} &= \frac{D \cdot A \cdot K_p}{h} \left( c_0 - \frac{V_{br} + V_{bl}}{V_{bl}V_{br}}Q(t) \right) \quad (3.3) \end{aligned}$$

For clarity of notation, I will rewrite  $DAK_p/h$  as 'a' and  $V_{br} + V_{bl} / V_{bl}V_{br}$  as 'b'. Therefore, the rate of diffusion can be represented via the separable differential equation

$$\frac{dQ}{dt} = a(c_0 - bQ) \quad (3.4)$$

Observing equation (3.4), the rate of diffusion displays a negative linear association with the total amount of diffusion. This means that the rate of diffusion will decrease as more drug is diffused into the brain, so it is expected that  $Q(t)$  will eventually flatten out and plateau as its derivative approaches zero.



**Figure 3.** Relationship between the rate of diffusion ( $dQ/dt$ ) and total diffusion ( $Q(t)$ )

By solving this differential equation, I can then substitute  $Q(t)$  back into equations (3.1) and (3.2) to work out the concentration of the drug as a function of time. By rearranging the equation,

$$\frac{1}{c_0 - bQ} dQ = a dt$$

Therefore, I can integrate both sides of the equation with respect to  $Q$  and  $t$  respectively.

$$\int \frac{1}{c_0 - bQ} dQ = \int a dt$$

To evaluate the integral on the left, I used integration by substitution.

$$\text{Let } u = c_0 - bQ ; du = -bdQ \Rightarrow dQ = \frac{-1}{b} du$$

$$\therefore \int \frac{1}{c_0 - bQ} dQ = \frac{-1}{b} \int \frac{1}{u} du = \frac{-1}{b} \ln|u| = \frac{-1}{b} \ln|c_0 - bQ|$$

Something I noticed here is that  $c_0 - bQ$  (the concentration gradient) can never be negative, so the absolute value can be dropped. This is because, by the time the concentration gradient is zero, the diffusion would stop and the concentration gradient cannot further decrease and be negative. Hence,

$$\frac{-1}{b} \ln(c_0 - bQ) = at + C, C \in \mathfrak{R}$$

The  $-b$  term can then be multiplied on both sides. Furthermore, since a constant multiplied by another constant is still just a constant, I can continue to write  $+C$  on the right-hand side for some unknown  $C$ .

$$\ln(c_0 - bQ) = -abt + C$$

Finally, by exponentiating both sides of the equation and rearranging,

$$c_0 - bQ = e^{-abt+C} = Ce^{-abt}$$

$$Q(t) = \frac{1}{b}(c_0 - C \cdot e^{-abt}) \quad (3.5)$$

To find  $C$ , I used the initial condition  $Q(0) = 0$  (no drug diffused into the brain initially). Therefore

$$\frac{1}{b}(c_0 - C \cdot e^{-ab \cdot 0}) = \frac{1}{b}(c_0 - C) = 0 \Rightarrow C = c_0$$

Substituting the value of  $C$  back into equation (3.5), the total amount diffused over time is given by

$$Q(t) = \frac{c_0}{b}(1 - e^{-abt}) \\ = \frac{c_0 \cdot V_{bl} \cdot V_{br}}{V_{bl} + V_{br}} \left( 1 - e^{-\left(\frac{D \cdot A \cdot K_p}{h}\right) \left(\frac{V_{br} + V_{bl}}{V_{bl} V_{br}}\right) t} \right) \quad (3.6)$$

Furthermore, the rate of diffusion can be found by differentiating this function:

$$\frac{dQ}{dt} = a \cdot c_0 e^{-abt} \quad (3.7)$$

As time progresses, the rate of diffusion slows down, eventually tending towards zero. This matches my previous predictions, suggesting that the concentrations should indeed converge. To find the exact equation, I first calculated the values of 'a' and 'b' based on the coefficients defined in section 2.2:

$$a = \frac{D \cdot A \cdot K_p}{h} = \frac{4.56 \cdot 10^{-10} \cdot 25.1986 \cdot 0.78}{4.0 \cdot 10^{-7}} \\ \approx 0.0224$$

$$b = \frac{V_{br} + V_{bl}}{V_{bl} V_{br}} = \frac{1}{V_{bl}} + \frac{1}{V_{br}} \\ = \frac{1}{7.85 \cdot 10^{-5}} + \frac{1}{1.51 \cdot 10^{-3}} \approx 13400$$

Therefore,

$$Q(t) = \frac{c_0}{13400}(1 - e^{-0.0224 \cdot 13400t}) \\ = \frac{c_0}{13400}(1 - e^{-300t}) \quad (3.8)$$

Finally, to solve for the functions of concentration with respect to time,

$$c_{brain}(t) = \frac{1}{V_{br}} Q(t) \\ = \frac{1}{1.51 \cdot 10^{-3}} \cdot \frac{c_0}{13400}(1 - e^{-300t}) \\ = 0.494c_0(1 - e^{-300t}) \quad (3.9)$$

Similarly, for the concentration of the drug remaining in the bloodstream,

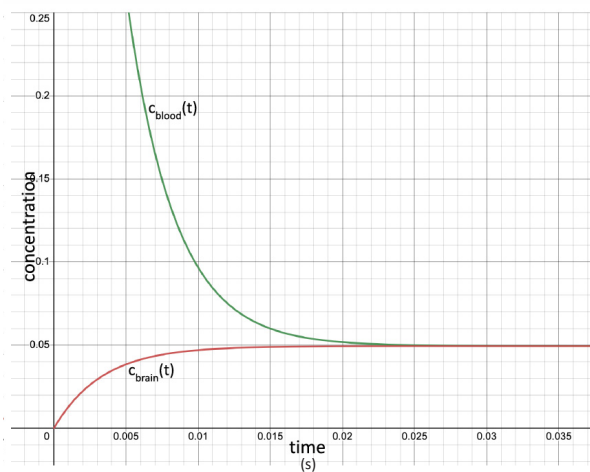
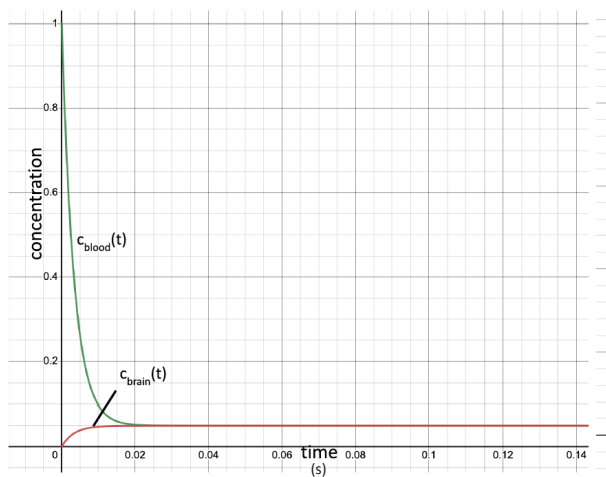
$$c_{blood}(t) = c_0 - \frac{1}{V_{bl}} Q(t) \\ = c_0 - \frac{1}{7.58 \cdot 10^{-5}} \cdot \frac{c_0}{13400}(1 - e^{-300t}) \\ = c_0(0.0494 + 0.951e^{-300t}) \quad (3.10)$$

Initially, when I did the calculations using the rounded values listed above, I noticed that the two equilibrium concentrations did not match, very possibly due to rounding errors from a lower degree of accuracy. Therefore, although the values displayed here are only to 3 significant figures for clarity, the final values were computed using the exact values on the calculator. Hence, to summarize,

$$c_{blood}(t) = c_0(0.0494 + 0.951e^{-300t});$$

$$c_{brain}(t) = 0.0494c_0(1 - e^{-300t}) \quad (3.11)$$

These two equations are graphed below (setting  $c_0 = 1$ ):



**Figure 3.** Concentration of drug in blood and brain over time under passive diffusion

As seen from equation (3.11), although the constant term is the same, the coefficient of the exponential term is greater for  $c_{blood}(t)$ . This suggests that the concentration in the blood will decrease at a faster rate. Since the volume of the blood is nearly 20 times smaller than the volume of the brain ( $7.58 \times 10^{-5}$  vs  $1.51 \times 10^{-3}$ ), the same mass leaving the blood and entering the brain would represent a higher change in the concentration of the blood. From equation (3.11), both exponential terms will tend to zero as  $t$  tends to infinity, so both concentrations will converge to the same horizontal asymptote of  $c = 0.0494c_0$ . This coefficient of 0.0494 represents the ratio of the volume of the blood to the total volume.

Finally, it is also important in a physical context to know how quickly the drug concentration converges to equilibrium. However, since the equilibrium is a horizontal asymptote and will never actually reach that value, I can only measure how long it takes to reach a certain proportion ( $p$ ) of the equilibrium:

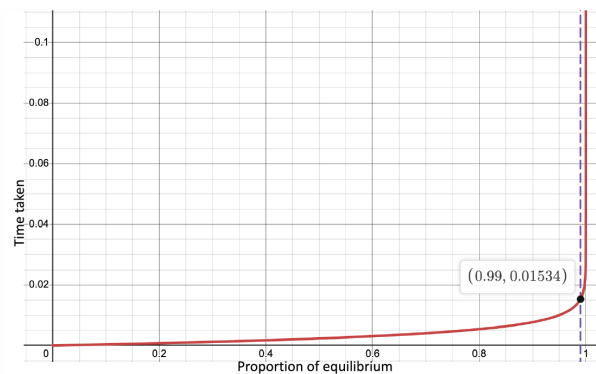
$$c_{blood}(t) = p \left( c_0 \frac{V_{bl}}{V_{bl} + V_{br}} \right), 0 \leq p < 1$$

$$0.0494c_0(1 - e^{-abt}) = p(0.0494c_0)$$

$$e^{-abt} = 1 - p$$

$$-abt = \ln(1 - p)$$

$$t = \frac{-\ln(1 - p)}{ab} \quad (3.11)$$



**Figure 4.** Time taken to reach a finite proportion of the equilibrium concentration

For example, to reach 99% of the equilibrium concentration,

$$t = \frac{\ln(1 - 0.99)}{0.0224 \cdot 13400} = 0.0153s$$

It is fascinating to see how quickly this diffusion process occurs. Even for 99% of the diffusion, it only takes a matter of milliseconds. In the Figure 3, although the scale on the x-axis is set from 0 to 0.14s, for most of it there is already no noticeable difference in the concentrations in the blood and the brain. However, in reality, the drug will not immediately register its effects, since it also takes time for the drug to travel from the site of administration to the brain capillaries.

#### 4. Diffusion-Absorption Equation

Section 3 allows us to describe the diffusion process. But in reality, the drug will not stay in the body forever. Instead, as the drug is absorbed by the brain (e.g. reacted to form other chemical products), a new concentration gradient is formed and the drug should continue to diffuse into the brain until there is no drug remaining. In this section, I will consider how diffusion and absorption occur simultaneously and how this affects the concentration of the drug in the blood and brain over time.

Since the concentration in the blood only depends on the initial concentration and rate of diffusion, the expression for the blood concentration is still the same as in section 3, though the actual equation should be different as the exact solution for  $Q(t)$  may differ.

$$C_{blood}(t) = c_0 - \frac{1}{V_{bl}} Q(t) \quad (4.1)$$

However, the concentration in the brain can no longer be expressed explicitly because the rate of absorption also depends on the concentration itself. It is assumed that the absorption process obeys first-order kinetics, meaning that the rate of absorption is proportional to the concentration at any time  $t$  by a factor of  $k$  (the rate constant).

$$\frac{d(abstract)}{dt} = kc_{brain}(t)$$

Therefore, the rate of change (derivative) of the concentration would be equal to the rate at which the drug is diffusing in from the blood subtracted by the rate at which it is being absorbed, i.e.

$$\begin{aligned} \frac{dc_{brain}(t)}{dt} &= rate_{in} - rate_{out} \\ &= \frac{1}{V_{br}} \frac{dQ}{dt} - kc_{brain} \quad (4.2) \end{aligned}$$

To be able to use equation (1.1) to solve for  $Q(t)$ , I first need to solve the differential equation (4.2) for an explicit solution of  $c_{brain}(t)$ . I noticed that the equation can be written in the standard form  $y'(t) + p(t)y(t) = q(t)$  (where  $y = c_{brain}$ ,  $p(x) = k$ ,  $q(t) = 1/V_{br} dQ/dt$ ), so the integrating factor method can be applied:

$$\frac{dc_{brain}}{dt} + kc_{brain} = \frac{1}{V_{br}} \frac{dQ}{dt}$$

The integrating factor is given by

$$\mu(t) = e^{\int p(t)dt} = e^{\int kdt} = e^{kt}$$

Therefore, by multiplying the integrating factor to both sides of the equation,

$$e^{kt} + \frac{dc_{brain}}{dt} + ke^{kt} \cdot c_{brain} = \frac{e^{kt}}{V_{br}} \frac{dQ}{dt}$$

Notice that from the product rule, the derivative of  $c_{brain}(t) e^{kt}$  is given by

$$\frac{dc_{brain}}{dt} e^{kt} + c_{brain}(ke^{kt})$$

which is equal to the left-hand side of the equation above. Therefore, I can rewrite the left-hand side as

$$\frac{d}{dt}(c_{brain} \cdot e^{kt}) = \frac{e^{kt}}{V_{br}} \frac{dQ}{dt}$$

To isolate  $c_{brain}(t)$ , I can integrate both sides of the equation over the interval  $[0, t]$  with respect to  $t$ ,

$$\int_0^t \frac{d}{dt}(c_{brain} \cdot e^{kt}) = \frac{1}{V_{br}} \int_0^t e^{kt} \frac{dQ}{dt} dt$$

Since the antiderivative of the derivative of a function is just the function itself,

$$e^{kt} c_{brain}(t) - e^{k \cdot 0} c_{brain}(0) = \frac{1}{V_{br}} \int_0^t e^{kt} \frac{dQ}{dt} dt$$



Furthermore, because the initial concentration in the brain is just zero,

$$c_{brain}(t) = \frac{1}{V_{br}} e^{-kt} \int_0^t e^{kt} \frac{dQ}{dt} dt \quad (4.3)$$

Based on this, I would predict that the concentration function is still exponential, similar to equation (3.11). However, although there is an  $e^{-kt}$  term outside the integral and an  $e^{kt}$  term inside, I cannot simply cancel the two terms because the value of the definite integral also depends on the  $e^{kt}$  term inside.

Therefore, by substituting the concentration equations (4.1) and (4.3) back into equation (1.1),

$$\begin{aligned} \frac{dQ}{dt} &= \frac{D \cdot A \cdot K_p}{h} (c_{blood} - c_{brain}) \\ &= \frac{D \cdot A \cdot K_p}{h} \left( c_0 - \frac{1}{V_{bl}} Q(t) - \frac{1}{V_{br}} e^{-kt} \int_0^t e^{kt} \frac{dQ}{dt} dt \right) \end{aligned} \quad (4.4)$$

Unlike equation (3.3), standard methods do not apply since it involves a definite integral term in the equation. Initially, this equation looks impossible to evaluate analytically. However, with a clever substitution, it can be transformed into a familiar ordinary differential equation. To do so, I first need to replace the integral term.

$$\text{Let } U = \int_0^t e^{kt} \frac{dQ}{dt} dt$$

Therefore, (I will rewrite  $dQ/dt$  as  $Q'$  for conciseness), equation (4.4) can be expressed in terms of  $U$ :

$$Q' = \frac{D \cdot A \cdot K_p}{h} \left( c_0 - \frac{1}{V_{bl}} Q(t) \right) - \frac{D \cdot A \cdot K_p}{h} \frac{1}{V_{br}} e^{-kt} U$$

For conciseness, I let  $\frac{D \cdot A \cdot K_p}{h} = a$

By rearranging the terms,

$$\begin{aligned} U &= \frac{Q' + \frac{a}{V_{bl}} Q - ac_0}{-\frac{a}{V_{br}} e^{-kt}} \\ &= -V_{br} e^{kt} \left( \frac{1}{a} Q' + \frac{1}{V_{bl}} Q - c_0 \right) \end{aligned} \quad (4.5)$$

Taking the derivative of  $U$  with respect to  $t$  and applying the product rule,

$$U' = -V_{br} \left( k e^{kt} \cdot \left( \frac{1}{a} Q' + \frac{1}{V_{bl}} Q - c_0 \right) + e^{kt} \left( \frac{1}{a} Q'' + \frac{1}{V_{bl}} Q' \right) \right)$$

By combining like terms,

$$U' = -V_{br} e^{kt} \left( \frac{1}{a} Q'' + \left( \frac{k}{a} + \frac{1}{V_{bl}} \right) Q' + \frac{k}{V_{bl}} Q - k \cdot c_0 \right)$$

However, by the fundamental theorem of calculus, the derivative of an integral is equal to the function inside the integral itself, so  $U'$  can also be expressed as

$$U' = \frac{d}{dt} \int_0^t e^{kt} \frac{dQ}{dt} = e^{kt} \frac{dQ}{dt} = e^{kt} Q' \quad (4.6)$$

As such, equations (4.5) and (4.6) must be equal to each other since they are both the derivative of  $U$ :

$$-V_{br} e^{kt} \left( \frac{1}{a} Q'' + \left( \frac{k}{a} + \frac{1}{V_{bl}} \right) Q' + \frac{k}{V_{bl}} Q - k \cdot c_0 \right) = e^{kt} Q'$$

Since  $e^{kt}$  is on both sides of the equation, it can be canceled out. Furthermore, by rearranging the terms,

$$\frac{V_{br}}{a} Q'' + \left( \frac{V_{br}k}{a} + \frac{V_{br}}{V_{bl}} + 1 \right) Q' + \frac{V_{br}k}{V_{bl}} Q - k \cdot c_0 V_{br} = 0$$

Therefore, I can now rewrite the equation as a second order linear differential equation:

$$\frac{V_{br}}{a} Q'' + \left( \frac{V_{br}k}{a} + \frac{V_{br}}{V_{bl}} + 1 \right) Q' + \left( \frac{V_{br}k}{V_{bl}} \right) Q = k \cdot V_{br} \cdot c_0 \quad (4.7)$$

Furthermore, by substituting the coefficients that I defined in section 2.2,

$$\begin{aligned} &\frac{1.51 \cdot 10^{-3}}{0.0224} Q'' \\ &+ \left( \frac{1.51 \cdot 10^{-3} \cdot 4.31 \cdot 10^{-3}}{0.0224} + \frac{1.51 \cdot 10^{-3}}{7.85 \cdot 10^{-5}} + 1 \right) Q' \\ &+ \left( \frac{1.51 \cdot 10^{-3} \cdot 4.31 \cdot 10^{-3}}{10^{-5} \cdot 0.0224} \right) Q \\ &= 1.51 \cdot 4.31 \cdot 10^{-6} \cdot c_0 \end{aligned}$$

Hence,

$$0.0674Q'' + 20.2Q' + 0.0828Q = 6.50 \cdot 10^{-6}c_0 \quad (4.8)$$

This differential equation is now much easier to solve with standard methods, and it is fascinating how two equations (4.4 and 4.8) that look entirely different are the same equation in disguise. Here, the second derivative represents the rate of change of the diffusion rate, or proportionally, the rate of change of the concentration gradient. This equation also resembles the equation of a damped simple harmonic oscillator from physics, so the second derivative might represent a 'restoring force' that always drives the system back to equilibrium.

From my research, I found that the general solution to a non-homogeneous second-order linear differential equation with constant coefficients (Grayling, 2019)

$$ax'' + bx' + cx = d \quad (4.9)$$

is given by the sum of the complementary function and particular integral:

$$x(t) = x_c(t) + x_p(t) = (c_1 e^{r_1 t} + c_2 e^{r_2 t}) + c_3$$

where  $r_1$  and  $r_2$  are the roots of the characteristic equation

$$ax^2 + bx + c = 0$$

Furthermore,  $x_c(t)$  satisfies the equation  $ax'' + bx' + cx = 0$ ; while  $x_p(t)$  satisfies equation (4.9).

Therefore, to solve equation (4.8), I first need to find the complementary solution by finding the roots of the quadratic equation

$$0.0674r^2 + 20.2x + 0.0828 = 0$$

Using the quadratic formula,

$$r = \frac{-20.2 \pm \sqrt{20.2^2 - 4(0.0674)(0.0828)}}{2 \cdot 0.0674}$$

$$= -4.09 \cdot 10^{-3} \text{ or } -300$$

Therefore, the solution to the complementary equation  $0.0674Q'' + 20.2Q' + 0.0828Q = 0$

$$Q_c(t) = c_1 e^{-4.09 \cdot 10^{-3} t} + c_2 e^{-300t} \quad (4.10)$$

Furthermore, to find the particular integral, I know that  $Q_p(t) = c_3$ , where  $c_3$  is a constant value. Since the derivative of a constant is zero, this only impacts the  $Q$  term in the differential equation:

$$0.0674Q_c'' + 20.2Q_c' + 0.0828(Q_c + c_3)$$

$$= 6.50 \cdot 10^{-6} c_0$$

$$(0.0674Q_c'' + 20.2Q_c' + 0.0828Q_c) + 0.828c_3$$

$$= 6.50 \cdot 10^{-6} c_0$$

By definition,  $Q_c(t)$  is a solution to the equation  $0.0674Q'' + 20.2Q' + 0.0828Q = 0$ , so

$$0.0828c_3 = 6.50 \cdot 10^{-6} c_0$$

$$c_3 = \frac{6.50 \cdot 10^{-6}}{0.828} c_0 = c_0 k V_{br} \div \frac{V_{br} k}{V_{bl}} = c_0 k V_{br} \cdot \frac{V_{bl}}{V_{br} k}$$

$$= c_0 V_{bl}$$

$$\therefore Q(t) = c_1 e^{-4.09 \cdot 10^{-3} t} + c_2 e^{-300t} + c_0 V_{bl} \quad (4.11)$$

Compared to equation (3.5), there is an extra exponential decay term, potentially representing the absorption part of the process. Finally, to find  $c_1$  and  $c_2$ , I substituted in the initial conditions  $Q(0) = 0$  and

$$Q'(0) = a \cdot c_0 \left( a = \frac{D \cdot A \cdot K_p}{h} \right)$$

This is because at  $t=0$ , no drug has diffused yet, so

$$Q'(0) = \frac{dQ}{dt} \Big|_{t=0} = \frac{D \cdot A \cdot K_p}{h} (c_{bl}(0) - c_{br}(0))$$

$$= \frac{D \cdot A \cdot K_p}{h} (c_0 - 0) = a \cdot c_0$$

Therefore,

$$Q(0) = c_1 e^{r_1 \cdot 0} + c_2 e^{r_2 \cdot 0} + c_0 V_{bl} = c_1 + c_2 + c_0 V_{bl} = 0$$

$$Q'(0) = c_1 r_1 e^{r_1 \cdot 0} + c_2 r_2 e^{r_2 \cdot 0} = c_1 r_1 + c_2 r_2 = a \cdot c_0$$

Therefore, the values of the constants  $c_1$  and  $c_2$  can be represented by a system of linear equations

$$\begin{cases} c_1 + c_2 = -c_0 V_{bl} \\ c_1 r_1 + c_2 r_2 = a \cdot c_0 \end{cases} \quad (4.12)$$

To solve this, I can multiply the first equation by  $r_1$  on both sides and subtract (2) from (1):

$$\begin{aligned} c_1 r_1 + c_2 r_1 - (c_1 r_1 + c_2 r_2) &= -c_0(r_1 V_{bl} + a) \\ (r_1 - r_2)c_2 &= -c_0(r_1 V_{bl} + a) \\ c_2 &= \frac{-(r_1 V_{bl} + a)}{r_1 - r_2} c_0 \\ &= \frac{-(4.09 \cdot 10^{-3} \cdot 7.58 \cdot 10^{-5} + 0.0224)}{4.09 \cdot 10^{-3} - (-300)} c_0 \\ &= -7.46 \cdot 10^{-5} c_0 \end{aligned}$$

Similarly, to solve for the other constant  $c_1$ , I can substitute this value of  $c_2$  back into equation (1),

$$\begin{aligned} c_1 &= -c_0 V_{bl} - c_2 = -c_0 V_{bl} + \frac{(r_1 V_{bl} + a)}{r_1 - r_2} c_0 \\ &= c_0 \left( \frac{-(r_1 - r_2)V_{bl}}{r_1 - r_2} + \frac{(r_1 V_{bl} + a)}{r_1 - r_2} \right) = \frac{a + r_2 V_{bl}}{r_1 - r_2} c_0 \\ &= \frac{0.0224 + (-300) \cdot 7.85 \cdot 10^{-5}}{4.09 \cdot 10^{-3} - (-300)} c_0 \\ &= -3.88 \cdot 10^{-6} c_0 \end{aligned}$$

Hence,

$$\begin{aligned} Q(t) &= c_1(-3.88 \cdot 10^{-6} e^{-4.09 \cdot 10^{-3} t} \\ &\quad - 7.46 \cdot 10^{-5} e^{-300t} + 7.85 \cdot 10^{-5}) \quad (4.13) \end{aligned}$$

To solve for the concentration functions with respect to time,

$$\begin{aligned} c_{blood}(t) &= c_0 - \frac{1}{V_{bl}} Q(t) \\ &= c_0 - \frac{c_0}{7.85 \cdot 10^{-5}} (-3.88 \cdot 10^{-6} e^{-4.09 \cdot 10^{-3} t} \\ &\quad - 7.46 \cdot 10^{-5} e^{-300t} + 7.85 \cdot 10^{-5}) \\ &= c_0 (0.0494 e^{-4.09 \cdot 10^{-3} t} + 0.951 e^{-300t}) \quad (4.14) \end{aligned}$$

Furthermore, for the concentration of the drug in the brain, I need to substitute  $Q(t)$  from equation (4.13) back into the integral from equation (4.3),

$$\begin{aligned} c_{brain}(t) &= \frac{1}{V_{bl}} e^{-kt} \int_0^t e^{kt} \frac{dQ}{dt} dt \\ &= \frac{1}{V_{bl}} e^{-kt} \int_0^t e^{kt} (c_1 r_1 e^{r_1 t} + c_2 r_2 e^{r_2 t}) dt \\ &= \frac{1}{V_{br}} e^{-kt} \left[ c_1 r_1 \int_0^t e^{(k+r_1)t} dt + c_2 r_2 \int_0^t e^{(k+r_2)t} dt \right] \end{aligned}$$

I used integration by substitution to evaluate the integrals above

$$\begin{aligned} \text{Let } u &= (k+r)t \Rightarrow du = (k+r)dt \Rightarrow dt = \frac{1}{k+r} du \\ \therefore \int_0^t e^{(k+r)t} &= \frac{1}{k+r} \int_0^{(k+r)t} e^u du \\ &= \frac{1}{k+r} [e^u]_0^{(k+r)t} = \frac{1}{k+r} (e^{kt} e^{rt} - 1) \end{aligned}$$

Therefore,

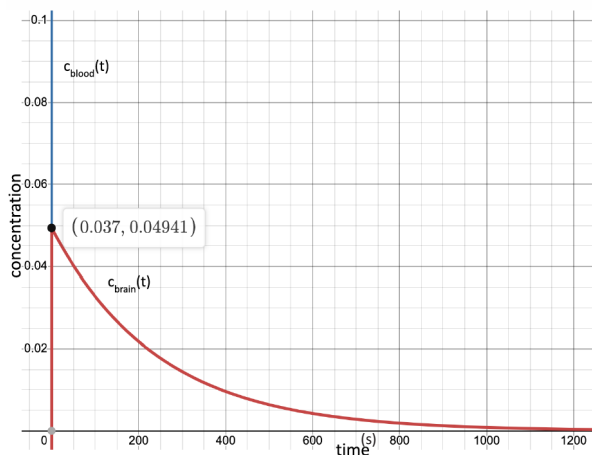
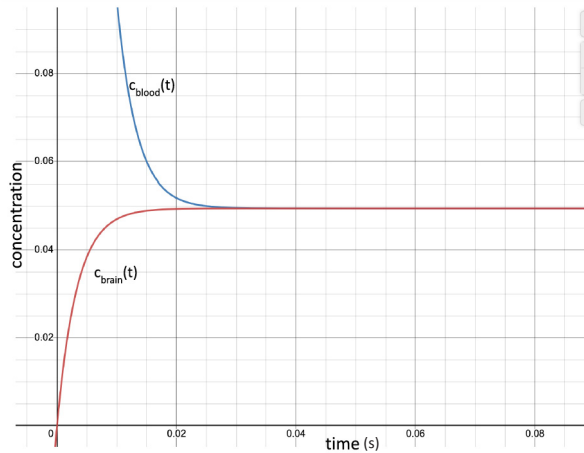
$$\begin{aligned} c_{brain}(t) &= \frac{1}{V_{bl}} e^{-kt} \left[ \left( \frac{c_1 r_1}{k+r_1} e^{kt} e^{r_1 t} - \frac{c_1 r_1}{k+r_1} \right) \right. \\ &\quad \left. + \left( \frac{c_2 r_2}{k+r_2} e^{kt} e^{r_2 t} - \frac{c_2 r_2}{k+r_2} \right) \right] \\ &= \frac{c_0}{V_{br}} \left( \frac{c_1 r_1}{k+r_1} e^{r_1 t} + \frac{c_2 r_2}{k+r_2} e^{r_2 t} \right. \\ &\quad \left. - \left( \frac{c_1 r_1}{k+r_1} + \frac{c_2 r_2}{k+r_2} \right) e^{-kt} \right) \quad (4.15) \end{aligned}$$

By substituting in all the constant values,

$$\begin{aligned} c_{brain}(t) &= \frac{c_0}{1.51 \cdot 10^{-3}} (7.46 \cdot 10^{-5} e^{-4.09 \cdot 10^{-3} t} \\ &\quad - 7.46 \cdot 10^{-5} e^{-300t} - 6.44 \cdot 10^{-17} e^{-4.31 \cdot 10^{-3} t}) \quad (4.16) \end{aligned}$$

\*Equations 4.17-4.19 that verify the coefficients can be found via the QR code at the end of the article.

## 5. Analysis of Diffusion-Absorption Equation



**Figure 5.** Concentration of drug in blood and brain over time under diffusion and absorption

The concentration-time graphs look starkly distinct from different perspectives. When I zoomed out to see the entire curve, the increasing section looked like a vertical line and then slowly began to decay. However, when I then zoomed in, setting the x-axis to  $[0, 0.1]$ , the graph looked very similar to Figure 3, where the two concentrations converged towards an equilibrium. This may be because, at the very start, diffusion dominates absorption, while as time passes, the rate of diffusion becomes near zero and the absorption process dominates diffusion. This also supports my hypothesis that  $e^{-4.09 \cdot 10^{-3}t}$  and  $e^{-300t}$  could represent the absorption and diffusion respectively because the impact of diffusion will decrease at a much faster rate since its coefficient in the exponential decay term is greater. When the value of  $t$  is large,  $e^{-300t}$  will be very small compared to  $e^{-4.09 \cdot 10^{-3}t}$  so its impact on the overall equation is minimal.

Given the coefficients that I used, the time taken to reach peak concentration in the brain is very rapid. In

particular, it only takes 0.0373s to reach the maximum regardless of the initial concentration. This may be because the surface area to volume ratio of the blood is very high ( $3.21 \times 10^5$ ), so the drug can diffuse across the barrier very quickly. Furthermore, although a higher initial concentration implies a steeper concentration gradient, there are also more drug molecules needing to diffuse through, so the time taken to reach maximum concentration is independent of the initial concentration. Then, the drug is absorbed at a significantly slower rate, eventually converging to zero.

### Peak concentration in the brain:

To find the peak concentration, I calculated the maxima point by finding the derivative of  $c_{brain}(t)$  with respect to time and setting it to zero:

$$\frac{dc_{brain}}{dt} = \frac{d}{dt} 0.0494c_0(e^{-4.09 \cdot 10^{-3}t} - e^{-300t})$$

$$\frac{dc_{brain}}{dt} = 0.0494 \cdot c_0(r_1 e^{r_1 t} - r_2 e^{r_2 t}) = 0$$

$$r_1 e^{r_1 t} - r_2 e^{r_2 t} = 0 \Rightarrow r_1 e^{r_1 t} = r_2 e^{r_2 t}$$

$$\frac{r_1}{r_2} = \frac{e^{r_1 t}}{e^{r_2 t}} = e^{(r_2 - r_1)t}$$

$$t = \frac{1}{r_2 - r_1} \ln\left(\frac{r_1}{r_2}\right) \quad (4.20)$$

$$= \frac{1}{-300 - (4.09 \cdot 10^{-3})} \ln\left(\frac{4.09 \cdot 10^{-3}}{300}\right) = 0.0373s$$

The maximum concentration is therefore given by substituting 0.0373 back into  $c_{brain}(t)$

$$c_{max} = c_{brain}(0.0373) = 0.049406c_0$$

To avoid confusion, I have used more than 3 significant figures to differentiate between coefficients with similar values.

### Time before re-administration:

Finally, from a medical perspective, it is also important to know how long it takes to be absorbed by the body. As the concentration of the drug in the brain decreases, the drug may need to be re-administered to maintain its effects for the patient. Therefore, I will find the time it takes for the concentration to fall below a certain proportion of the maximal concentration. In particular, I will solve for time  $t$  such that

$$c_{brain}(t) = p(c_{max}), \quad 0 < p \leq 1$$

Therefore

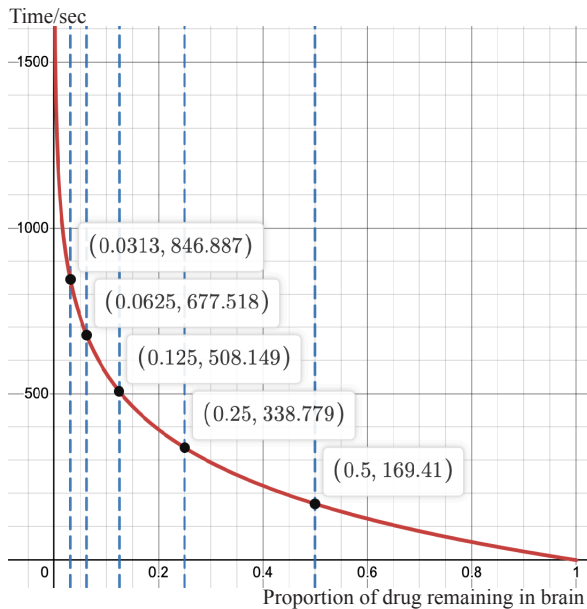
$$0.049415c_0(e^{-4.09 \cdot 10^{-3}t} - e^{-300t}) = p \cdot (0.049406c_0)$$

$$e^{-4.09 \cdot 10^{-3}t} - e^{-300t} = 0.9998p \quad (4.21)$$

This equation does not have a closed-form solution for  $t$  in terms of  $p$ . Therefore, I graphed this relationship implicitly using the equation

$$e^{-4.09 \cdot 10^{-3}y} - e^{-300y} = 0.9998x, \quad 0 < x \leq 1$$

where the y-axis is the time taken and the x-axis is the proportion left in the brain. Furthermore, since I am concerned with the time taken to absorb that amount, the range of time ( $y$ ) should be restricted to only after the concentration has peaked (ie.  $y \geq 0.0373$ )



**Figure 6.** The time taken as a function of the proportion of drug remaining in the brain

For example, if the drug needs to be re-administered when only 1/32 of the maximum concentration is remaining in the brain, then the drug will need to be re-administered every 846.887 seconds, which is around 11 minutes. I also noticed that the time taken as a function of the proportion remaining in the brain seemed to follow an exponential decay relationship, with similar times taken to reduce by half. To verify this, I calculated the first five half-lives (time taken for concentration to reduce by  $1/2$ ):

As seen from Table 1, except for the first half-life, the time taken for the drug to half its concentration in the brain is always constant, with only minute differences of 0.001 potentially due to the rounding of the times. However, it is quite interesting how this half-life of 169.369 seconds that I have calculated is greater than the initial half-life of 161 seconds that I used in section 2 to derive the rate constant of the absorption process. This may be because there is always still a small amount of drug diffusing into the brain, which in turn offsets the amount that is absorbed, so the total time taken to decrease to half of its original amount is slightly greater than if only absorption was present.

## Conclusion

In this exploration, the concentration of a drug in the blood and brain as a function of time under diffusion-absorption dynamics was found. In section 3, I considered just the diffusion part, while section 4 incorporates both absorption and diffusion. The two sets of equations display a high degree of resemblance, though the coefficients have minute differences ( $<0.00001$ ) and the constant term is replaced by an additional exponential decay term in the diffusion-absorption equation. A significant finding is how quickly passive diffusion can occur. In section 3, it only takes

Nth half-life	Remaining $c_{\text{brain}} (c_{\text{max}})$	Total time taken (s)	Half-life (s)
0	1	0.0373	n/a
1	1/2	169.410	169.373
2	1/4	338.779	169.369
3	1/8	508.149	169.370
4	1/16	677.518	169.369
5	1/32	846.887	169.369

**Table 1.** Half-life of the concentration of the drug in the brain

0.0153 s for 99% of the equilibrium concentration to diffuse; in section 4, the concentration of the drug in the brain only took 0.0373 s to reach the maximum. However, the time taken for the drug to be absorbed is significantly slower, exhibiting an exponential decay relationship with a half-life of around 170 seconds.

However, my model also has several limitations. For example, it does not account for the time taken for the drug to flow from the injection site to the blood capillaries, since it is unlikely that a drug will be directly injected into someone's skull. This will also cause the concentration of the drug in the blood to be non-uniformly distributed, so one would have to integrate over local concentration gradients to find the total rate of diffusion, adding an additional layer of complexity. Furthermore, due to the limited space in this exploration, I only focused on morphine for my drug parameters, but it would also be interesting to compare how different drugs (different partition coefficients and rate constant) would impact the concentrations over time.

**Full article as submitted to the IB,  
including Appendices**



## References

- Bhosle, V. K., Altit, G., Autmizguine, J., & Chemtob, S. (2017). *Basic Pharmacologic Principles. Fetal and Neonatal Physiology*, 187–201. <https://doi.org/10.1016/b978-0-323-35214-7.00018-4>
- Cipolla, M. J. (2009). Anatomy and Ultrastructure. In *The Cerebral Circulation*. Morgan & Claypool Life Sciences. Retrieved August 31, 2022, from <https://www.ncbi.nlm.nih.gov/books/NBK53086/>.
- Duke University. (2022). Content background: *How the route of cocaine administration affects its rate of entry into the brain*. The Pharmacology Education Partnership. Retrieved August 31, 2022, from <https://sites.duke.edu/thepeproject/module-1-acids-bases-and-cocaine-addicts/content-background-how-the-route-of-cocaine-administration-affects-its-rate-of-entry-into-the-brain/>
- Ederoth, P., Tunblad, K., Bouw, R., Lundberg, C. J., Ungerstedt, U., Nordström, C.-H., & Hammarlund-Udenaes, M. (2004). Blood-brain barrier transport of morphine in patients with severe brain trauma. *British Journal of Clinical Pharmacology*, 57 (4), 427–435. <https://doi.org/10.1046/j.1365-2125.2003.02032.x>
- Grayling, M. (2019). *Second order differential equations*. NRICH. Retrieved August 31, 2022, from <https://nrich.maths.org/11054>
- Lüders, E., Steinmetz, H., & Jäncke, L. (2002). Brain size and grey matter volume in the healthy human brain. *NeuroReport*, 13 (17), 2371–2374. <https://www.uclahealth.org/reversibility-network/workfiles/resources/publications/luders-brain-size.pdf>
- Piantino, M., Figarol, A., & Matsusaki, M. (2021). Three-Dimensional *in vitro* Models of Healthy and Tumor Brain Microvasculature for Drug and Toxicity Screening. *Frontiers in Toxicology*, 3: 656254. <https://doi.org/10.3389/ftox.2021.656254>
- Shamloo, A., Pedram, M. Z., Heidari, H., & Alasty, A. (2016). Computing the blood brain barrier (BBB) diffusion coefficient: A molecular dynamics approach. *Journal of Magnetism and Magnetic Materials*, 410, 187–197. <https://doi.org/10.1016/j.jmmm.2016.03.030>
- Smith, A. F., Doyeux, V., Berg, M., Peyrounette, M., Haft-Javaherian, M., Larue, A.-E., Slater, J. H., Lauwers, F., Blinder, P., Tsai, P., Kleinfeld, D., Schaffer, C. B., Nishimura, N., Davit, Y., & Lorthois, S. (2019). Brain capillary networks across species: A few simple organizational requirements are sufficient to reproduce both structure and function. *Frontiers in Physiology* 10: 233. <https://doi.org/10.3389/fphys.2019.00233>
- Zlokovic, B. V. (2009). Blood–brain barrier and neurovascular mechanisms of neurodegeneration and injury. *Encyclopedia of Neuroscience*, 265–271. <https://doi.org/10.1016/b978-008045046-9.00491-5>

---

# Hua Tuo's Development of the Idea of *Daoyin* in Traditional Chinese Medicine: the Five Animal Frolics

Giselle Wong

---

## Introduction

The Five Animal Frolics (五禽戲) is one of the most popular *daoyin* (導引, “pulling and guiding”) exercises in the history of Traditional Chinese Medicine (TCM). *Daoyin* is a traditional form of orthopedic therapy. In ancient Chinese history, medical *daoyin* practitioners believed that by performing specific physical movements, breathing methods, and mental strategies, *daoyin* would improve and rejuvenate the human body (Lo, 2014). Many ancient, well-known Chinese physicians utilized their knowledge of medicine and bodily anatomy to invent a set of unique and intricate *daoyin* movements and breathings to target the amelioration of different bodily functions. Traditional *daoyin* practices passed down through generations and are still used in society today. Learning about *daoyin* allows one to gain an insight into the types of practices ancient Chinese practitioners would rely on in societies with limited procedural medicine, and the significance in the value and function of *daoyin* that causes this form of medical practice to be utilized for rejuvenation and replenishment purposes across future generations.

Hua Tuo, a TCM practitioner from the late Eastern Han dynasty, occupies a significant place and is remembered as one of China's most famous medical practitioners. Combined with his years of experience in numerous fields of medicine and with creations that have changed the way practitioners perform Chinese Medicine, such as acupuncture and anesthesia, Hua Tuo utilized his knowledge on the fundamentals of *daoyin* practices to create the Five Animal Frolics. His original *daoyin* practice contains a series of animal movements specifically created to help relieve one's physical, and sometimes even mental stress and pain. As the Five Animal Frolics is arguably one of the most well-known *daoyin* exercises, it is essential to recognize why this specific form of *daoyin* has gained its popularity and how Hua Tuo built on the idea of *daoyin* to create the Five Animal Frolics (May *et al.*, 2000).

This paper aims to explain the history and ancient uses of *daoyin*, situate Hua Tuo in the *daoyin* tradition and elucidate Hua Tuo's Five Animal Frolics. Although Hua Tuo did not leave a personal record of his work regarding the Five Animal Frolics, there are records of his work written in other texts during his period, such as *San Guo Zhi* (三國志) and *Hou Han Shu* (後漢書). These are the two main primary sources I will be referencing in this essay.

*Daoyin* and Hua Tuo's creation of the Five Animal Frolics have played a significant role in Chinese culture and have been incorporated into medical exercises and martial art training. This paper highlights Hua Tuo's approach in including animal movements into his form of *daoyin* exercise and the significance of the Five Animal Frolics on contemporary *daoyin* practices and on Chinese medicine as a whole.

## 1. *Daoyin* and its Utility

*Daoyin* is essentially a form of exercise originating in ancient China that combines breathing, the stretching and twisting of limbs, and mental focus to direct the flow of *qi* [breath, energy] and restore the body's internal balance. It is practiced as a form of Daoist *nei gong* (內功, spiritual and breathing meditations associated with Daoism and Chinese martial arts) as the underlying theory for the correlation of *daoyin* with Daoist beliefs. Different *daoyin* exercises target the healing of different parts and problems in the body. The name *daoyin* can be separated into two parts: *dao* means the action of guiding, and *yin* means to guide and stretch the body in order to gain strength and flexibility (Chen *et al.*, 2019).

In Chinese medicine, it is believed that our bodies were created to be balanced. Health and long life are manifested in the overall balance of *qi* in the body by working with the force to the best of one's ability, to enable attainment of perfect internal balance and utmost harmony. Imbalances of *qi* in body systems can be caused by actions and environments that harm

---

The above article was written as a culminating essay for the Shuyuan (italicize Shuyuan) NRI Scholar's Summer Retreat, 2022.

physical, emotional and mental states, thus causing the body to be prone to illnesses and disease. After the Manual of Therapeutic Gymnastics (*Yinshu*, 引書) was excavated from Mawangdui Tomb 3 in 1974, it was believed that the origin of *daoyin* can be traced back thousands of years. What is now known as the “Pulling and Guiding Chart” (*Daoyin Tu*, Figure 1) was found among the artifacts discovered that were sealed around 168 B.C.E. It is a chart painted on silk that depicts figures demonstrating the movements of more than 44 different *daoyin* exercises used during ancient times to improve health. During that period of time, people were not only looking into the physical movements of *daoyin*, but also the underlying theory (Chen *et al.*, 2019). Chinese philosophers and medical practitioners who experimented with the function of *daoyin* believe that its practice will help maintain the harmony of *qi* and blood in the body, useful in preventing disease, improving health, accelerating the recovery of limb function, and developing a vital and healthy spirit (Chen *et al.*, 2019). Because of this, *daoyin* was and still is widely applied to medical treatments and health preservation procedures.



**Figure 1.** Reconstruction of “Guiding and Pulling Chart” (Wellcome Collection)

*Daoyin* plays a significant role in understanding of transformation being reflected in external and internal alchemy, as it was first practiced in Chinese Daoist monasteries. Later on, it was also used as a means to achieve immortality. One type of *qi* is *jing* (精), which is the energy that provides one with vitality and strength. Daoists and Chinese doctors believe that although having a perfect inner balance and body function can allow us to live up to 120 years, it is natural to lose *jing* regularly, thus causing the body to go through gradual physical decline and death. However, practicing *daoyin* will allow this process to slow down and extend one’s lifespan (Chen *et al.*, 2019).

*Daoyin* was incorporated in many Chinese philosophical teachings, such as the *Zhuangzi* (莊子). In the chapter “Ingrained ideas”, it says:

吹响呼吸，吐故納新，熊經鳥申，為壽而已矣，此道引之士，養形之人，彭祖壽考者之所好也。

Blowing and exhaling, expelling the old and taking in the new, studying the classics of bear and bird, only for the sake of longevity. This is the practice of those who pursue it, nourishing the body and the mind. It is also favoured by those who seek long life, such as Pengzu.

*Zhuangzi* explains how those who nourish the body manipulate their breath by blowing and breathing, inhaling and exhaling the breath with an open mouth, and passing their time like the dormant bear, as well as stretching and twisting the neck like a bird to achieve longevity. However, *Zhuangzi* may have been skeptical about the effectiveness of *daoyin*. Looking at ancient sources such as the “Guiding and Pulling Chart”, *daoyin* is portrayed as an exercise to nourish the inner and outer body. But according to quote above, the phrase *yang xing zhi ren* (養形之人) translates to the nourishment of just the outer appearance. This shows how *Zhuangzi* may have misunderstood the intention of *daoyin*.

## 2. Hua Tuo and the Five Animal Frolics

Also known as China’s most famous ancient surgeon, Hua Tuo is also known for his herbal remedies, moxibustion, and other ideas on *daoyin*. He was born around 111 C.E. in the Kingdom of *Wei* 魏 (modern day *Jiangsu* 江蘇 Province).

Hua Tuo’s ultimate fame came from his invention of general anesthesia. He used hemp, a botanical class of cannabis specifically grown for medicinal and industrial use, and wine to create an oral herbal medication that would help patients temporarily desensitize to pain. This medicine was known as *mafeisan* 麻沸散, the first anesthetic ever created in the history of China, and was reportedly very effective (Kohn, 2008).

Even though Hua Tuo did not leave any personal record after his death, his reputation among Chinese society can be seen through ancient texts such as *The Book of the Later Han*. Records say that even though Hua Tuo lived to be 100 years old, he looked much younger and acted like a sprightly sixty-year-old throughout his life. People thought he had divine powers and named him “The Divine Doctor”. Quoting *The Book of the Later Han*, “Divinity could also stem from his extremely accurate diagnoses, which bordered on fortune-telling. He could mix medicinal ingredients so well that he never needed to measure them.” Figure 2 is an ancient



print of an outsized Hua Tuo underneath the red temple, with offerings of different fruits, portraying him as a figure worth respecting and worshipping. The Chinese phrase “華佗神醫” displayed on the print means “Divine medic Hua Tuo”, exhibiting how respected he was during the Later Qing Dynasty period.



**Figure 2.** “華佗神醫” ancient painting during the Later Qing Dynasty period (National Museum of History)

Hua Tuo created his very own *daoyin* exercise named the Five Animal Frolics. Instead of treating solely by medication, Hua Tuo would recommend physical exercise for people as a method of recovery, rejuvenation and most importantly, disease prevention. The practice of the exercises include embodying the qualities of animals (tiger, deer, bear, monkey and bird) within physical movements, which Hua Tuo recommended to practice in sequence. The entire exercise consists of ten movements, two for each animal. Each animal closely aligns with a specific season, organ and emotion. The five main aspects of the universe’s ongoing existence and development (fire, earth, water, metal and wood), important to both Daoism and TCM, are also aligned with the five animals and exercises. Each animal movement is said to provide specific health benefits, and the distinctive hand forms incorporated into the exercise would help improve manual dexterity and increase one’s grip strength (Ru, 1999).

The chapter “The Legend of Hua Tuo” in *The Book of the Later Han* records the function and purpose of Hua Tuo’s Five Animal Frolics:

吾有一術，名五禽之戲：一曰虎，二曰鹿，三曰熊，四曰猿，五曰鳥。亦以除疾，兼利蹄足，以當導引。體有不快，起作一禽之戲，怡而汗出，因以著粉，身體輕便而欲食。

I have a skill called the “Five Animal Play”: the first is the tiger, the second is the deer, the third as to guide and lead. When the body is uncomfortable, performing the movements of one of the animals can bring joy and make one sweat. Afterwards, applying powder can make the body feel light and agile, and increase appetite.

Hua Tuo also believed that the human body wants to work, but it should not be pushed over the limit. Accordingly to him, when we cooperate with the body, the blood will circulate, and diseases will not emerge (May *et al.*, 2000).

In later generations, the tiger would become associated with the element of wood, the season of spring, the body’s liver and gallbladder, as well as the emotion of anger. The individual’s eyes should be glaring with ferocity, and the hand should be strengthening the sinews. In TCM, the liver governs the body’s tendons and sinews, allowing the body to move. The routine of the tiger would require balance, strength and flexibility as those are the key traits a tiger would need to catch its prey and survive. This routine should be performed strenuously but containing inner softness (Balaneskovic, 2018).

The monkey was associated with the element of fire, the season of summer, the body’s heart and small intestine, as well as the emotion of joy. The first part of the routine would require movements into the individual’s chest allowing the heart to pump, and blood to be directed throughout the body. The second part of the routine would balance out the heart’s fire with water from the kidneys by raising the ball of the trailing foot. Since monkeys are flexible, sprightly beings, the quick hand movements would require great amounts of coordination and concentration (Balaneskovic, 2018).

The bear was associated with the element of earth, the season of late summer, the body’s stomach and spleen, as well as the emotion of worry. A bear is solid, stable and grounded, resembling the earth element, which will require the individual to perform slowly with strength and steadiness. The first part of the exercise would require the massage of the stomach and spleen in order to aid digestion, while at the same time rotating the upper body in order to improve mobility of the waist and spine (Balaneskovic, 2018).

The crane was associated with the element of metal, the season of autumn, the body’s lungs and large intestine, and the emotion of sadness. As the crane represents longevity and grace by standing on one

leg effortlessly for hours, the individual should also perform this routine in a carefree and relaxed manner. The focus of this exercise is balance and concentration, especially during the weight-transfer from one leg to the other. The individual should move their hands gracefully, representing a crane when moving its wings (Balaneskovic, 2018).

Lastly, the deer was associated with the element of water, the season of winter, the body's kidneys and bladder, as well as the emotion of fear. The individual should perform this routine in a gentle but lively manner, and listen to their surroundings as it embodies the quality of the water element. The frequent twisting movements would activate one kidney and close the other, creating a pumping effect among both kidneys. This routine targets multiple functions of the human body, allowing the individual's chest to open, muscles to relax and improves shoulder and spinal mobility (Balaneskovic, 2018).

In the book “*Baopuzi* : Inner Chapters” (chapter “The Truth”), it is rumored that Hua Tuo had a disciple named Wu Pu, who learned the Five Animal Frolics from Hua Tuo and was determined to practice daily. After rigorously practicing everyday for the rest of his life, Wu Pu grew older than a hundred years old, also miraculously maintaining his dark black hair and full set of teeth. Wu Pu was an ancient epitome of how the Five Animal Frolics may have been the reason behind his longevity and youthful appearance, which persuaded other people to engage in this practice.

## 2.1 The Five Animal Frolics : Creation Inspirations

Historians were able to associate aspects of the Five Animal Frolics with *Zhuangzi's* spiritual practice. Within *Zhuangzi's* writings, there were mentions of the vibrant culture of *yangsheng* 養生 and the physical methods of nourishing life. *Yangsheng* is essentially a compilation of macrobiotic practices that focus on increasing one's longevity, even to the point of immortality. These practices include breath work, fasting, *daoyin* exercises, sexual practices and lifestyle taboos. Both *yangsheng* and *daoyin* have the same goal, however Hua Tuo combined the aspects of breath work and *daoyin* exercises together in order to boost efficiency and effectiveness, as performing both at the same time will allow one to guide more *qi* and channel more energy into curing diseases (May *et al.*, 2000). Furthermore, both exercises require the practitioners to have mental focus and attentiveness; solely completing the physical movements will not help an individual reach their desired outcome. *Zhuangzi* believed that

anything could be considered a method of *yangsheng* as long as one's spiritual state of heightened awareness is present. Within the Five Animal Frolics, one will need to be attentive to every move they perform, as well as feeling the mental behaviors and characteristics of each animal. Each animal exercise will need to be performed with different mindsets in order to achieve perfect internal balance. In wanting to create an exercise that could target almost all diseases and problems, Hua Tuo is believed to have chosen the five animals because they symbolize different aspects of the human body and nature, creating a perfect balance when practicing the entirety of the exercise (Balaneskovic, 2018).

## 2.2 The Five Animal Frolics & *Daoyin*: Popularity in Modern Society

Medical practitioners say that *daoyin* can also be used for therapeutic effects on central nervous system and peripheral musculoskeletal disorders, as well as heart diseases. A *daoyin* practitioner extends and flexes the body under the guidance of his or her active consciousness (Ru, 1999). The stretching balances the muscle contraction force around the joints of the limbs, and increases the volume of the limb tissue fluid, forming a stretch-fluid loop. If such exercise is practiced for a long period of time, it benefits the central nervous system's ability by regulating and controlling the muscles, which then enhances limb flexibility, physical agility and rehabilitates musculoskeletal diseases. For heart diseases, based on a scrutiny of literature, it is found that the practice of *daoyin*, specifically the Five Animal Frolics, increases blood volume of venous return but also strengthens the contractility of cardiac muscle tissue, therefore allowing enhancing the pumping force of the heart in the long run (Chen, *et al.*, 2019).

*Daoyin* has been incorporated into other aspects of Chinese culture. For example, it is now the primary ingredient in one of the main forms of traditional Chinese martial arts, *Tai chi quan* (太極拳). *Tai chi quan* works with *qi* to explore the balance between the sky and earth, the yin and yang of life. In modern society, *daoyin* is more frequently referred to as *qigong*, even though *qigong* refers to the use of *daoyin* in *Tai chi quan*. The softening and loosening of the body and joints, as well as the turning and twisting of limbs in many movements of *Tai chi quan* stimulates, massages and brings blood circulation to the internal organs, and increase one's energy quotient (Ru, 1999).

There are two main reasons as to why the Five Animal Frolics Exercise became so well-known. Firstly, as

a figure so well-respected and worshiped in ancient Chinese history for the invention of anesthetics and his surgical skills, people romanticized and glorified Hua Tuo's work, allowing his other inventions to come into fame. Secondly, Chinese martial artists have had the constant belief that humans never developed the natural instincts and behaviors that animals use to survive in the wild. Therefore, Hua Tuo's development on the idea that humans could utilize the characteristics of animals to improve and rejuvenate human bodily functions, is a unique exploration.

## Conclusion

In conclusion, *daoyin* is a type of non medicinal treatment that combines physical movements, breathing, and mental focus to target general or specific problems in the human body. Hua Tuo may have taken inspiration from other ancient texts and charts in developing his own exercise, also known as the Five Animal Frolics, one of the most well-known forms of *daoyin*. The physical movements and instructions were designed in a way that direct the flow of *qi* and restore the body's internal balance. The Five Animal Frolics has been taught and passed down for generations, leaving a lasting impact on traditional Chinese *daoyin* and martial arts.

## References

- Balaneskovic, Saša. (2018). *Hua Tuo's Wu Qin Xi (Five Animal Frolics) Movements and the Logic behind It*. [online] 1(3), 127–134. doi:[https://doi.org/10.4103/cmac.cmac\\_32\\_18](https://doi.org/10.4103/cmac.cmac_32_18).
- Chen, X., Cui, J., Li, R., Norton, R., Park, J., Kong, J. and Yeung, A. (2019). Dao Yin (a.k.a. Qigong): Origin, Development, Potential Mechanisms, and Clinical Applications. *Evidence-Based Complementary and Alternative Medicine*, 1-11. doi:<https://doi.org/10.1155/2019/3705120>.
- Divine Medic Hua Tuo* (神醫華陀). *National Museum of History 國立歷史博物館*, 2023, <https://funchengnan2.nmh.gov.tw/fun/view?id=90cefb7bb72f450281608567f78093dc>. Accessed 6 Jul. 2023.
- Hong, Ge. (2016) *Baopuzi: Inner Chapters*. (抱樸子:內篇). Translation by Chinese Text Project, <https://ctext.org/baopuzi/zh>. Accessed 30 Jan. 2023.
- Hou Han Shu*. (後漢書) Chinese Text Project, 2016, [ctext.org/](https://ctext.org/). Accessed 30 Jan. 2023.
- Kohn, Livia. (2008). In: *Chinese Healing Exercises: The Tradition of Daoyin*. Honolulu, Hawaii: University of Hawaii Press, pp.1–28.
- Lo, V. (2014). *How to do the Gibbon Walk: a Translation of the Pulling Book* (ca 186 BCE). Cambridge: Needham Research Institute Working Papers.
- May, B., Tomoda, T. and Wang, M. (2000). The Life and Medical Practice of Hua Tuo. *Pacific Journal of Oriental Medicine*, 14, 40–54.
- Ru, K. (1999). The analysis on movement of China Dao Yin skill and its inspiration. *Journal of Capital University of Physical Education and Sports*, 2, 90–91.

## Bibliography

- Hua Tuo | Chinese physician and surgeon | Britannica. (2019). In: *Encyclopædia Britannica*. [online] Available at: <https://www.britannica.com/biography/Hua-Tuo>.
- “Zhuangzi | Internet Encyclopedia of Philosophy.” *Internet Encyclopedia of Philosophy*, 2015, [iep.utm.edu/zhuangzi-chuang-tzu-chinese-philosopher/#SH3c](http://iep.utm.edu/zhuangzi-chuang-tzu-chinese-philosopher/#SH3c). Accessed 30 Jan. 2023.

# How do Anti-reflective Coatings Affect the Power Generation of Solar Panels?

Skylar Rach

## 1. Research Background

The use of photovoltaic cells in solar panels remains a leading source of growth in renewable electricity generation (Figure 1), with a capacity of almost 160 GW according to the International Renewable Energy Agency (IEA, 2021). Figure 2 shows the core principles of operation of solar cells. Unfortunately, only 20% of the energy from residential solar panels is actually turned into electrical energy (Zito, 2023) One source of solar energy loss is the reflection of light off of the panels.

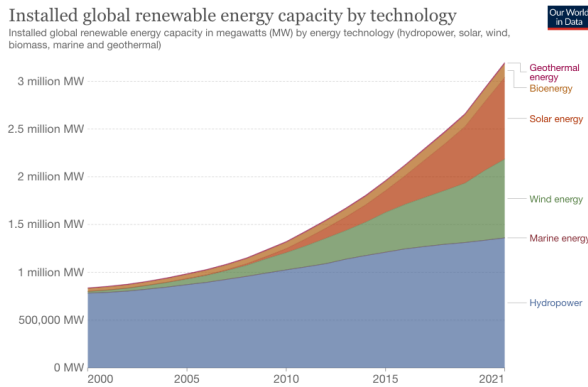


Figure 1. Renewable Energy Capacity

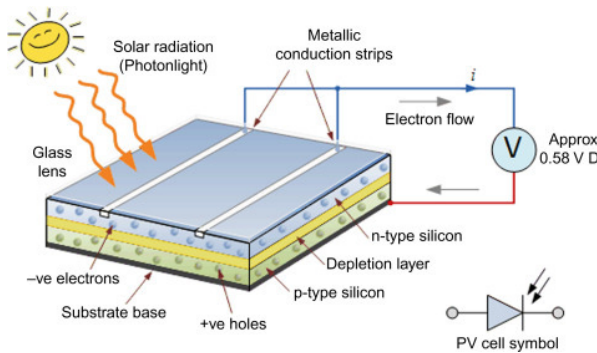


Figure 2. PV Panel Operations

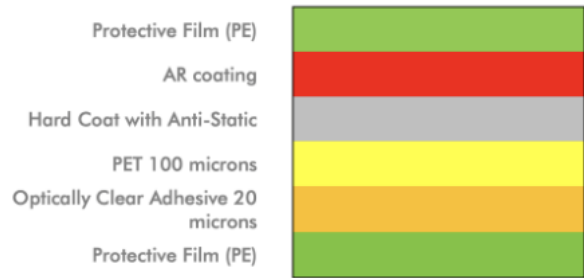


Figure 3. Layers in PV Panels including AR Coating

The Sustainable Development Goal that relates to my research is Goal 9: Industry, Innovation, and Infrastructure (Figure 5). Given the significant increase in the use of solar energy in the past 10 years, (*Solar energy*, no date) my study focuses on determining a specific method to increase the efficiency of PV solar panels through the use of anti-reflective coatings (ARC) using nano-structures that offer improvements of 2-3% in efficiency. Even a small increase in efficiency will have a massive impact on the power generation of solar farms around the world: more than one GW - equivalent to 3.125 million additional solar panels (Fasching & Ray, 2022).

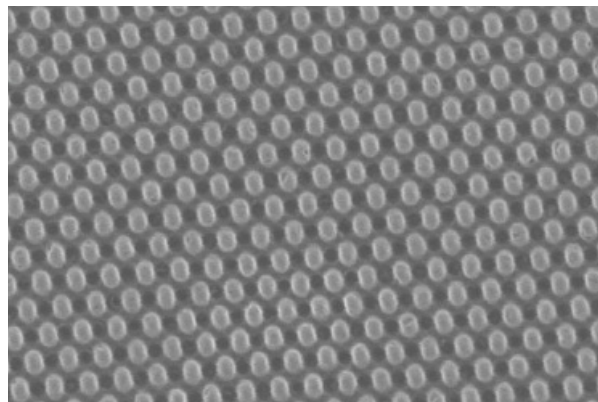


Figure 4. SEM image of moth-eye nanostructures

The above article was written as a culmination of research presented at the Fall Meeting of the American Geophysical Union (AGU), 2022.

The use of nanocoatings initially focused on the reduction of fouling of the solar panels by dust, pollution, rain, and bird droppings (Yadav & Mishra, 2013) by developing coatings with unique properties to repel water, or smooth the surface, thereby reducing maintenance and operational costs. A further area of research has been focused on the increased efficiency with the deposition of anti-reflection (AR) layers onto the photovoltaic (PV) substrate to enhance its light-collection efficiency (Figure 3). Harder *et al.* (2005) simulated this effect and Chang *et al.* (2013) used a mesoporous silicon dioxide (SiO<sub>2</sub>) film as an AR layer to achieve up to 6% enhancement in the photocurrent generation of a solar cell (Lan *et al.*, 2021).



Figure 5. SGD Number 9

## 2. Methodology

This experiment used a 25-watt PV solar panel in combination with the Diamox AR1617 anti-reflective film from Diamond Coatings. Voltage was recorded using a voltmeter in the experimental setup as shown.

The solar panel was placed on a table with LED lights placed one meter above to serve as a control for the lighting though it is noted that LED lights are not a perfect replication of the wavelengths of the solar energy of the Sun. Initial readings were recorded with no film. Then, using the anti-reflective (AR) coating, one layer was placed over the panel and voltage readings were taken. As AR coatings work based on the angle of light, the experiment was repeated with the panel elevated 25 and 45 degrees for three trials (Figure 6).

A further investigation of AR Coating and Solar Cell cross section was conducted with the Scanning Electron Microscope (SEM) with the results shown (Figures 7 and 8).



Figure 6. This SEM image shows the cross-section of AR coating

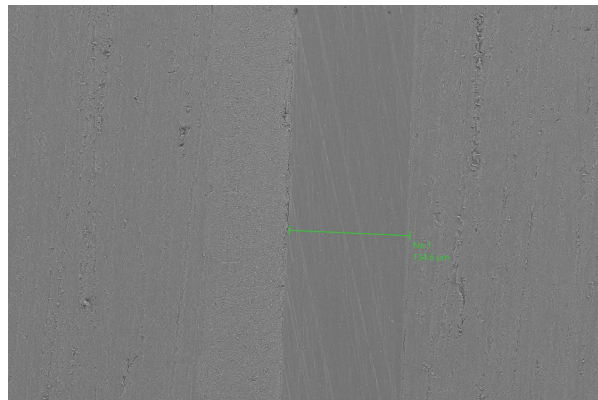


Figure 7. This SEM image shows the cross-section of AR coating

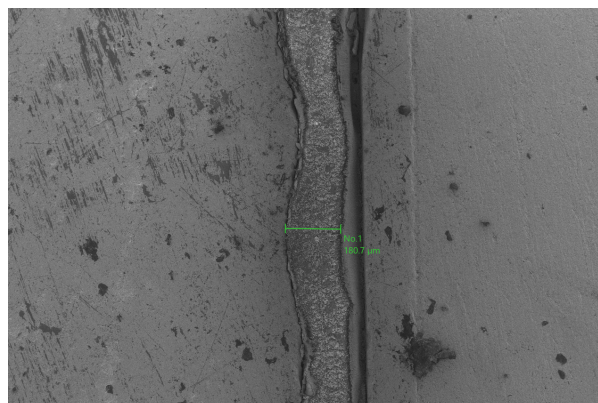


Figure 8. This SEM image shows the cross-section of a solar cell

### 3. Experimental Results

Unexpectedly, the use of the AR film did not result in an increase in the voltage generated (Figures 9 and 10). In reviewing the material specifications of the Diamox film coating (Diamond Coatings, 2022), it states the coating has a luminous transmission of 94.4% (meaning a net loss of light energy passed through the coating) which could account for this experimental error. The supplier has stated that this coating was appropriate for use in solar installations but made no claims of an increase in efficiency in the use of solar cells with the coating. It may be that the intended use is for anti-reflectivity for other purposes.

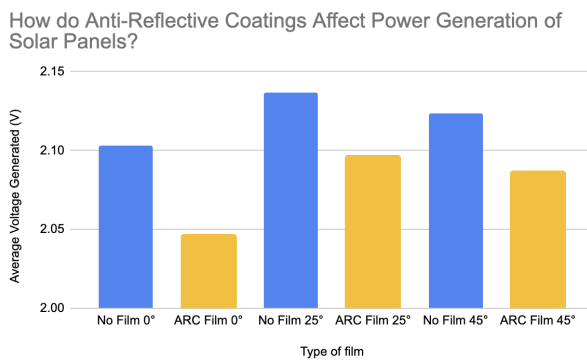


Figure 9. Experimental results

Trials	Volts Generated					
	No Film 0°	ARC Film 0°	No Film 25°	1 Layer 25°	No Film 45°	1 Layer 45°
1	2.10	2.05	2.14	2.10	2.12	2.09
2	2.11	2.04	2.13	2.09	2.13	2.08
3	2.10	2.05	2.14	2.10	2.12	2.09

Figure 10. Experimental data

### Conclusion

From the literature review conducted, it was expected that the trials with the AR film would result in increased voltage or PCE. Further insight would be gained from varying the angle of incidence closer to 90 degrees in order to quantify any measurable effect of the nano-structures in the AR coating. Ideally, the light should be perpendicular to the PV panel to maximize the penetration of the sunlight into the panel, but this is often difficult for fixed panels (the majority of installations).

Unfortunately, the experimental data did not show positive results. By testing multiple times, experimental error was reduced. However, there are other possible explanations of these results including: 1) the tested solar panels may have an anti-reflective layer/coating applied in manufacture that conflicts with the added AR film and 2) this particular AR Film may not be optimized for solar cell efficiency. Discussions with the supplier were inconclusive - their specifications mentioned a 94.4% transmission of light which would account for the decrease in voltage observed.

Ongoing research is being conducted with alternate suppliers of AR films and spray coatings to determine suitability for solar panel efficiency improvement. Further experimental trials will be conducted to produce the expected gains in efficiency.

## AGU 2023 Poster



## Solar-related SEM Images



## References

Chang, Y. M., Su, Y. Y., & Leu, C. Y. (2013). Improvement in power conversion efficiency of organic photovoltaic devices by using excimer ultraviolet-radiation induced mesoporous silica anti-reflection coating. *Thin Solid Films*, 534, 492–496. <https://doi.org/10.1016/j.tsf.2013.02.078>

Diamond Coatings. (2022). Diamond Coatings AR1617 *Anti-Reflective PET Film*. [online] Available at: <https://diamondcoatings.co.uk/diamond-coatings-ar1617-anti-reflective-pet-film/> [Accessed 30 Nov. 2022].

Fasching, E. and Ray, S.. (2022). Solar power will account for nearly half of new U.S. electric generating capacity in 2022. *EIA*. [online] Available at: <https://www.eia.gov/todayinenergy/detail.php?id=50818> [Accessed 27 Aug. 2023].

Harder, N. P., Blieske, U., Neander, M., Neumann, D., Mahe, E., & Mogensen, P. (2005). Evaluation of anti-reflection coatings on cover glasses for solar modules; getting down to the nitty gritty. *Conference Record of the Thirty-First IEEE Photovoltaic Specialists Conference*, 2005, 1792-1795. <https://doi.org/10.1109/pvsc.2005.1488499>

IEA (2021), *Renewables 2021, IEA*, Paris <https://www.iea.org/reports/renewables-2021>, License: CC BY 4.0

Lan, W.; Chen, D.; Guo, Q.; Tian, B.; Xie, X.; He, Y.; Chai, W.; Liu, G.; Dong, P.; Xi, H.; *et al.* Performance Enhancement of All-Inorganic Carbon-Based CsPbIBr<sub>2</sub> Perovskite Solar Cells Using a Moth-Eye Anti-Reflector. *Nanomaterials* 2021, 11, 2726. <https://doi.org/10.3390/nano11102726> [Accessed 30 Nov. 2022].

*Solar energy* (no date). <https://www.irena.org/Energy-Transition/Technology/Solar-energy>.

Yadav, V. and Mishra, A., 2013. Role of nanocoating in maintaining solar PV efficiency: n overview. In Conference: *National Seminar on Recent Trends and Development in Nano Materials, At IIMT Engineering College, Meerut, UP*.

Zito, B. (2023). Most Efficient Solar Panels Of 2023. *Forbes*. [online] 12 Jun. Available at: <https://www.forbes.com/home-improvement/solar/most-efficient-solar-panels/> . [Accessed 19 Jun. 2023].

---

# Connections and Comparisons: a Study of Science, Societal Psychology, and Geopolitics in the Manchurian Plague

*Katrina Chan*

---

## Introduction

The Manchurian Plague originated in 1910, when the region's thriving and prominent fur trade accelerated the disease's spread from local marmots to humans. A common hunting area for the marmots was in northeast China. The climate there was dry, arid, and grueling. The hunters often, the hunters failed to satiate their basic needs, instead resorting to "eating the flesh of the marmot and drinking water squeezed out of the towel which has been left on the grass during the night to catch the dew" (Summers 123). They lived in cramped cabins, with the windows seldom, if ever opened; there was a constant foul stench emanating from the occupants and the marmot carcasses. As such, the hunters' immune systems were naturally weakened and prone to infection. This suggests that prior to the plague, health precautions were not addressed, especially within the hunter population, which led to Manchuria's inexperience with the spread of disease. Meanwhile, Manchuria was a place of political interest to many superpowers. In China's weakened state after the fall of the Qing dynasty, Russia and Japan built railways leading into Manchuria; however, these tracks were not closely monitored. These factors combined, when the marmot hunters began to contract a blood-spitting disease, it spread quickly across the railways and escalated into the full-blown epidemic known as the Great Manchurian Plague.

The Manchurian Plague is particularly pertinent to current affairs as the world emerges from the devastating COVID-19 pandemic. This paper presents an analysis of the science, societal psychology, and geopolitics during 1910–1911 in Manchuria with the aim of drawing insightful points of consideration to the present situation.

## 1. Science in the Manchurian Plague

### 1.1 Dr. Wu Lien Teh's Involvement

Dr. Wu Lien-Teh was born to a family of Chinese immigrants in Penang, Malaysia. He was the first student of Chinese descent to earn a medical degree from Cambridge and was appointed to investigate the Manchurian Plague, working with government officials to establish plague prevention measures. The first mask with multiple filtering layers of gauze and cloth was invented by him and was widely recommended for wear during the plague. It is believed to be "the precursor to the N95 mask" (Dr. Wu Lien-teh's 142nd Birthday). He hosted the International Plague Conference and after the plague, became the founder of the Chinese Medical Association in 1915, China's largest and oldest medical non-governmental organization (NGO).

The Manchurian Plague had been classified as bubonic by the Russia in early 1911, whilst Dr. Wu Lien-Teh had found it was actually a pneumonic variant (Summers 21). He attempted to warn the Russians of his findings, to no avail, and Russian investigations of the plague began without taking the necessary respiratory precautions. A rat-catching and dissecting program commenced, and the epidemic was referred to as the bubonic plague. Things worsened when prominent French physician and head professor of the Peiyang Medical College, Dr. Girard Mesny, "refused to accept Wu's evaluation and failed to take precautions" (Summers 21) when sent to Harbin to investigate. He died six days later. His death was a turning point: after all, if an experienced Western physician could succumb to the plague, citizens would not be spared.

Wu's evaluation was accepted and the Chinese government consequently sent soldiers and police to Manchuria in order to control population movements and enforce quarantines, with Wu himself sent to Harbin to investigate in December. This implies a major change in societal thinking: initially, citizens were evidently more inclined to accept Western opinion; however, their

---

The above article was written as a culminating essay for the *Shuyuan* NRI Scholar's Summer Retreat, 2021.



fear of death overcame their bias and they turned to Wu's more trustworthy opinion. The plague prevention efforts eventually proved effective, and within 4 months of Wu being tasked to combat and control the spread of the plague, the crisis had been averted. The final case reported in Harbin was on 1 March 1911, with the final death toll being around 45,000 to 60,000 (Summers 78). The International Plague Conference was held in the aftermath in Mukden, during which the North Manchurian Plague Prevention Service was created, marking the beginning of public health in China.

A less severe relapse of the plague broke out again in 1920–1921, this time mainly in Korea, and Manchuria was effective in an almost immediate halt of the spread of the plague.

## 1.2 Plague Prevention Measures

Due to his modern medical training in Europe, Wu was able to use approaches that were admired and agreed on by European, American and Japanese medical authorities. This instance likely marked one of the first times in which Western medicine began to acquire knowledge from a Chinese doctor regarding modern diseases. (Summers 21).

When the plague was discovered, the mortality rate was near 100%. At one point Wu had reported seeing “two thousand coffins in rows, with more dead on the ground because of a shortage of coffins” (Summers 21). He began to worry that rats and pests alike would be infected by eating the dead, so enlisting the support of local officials, he wrote a memorial to the throne requesting mass cremation of the dead, which was granted. For the first time in Chinese history, authorized autopsies on unclaimed bodies of plague victims were also granted. The initial approach to plague prevention was more forceful in order to keep the widespread panic under control. Government officers were instructed to shoot anyone trying to escape, and the police went door to door looking for the dead from the plague (Yan). It is interesting to consider this concept of countering death with death; however, this was likely utilizing the approach of 殺雞儆猴 [kill the chicken to warn the monkey], a idiom referring to the theory that threat of punishment will deter people from violating the law, especially in the case where the punishment is reinforced once, thereby proving its actuality and reducing the probability of further incidences.

The Commercial Guild of Mukden opened a plague hospital in February 1911, but most patients and staff died due to poor attention and maintenance of hygiene: patients were often unfed for up to 24 hours, rooms

were unheated despite the plague having been found to thrive under cooler conditions. Patients were able to escape through the lax guard, police officers were being bribed to allow secret burials by desperate families, and staff were found stealing the belongings of dead or dying patients (Nathan 13-16).

As a result, an order was handed down to close the merchant hospital and to arrest the guild's police. There was a mortality rate of 44% of native doctors involved. This demonstrates that the plague was not taken seriously at first and there were consequences in terms of mortality, which led to the doctors' realization of the importance of punishing those who were not diligent in plague prevention in order to set an example for the citizens; this likely increased the community's trust in the medical personnel and in turn made them more receptive to plague prevention.

By mid-December of 1910, governor General Affanasiev of Russia had published a list of plague prevention measures, one of which was a military-enforced cordon around *Fuchiatien* 傅家甸, the Chinese-governed section of Harbin (Summers 57). Violators of the cordon would—similarly to escapees—be met with a punishment of death. All travelers were subject to a five day quarantine and disinfection of all tarbagan (marmot) skins were required. There was a mandatory separation of passengers and cargo. Exports of leather, furs, animals and food from plague regions were retained, if not strengthened; and the conference recommended anti-rat campaigns in such regions.

Russian and Chinese authorities agreed to enforce quarantines and population movements. The only reliable signs of plague infection were the symptoms of declining health then, so the medical authorities decided to carry out the simplest measures possible under the pressure of the possibility of a mass epidemic. Groups of potentially exposed individuals were quarantined inside railway cars accommodating up to several dozen people for 5–10 days at a time. If no signs of impending death were observed in the group, all individuals were deemed uninfected and were safely released. To identify these healthy individuals, they were tagged with wristbands indicating that they had been quarantined, examined and certified plague-free, and were thus allowed to resume their activities (Summers 57-59). There were some limitations to this approach, however: one singular case of plague in one of these railway cars meant a near-certain death for all those inside the same compartment as the confinement in close quarters maximized the spread of the disease. The death of innocent passengers sparks a moral debate on the topic; however, it is worth considering that this

method allowed control over the exact mortality count instead of the alternative, where the plague could potentially spread at exponential rates. It was thence deemed appropriate to sacrifice the immediate lives of few individuals in exchange for a projected lower infection rate overall.

### 1.3 Medical Investigations and Innovations

As part of his training, Wu had previously studied infectious diseases in Paris. Previously, a one-layer surgical mask had been used. Wu added on to this mask with air-filtering layers of gauze and cloth that were effective in intercepting and absorbing pathogen-laden airborne particles before they were inhaled, turning the masks into a “two-way disease defense” (Yang) for the first time and invented the multi-layered mask that is now widely known as the precursor to the N95 mask, said to offer the best protection against COVID-19 today (Ma).

Wu also managed to perform a limited autopsy on a woman who had just died on his third day in Harbin. This was surprising and fortunate considering cultural taboos associated with interfering with the dead during that time (Summers 64). He was able to observe massive infections of the lungs, heart, spleen and liver of the Yersin’s plague bacillus, which allowed him to prove that the plague was pneumonic and not bubonic as Russian scientists had previously stated. During the second spread of the plague, Wu was able to carry out many experiments on the plague bacilli and came to a series of conclusions (Wu *et al.* 328):

1. The plague bacilli *B. pestis* found in sputum were found to be resistant to cold but weak to sunlight—even in  $-3^{\circ}\text{C}$  weather, *B. pestis* was killed within 9 hours of direct sunlight.
2. Mere drying of the plague sputum was found ineffective in termination of the plague.
3. Strong disinfectants and antiseptics, for example, carbolic acid lotion 1:10, required 5 minutes to prevent growth of *B. pestis* in sputum. Concentrated alcohol was found to be the surest means of sterilizing.
4. The disinfection of surfaces and clothing were highly necessary.
5. The cotton-gauze mask, when properly applied, was the most effective means of protection against respiratory infection. For practitioners in constant and immediate contact with patients, wearing an additional hood with a piece of silk sewn on in front with the usage of goggles was highly recommended.

These conclusions later allowed him to make recommendations to the general public as to methods of disinfection and plague prevention.

Throughout the plague, considerable impacts were made on advances of medicine and the North Manchurian Plague Prevention Service proved to be significant in China’s modernization. It is still operational today under a slightly different name: the Manchurian Plague Prevention Service.

## 2. Societal Psychology in the Manchurian Plague

There was an attempt to distribute leaflets and bulletins urging the villagers on plague prevention measures as most villages had no modern medical attention. Some villages had Chinese medical practices, but Chinese medicine was found completely powerless against the plague (Nathan 6), which likely contributed to the initial inclinations towards Western opinion rather than Chinese. In most places, people first reacted with fatalism, apathy in disbelief in the necessity and efficacy of anti-plague measures. The typical native response was (translated):

“This is the scourge of Heaven... All will die whose time has come, and no others. Then why take people away to isolation stations? Why burn good clothes and bedding?” (Nathan 11)

One could conjecture that people did not carry as much fear or care for death back then— this could be attributed to the common Taoist approach of 順其自然 [going with the flow], i.e. a “come what may” attitude— and resources were scarce and hard to come by, therefore, such a reaction was commonly given. This changed, however, at the news of Dr. Girard Mesny’s death, and locals began to realize the severity of the situation. Though their culture rendered them more accepting towards death, it was probable that observing close ones— including spouses, parents, and young children— die around oneself, and the possibility of whole households or even societies being upended as a result left citizens terror-stricken.

The flames of terror were also fuelled by the knowledge that there was no cure, and some villages even independently followed the cities’ example and cremated the dead. A number of villages isolated themselves by turning away foreign guests and limiting marketing activities. These villages, successfully, had no plague. However, many locals were also hesitant to report plague cases: “To report a suspected case could mean the removal of the victim’s entire family to an

isolation station, where they might well catch plague from other inmates” (Nathan 11-12). The family’s furniture, or worse, even the house itself, would be burned or destroyed. To report the death of a loved one meant a cremation or a burial in a mass grave; to report an infection within a business would interfere with, if not, shut it down. Hence, many plague cases were not reported.

Despite their fear, people retained their cultural preoccupations. While this may initially seem shortsighted, their views were considerably justifiable: the burial was seen as a rite of passage to the afterlife and was therefore not to be taken lightly; businesses then were passed down over generations and held great amounts of historical and familial significance. The dread regarding such measures was countered somewhat: there was compensation for destroyed goods, a daily plague newspaper was published with printed explanations as to the importance of plague prevention, which seemed to prove more effective than speeches given by government officials or doctors (Nathan 12). This increased reception was likely due to the form of media being closer to citizens in terms of physical and societal proximity.

On the last day of January 1911, the Anti-Plague Bureau printed 24,000 leaflets calling on the people of Harbin to celebrate Chinese New Year by setting off their firecrackers inside the house that year (Summers 77). Traditionally, firecrackers in Chinese culture are believed to dispel evil spirits that bring bad luck. Evidently, Wu understood the cultural considerations of citizens and used this to his advantage, thus rendering this method one of the most effective within the plague. He suggested that— because the plague represented an extraordinary evil influence— “it might take more than the usual diligence to rid their homes and belongings of the evil spirits” (Summers 77). The scientific motive, however, was to exploit the sulfurous vapors from the firecrackers to disinfect the homes and reduce the presence of plague bacilli in the intimate surroundings of the population.

With the reverence residents and officials had for him as a figure of authority, Wu was able to promote widespread usage of masks. They were affordable and accessible for both the manufacturer and the customer and easy to use with strings so the user could secure it to their head. In the International Plague Conference, respirators and masks were a focal point of conversation. Western scholars believed they could effectively prevent plague and citizens were thus recommended to wear masks in public spaces to prevent meningitis or cholera. They became symbols of hygienic modernity, contributing to

a greater acceptance of the practice of mask-wearing in China today (Yan).

Throughout the plague, superstitions regarding the foreign doctors were directed almost as strongly against the modern-trained Chinese physicians. There is an interesting phenomenon worth considering on how the people oscillated between trusting Western and Chinese practitioners’ views throughout the plague: Chinese medicine was first tried against the plague; when that failed, they placed their trust in Western physicians; and finally became more receptive to Chinese practitioners when Western judgment failed. From this, it is interesting to note that although a sense of loyalty to the local practice was initially present, beliefs were quickly swayed toward whichever form of medicine had not yet proven to be ineffective, demonstrating that the notion of the “acceptance of death” had been overturned and people were instead desperate to survive at all costs. The presence of superstition was a notable manifestation of the desire to pinpoint a specific cause or blame, an attempt to alleviate the fear brought about by the prospect that the plague was inevitable and unstoppable. Yet ultimately, these feelings of hostility dwindled: it was simply pointless or even detrimental to resist any medical efforts when all parties, regardless of individual motives, were working toward the common goal of eradicating the plague.

### **3. Geopolitics in the Manchurian Plague**

World War I in Asia had just barely passed. The most obvious and public competitors at the time were Russia and Japan, who wanted control over Manchuria for their own geopolitical goals. The plague provided a good opportunity for both countries to assert a foothold into Manchuria. As a result, China was “particularly sensitive to both Russian and Japanese military threats of any kind” (Summers 63). In addition to external tensions, there were also internal disputes at the time resulting from an influx of Han immigrants into Manchuria. With Han nationalism and anti-Manchu racism, politics were further complicated (Summers 147).

Dr. Wu-Lien Teh became the official president of the International Plague Conference, held in Mukden during April 1911 (Summers 24). His fluency in English and not Chinese and preference for English dress were said to “rankle” some of his Western colleagues. His position also upset some Japanese, who were appalled that a young Chinese attaining international prestige of such a high position. Nonetheless, Wu’s political skill

and scientific knowledge were able to win over the respect and acceptance of most delegates. This points to the professionalism of all practitioners that despite their initial qualms and bias present, they were able to take an objective perspective in judging his competency.

The events of the first Sino-Japanese War (1894-1895) led to the Japanese being the dominant geopolitical force in East Asia. The configuration of Manchuria during the plague was a direct result of Korean policies made by Japan, China and Korea. For this reason, Chinese peasants hated and feared the Japanese. Old slanders formerly directed against all foreigners then applied to only the Japanese, who were also credited with encouraging or even causing the epidemic in order to destroy people and possess land (Nathan 29).

The Japanese Railroad was located in South Manchuria and the South Manchuria Railway Company was ordained in June 1907. Though the railway was said to be “primarily an instrument of colonization and only secondarily a transportation company, the Japanese built “impressive” public infrastructure around the railways such as roads, sewage systems, bridges, water supplies, hospitals, parks, and cemeteries (Summers 137-138). This increase in public and medical infrastructure better prepared South Manchuria to adapt to the Manchurian Plague.

Rumors spread, including ones such as a Japanese agent “taking some poison in his hand and sticking it on the queues of the Chinese, this causing insensibility, spitting of blood, and finally death” (Nathan 29), and of old men and women accused of witchery and tortured until admitting they were secret agents of the Japanese. Yet the Japanese anti-epidemic effort was more elaborate. Unlike the Russians, they worked alone, having been described as “went so far and gave such publicity to their protective measures as to appear unnecessarily ostentatious, evidently for the purpose of impressing other resident foreigners with their zeal and effectiveness” (Nathan 27). According to the Japanese, China’s neglect in suppressing the epidemic proved to the world that China should have been relieved of their responsibilities in Manchuria. Though this may contribute to the argument that the Japanese had their external motives for participating in the plague prevention, their contribution to the efforts cannot be denied.

Russia was wary of Japanese intentions at the time of the plague as they were the dominant geopolitical force in the area. They believed that Japan was “systematically making speedy preparations for a new war and using all of South Manchuria and Korea as a hinterland from

which to attack” (Summers 143). After their defeat in the Russo-Japanese War (1904-1905), Russia’s foothold in Manchuria weakened significantly. They sent staff and military troops into Manchuria and persistently tried to bring issues before the diplomatic body, requiring multilateral aid, resulting in China raising to the other powers that Russia was trying to defeat the project (Nathan 24-25). It can be conjectured that though both wanted to establish geopolitical power in Manchuria, Russia was more apparent than Japan in their attempts at doing so during the time of the pandemic. Yet without the guise of aiding the plague prevention efforts, China had no political reason to tolerate Russia’s methods as opposed to Japan, and therefore they were less successful in achieving their aims.

The plague endangered China both medically and politically. The North Manchurian Plague Prevention Service was partially built as a response. It was stated that Russian influence had declined because “the Plague Prevention Service was competent and prepared, it was able to pressure the Russians” (Nathan 64). Japan became more assertive, but was able to cooperate with China as medical equals, removing it from the political arena. The United States files of Chinese plague prevention were mostly silent after the Manchurian Plague of 1910-1911, signifying a great achievement in that outbreaks deemed of similar severity were few and far between.

## Conclusion

The events of the Manchurian Plague saw various developments in science, societal psychology, and geopolitics across not only Manchuria but also particularly the rest of China. The events of the plague directly led to the invention of the (pivotal) N95 mask that is widely used today, as well as demonstrating an acute consideration of not only scientific methods, but also societal psychology in the plague prevention efforts. The plague also saw— for the majority— various countries put aside their political motives and hostilities to combine efforts in plague prevention and eradication.

While similar phenomena may be observed in the present situation, the research demonstrates that there is a considerable difference in context between these two pandemics— namely, the extent of scientific and technological innovation that has advanced our world in terms of medicine, travel, and overall structure; the information available in this age of communication that has significantly impacted the psychology of the current population; the wholly different power dynamics and political states of each country as compared to a century

prior. This renders it impractical to draw a conclusion as to whether, and if so, how the COVID-19 prevention efforts could have been amended or improved based on the events of the Manchurian Plague.

Nonetheless, studying the history of science still provides a multitude of benefits. This study of the Manchurian Plague provides a lens through which to view the current pandemic: numerous scientific innovations, interesting perspectives, as well as political events can be documented. For instance, similarly to the invention of the mask and the plague conferences during the Manchurian Plague, COVID-19 saw rising international collaborations (Maher and Noorden) to yield rapid-antigen tests, various effective vaccines such as the Pfizer, as well as clinical trials for drugs that significantly reduce the death rate of COVID (Callaway *et al.*). Though knowledge of virus prevention is more widespread with the use of technology, there was surprising hesitation: in Germany, around 30% of people did not want to be vaccinated after the introduction of the vaccine in 2020 (Fieselmann *et al.*); numerous COVID-conspiracy theories were also spread (Raballo *et al.*). Political conflict also rose: for example, in Syria, “state-sponsored media instrumentalized the pandemic to vilify the United States, while lauding Russian, Iranian, and Chinese pandemic response measures”, with similar phenomena observed in other countries (Blanc and Brown).

However, the merits are not yet fully considered. It can be said that the more experience humanity gains, the more prepared it is for future situations. However, situations such as pandemics do not commonly occur; much less on a similar scale to COVID-19, and evidently cannot be emulated in experimentation because it is unethical and unfeasible to carry out. Instead, humanity prepares by using thought experiments to predict the trajectory of an event, and therefore, the events of the Manchurian Plague can be used to verify or deny the results of a thought experiment set according to the historical context at the time; similarly, the events of COVID-19 can be used in consideration for a thought experiment set according to the current time. Notable effective or ineffective predictions, such as the role of such pandemics in spurring scientific progress and global cooperation, may then be used to promote the actions necessary to better prepare the world for the next pandemic.

## References

- Blanc, J. and Brown, F.Z. (2020). *Conflict Zones in the Time of Coronavirus: War and War by Other Means*. Carnegie Endowment for International Peace. Available at: <https://carnegieendowment.org/2020/12/17/conflict-zones-in-time-of-coronavirus-war-and-war-by-other-means-pub-83462>
- Callaway, E., Ledford, H., Viglione, G., Watson, T., & Witze, A. (2020). COVID and 2020: An extraordinary year for science. *Nature*, 588(7839), 550–552. <https://doi.org/10.1038/d41586-020-03437-4>
- Fieselmann, J., Annac, K., Erdsiek, F., Yilmaz-Aslan, Y., & Brzoska, P. (2022). What are the reasons for refusing a COVID-19 vaccine? A qualitative analysis of social media in Germany. *BMC Public Health*, 22(1), 846. <https://doi.org/10.1186/s12889-022-13265-y>
- Google (2021). Dr. Wu Lien-teh’s 142nd Birthday, Google Doodles, March 10, 2021. <https://doodles.google/doodle/dr-wu-lien-tehs-142nd-birthday/>
- Irwin, J. F. & Smith, J. L. (2020). On Disaster, *Isis*, 111(1), 98-103. <https://doi.org/10.1086/707818>
- Gamsa, M. (2006). The Epidemic of Pneumonic Plague in Manchuria, *Past and Present*, 190, 147-184. <https://doi.org/10.1093/pastj/gtj001>
- Ma, J. (2021). N95, surgical or cloth: which face mask offers the best protection against Covid-19 and the Omicron variant?, *South China Morning Post*, December 26. Available at: <https://www.scmp.com/coronavirus/explainers-faqs/article/3161005/which-face-mask-offers-best-protection-against-covid-19>
- Maher, B., & Van Noorden, R. (2021). How the COVID pandemic is changing global science collaborations. *Nature*, 594(7863), 316–319. <https://doi.org/10.1038/d41586-021-01570-2>
- Raballo, A., Poletti, M., & Preti, A. (2022). Vaccine Hesitancy, Anti-Vax, COVID-Conspirationism: From Subcultural Convergence to Public Health and Bioethical Problems. *Frontiers in Public Health*, 10: 877490. <https://doi.org/10.3389/fpubh.2022.877490>
- Summers, W. C. (2012) *The Great Manchurian Plague of 1910-1911: The Geopolitics of an Epidemic Disease*. Yale University Press (New Haven, London).
- Wu, L. T. (1918) The North Manchurian Plague Prevention Service. *National Medical Journal of China*, 4(4), 810-811.
- Wu, L. T., Han, C. W., & Pollitzer, R. (1923). Plague in Manchuria: I. Observations made during and after the Second Manchurian Plague Epidemic of 1920-21. II. The Rôle of the Tarabagan in the Epidemiology of Plague. *The Journal of Hygiene*, 21(3), 307–358. <https://doi.org/10.1017/s0022172400031521>
- Yan, W. (2021). What Can and Can’t Be Learned From a Doctor in China Who Pioneered Masks. *The New York Times*. Available at: <https://www.nytimes.com/2021/05/19/health/wu-lien-teh-china-masks.html>
- Yang, J. (2021). *The trailblazing doctor who invented the face mask*, CNN. Available at: <https://www.cnn.com/2021/03/10/opinions/google-doodle-dr-wu-lien-teh-yang/index.html>

---

# An Investigation on the Antioxidants and Antioxidant Capacity of *Polygoni cuspidati* Roots

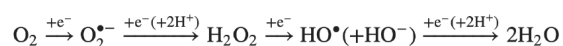
Ashley H.K. Wong

---

## 1. Background

### 1.1 Free Radicals and Antioxidants

Free radicals are species that contain one or more unpaired electrons in atomic or molecular orbitals, giving rise to a high degree of reactivity (Valko *et al.*, 2007). There are many classes of radicals, but the most important class of radical species generated in living organisms are derived from oxygen, since oxygen is necessary for any oxidative metabolism in aerobic organisms, known as reactive oxygen species (ROS). Although ROS in organisms plays an integral role in homeostasis, cell signalling, regulation, metabolism, and memory formation via DNA methylation; excess ROS can cause damage to biomolecules causing oxidative stress, leading to neurodegenerative diseases, atherosclerosis, cancer and other disorders (Collin, 2007). They are generated naturally from molecular oxygen in four successive single-electron reductions (Equation 1)



**Equation 1.** Four successive single-electron reductions

Due to the radical's high reactivity, formation of superoxide anion ( $\text{O}_2^{\bullet-}$ ) radical leads to a cascade of other ROS -hydrogen peroxide ( $\text{H}_2\text{O}_2$ ) and hydroxyl radical ( $\text{HO}^{\bullet}$ ). The  $\text{O}_2^{\bullet-}$ ,  $\text{H}_2\text{O}_2$  and  $\text{HO}^{\bullet}$  will react with other molecules forming new radicals, resulting in a chain reaction. Antioxidants act as free radical scavengers as they can inhibit oxidation and terminate chain reactions, (Azat Aziz *et al.*, 2019). Antioxidants can deactivate free radicals either by hydrogen atom transfer, transfer of a single electron, sequential proton loss electron transfer, or by the chelation of transition metals (Zeb, 2020). Therefore, antioxidants are often found in foods or employed as dietary supplements as protection against the deleterious effects of free radical oxidation (Azat Aziz *et al.*, 2019).

Antioxidants can be classified into two groups: synthetic and natural. Synthetic antioxidants are man-made, present higher stability and performance, but consumption of them may give rise to health issues (Lourenço *et al.*, 2019). Natural antioxidants are obtained from food and medicinal plants, such as fruits, vegetables, spices and traditional medicinal herbs (Xu *et al.*, 2017). Natural antioxidants from plants may be classified into three main classes: phenolic compounds, vitamins and carotenoids (Lourenço *et al.*, 2019). To which phenolic compounds exhibit strong antioxidant activity due to the presence of the phenolic hydroxyl groups.

Phenolic hydroxyl groups (-OH) are good hydrogen atom donors. After donation of a hydrogen atom, the phenol's stability is maintained through the interaction between the delocalized  $\pi$ -electrons of the benzene ring and the phenolic hydroxyl group (Pereira *et al.*, 2009).

### 1.2 Traditional Chinese Medicine (TCM) and *Polygoni cuspidati* Roots

Traditional Chinese Medicine (TCM) is a systematic healthcare system that has been in practice for over 5000 years (Pan *et al.*, 2014) and is used to treat diseases and enhance health (Matos *et al.*, 2021).

Despite herbal medicine's long history of effective use, practitioners of mainstream medicine have challenged the TCM approach due to the lack of scientific evidence in the context of contemporary medicine. However, more recently, due to the adverse side effects and antimicrobial resistance associated with pharmaceuticals, herbal medicine has increased in demand worldwide (Pan *et al.*, 2014). It has been increasingly common for people with chronic diseases to turn to TCM for better and less adverse effect treatments (Zhang *et al.*, 2013). Thus, the understanding of herbal medicine mechanisms is of particular importance.

---

The above article was written as an Extended Essay in Chemistry, in partial fulfillment of the IB Diploma Programme, 2023.

More than 85% of commonly used TCM ingredients listed in the *Chinese Materia Medica Encyclopedia* originate from plants (Pan *et al.*, 2014). The reason why plants are so effective is because they contain phenolic compounds which are generated when plants undergo photosynthesis through the phenylpropanoid pathway (Ralston *et al.*, 2005).

*Polygoni cuspidati* is a herbaceous perennial plant, its dried roots are officially listed in the Pharmacopeia of the People's Republic of China under the name "Hu Zhang". Known for its abundance in resveratrol (Wang *et al.*, 2011), *Polygoni cuspidati* roots have many therapeutic and pharmacological effects (Zhang *et al.*, 2013). The major active ingredients isolated from *Polygoni cuspidati* roots contain polyphenols such as 6-methyl-1,3,8-trihydroxyanthraquinone (emodin) and 3,5,4'-trihydroxy-*trans*-stilbene (*trans*-resveratrol), other antioxidants like physcion, 8-O- $\beta$ -D-glucopyranoside, 2-methoxy-6-acetyl-7-methyljuglone, citreorosein, (+)-catechin, polydatin (Zhang *et al.*, 2013).

### Antioxidant Capacity

Antioxidant capacity is the measure of the amount of free radicals scavenged by a test solution (Rubio *et al.*, 2016), thus reflecting the concentration of antioxidants present in a sample. There are many methods to determine the antioxidant capacity of a substance based on the antioxidant mechanism.

The method used in this investigation is the Briggs Rauscher reaction (Cervellati *et al.*, 2001), which uses relatively inexpensive reagents and apparatus that are commonly present in chemical laboratories. Briggs Rasucher is an oscillating reaction that has the ability to measure the antioxidant capacity of a sample due to the presence of the hydroperoxyl radical (one of the intermediates) (Gajdoš Kljusurić *et al.*, 2005). When antioxidants are added to the Briggs Rauscher reaction, antioxidants deactivate the radicals, which elongates the oscillation period. The elongation caused by antioxidants (inhibition time) is linearly proportional to the concentration of antioxidants added (Cervellati *et al.*, 2001).

The overall reaction of Briggs Rauscher is:  $\text{IO}_3^- + 2\text{H}_2\text{O}_2 + \text{CH}_2(\text{COOH})_2 + \text{H}^+ \rightarrow \text{ICH}(\text{COOH})_2 + 2\text{O}_2 + 3\text{H}_2\text{O}$  (Noyes and Furrow, 1982)

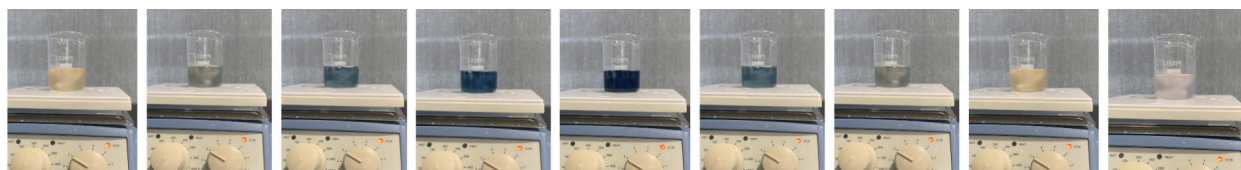
The Briggs Rauscher reaction is an oscillating reaction that changes colors between colorless, amber and dark blue in response to the changing concentrations of  $\text{I}^-$ ,  $\text{I}_2$  and  $\text{I}_3^-$ . Where colorless represents a shortage of iodine, amber represents an abundance of iodine and blue indicates the presence of iodate-starch complex (Figure 1).

### Antioxidant Stability

Naturally occurring polyphenolic compounds are damaged when exposed to UV and high pHs levels (Del Valle *et al.*, 2020; Friedman and Jürgens 2000; Chen *et al.*, 2007; Robinson *et al.*, 2015). Studies have found that the  $\text{H}_2\text{O}_2$  scavenging and  $\text{H}_2\text{O}_2$  producing activities present in plant extracts are pH dependent, more specifically, in an alkaline pH, the production of hydrogen peroxide is higher and the inhibition is lower, reflecting the decrease in antioxidant activity (Bayliak *et al.*, 2016).

*Polygoni cuspidati* is often mixed with many types of other herbs to yield different therapeutic effects (Bai *et al.*, 2016). *Lysimachia christinae* (金錢草), a common TCM mixed with *Polygoni cuspidati* to expel dampness and remove jaundice contains alkaloids (Chen and Hu, 1979; Gao *et al.*, 2013). The pH of most alkaloids ranges between 6-9, and a pH value greater than 10 when most alkaloids are deprotonated species (Wei *et al.*, 2016). Thus, the mixture of TCMs may cause a decrease in *Polygoni cuspidati* antioxidant capacity.

This study will focus on the effect of addition of different concentrations of sodium hydroxide (NaOH) on the antioxidant capacity of *Polygoni cuspidati* roots extract. NaOH is a common reagent used for the basification during polyphenol extraction from plants to increase the diffusion coefficients of polyphenol, hence increasing yield of extraction (Rajha *et al.*, 2014). However, NaOH is a strong base and antioxidants are susceptible to high pHs (Friedman and Jürgens, 2000). Thus, the change in pH during polyphenol extraction may affect the antioxidant capacity and possibly the structure of compounds.

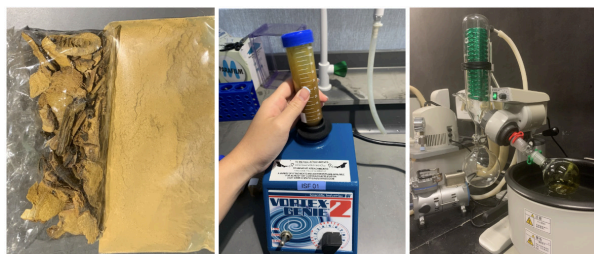


**Figure 1.** Oscillating reaction (yellow to blue to yellow to clear) taken from experiment

## 2. Method

### 2.1 Preparation of Ethanolic Extracts of *Polygoni cuspidati* Roots

The *Polygoni cuspidati* roots extraction method was adapted from Hsu *et al.* (2007) with some modifications due to equipment constraints. 2.5000 g  $\pm$  0.0001 of dried (blended) roots were extracted using 25.0 cm<sup>3</sup>  $\pm$  0.1 of 100% ethanol at 25 °C with 15 minutes of shaking via vortex. The extract was centrifuged twice at 5000 rpm for 3 minutes. 20.0 cm<sup>3</sup>  $\pm$  0.1 of supernatant was collected and ethanol removed under reduced pressure in the rotary evaporator at 40 °C (water bath) until all ethanol was evaporated (Figure 2). The mass of the dried extract was determined by measuring the initial and final mass of the round bottom flask after the evaporation, 50% ethanol was used to prepare a 0.1 g/cm<sup>3</sup> stock solution.



**Figure 2.** (left to right): *Polygoni cuspidati* roots in dried and powdered form; shaking via vortex; rotary evaporation of extract

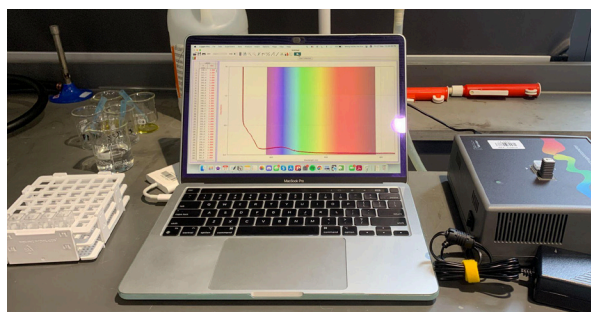
### 1.2 Confirmation of Presence of Antioxidants

#### Thin Layer Chromatography (TLC) of *Polygoni cuspidati* Extracts

TLC was carried out to identify resveratrol's presence in *Polygoni cuspidati* root extract. Aluminium plates precoated with silica gel were cut with scissors to 5 cm x 5 cm each. Plate markings were made with soft pencil about 1 cm from the bottom of the plate. Glass capillaries were used to spot the sample onto the TLC plate at a distance 1 cm away from the edge of the plate. The plates were developed in a glass chamber using a solvent system: (1) ethyl acetate, cyclohexane, *n*-butanol 9:9:2 v/v/v (Lotz *et al.*, 2015); and (2) *n*-pentanol-pyridine-methanol 6:4:3, v/v/v (Räisänen *et al.*, 2000). Prior to plate development, the glass chambers were pre-saturated with the solvent system for 5 minutes. The plates were dried using a blowdryer and visualized under normal daylight and ultraviolet light (254 nm and 365 nm).

### Absorbance Measurement

The *Polygoni cuspidati* roots extract were diluted to 1:29 with deionised water. The extracts were scanned in the wavelength range from 220 - 850 nm using the Vernier Fluorescence/UV-Vis spectrophotometer to detect characteristic peaks after calibration using deionised water as a blank. The scanning record was recorded through the Logger Pro software (Figure 3).



**Figure 3.** Spectrophotometer set up

### Briggs Rauscher

The Briggs Rauscher reaction consists of three solutions (solutions A, B and C). For solution A, 12.9040  $\pm$  0.0001 g of KIO<sub>3</sub> and 30.00  $\pm$  0.05 cm<sup>3</sup> of 1 mol.dm<sup>-3</sup> H<sub>2</sub>SO<sub>4</sub> was mixed with 270.0  $\pm$  0.3 cm<sup>3</sup> of deionised water. For solution B, 120.00  $\pm$  0.15 cm<sup>3</sup> of 1% starch solution was mixed with 1.2170  $\pm$  0.0001 g of MnSO<sub>4</sub>•H<sub>2</sub>O, 4.4950  $\pm$  0.0001 g of malonic acid and 180.0  $\pm$  0.2 cm<sup>3</sup> of deionised water. For solution C, 90.0  $\pm$  0.1 cm<sup>3</sup> of 30% H<sub>2</sub>O<sub>2</sub> was mixed with 210.00  $\pm$  0.25 cm<sup>3</sup> of deionised water. 10.0  $\pm$  0.2 cm<sup>3</sup> of solution A and B were added to a 100 cm<sup>3</sup> beaker whilst stirred to form a vortex. Upon addition of 10.0  $\pm$  0.2 cm<sup>3</sup> of solution C, the solution turned amber and then dark blue. On the second oscillation, 100  $\pm$  0.8  $\mu$ L of sample was added. The duration of the second oscillation was measured to indicate antioxidant capacity.

### 1.3 NaOH (aq) Concentration Dependent Study

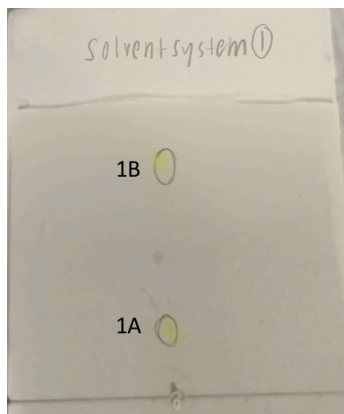
Five different concentrations (0.0001, 0.001, 0.01, 0.05, 0.1 mol.dm<sup>-3</sup>) of NaOH were prepared via serial dilution using a 1 mol.dm<sup>-3</sup> stock solution. 100.0  $\pm$  0.8  $\mu$ L of different NaOH concentrations were added into 1000  $\pm$  6  $\mu$ L of 1000  $\mu$ g/cm<sup>3</sup> root extract. 1000  $\pm$  6  $\mu$ L of pure extract was prepared as control. These solutions were further analyzed via spectrophotometrically and via the Briggs Rasucher reaction. Where the spectrophotometric analysis and the Briggs Rauscher analysis followed the methods in section 2.2.2 and 2.2.3 respectively.



## 2. Results

### 2.1 Confirmation of Presence of Antioxidants

#### TLC of *Polygoni cuspidati* Roots



**Figure 4.** TLC plate developed using (1) ethyl acetate, cyclohexane, *n*-butanol 9:9:2 v/v/v solvent system, visualized under normal daylight

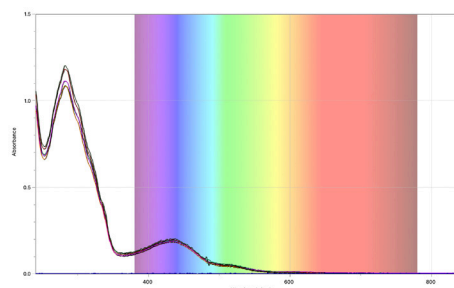


**Figure 5.** TLC plate developed using (2) *n*-pentanol-pyridine-methanol 6:4:3, v/v/v, visualized under normal daylight

The TLC results show the presence of two spots (1A and 1B) in Figure 4. Spot 1A has an  $R_f$  value of 0.22 (which is currently unidentified) and spot 1B has an  $R_f$  value of 0.78, which corresponds to the  $R_f$  value of *trans*-resveratrol (Lotz *et al.*, 2015). Another TLC with

a different solvent system was performed (Figure 5) which shows the presence of one spot (2A). 2A has an  $R_f$  value of 0.8, corresponding to the literature  $R_f$  value of emodin (Räisänen *et al.*, 2000). Hence, suggesting that spot 1A in Figure 4, may be emodin.

#### Absorbance Analysis



**Figure 5.** Spectrophotometer results of pure extract

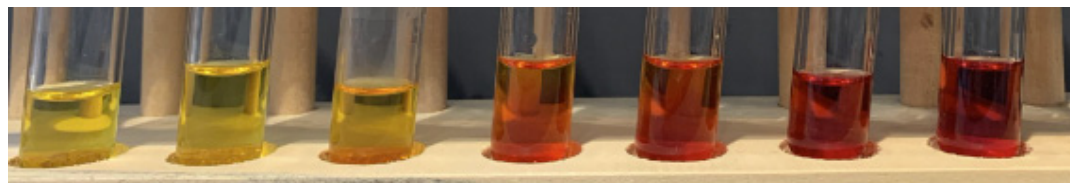
In the pure ethanolic extract, two peaks at 282.3 nm and 433.0 nm were detected, with the first peak at a much higher absorbance than the second peak (Figure 6). The UV peak observed corresponds to the literature absorbance maximum of *cis*-resveratrol at 288 nm (Trela and Waterhouse, 1996). The visible peak observed corresponds to the literature absorbance maximum of emodin at 438 nm (Räisänen *et al.*, 2000).

#### Briggs Rauscher

Upon addition of 100  $\mu$ L of *Polygoni cuspidati* extracts, the mean inhibition time is  $144.67 \pm 0.02$  seconds, whilst the inhibition time when no antioxidants were added is  $14.12 \pm 0.02$  seconds. Thus, the Briggs Rauscher reaction confirmed the presence of antioxidants in *Polygoni cuspidati* root extracts.

### 2.2 NaOH (aq) Concentration Dependent Study Findings

Upon addition of NaOH to *Polygoni cuspidati* root extract, a color change was observed. The extract is originally yellow in color, but as the concentration of NaOH increased, the sample turned increasingly red (Figure 7).



**Figure 7.** (left to right): 0, 0.0001, 0.001, 0.01, 0.05, 0.1, 1 mol.dm<sup>-3</sup> of 100  $\mu$ L NaOH added to sample. Note: different test tubes were used, but the total volume of solution is identical in each test tube.

## Spectrophotometric Analysis

The different peaks in the UV-Vis spectrum reveal the composition of the mixture at different concentrations of NaOH. As the concentration of NaOH increases, the wavelengths of the absorbance maxima increase. The peak in the UV spectrum shifted from 282.3 nm to 282.9 nm, 283.5 nm, 304.3 nm, 308.3 nm, 309.5 nm, 310.3 nm, while the peak in the visible spectrum shifted from 433.0 nm to 434.4 nm, 434.6 nm, 496.2 nm, 506.2 nm, 509.9 nm, 511.2 nm, upon addition of 0.0001, 0.001, 0.01, 0.05, 0.1, 1 mol.dm<sup>-3</sup> of NaOH respectively (Figure 8).

## Briggs Rauscher

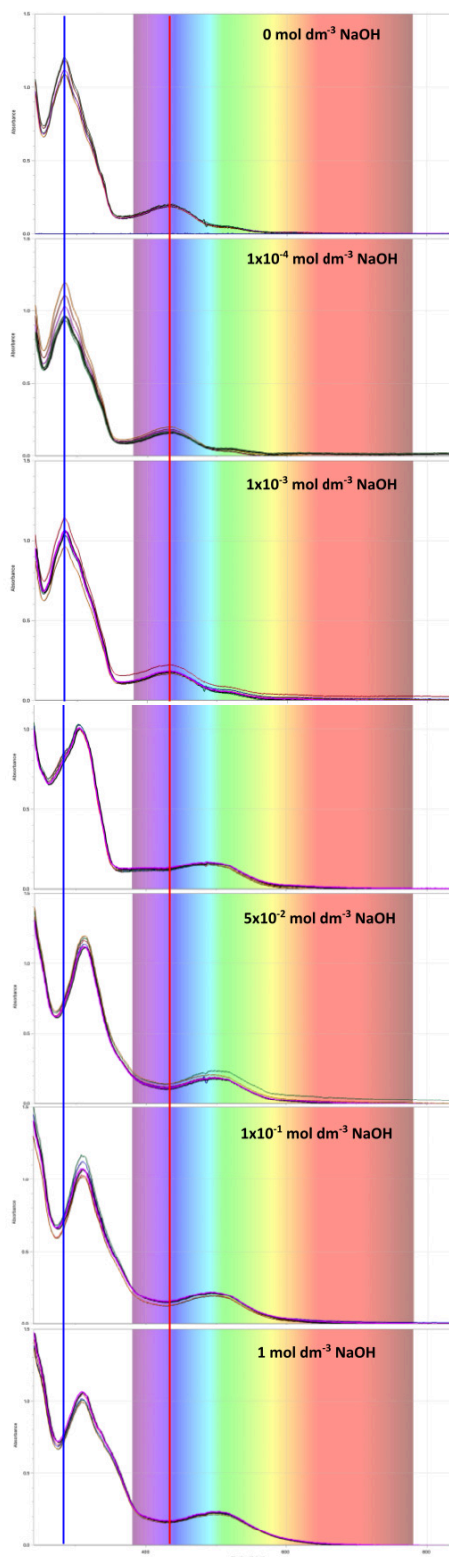
The results from the Briggs Rauscher reaction shows that as the NaOH concentration in *Polygoni cuspidati* root extract increases, the mean Briggs Rauscher inhibition time decreases (Table 1 and 2).

## 3. Discussion

### 3.1 Absorbance Shift

The TLC results show that *trans*-resveratrol most likely present in the *Polygoni cuspidati* roots extract as spot 1B (Figure 4) and spot 2A is emodin (Figure 5), which corresponds to the reports of protykin (a high-potency, standardized extract found in *Polygoni cuspidati*) of *trans*-resveratrol (20%) and emodin (10%) (Sato *et al.*, 2000).

*Trans*-resveratrol and *cis*-resveratrol are isomers of resveratrol (Figure 9). *Trans*-resveratrol has higher potency and higher biological activity than *cis*-resveratrol due to its lower steric hindrance (Anisimova *et al.*, 2011; Pannu and Bhatnagar, 2019). According to Kriel (2020), *cis*-resveratrol does not naturally occur due to the steric hindrance of the two aromatic rings but is derived from isomerisation of *trans*-resveratrol. Studies have found that after 48 min of UV irradiation, greater than 82% of *trans*-resveratrol will be photoconverted to its *cis*-stereoisomer (Bernard *et al.*, 2007). (See Figure 9)



**Figure 8.** Spectrophotometer reading of *Polygoni cuspidati* ethanolic extract with different concentrations of NaOH; blue and red vertical lines represent the signal in pure extract (without addition of NaOH), in uv and visible spectrum respectively.

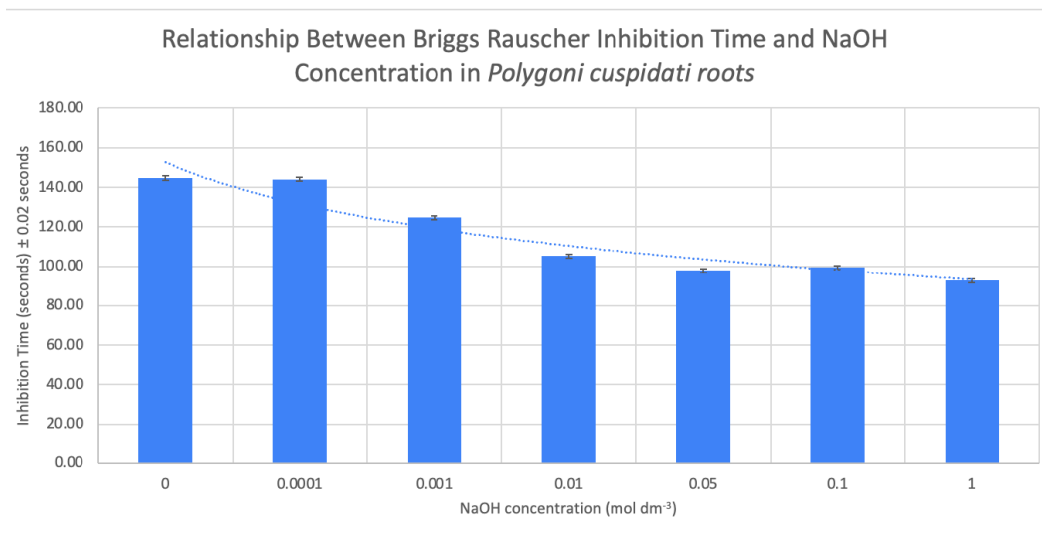
Concentration of NaOH (mol. dm <sup>-3</sup> )	Time (seconds) ± 0.01 seconds									
	trial 1		trial 2		trial 3		trial 4		trial 5	
	start	end	start	end	start	end	start	end	start	end
0	35.34	181.04	36.81	175.54	33.94	182.14	63.01	200.95	29.91	182.67
1x10 <sup>-4</sup>	42.12	182.78	38.55	192.89	37.76	180.09	36.81	179.94	39.12	178.32
1x10 <sup>-3</sup>	40.32	160.09	38.50	151.18	38.17	154.54	41.02	158.31	38.73	195.76
1x10 <sup>-2</sup>	46.76	140.15	42.71	165.24	34.78	140.04	38.12	142.45	32.48	133.00
5x10 <sup>-2</sup>	41.40	135.46	40.27	146.90	42.08	147.46	41.34	133.59	40.16	131.04
1x10 <sup>-1</sup>	33.71	148.79	41.68	153.45	39.53	124.86	38.43	113.98	40.58	149.87
1	40.32	151.51	43.96	132.13	38.47	128.59	36.08	118.49	36.26	128.00

**Table 1.** Table 1: Raw data of Briggs Rauscher experiments

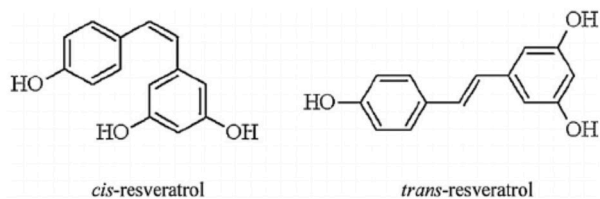
Concentration of NaOH (mol. dm <sup>-3</sup> )	Absolute uncertainty of NaOH	Time (seconds) ± 0.02 seconds						
		trial 1	trial 2	trial 3	trial 4	trial 5	mean change	
		change	change	change	change	change		
0	0.00	145.70	138.73	148.20	137.94	152.76	144.67	
1x10 <sup>-4</sup>	6.0x10 <sup>-3</sup>	140.66	154.34	142.33	143.13	139.20	143.93	
1x10 <sup>-3</sup>	1.3x10 <sup>-3</sup>	119.77	112.68	116.37	117.29	157.03	124.63	
1x10 <sup>-2</sup>	1.8x10 <sup>-3</sup>	93.39	122.53	105.26	104.33	100.52	105.21	
5x10 <sup>-2</sup>	2.5x10 <sup>-4</sup>	94.06	106.63	105.38	92.25	90.88	97.84	
1x10 <sup>-1</sup>	3.8x10 <sup>-5</sup>	115.08	111.77	85.33	75.55	109.29	99.40	
1	5.8x10 <sup>-6</sup>	111.19	88.17	90.12	82.41	91.74	92.73	

**Table 2.** Processed data of Briggs Rauscher experiments

<p><b>Change</b>          = End time - Start time          = 181.04-35.34          = 145.70 seconds (correct to 2 decimal places)</p>	<p><b>Mean change</b>          =  <math display="block">\frac{T1\ change + T2\ change + T3\ change + T4\ change + T5\ change}{5}</math>         = <math>\frac{145.7+138.73+148.20+137.94+152.76}{5}</math>          = 144.67 seconds (correct to 2 decimal places)</p>
<p><b>Absolute uncertainty of change</b>          = absolute uncertainty of start time + absolute uncertainty of end time          = 0.01 + 0.01          = ±0.02 seconds</p>	<p><b>Absolute uncertainty of mean change</b>          = absolute uncertainty of change          = ±0.02 seconds</p>



**Graph 1.** Relationship between Briggs Rauscher inhibition time and NaOH concentration in *Polygoni cuspidati* roots. 5 trials have been performed for each concentration and the error bars represent the absolute uncertainty in seconds.



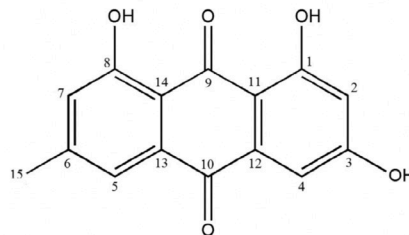
**Figure 9.** Molecular structure of resveratrol *trans*- and *cis*-isomers (Venuti *et al.*, 2014)

The UV peak observed (Figure 6) in the pure extract (282.3 nm) corresponds to the literature spectrophotometric reading of *cis*-resveratrol 288 nm (Trela and Waterhouse, 1996), indicating that the *trans*-resveratrol in the sample degraded since the TLC measurement (as the spectrophotometric and TLC measurement was conducted a week apart). Upon addition of NaOH, the peak in the UV spectrum (*cis*-resveratrol) undergoes bathochromic (red) shift and towards the spectrophotometric reading of *trans*-resveratrol at 308 nm (Trela and Waterhouse, 1996). A possible explanation of this bathochromic shift is isomerization of *cis*-resveratrol to *trans*-resveratrol. However, the isomerization pattern does not match with literature reports. On the contrary, reports say that low pHs induce the isomerization of *cis*-isomer to *trans*-isomer (Trela and Waterhouse, 1996), whereas the isomerization of *trans*-resveratrol to *cis*-resveratrol occurs in high pHs (pH >11) (Pannu and Bhatnagar, 2019). Hence, isomerization of resveratrol may not have been the most accurate explanation for this phenomenon.

Another possible explanation for this bathochromic shift is the solvent effect of NaOH. An aqueous solution of NaOH is known to cause a bathochromic shift in the absorbance spectrum. The absorption peaks in NaOH undergo bathochromic shifts in the UV absorbance with the increasing solution concentration by comparing the UV spectra of various concentrations (Tong *et al.*, 2020). This is consistent with my findings, because as the NaOH concentration added to the samples increased, the absorbance in the UV peak also increased (bathochromic shift).

### 3.2 Pro-oxidant Effect of Emodin

Other than the shift in UV peak, the addition of NaOH to the ethanolic extract of *Polygoni cuspidati* roots caused a shift in the peak in the visible spectrum, resulting in a color change from yellow to red (Figure 7). The change in color of the extract is most likely due to emodin as shown in the spectrophotometric analysis (Figure 8). The neutral form of emodin (EMH) (Figure 10) is yellow, but in alkaline pH solutions, deprotonation of emodin will occur, causing the anionic/deprotonated form (EM<sup>-</sup>, EM<sup>2-</sup>) to be red (Da Cunha *et al.*, 2014).



**Figure 10.** Chemical structure of emodin in its neutral form (EMH) (Da Cunha, *et al.*, 2014)

Polyphenols are generally more stable at low pH as the acidic conditions help polyphenols stay neutral (Tsoo 2010). Whereas high pHs causes polyphenols to be unstable, auto-oxidate and exhibit prooxidant activities (Babich *et al.*, 2010). Prooxidants refers to the species that induce oxidative stress, through formation of ROS or by inhibiting the antioxidant system (Sotler *et al.*, 2019).

The different properties displayed by antioxidants under different pH reported by studies (Friedman and Jürgens 2000, Chen *et al.*, 2007; Robinson *et al.*, 2015, Bayliak *et al.*, 2016) are consistent with the Briggs Rauscher findings of this investigation. Since the Briggs Rauscher inhibition time is proportional to the antioxidant capacity (Gajdoš Kljusurić *et al.*, 2005), the Briggs Rauscher results show that as the NaOH concentration increases, the antioxidant capacity of *Polygoni cuspidati* root extract decreases.

In the pure extract, the mean inhibition time is  $144.67 \pm 6.01$  seconds whereas when  $1 \text{ mol.dm}^{-3}$  of NaOH is added to the pure extract, the inhibition time is  $92.73 \pm 10.91$  seconds (Table 2). The longest inhibition time is when no NaOH is added, whereas the shortest inhibition time is when  $1 \text{ mol dm}^{-3}$  of NaOH is added, indicating that there is an inverse relationship between the concentration of NaOH and antioxidant capacity of the extract. Between  $0.001$  and  $0.01 \text{ mol.dm}^{-3}$  of NaOH there is a significant fall in inhibition time, from a mean inhibition time of 124.63 to 105.21 seconds (Table 2), with a difference of 19.42 seconds. This significant decrease in inhibition time is also reflected in the spectrophotometric analysis, where the largest shift occurred in both the UV and visible spectrum between  $0.001$  and  $0.01 \text{ mol.dm}^{-3}$  of NaOH, with a difference of 20.8 nm and 61.6 nm in the UV and visible spectrum respectively (Figure 8).

The inverse relationship between the concentration of NaOH and the antioxidant capacity of the extract can be explained by the unstable nature of resveratrol and the deprotonation of emodin at high pH. Resveratrol's half-life ranges from almost a year at pH 1.2 to 20 days at pH 6.8, but it decreases exponentially at basic pHs:

2 days at pH 7.4, hours at pH 8, and minutes at pH 9 and 10 (Konopko and Litwinienko, 2021; Zupančič *et al.*, 2015). Moreover, at high pH, emodin will deprotonate, causing the antioxidant to exhibit prooxidant properties meaning a decrease in the antioxidant capacity (Babich *et al.*, 2021).

### 3.3 Proposed Mechanism

Upon addition of NaOH, the color of the solution changes from yellow to red (Figure 7), meaning that the wavelength absorbed increases from violet (400 nm - 424 nm) to green (491 nm - 575 nm), which is congruent to the proposed mechanism, because the proposed mechanism in Figure 11, suggests that deprotonation of emodin from EMH to EM<sup>-</sup> and EM<sup>2-</sup> creates a higher degree of conjugation (as shown in the molecule highlighted in blue). The more conjugation present in a molecule, the closer the distance is between the ground states and excited states. Which means that lower energy is required to excite electrons in conjugated systems, thus lower energy light (longer wavelength) will be absorbed by conjugated systems (Samal, 2010).

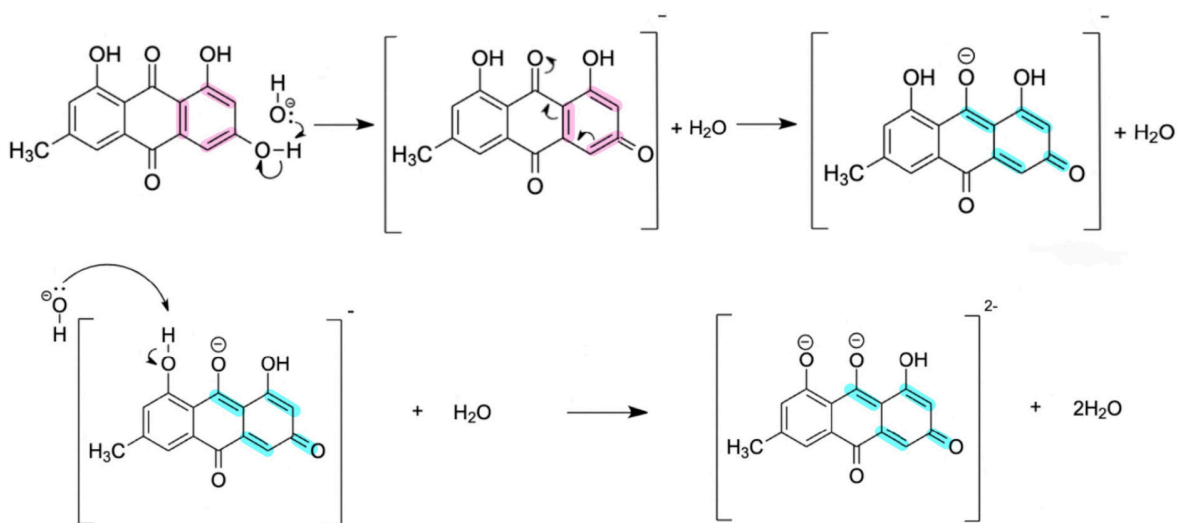
### Conclusion

The TLC and spectrophotometric analysis confirms that emodin and resveratrol are both present in the dried *Polygoni cuspidati* root extract. These results are consistent with the previous studies that have extracted protykin, an all-natural, high potency standardized extract of *trans*-resveratrol (20%) and emodin (10%) derived from dried rhizomes of *Polygoni cuspidati* (Sato *et al.*, 2000).

The Briggs Rauscher results suggest that the antioxidants present in *Polygoni cuspidati* root extracts are sensitive to high pHs (high NaOH concentrations). Despite the numerous health benefits offered by antioxidants, the results obtained suggest that under high pH environments, antioxidants might exhibit prooxidant properties and cause greater harm than good. Hence, the dual effect of antioxidants should be carefully considered when consumed with other TCMs or foods with high pHs.

The experimental percentage uncertainty was calculated to be 13.66% (Appendix A, Table 5). This shows that there is an overall small degree of uncertainty throughout the experiment, but there are improvements that can further reduce experimental inaccuracies. Though the Briggs Rauscher reaction is a widely used method for testing the antioxidant capacity of a substance, different antioxidant assays have different objectives (Rodríguez-Bonilla *et al.*, 2017). For example, the Oxygen Radical Absorbance Capacity (ORAC) assay measures the hydrogen atom transfer reaction, whereas the ABTS<sup>•+</sup> and the 2,2-diphenyl-1-picrylhydrazyl (DPPH) assay measures the single electron transfer reaction (Rodríguez-Bonilla *et al.*, 2017). Therefore, multiple assays can be used to assess a broader range of antioxidant mechanisms.

Furthermore, the change in color of the extracts suggests that emodin deprotonates. This deprotonation may cause emodin to exhibit prooxidant effects rather than antioxidant effects. However, the color change is only a small indication of this and can be further explored by



**Figure 11.** Proposed mechanism of emodin deprotonation

measuring the prooxidant activity in *Polygoni cuspidati* root extracts, such as measuring H<sub>2</sub>O<sub>2</sub> production (as per Bayliak *et al.*, 2016).

The addition of NaOH induced a response in the *Polygoni cuspidati* roots extract by changing its color and changing its antioxidant capacity. However, it is not certain whether pH is the sole factor that affects the extract. Hence, the use of buffers and a wider pH range can be tested, possibly finding the optimal pH for maximum antioxidant capacity.

To better improve the identification of organic compounds present in the *Polygoni cuspidati* extracts, a high-performance liquid chromatography (HPLC) could be used. Resveratrol undergoes photoisomerization with UV. Due to the nature of the UV spectrophotometer measurement mechanism, the spectrophotometer is not necessarily the best identification tool for the quantification of resveratrol, more specifically UV/VIS spectroscopy resulted in false higher *trans*-resveratrol concentrations in conditions under which it was not stable (Zupančič *et al.*, 2015). To better understand the range of compounds present in the extracts, different solvent mixtures for TLC suitable for various groups of compounds (*e.g.* polyphenols) could be used.

## References

- Anisimova, N. Y., Kiselevsky, M. V., Sosnov, A. V., Sadovnikov, S. V., Stankov, I. N., & Gakh, A. A. (2011). *Trans*-, *cis*-, and dihydroresveratrol: a comparative study. *Chemistry Central Journal*, 5: 88. doi: 10.1186/1752-153X-5-88
- Azat Aziz, M., Shehab Diab, A., & Abdulrazak Mohammed, A. (2019). Antioxidant Categories and Mode of Action. *Antioxidants*. doi: 10.5772/intechopen.83544
- Babich, H., Schuck, A. G., Weisburg, J. H., & Zuckerbraun, H. L. (2011). Research Strategies in the Study of the Pro-Oxidant Nature of Polyphenol Nutraceuticals. *Journal of Toxicology*, 2011: 467305. doi: 10.1155/2011/467305
- Bai, Y.L., Tong, R.S., Li, P.Q. (2016) 不同劑量和配伍對虎杖功效發揮的影響概述. *China Pharmacy*, 27(1), 105-107. doi: 10.6039/j.issn.1001-0408.2016.01.34
- Bayliak, M. M., Burdyliuk, N. I., & Lushchak, V. I. (2016). Effects of pH on antioxidant and prooxidant properties of common medicinal herbs. *Open Life Sciences*, 11(1), 298-307. doi: 10.1515/biol.2016.0040
- Bernard, E., Britz-McKibbin, P., & Gernigon, N. (2007). Resveratrol Photoisomerization: An Integrative Guided-Inquiry Experiment. *Journal of Chemical Education*, 84(7): 1159-1161. doi: 10.1021/ed084p1159
- Cervellati, R., Höner, K., Furrow, S. D., Neddens, C., Costa, S. (2001) The Briggs-Rauscher reaction as a test to measure the activity of antioxidants. *Helvetica Chimica Acta*, 84(12), 3533-3547. doi: 10.1002/1522-2675(20011219)84:12<3533::aid-hlca3533>3.0.co;2-y
- Chen, F. H., Hu, C. M. (1979) Taxonomic and phytogeographic studies on Chinese species of *Lysimachia*. *Acta Phytotaxonomica Sinica*, 17(4), 21-53. <https://www.jse.ac.cn/EN/Y1979/V17/I4/21>
- Chen, Y.B., Sun, B.X., Chen, J. (2007) Study on the stability of resveratrol in rhizoma *Polygoni cuspidati*. *Journal of Chinese Medicinal Materials*, 30(7), 805-807. PMID: 17944191
- Collin, F. (2019) Chemical Basis of Reactive Oxygen Species Reactivity and Involvement in Neurodegenerative Diseases. *International Journal of Molecular Sciences*, 20(10): 2407. doi: 10.3390/ijms20102407.
- Da Cunha, A. R., Duarte, E. L., Lamy, M. T., & Coutinho, K. (2014). Protonation/deprotonation process of emodin in aqueous solution and pKa determination: UV/Visible spectrophotometric titration and quantum/molecular mechanics calculations. *Chemical Physics*, 440, 69–79. doi: 10.1016/j.chemphys.2014.06.009
- Del Valle, J. C., Buide, M. L., Whittall, J. B., Valladares, F., Narbona, E. (2020) UV radiation increases phenolic compound protection but decreases reproduction in *Silene littorea*. *PLoS One*, 15(6): e0231611. doi: 10.1371/journal.pone.0231611
- Friedman, M., & Jürgens, H. S. (2000). Effect of pH on the Stability of Plant Phenolic Compounds. *Journal of Agricultural and Food Chemistry*, 48(6), 2101–2110. doi: 10.1021/jf990489j
- Gajdoš Kljusurić, J., Djaković, S., Kruhak, I., Kovačević Ganić, K., Komes, D., & Kurtanjek, Ž. (2005). Application of Briggs-Rauscher reaction for measurement of antioxidant capacity of Croatian Wines. *Acta Alimentaria*, 34(4), 483–492. doi: 10.1556/aalim.34.2005.4.15

- Gao, F. F., Zhao, D., Deng, J. (2013) New Flavonoids from *Lysimachia christinae* Hance, *Helvetica Chimica Acta*, 96(5), 985-989. doi: 10.1002/hlca.201200328
- Hsu, C. Y., Chan, Y. P., & Chang, J. (2007). Antioxidant activity of extract from *Polygonum cuspidatum*. *Biological Research*, 40(1), 13–21. doi: 10.4067/s0716-97602007000100002
- Konopko, A., & Litwinienko, G. (2022). Unexpected Role of pH and Microenvironment on the Antioxidant and Synergistic Activity of Resveratrol in Model Micellar and Liposomal Systems. *The Journal of Organic Chemistry*, 87(3), 1698–1709. doi: 10.1021/acs.joc.1c01801
- Kriel, C. (2020). *The extraction of resveratrol and other polyphenols from solid winery waste and an investigation into alternative resveratrol recovery techniques*. Thesis (M.Eng.), Stellenbosch University. Available at: <https://hdl.handle.net/10019.1/108171>
- Lotz, A., Milz, B., & Spangenberg, B. (2015). A New and Sensitive TLC Method to Measure Trans-Resveratrol in Red Wine. *Journal of Liquid Chromatography & Related Technologies*, 38(11), 1104-1108. doi: 10.1080/10826076.2015.1028288
- Lourenço, S. C., Moldão-Martins, M., Alves, V. D. (2019) Antioxidants of Natural Plant Origins: From Sources to Food Industry Applications. *Molecules*, 24(22): 4132. doi: 10.3390/molecules24224132.
- Matos, L. C., Machado, J. P., Monteiro, F. J., Greten, H. J. (2021) Understanding Traditional Chinese Medicine Therapeutics: An Overview of the Basics and Clinical Applications. *Healthcare*, 9(3): 257. doi: 10.3390/healthcare9030257.
- Noyes, R. M., & Furrow, S. D. (1982). The oscillatory Briggs-Rauscher reaction. 3. A skeleton mechanism for oscillations. *Journal of the American Chemical Society*, 104(1), 45–48. doi: 10.1021/ja00365a011
- Pan, S. Y., Litscher, G., Gao, S. H., Zhou, S. F., Yu, Z. L., Chen, H. Q., Zhang, S. F., Tang, M. K., Sun, J. N., & Ko, K. M. (2014). Historical perspective of traditional indigenous medical practices: the current renaissance and conservation of herbal resources. *Evidence-based complementary and alternative medicine*, 2014: 525340. doi: 10.1155/2014/525340.
- Pannu, N., & Bhatnagar, A. (2019). Resveratrol: from enhanced biosynthesis and bioavailability to multitargeting chronic diseases. *Biomedicine & Pharmacotherapy*, 109, 2237–2251. doi: 10.1016/j.biopha.2018.11.075
- Pereira, D., Valentão, P., Pereira, J., & Andrade, P. (2009). Phenolics: From Chemistry to Biology. *Molecules*, 14(6), 2202–2211. doi: 10.3390/molecules14062202
- Räisänen, R., Björk, H., & Hynninen, P. H. (2000). Two-dimensional TLC separation and mass spectrometric identification of anthraquinones isolated from the fungus *Dermocybe sanguinea*. *Zeitschrift für Naturforschung*. 55(3-4), 195-202. doi: 10.1515/znc.2000-3-410
- Rajha, H. N., Abou Jaoude, N., Louka, N., Maroun, R. G., & Vorobiev, E. (2014). Industrial byproducts valorization through energy saving processes. Alkaline extraction of polyphenols from vine shoots. In International Conference on Renewable Energies for Developing Countries 2014. *2014 International Conference on Renewable Energies for Developing Countries (REDEC)*. doi: 10.1109/redec.2014.7038537
- Ralston, L., Subramanian, S., Matsuno, M., & Yu, O. (2005). Partial reconstruction of flavonoid and isoflavonoid biosynthesis in yeast using soybean type I and type II chalcone isomerases. *Plant Physiology*, 137(4), 1375–1388. doi: 10.1104/pp.104.054502.
- Robinson, K., Mock, C., & Liang, D. (2015). Pre-formulation studies of resveratrol. *Drug Development and Industrial Pharmacy*, 41(9), 1464–1469. doi: 10.3109/03639045.2014.958753.
- Rodríguez-Bonilla, P., Gandía-Herrero, F., Matencio, A., García-Carmona, F., & López-Nicolás, J. M. (2017). Comparative Study of the Antioxidant Capacity of Four Stilbenes Using ORAC, ABTS+, and FRAP Techniques. *Food Analytical Methods*, 10(9), 2994–3000. doi: 10.1007/s12161-017-0871-9
- Rubio, C. P., Hernández-Ruiz, J., Martínez-Subiela, S., Tvarijonavičiute, A., & Ceron, J. J. (2016). Spectrophotometric assays for total antioxidant capacity (TAC) in dog serum: an update. *BMC Veterinary Research*, 12(1): 166. doi: 10.1186/s12917-016-0792-7
- Samal, P. (2010) *A Brief Discussion on Color*. University of Massachusetts. <https://people.chem.umass.edu/samal/269/color.pdf>
- Sato, M., Maulik, G., Bagchi, D., & Das, D. K. (2000). Myocardial protection by Protynin, a novel extract of trans-resveratrol and emodin. *Free Radical Research*, 32(2), 135–144. doi: 10.1080/1071576000300141
- Sotler, R., Poljšak, B., Dahmane, R., Jukić, T., Pavan Jukić, D., Rotim, C., Trebše, P., & Starc, A. (2019). Prooxidant activities of antioxidants and their impact on health. *Acta Clinica Croatica*, 58(4), 726–736. doi: 10.20471/acc.2019.58.04.20.
- Tong, A., Tang, X., Zhang, F., & Wang, B. (2020). Study on the shift of ultraviolet spectra in aqueous solution with variations of the solution concentration. *Spectrochimica Acta Part A: Molecular and Biomolecular Spectroscopy*, 234: 118259. doi: 10.1016/j.saa.2020.118259
- Trela, B. C., & Waterhouse, A. L. (1996). Resveratrol: Isomeric Molar Absorptivities and Stability. *Journal of Agricultural and Food Chemistry*, 44(5), 1253–1257. doi: 10.1021/jf9504576
- Tsao, R. (2010). Chemistry and Biochemistry of Dietary Polyphenols. *Nutrients*, 2(12), 1231–1246. doi: 10.3390/nu2121231.
- Valko, M., Leibfritz, D., Moncol, J., Cronin, M. T. D., Mazur, M., & Telsler, J. (2007). Free radicals and antioxidants in normal physiological functions and human disease. *The International Journal of Biochemistry & Cell Biology*, 39(1), 44–84. doi: 10.1016/j.biocel.2006.07.001
- Venuti, V., Cannavà, C., Cristiano, M. C., Fresta, M., Majolino, D., Paolino, D., Stancanelli, R., Tommasini, S., & Ventura, C. A. (2014). A characterization study of resveratrol/sulfobutyl ether- $\beta$ -cyclodextrin inclusion complex and in vitro anticancer activity. *Colloids and Surfaces B: Biointerfaces*, 115, 22–28. doi: 10.1016/j.colsurfb.2013.11.025
- Wang, Y., Xu, H., Fu, Q., Ma, R., Xiang, J. (2011) [Resveratrol derived from rhizoma et radix *Polygoni cuspidati* and its liposomal form protect nigral cells of Parkinsonian rats]. *Zhongguo Zhong Yao Za Zhi*, 36(8): 1060-6. PMID: 21809586.
- Wei, X., Shen, H., Wang, L., Meng, Q., & Liu, W. (2016). Analyses of Total Alkaloid Extract of *Corydalis yanhusu* by Comprehensive RP  $\times$  RP Liquid Chromatography with pH Difference. *Journal of Analytical Methods in Chemistry*, 2016: 1-8. doi: 10.1155/2016/9752735

Xu, D. P., Li, Y., Meng, X., Zhou, T., Zhou, Y., Zheng, J., Zhang, J. J., & Li, H. B. (2017). Natural Antioxidants in Foods and Medicinal Plants: Extraction, Assessment and Resources. *International Journal of Molecular Sciences*, 18(1): 96. doi: 10.3390/ijms18010096.

Zeb, A. (2020). Concept, mechanism, and applications of phenolic antioxidants in foods. *Journal of Food Biochemistry*, 44(9): e13394. doi: 10.1111/jfbc.13394.

Zhang, H., Li, C., Kwok, S. T., Zhang, Q. W., & Chan, S. W. (2013). A review of the pharmacological effects of the dried root of *Polygonum cuspidatum* (Hu Zhang) and its constituents. *Evidence-based Complementary and Alternative Medicine*, 2013: 208349. doi: 10.1155/2013/208349

Zupančič, Š., Lavrič, Z., & Kristl, J. (2015). Stability and solubility of trans-resveratrol are strongly influenced by pH and temperature. *European Journal of Pharmaceutics and Biopharmaceutics*, 93, 196–204. doi: 10.1016/j.ejpb.2015.04.002

## Bibliography

Catalgol, B., Batirel, S., Taga, Y., Ozer, N. K. (2012) Resveratrol: French paradox revisited. *Frontiers in Pharmacology*, 17(3): 141. doi: 10.3389/fphar.2012.00141.

Munteanu, I. G., & Apetrei, C. (2021). Analytical Methods Used in Determining Antioxidant Activity: A Review. *International Journal of Molecular Sciences*, 22(7), 3380. doi: 10.3390/ijms22073380.

Renaud, S., & de Lorgeril, M. (1992). Wine, alcohol, platelets, and the French paradox for coronary heart disease. *The Lancet*, 339(8808), 1523–1526. doi: 10.1016/0140-6736(92)91277-f

**Access the full article submitted to the IB,  
including Appendices:**





---

# EnviroDroid: a Trash-Picking Robot

Harry Wang

---

## 1. Project Outline

This project intends to investigate the effectiveness of a smart trash-picking robot with a camera that allows it to recognize and locate trash. It can potentially be applied in a wide range of settings, from indoor spaces to beaches with rubbish.

### 1.1 Original Plan

The product tested in this project is a robot that drives around autonomously while picking up trash. The robot was intended to be powered by a single-board computer (e.g. a Raspberry Pi or an Nvidia Jetson Nano), which would run an AI algorithm to detect trash via the robot's camera. Once it detects trash, it would automatically pick it up using its robotic arm (driven by servo motors) and bring it into the nearest bin. In addition, the robot would need to have other sensors like laser rangefinders and ultrasonic sensors for it to drive autonomously.

### 1.2 Success Criteria:

A success criteria rubric was created specifying the goals the robot aims to achieve in this project. The following aspects contributed to the success criteria:

#### Safety

- To be safe, the Envirodroid must consist of no sharp edges, exposed wiring, or potentially dangerous components.
- It should also be able to avoid humans at will, for it could pose a tripping hazard.

#### Function

- The robot should detect trash with accuracy (e.g. it shouldn't accidentally recognize something that isn't trash).
- My robot should be able to pick up trash on the floor with speed and efficiency.

#### Physical Performance

- The robot should be able to drive in all directions with speed and mobility.
- The robot should have a long battery life, able to move for at least a few hours without having to charge.
- It should be durable and able to survive some damage.

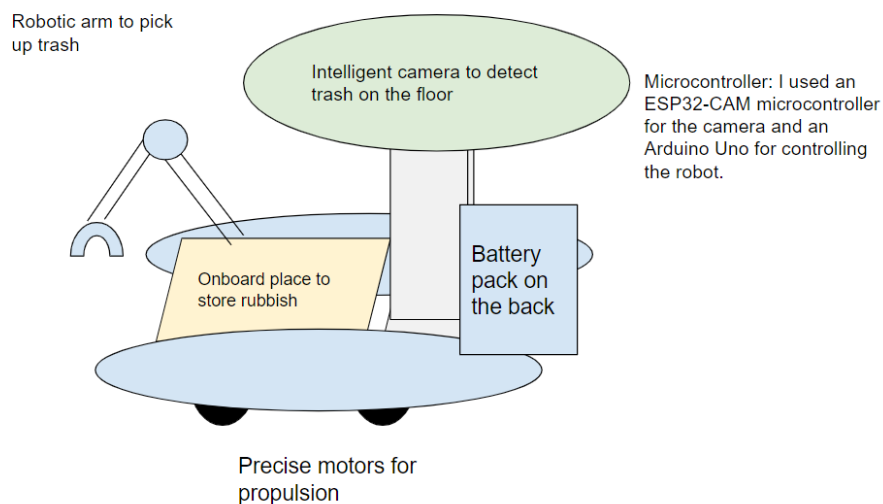
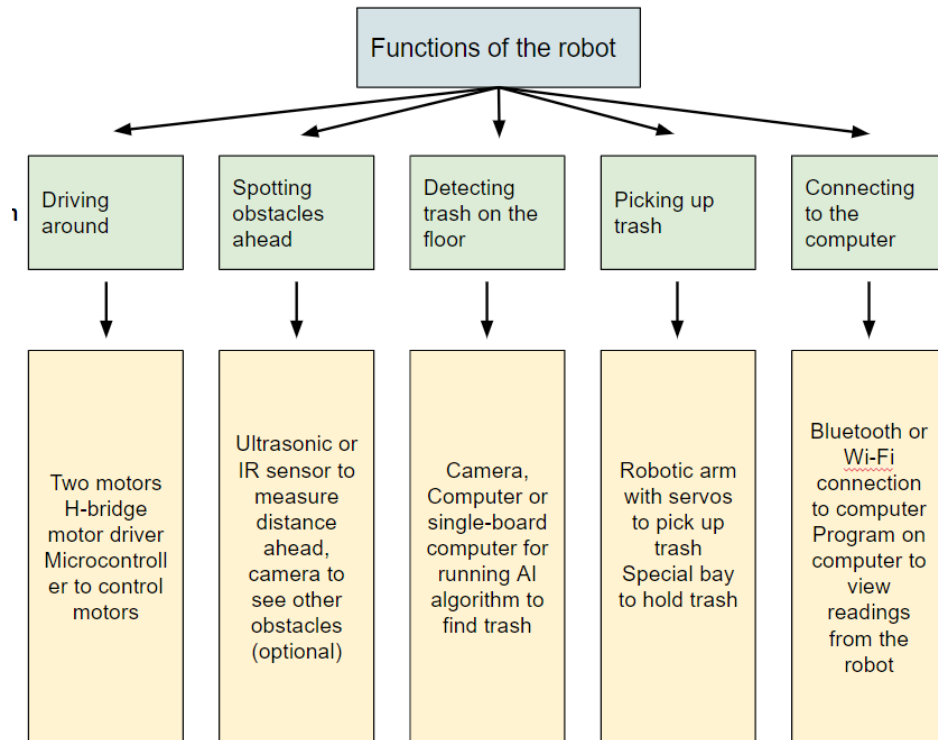


Figure 1. An initial design for the robot

---

The above article was written as a Personal Project, in partial fulfillment of the Middle Years Programme, 2023.



**Figure 2.** A diagram outlining the main functions of the robot

### Automation

- The robot should be able to drive around autonomously and move between rooms without constant human control (e.g. it should return to a point to charge if it is low on battery instead of requiring a human to charge it regularly).
- It should also be reliable, not needing regular maintenance.

### Cost

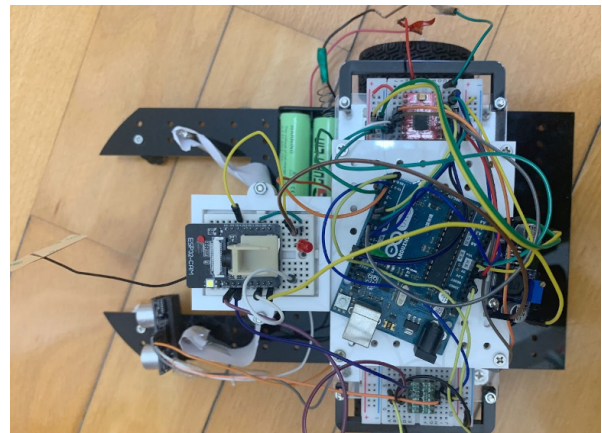
- The Envirodroid should be made out of parts readily available at my home or at school.
- Parts that need to be bought must be at a reasonable price

### Aesthetics

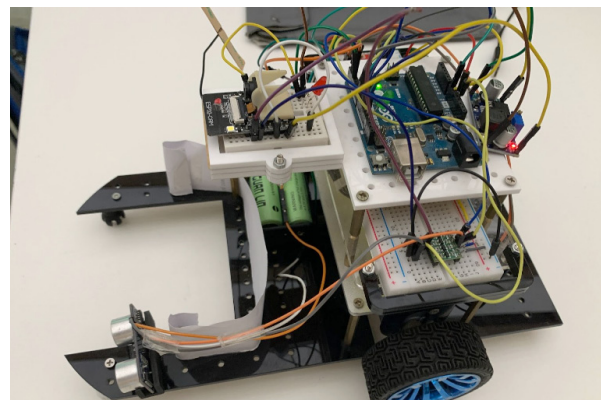
- The robot should look friendly so people will have a good impression of it.

## 2. Creation Process and Details

Upon the creation of the product plan, the robot was built over the next few months. In addition, a motion-controlled remote control was created for convenient control of the robot. Final pictures of the robot and the controller are shown in Figures 3-6.



**Figure 3.** A top view of the robot



**Figure 4.** A side view of the robot

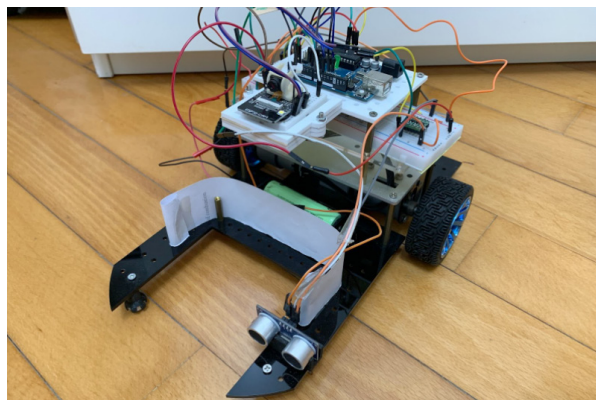


Figure 5. A front view of the robot

Some changes were made to the original plans. In terms of hardware, the robot was considerably smaller than the original design, and to reduce the complexity of the robot, a simple trash-scooping bay was made instead of a robotic arm for picking up trash. In addition, the autonomous capabilities were lessened due to the sensors being unavailable. In the end, only an ultrasonic obstacle sensor was used. Finally, due to single-board computers such as the Raspberry Pi not being available, the ESP32-CAM, a microcontroller with a camera was used instead. The image processing was done on a computer, as shown in the diagram below. While this new design limited its capabilities, it nevertheless worked.

The following compares the details about the robot creation designs:

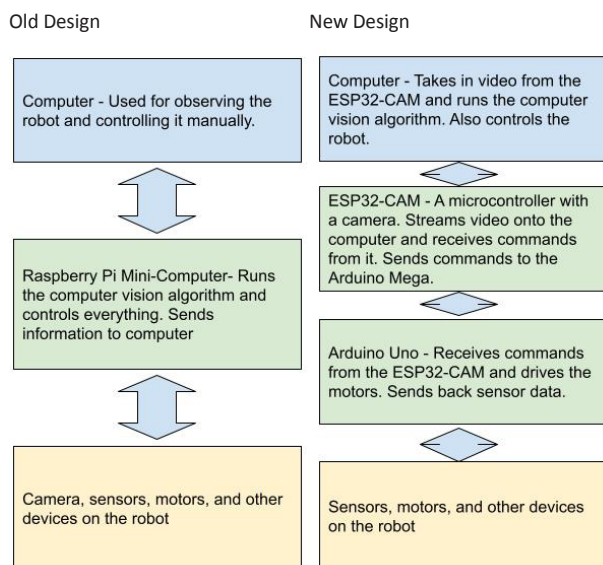


Figure 7. In comparing old and new designs for the robot, the main controller was switched from a single-board computer to a microcontroller and the image processing was shifted to the computer.

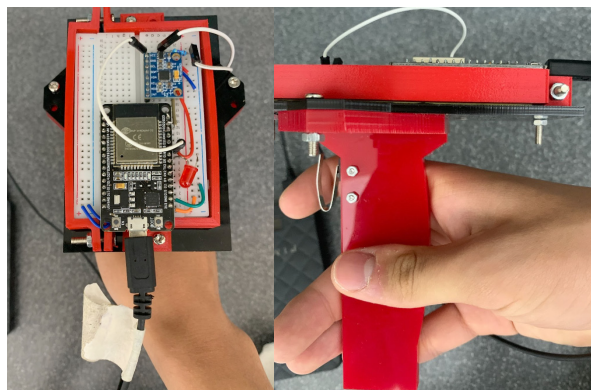


Figure 6. The motion-detecting remote controller as seen from different angles

## 2.1 Hardware

The robot was designed with CAD using Fusion 360, as seen in Figure 8. The frame of the robot was laser-cut using acrylic, while the front wheels of the robot were 3D-printed using PLA filament.

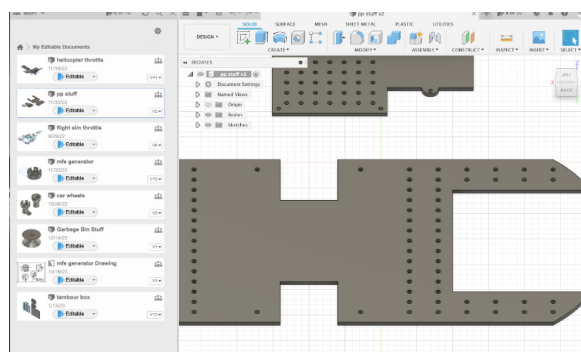


Figure 8. The design of the robot frame in Fusion 360

## Electronics

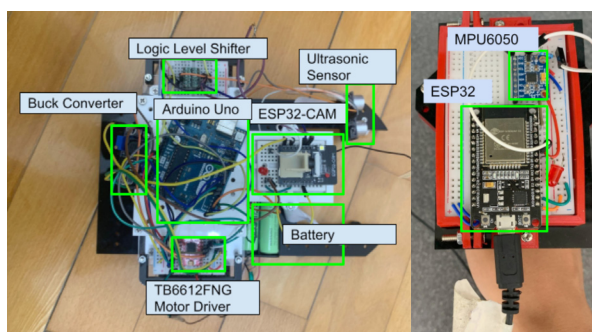


Figure 9. An outline of the electronic components of the robot and the remote controller

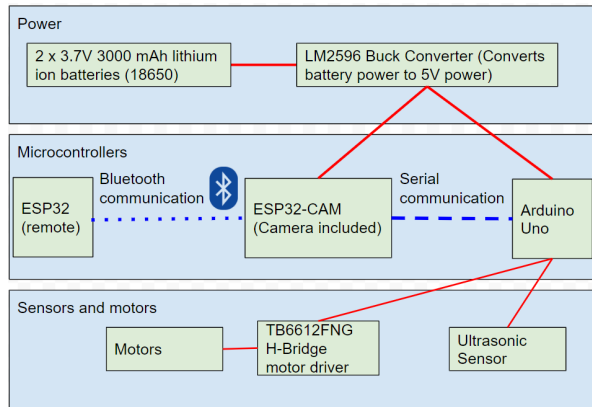


Figure 10. A block diagram showing the key components of the robot

## Main Control

Figure 10 shows how the main controller of the robot is an ESP32-CAM module, which is an ESP32 microcontroller connected to a camera. The ESP32-CAM will capture images using the camera and relay them back to the computer. It will receive Wi-Fi and Bluetooth signals from the computer or the Bluetooth remote, which it would process and deal with accordingly (e.g. if it receives a Bluetooth control signal from the controller, it would send a signal to the Arduino to drive it). The ESP32-CAM module requires precisely 3.3V to run, and hence a buck converter was needed to step the 7.4V power from the battery down to 3.3V, which the ESP32-CAM could easily use.

## Motor Control

As the ESP32-CAM does not have sufficient GPIO (General-Purpose Input-Output) pins to drive the motors, an extra Arduino Uno was used to control the motors. The ESP32-CAM sends signals using the UART (Universal Asynchronous Receiver / Transmitter) protocol to the Arduino. The Arduino then controlled the speed and direction of the motors using a TB6612FNG H-bridge module. H-bridges are circuits consisting of four switches as shown in the circuit diagram (Figure. 11). They enable motors to drive in both directions.

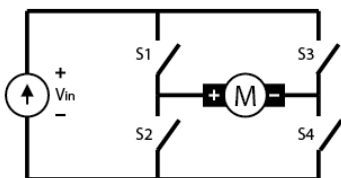


Figure 11. A functional diagram of the H-bridge used to control the robot's motors (Franz, 2023).

## Obstacle detection

An HC-SR04 ultrasonic distance sensor was placed at the front of the robot to sense obstacles straight ahead. It was connected to the Arduino Uno, which would stop the robot from going forwards if an obstacle were detected ahead. Unfortunately, due to the short range (during tests, it had a range of just 1 m) and the limited field of view, the sensor proved to be ineffective in helping the robot navigate.

## Controller

The Bluetooth motion controller uses an ESP32 to transmit signals to the robot's ESP32-CAM. It detects motion using an MPU6050 accelerometer module. The MPU6050 measures the acceleration in the X, Y, and Z axis and locates the direction of the ground, allowing it to measure the tilt relative to the ground.

## Power

The power for the robot comes from two 18650 batteries, each at 3.7V with 3000 mAh. The total capacity of the two batteries is 22.2 Wh of power. During tests, the batteries sustained the robot to drive for many hours.

## 2.2 Software

### Code

The code for the Arduino Uno and ESP32-CAM was written in C++ using the Arduino IDE. The following shows part of the ESP32-CAM code:

Figure 12. A part of the program for the robot

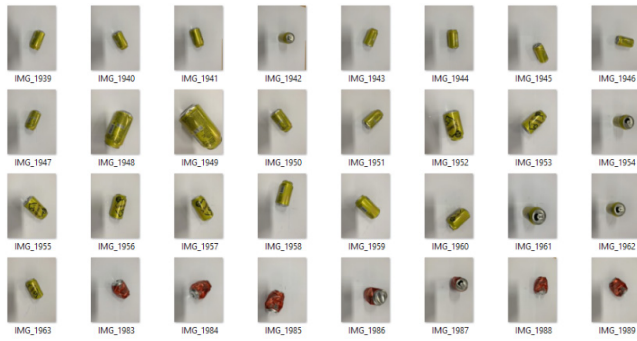
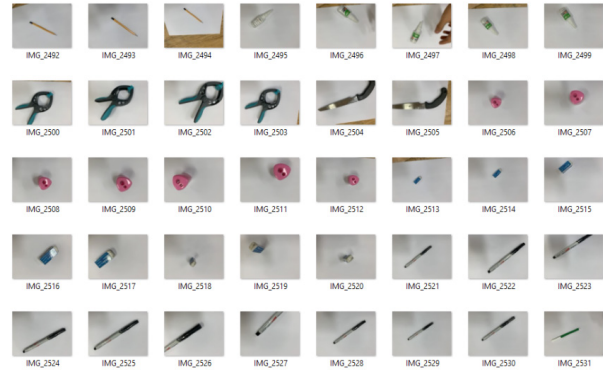


Figure 13. Images that were used for training the trash-classifying model



## Robot Control

The ESP32-CAM receives Bluetooth or WiFi signals from the computer or controller, which it sends to the Arduino Uno that would drive the motors.

## Streaming Images

The ESP32-CAM runs a web server on its own Wi-Fi access point. To read images from the ESP32-CAM, a device connects to the ESP32-CAM and sends a request via the Hyper Text Transfer Protocol (HTTP). The ESP32-CAM then sends the image back in JPG format.

## Image Recognition

A computer program is used to receive the camera data from the ESP32-CAM to recognize trash. A Tensorflow model was used to classify the images between metal, paper, plastic, and trash based on a custom-made dataset consisting of over 2000 self-taken pictures and online pictures of trash in white backgrounds (Figure 13).

Originally, the model was trained with a custom-made neural network made with TensorFlow Keras API. However, only low accuracies were achieved using this method. As seen in Figure 14, despite countless attempts, the validation accuracies in the red lines only achieved a maximum of 80%. Significant overfitting was detected and the model was very slow.

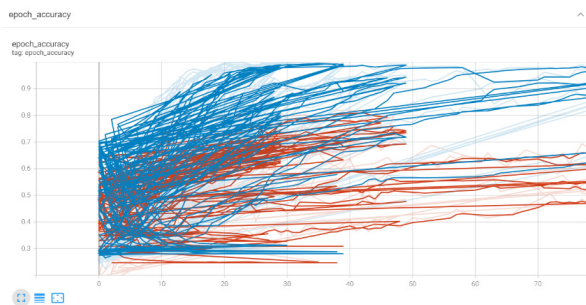


Figure 14. The countless failed attempts to train a neural network to classify trash, as seen from Tensorboard. The large gap between the red and blue lines indicates overfitting.

Due to these problems, the model was retrained on Teachable Machine. Using Teachable Machine, the model achieved near-perfect accuracy in optimal conditions. In addition, it was a lot faster, taking just 25 milliseconds to run on an Intel Macbook Air.

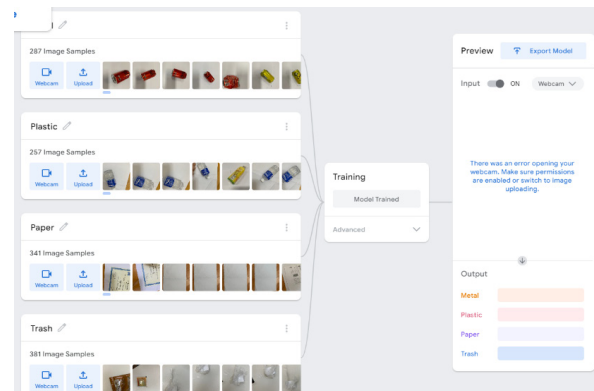


Figure 15. The Teachable Machine model used for classifying images in the end.

## 3. Testing Process

### 3.1 Test Results and Evaluation

The following is footage of some tests conducted on the robot.



Figure 16. The motion-controlled controller drives the robot



Figure 17. The robot streams footage while being controlled by arrow keys

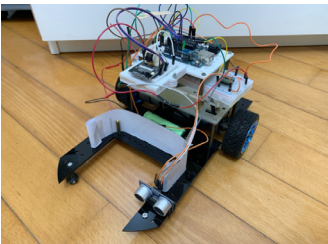


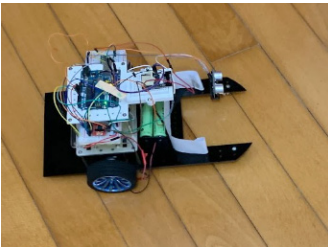
Figure 18. The robot recognizes the trash type using its camera

Throughout the tests, the robot demonstrated the following capabilities:

- It could drive in any direction swiftly. The battery can allow it to drive for hours.
- It can be controlled by many methods such as via a Bluetooth motion controller, or via Wi-Fi on a laptop.
- It has a camera that can stream video to the computer. The computer can run a trash-detecting algorithm for it to recognize trash. However, it is highly inaccurate and cannot pinpoint the position of the piece of trash.
- It has an ultrasonic sensor in front that can detect obstacles. This can allow it to drive with some degree of autonomy, being able to avoid obstacles up ahead (not shown in video).

### 3.2 Evaluation of Original Success Criteria

Success Criteria Aspect	Comments and rating from 1 - 10
<p>Safety</p> <ul style="list-style-type: none"> <li>• To be safe, my robot must consist of no sharp edges, exposed wiring, or potentially dangerous components.</li> <li>• It should also be able to avoid humans at will, for it could pose a tripping hazard.</li> </ul>	<p>Strengths</p> <ul style="list-style-type: none"> <li>• The robot can avoid obstacles ahead with the ultrasonic sensor.</li> <li>• The robot operates on just 7.4 volts, which is safe.</li> </ul> <p>Weaknesses</p> <ul style="list-style-type: none"> <li>• The robot has almost all of its wires exposed which are potential hazards as seen here.</li> </ul>  <ul style="list-style-type: none"> <li>• The front of the robot is sharp, which is a potential danger.</li> </ul> <p>Overall, safety rating = 4/10.</p>

<p>Function</p> <ul style="list-style-type: none"> <li>The robot should detect trash with accuracy (e.g it shouldn't accidentally recognize something that isn't trash).</li> <li>The robot should be able to pick up trash on the floor with speed and efficiency.</li> </ul>	<p>Strengths</p> <ul style="list-style-type: none"> <li>The robot can recognize pieces of trash to easy conditions (i.e they are very obvious to spot).</li> <li>The robot can push pieces of trash and gather them into locations.</li> </ul> <p>Weaknesses</p> <ul style="list-style-type: none"> <li>The algorithm on the robot is flawed and cannot properly distinguish between objects. Since it finds objects of certain colors, objects of the same color as normal rubbish will be detected.</li> <li>Unlike my plan, the robot lacks a robotic arm to pick up things. It can only scoop things with the front.</li> </ul> <p>Overall, function rating = 2/10.</p>
<p>Physical Performance</p> <ul style="list-style-type: none"> <li>The robot should be able to drive in all directions with speed and mobility.</li> <li>The robot should have a long battery life, able to move for at least a few hours without having to charge.</li> <li>It should be durable and able to survive some damage.</li> </ul>	<p>Strengths</p> <ul style="list-style-type: none"> <li>The robot is highly mobile, with the battery providing sufficient power.</li> <li>The robot has a decent battery life as I successfully had it working for hours without running out of power.</li> </ul> <p>Weaknesses</p> <ul style="list-style-type: none"> <li>The robot isn't very durable as the wires are all exposed. It might crash and break due to a wire disconnecting.</li> <li>The robot ran into a short-circuit during testing. If this ever happens in a real operation, it will make the robot less durable.</li> </ul> <p>Overall, physical performance rating = 6/10</p>
<p>Automation</p> <ul style="list-style-type: none"> <li>The robot should be able to drive around autonomously and move rooms without human control regularly(e.g it should return to a point to charge if it is low on battery instead of requiring a human to charge it regularly).</li> <li>It should also be reliable, not needing regular maintenance.</li> </ul>	<p>Strengths</p> <ul style="list-style-type: none"> <li>The obstacle sensor can help detect basic obstacles to help the robot drive around with basic automation.</li> </ul> <p>Weaknesses</p> <ul style="list-style-type: none"> <li>The autonomous driving program for the robot is highly unsophisticated and lacks many capabilities. It cannot map a room, and therefore will not be able to traverse around it.</li> </ul>  <ul style="list-style-type: none"> <li>In a test in my room, the robot kept driving in circles and failed to get out of it (see picture above).</li> <li>The robot has many issues regarding reliability. It frequently stops working in the middle of operation. There are also network problems that impede its ability to operate independently.</li> </ul> <p>Overall, automation rating = 2/10. It can seldom work without human intervention.</p>

<p>Cost</p> <ul style="list-style-type: none"> <li>• I should make the robot out of parts readily available at my home or at school.</li> <li>• Parts that need to be bought must be at a reasonable price</li> </ul>	<p>Strengths</p> <ul style="list-style-type: none"> <li>• It cost no money at all, and I managed to <i>get all</i> the parts from what I had.</li> <li>• In addition, the parts such as microcontrollers, wires, motors, and other parts on the robot were all very cheap.</li> </ul> <p>Overall, cost rating = 9/10.</p>
<p>Aesthetics</p> <ul style="list-style-type: none"> <li>• The robot should look friendly so people will have a good impression of it.</li> </ul>	<p>Strengths</p> <ul style="list-style-type: none"> <li>• The robot has some shiny-looking parts cut from acrylic.</li> </ul> <p>Weaknesses</p> <ul style="list-style-type: none"> <li>• The robot has exposed wires, and no decorations.</li> </ul> <p>Overall, aesthetics rating = 5/10.</p>

#### 4. Real-life Applications of the Robot

There are many potential applications for this robot, as trash exists everywhere and needs to be cleaned in many places. Furthermore, the autonomous capabilities and smart camera on this robot can allow it to be used in other places.

Littering is a major problem in urban areas due to space and a large number of people. The strenuous and time-consuming nature of picking up trash makes it costly. This robot offers a cost-effective solution to picking up trash as it can drive around autonomously while picking up trash, possibly without the need of any human. In addition, since the robot can drive around autonomously, it could perform other tasks that require manual labor, such as delivering small objects around places, sanitizing the floors in the room, or actively reminding people around it to pick up trash.

The robot could be modified to be used in outdoor settings such as beaches, where it can pick up trash that would otherwise fall into the ocean. This can help reduce the amount of plastic in the environment, positively contributing to the UN Sustainable Development Goals (SDGs) of Climate Action, Life on Land, and Life Below Water. It could also be used to count the number of pieces of trash in an area to assess the amount of trash contamination.

The first-person-view capability of the robot camera allows it to drive without being in the line of sight, as the operator can see through the robot's camera stream. This implies that it can navigate potentially dangerous spaces that humans cannot access.

#### 5. Areas of Further Research and Development

The robot is currently imperfect and can benefit from further research and development in several aspects.

On the hardware side, the accuracy of the robot could be improved. The robot has no sensors or accurate methods of measuring its speed/direction, which can be a major hassle for it to make precise movements. Solutions to this problem could be to use the built-in encoders on the robot's motors or to use positioning sensors such as optical mouse sensors. Furthermore, obstacle-sensing sensors on the robot could be improved as the robot currently only has a forward-sensing ultrasonic sensor. An improvement could be to use a LIDAR (Light Detection and Ranging) scanners, which can rapidly scan the entire space surrounding the robot. This can allow the robot to map its surroundings simultaneously as it drives, allowing it to navigate complex spaces and become more autonomous. Finally, the overall layout of the robot could be improved. The large number of wires sticking out are a potential hazard and are at the risk of short-circuiting. A shell could be used to cover the robot to make it neater.

On the software side, the computer algorithm for detecting trash simply gets the whole image and categorizes it into metal, paper, plastic, or trash. It is not accurate to find trash, *let alone* at pinpointing the location of it. An improvement could be to use algorithms such as YOLO or SSD Mobilenet that pinpoint the exact location of trash identified to aid the robot to detect trash more accurately. Using or developing another, larger



dataset consisting of more varied pieces of trash could also be more helpful. Another improvement could be to the streaming capability of the robot. It can only stream at approximately 10 frames per second at best, even with just 240 x 320 - sized pictures. A possible solution could be to use the UDP protocol to stream video rather than TCP/IP. The absence of a handshake in UDP allows for it to stream at significantly higher speeds allowing the video to be streamed at higher framerates.

Beyond the software and hardware of this robot, further research could be conducted to apply the robot in different scenarios. For example, an investigation could be conducted on the feasibility of the robot for cleaning rooms or large indoor spaces automatically, or on the viability of the robot for delivering cargo across short distances indoors.

## Bibliography

altanai. "Computer Vision for Garbage Detection." *Medium*, Ramudroid, 5 Aug. 2020, [medium.com/ramudroid/computer-vision-for-garbage-detection-136029142b3c](https://medium.com/ramudroid/computer-vision-for-garbage-detection-136029142b3c). Accessed 30 Jan. 2023.

Andreu, Oriol. "Semantic Image Cropping." July 2021.

Baranyi, Peter. "Cognitive Image Analysis Based on a Parallel Computational Model." Jan. 2005.

"C++ - Reading an Opencv Image in Python through a Socket." *Stack Overflow*, 15 Jan. 2018, [stackoverflow.com/questions/47936365/reading-an-opencv-image-in-python-through-a-socket](https://stackoverflow.com/questions/47936365/reading-an-opencv-image-in-python-through-a-socket). Accessed 30 Jan. 2023.

CodeSavant. "Ball Detection Using OpenCV in Python." *www.youtube.com*, 26 Dec. 2021, [www.youtube.com/watch?v=RaCwLrKuS1w](https://www.youtube.com/watch?v=RaCwLrKuS1w). Accessed 28 Jan. 2023.

EdgeElectronics. "How to Set up TensorFlow Object Detection on the Raspberry Pi." *www.youtube.com*, 19 July 2018, [www.youtube.com/watch?v=npZ-8Nj1YwY](https://www.youtube.com/watch?v=npZ-8Nj1YwY). Accessed 30 Jan. 2023.

ET Online. "Tired of Sweeping Your House This Lockdown? Get a Robot - a New Way to Clean the Floors." *The Economic Times*, 6 Aug. 2020, [economictimes.indiatimes.com/small-biz/startups/features/tired-of-sweeping-your-house-this-lockdown-get-a-robot-a-new-way-to-clean-the-floors/slideshow/77365809.cms](https://economictimes.indiatimes.com/small-biz/startups/features/tired-of-sweeping-your-house-this-lockdown-get-a-robot-a-new-way-to-clean-the-floors/slideshow/77365809.cms). Accessed 30 Jan. 2023.

Etzioni, Oren, and Daniel Weld. "The First Law of Robotics (a Call to Arms)." 1994.

Evan. "EdgeElectronics/TensorFlow-Lite-Object-Detection-On-Android-And-Raspberry-Pi." *GitHub*, 15 Mar. 2021, [github.com/EdgeElectronics/TensorFlow-Lite-Object-Detection-on-Android-and-Raspberry-Pi](https://github.com/EdgeElectronics/TensorFlow-Lite-Object-Detection-on-Android-and-Raspberry-Pi). Accessed 30 Jan. 2023.

Hassan, Murtaza. "Object Detection OpenCV Python | Easy and Fast (2020)." *www.youtube.com*, 30 Aug. 2020, [www.youtube.com/watch?v=HXDD7-EnGBY](https://www.youtube.com/watch?v=HXDD7-EnGBY). Accessed 25 Jan. 2023.

---. "Object Tracking - Computer Vision Zone." *Computervision.zone*, 2021, [www.computervision.zone/topic/object-tracking-3/](https://www.computervision.zone/topic/object-tracking-3/). Accessed 30 Jan. 2023.

---. "Self-Driving Car Using Raspberry Pi." *Computer Vision Zone*, 10 Feb. 2019, [www.computervision.zone/courses/self-driving-car-using-raspberry-pi/](https://www.computervision.zone/courses/self-driving-car-using-raspberry-pi/). Accessed 25 Jan. 2023.

Horaczek, Stan. "This May Be the Friendly Robot Face You See before You Die." *Popular Science*, 24 Jan. 2019, [www.popsci.com/health-robot-companions/](https://www.popsci.com/health-robot-companions/). Accessed 30 Jan. 2023.

Kassah, Adel. "ESP32 Tutorial B-15: Streaming to OpenCV." *www.youtube.com*, 19 June 2021, [www.youtube.com/watch?v=JDlm0BhgHCE](https://www.youtube.com/watch?v=JDlm0BhgHCE). Accessed 30 Jan. 2023.

M-short. "TB6612FNG Hookup Guide - Learn.sparkfun.com." *Sparkfun.com*, 2016, [learn.sparkfun.com/tutorials/tb6612fng-hookup-guide/all](https://learn.sparkfun.com/tutorials/tb6612fng-hookup-guide/all). Accessed 25 Jan. 2023.

Maggi. "Computer Vision Color Detection." *Public Lab*, 9 July 2018, [publiclab.org/notes/MaggPi/07-09-2018/computer-vision-color-detection](https://publiclab.org/notes/MaggPi/07-09-2018/computer-vision-color-detection). Accessed 25 Jan. 2023.

Marr, Bernard. "The 4 Ds of Robotization: Dull, Dirty, Dangerous and Dear." *Forbes*, 16 Oct. 2017, [www.forbes.com/sites/bernardmarr/2017/10/16/the-4-ds-of-robotization-dull-dirty-dangerous-and-dear/?sh=30e2f5993e0d](http://www.forbes.com/sites/bernardmarr/2017/10/16/the-4-ds-of-robotization-dull-dirty-dangerous-and-dear/?sh=30e2f5993e0d). Accessed 30 Jan. 2023.

Modular Circuits (2012). H-Bridges – the Basics | Modular Circuits. [online] *Modularcircuits.com*. Available at: <https://www.modularcircuits.com/blog/articles/h-bridge-secrets/h-bridges-the-basics/>.

Payne, G. "ESP32 Camera Robot - FPV." *Instructables*, [www.instructables.com/ESP32-Camera-Robot-FPV-Teacher-Entry/#madeits](http://www.instructables.com/ESP32-Camera-Robot-FPV-Teacher-Entry/#madeits). Accessed 30 Jan. 2023.

Raval, S. "YOLO Object Detection (TensorFlow Tutorial)." *www.youtube.com*, 16 Nov. 2017, [www.youtube.com/watch?v=4eIBisqx9\\_g&t=1175s](http://www.youtube.com/watch?v=4eIBisqx9_g&t=1175s). Accessed 30 Jan. 2023.

Redmon, J. "YOLO: Real-Time Object Detection." *Pjreddie.com*, 2012, [pjreddie.com/darknet/yolo/](http://pjreddie.com/darknet/yolo/). Accessed 30 Jan. 2023.

Reichelt Elektronik. "ROBOT CAR KIT 01 - Robot Chassis Kit for All ARDUINO Systems." *Elektronik Und Technik Bei Reichelt Elektronik Günstig Bestellen*, [www.reichelt.com/de/en/robot-chassis-kit-for-all-arduino-systems-robot-car-kit-01-p219024.html](http://www.reichelt.com/de/en/robot-chassis-kit-for-all-arduino-systems-robot-car-kit-01-p219024.html). Accessed 30 Jan. 2023.

Santos, R. "ESP32 Access Point (AP) for Web Server | Random Nerd Tutorials." *Random Nerd Tutorials*, 9 Aug. 2018, [randomnerdtutorials.com/esp32-access-point-ap-web-server/](http://randomnerdtutorials.com/esp32-access-point-ap-web-server/). Accessed 30 Jan. 2023.

Shenoy, G. "The Importance of Aesthetics to Consumer Products." *www.onshape.com*, 22 May 2019, [www.onshape.com/en/blog/the-importance-of-aesthetics-to-consumer-products](http://www.onshape.com/en/blog/the-importance-of-aesthetics-to-consumer-products). Accessed 11 Jan. 2023.

TensorFlow. "Build an Image Classifier (ML Zero to Hero - Part 4)." *www.youtube.com*, 19 Sept. 2019, [www.youtube.com/watch?v=u2TjZzNuly8](http://www.youtube.com/watch?v=u2TjZzNuly8). Accessed 5 Nov. 2021.

---

# Investigating the Gut Microbiota of Domestic Dogs in Hong Kong by 16S Sequencing

James A. Schrantz

---

## Introduction

In humans and canines, gut health depends on the diversity of the gut microbiome. Dysbiosis is characterised as an imbalance in the gut microbiome. And, as in humans, dysbiosis in dogs is associated with diarrhoea, discomfort and a loss of condition, as well as immune system disorders.

Early-life colonisers strongly influence the profile of the adult human gut microbiome, so microbes introduced during vaginal delivery and breastfeeding, for example, can help to establish a stable, healthy gut ecosystem going forward (Martínez *et al.*, 2018; Sprockett *et al.*, 2018). The development of the neonatal canine microbiome has not been extensively studied, and its influence on gut health in adult dogs is unknown.

In this study, we assessed possible links between early-life experience and adult gut health by comparing rescued street dogs *vs.* dogs acquired as young puppies from breeders and pet shops by comparison with the Dysbiosis Index (AlShawaqfeh *et al.*, 2017). 16s sequencing was performed to determine the microbial profile in the samples. The 16s rRNA gene is an important ribosomal RNA, and its internal structure is composed of stable and variable regions. Unlike stable regions, which are common across all bacteria, the variable regions show characteristics specific to certain genera and species of bacteria, which enables PCR and sequencing analysis.

Understanding the impact of urban factors on gut health is crucial to building sustainable cities and communities, and learning how our living environment affects our physical well-being.

## 1. Methodology

Faecal samples were collected from a diverse group of domestic dogs around Hong Kong. Bacterial DNA was extracted from the faeces using the Qiagen DNeasy PowerSoil Kit. Following extraction, the FastStart high-fidelity PCR system was used for PCR amplification of the variable region 3-5 (V3-V5) of the bacterial 16s rRNA gene. The Illumina NovaSeq platform was used to sequence the samples. The processed DNA dataset was analysed using QIIME2. The dysbiosis of each sample was calculated using the following formula, index 2.8 from the Review of Applied Indexes for Assessment of Intestinal Microbiota Imbalances (Wei *et al.*, 2021):

$$\text{Dysbiosis Index} = \frac{\text{abundance of Firmicutes}}{\text{abundance of Bacteroidetes}}$$

This index was chosen for its time-efficiency. Google Sheets and ArcGIS mapping software were used to visualise the processed data.

## 2. Data

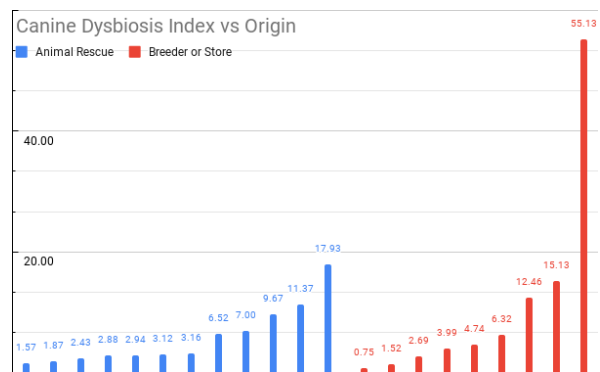


Figure 1. Canine Dysbiosis Index vs. Origin.

This graph shows the calculated dysbiosis of each sample, highlighted according to their origin.

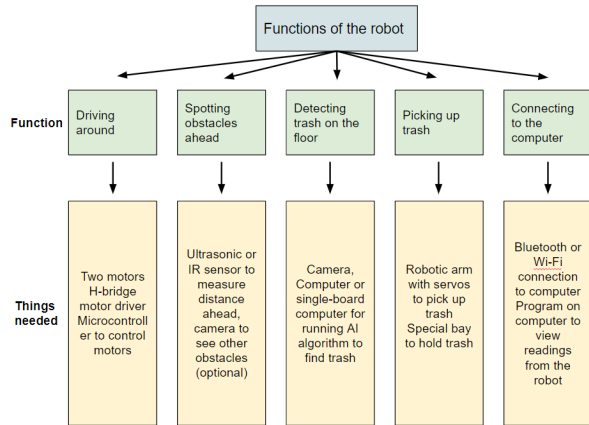


Figure 2. Bray-Curtis Dissimilarity Table

This table shows the Bray-Curtis similarity indices between each pair of samples. Values closer to one are more similar, highlighted in green. Values closer to zero are less similar, highlighted in red. Samples labelled “AR” represent rescue dogs, and samples labelled “B/S” represent breeder or store-bought dogs.

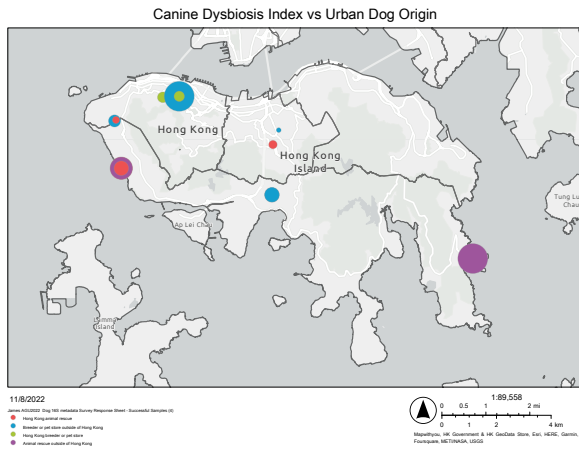


Figure 3. Canine Dysbiosis Index vs. Geographic Location

A map of Hong Kong Island. Each spot represents the living space of one selected sample<sup>1</sup>, the size of each dot represents the dysbiosis of the samples, and the colour represents the origin of the sample.

### 3. Analysis

Based on index 2.8, there is no clear correlation between a dog’s origin and the dysbiosis index (Figure 1). However, according to the Bray-Curtis dissimilarity results (Figure 2), which represent the similarity of 16s sequence data between samples, samples from dogs from breeders or pet stores are more similar than

samples from rescue dogs. This indicates that early life experiences in captivity may correlate with a noticeably different gut microbiome. It is important to recognize that the dysbiosis index and Bray-Curtis results represent different aspects of the samples. The former method describes the levels of dysbiosis according to the chosen index, whereas the latter describes the similarity between the bacterial profiles of the samples. In other words, the data indicates that rescue dogs have greater diversity of gut microbiomes, but not necessarily different levels of dysbiosis than breeder and store dogs.

### Conclusion

A more accurate index to represent the dysbiosis of a sample involves a quantitative PCR panel consisting of eight bacterial groups (AlShawaqfeh *et al.*, 2017), which we were unable to perform due to time constraints. With a relevant index, we could establish better correlations between urban factors and dysbiosis. The previously noted Bray-Curtis dissimilarity data indicate further investigation with a relevant index may yield more promising results.

<sup>1</sup> Samples collected by individuals unwilling to share their geographic data are marked in Cyberport Waterfront Park, shown in the westernmost red dot.

## Acknowledgements

This work was funded under the ISF Shuyuan Research Program. Special thanks to Dr Simon Griffin, Ms Grace Lai, Mr Leung Kung Ming, Ms Diana Ibarra, and Ms Sarah Ratzlaff. Additional thanks to the individuals who graciously contributed their dogs' faecal samples, as well as the dogs themselves for producing said samples.

## References

AlShawaqfeh, M. K., Wajid, B., Minamoto, Y., Markel, M., Lidbury, J. A., Steiner, J. M., Serpedin, E., Suchodolski, J. S. (2017). A dysbiosis index to assess microbial changes in fecal samples of dogs with chronic inflammatory enteropathy. *FEMS Microbiology Ecology*, 93(11), doi: 10.1093/femsec/fix136

Martínez, I., Maldonado-Gomez, M.X., Gomes-Neto, J.C., Kittana, H., Ding, H., Schmaltz, R., Joglekar, P., Cardona, R.J., Marsteller, N.L., Kembel, S.W., Benson, A.K., Peterson, D.A., Ramer-Tait, A.E., Walter, J. (2018) Experimental evaluation of the importance of colonization history in early-life gut microbiota assembly, *eLife*, 7, e36521. doi: 10.7554/eLife.36521

Sprockett, D., Fukami, T., & Relman, D. A. (2018). Role of priority effects in the early-life assembly of the gut microbiota. *Nature Reviews. Gastroenterology & Hepatology*, 15(4), 197–205. <https://doi.org/10.1038/nrgastro.2017.173>

Wei, S., Bahl, M. I., Baunwall, S. M. D., Hvas, C. L., & Licht, T. R. (2021). Determining Gut Microbial Dysbiosis: a Review of Applied Indexes for Assessment of Intestinal Microbiota Imbalances. *Applied and Environmental Microbiology*, 87(11), e00395-21. <https://doi.org/10.1128/AEM.00395-21>

---

# The Application of Don Norman's Principles in Designing and Shaping the User Experience of Digital Products

Jasmine J. L. Leung

---

## Introduction

The user experience is how a user interacts with and experiences a product, including the user's perceptions of utility, ease of use, and efficiency (Interaction Design Foundation, 2022). In today's society, we utilize apps, websites, and digital software across every aspect of our lives (Reid, 2019). As the market for current technologies gradually approaches obsolescence, companies continuously push for research and development into emerging technologies. Hence, designing for the user experience and preparing for technological advancements has never been more critical.

The term "User Experience" first originated in the early 1990s at Apple when used by cognitive psychologist Donald Norman. Norman was the first to ever hold the term "User Experience" in his title, and was the leading voice in developing the field of User Experience design. He introduced the user experience to encompass what had previously been known as human interface research, stating, "I invented the term because I thought Human Interface and usability were too narrow: I wanted to cover all aspects of the person's experience with a system, including industrial design, graphics, the interface, the physical interaction, and the manual" (UX Booth, 2013).

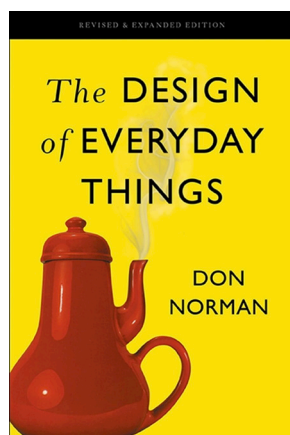


Figure 1. Don Norman's book: The Design of Everyday Things

To ensure designs are accessible and easy for users to use, Don Norman later published his book "The Design of Everyday Things" (Edpresso Team, 2020). Deemed the most influential book in the field of User Experience design, he details six universal principles that must be considered when designing the user experience: visibility, feedback, affordance, mapping, constraints, and consistency, allowing designers to maintain a balance between functionality and aesthetics. Despite there now being variations in these principles, Don Norman's six principles remain as the foundation.

To test the significance of his principles, I have chosen to create an app addressing the issue of sustainability in Hong Kong. Hong Kong currently aims to reach carbon neutrality by 2050 in alliance with the UN sustainability goal of climate change (United Nations, 2022). However, based on current statistics, it is a highly ambitious goal and is not widespread. I will thus be prototyping an app to promote sustainable practice in Hong Kong, by encouraging consumption at environmentally-friendly stores that implement eco-design into their products, as seen in Topic 2 of the IB syllabus. By utilizing and referencing Don Norman's principles when designing, I can then test and analyze the success of my app and these principles.

Regarded as one of the most distinguished researchers and designers in the field of user-centered design, Don Norman's principles of interaction design are still largely used today (Edpresso Team, 2020). With the expansion of the user experience design industry since the introduction of Don Norman's concepts, it is crucial to evaluate whether these principles can still best encompass the entire design of an interactive interface. Hence, this essay will aim to explore the pivotal role his principles play in digital design today, forming the research question "How have Don Norman's principles of design been significant in shaping the user experience, and how can they be utilized in designing a user-centered app interface for sustainability?"

---

The above article was written as an Extended Essay in Design, in partial fulfillment of the IB Diploma Programme, 2023.

# 1. Background

## 1.1 User Experience, User Interface and Interaction Design

User Experience, User Interface, and Interaction Design are often used interchangeably; however, they are not synonymous and must be differentiated (Sharma, 2021). The definitions are as follows:

- User Experience (UX): User experience design considers the entire process and experience of using a product by improving the usability, accessibility, and interactions between the user and product. UX design aims to give users a positive and satisfying experience after using the interface (Babich, 2019).
- Interaction Design (IXD): Interaction design defines the structure and behavior of interactive systems by transforming complex tasks into intuitive, easy-to-use, and accessible designs. IXD aims to redefine tasks to suit all groups of users, whether they are first-time users or experts.
- User Interface (UI): User interface design refers to the visual look and feel of a digital interface and the arrangement of elements such as fonts, buttons, colors, and text fields. UI design aims to make the interface user-friendly, making the user's interaction with the app or website as simple and efficient as possible.

Figure 2 is a diagram of how the three fields work with one another. In summary, UX design is the satisfaction a user derives from the interaction between the user and product (Thackara, 2022). IXD is a branch of UX design that advocates for the user to create intuitive, easy-to-use, and accessible designs. UI design is the section of IXD and UX that focuses on the elements of a website or app and how they work together to ease and simplify the user's interaction. All three terms contribute to achieving Don Norman's principles of design within an interface (Sharma, 2021).

## 1.2 Don Norman's Principles of Design

In this investigation, Don Norman's principles of design will primarily be used to assess and analyze the functionality of three existing digital interfaces and act as a guide in developing a framework for my own interface design. Don Norman's principles of design have been chosen as they are widely regarded as the most cohesive, credible and critical concepts for understanding the usability and learnability of interfaces (Service Design Sydney, 2017), and have also been

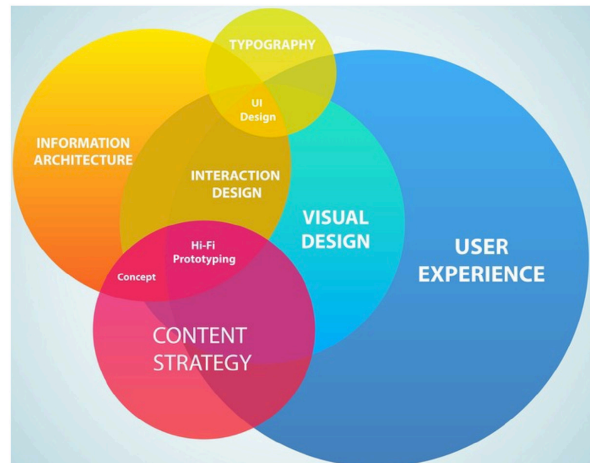


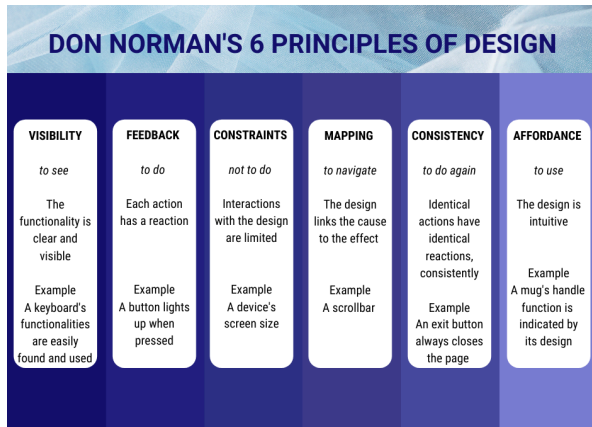
Figure 2. UI design is a part of both UX and IxD, and IxD is a branch of UX design (Dzera, 2017)

selected to be a part of the IB syllabus under Topic 7. Don Norman's six principles of design are outlined in Figure 3 (Engness, 2016), defined in the context of interface design (Rekhi, 2017).

## 1.3 Climate Change in Hong Kong and Sustainable Stores

The United Nations has long deemed climate change and global warming a significant global issue. In line with the worldwide trend, Hong Kong's temperatures have been warming in the last century, with the number of days with cool temperatures decreasing rapidly. Global warming has also caused sea levels to rise in Victoria Harbor. Aside from increasing temperatures, Hong Kong has experienced more frequent and heavy rainfall in recent years (GovHK, 2022). However, the consumption habits of Hong Kong citizens currently do not line up to help combat these trends.

In 2021, the Hong Kong government announced two climate action plans, climate action plan 2030+ and 2050. The government has set an ambitious carbon intensity target of 65% to 70% by 2030; to reduce carbon emissions by 50% before 2035; and to reach carbon neutrality before 2050. It aims to do this using four major decarbonization strategies, namely "net-zero electricity generation," "energy saving and green buildings," "green transport," and "waste reduction." It has started numerous programs to educate citizens about their carbon footprint, stating that small changes to every individual's daily life are the best way to combat climate change. One such way is the introduction of zero-waste, where citizens are encouraged to reuse or recycle used materials as much as possible (HKGov, 2022).



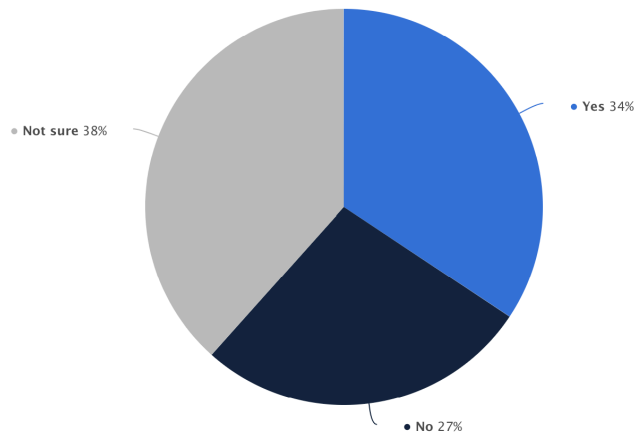
**Figure 3.** Definitions and Examples of Don Norman’s Principles of Design (Prisma Network, 2021)

In Hong Kong, many stores and local businesses have also introduced the zero-waste model to take a more eco-friendly approach to commerce. They do this by making more environmentally conscious choices in packaging and materials, selling reusable or recyclable products, offering refills, and many more. However, many of these stores are currently not well known or are targeted at a very small demographic, in which people are actively searching for these stores. The population stereotype is generally that most people are currently less conscious of their consumption habits, especially younger generations who are often unaware that these stores exist.

Rakuten Insight surveyed 3,910 citizens across Hong Kong of all ages on sustainable consumption in February 2022. They posed the question “Have you adopted any sustainable practices when purchasing items in the last 12 months?”

Approximately 34% of local consumers stated that they had adopted sustainable shopping practices in the past 12 months. In comparison, 27% of respondents had not adopted any sustainable practices during the same time period, with the remaining 38% stating they were unsure (Ma, 2022). Although the survey was only conducted on a small percentage of the Hong Kong population, it can be seen that guidance and encouragement is needed to inform citizens on eco-consumption.

Hence, my app will aim to solve this need by spreading awareness about the existence of these eco-friendly stores, encouraging students to consume at these stores to learn how to reduce their carbon footprint, and applying Don Norman’s principles to create my design.



**Figure 4.** Results from a survey by Rakuten Insight on sustainable consumption in Hong Kong (Ma, 2022)

## 2. Methodology

The research will be divided into two stages to better address my research question. The first stage will mainly answer the first half of my research question, “To what extent have Don Norman’s principles of design been significant in shaping the user experience?”. The latter half “how can they be utilized in designing a user-centered app interface for sustainability?” will be addressed in the second stage.

In the first stage of research, a variety of books, online articles, academic journals, and research papers will be utilized to understand how different frameworks are used in evaluating existing user interfaces. The frameworks from the case studies will be compared to Don Norman’s framework to see if there are overlapping principles or differences.

Two primary research methods are used to gain insight into the significance of Don Norman’s principles in existing interfaces. I will first conduct a questionnaire to obtain user feedback on the user experience of existing interface designs based on how well they conform to Don Norman’s principles. Users will be asked whether they thought the specifications cohesively covered the user experience or if there was any aspect they feel is omitted.

In addition, a product analysis will be conducted on multiple interfaces for further qualitative information. Both primary research methods will allow me to understand if a good user interface follows Don Norman’s principles, and if his principles can best encompass the entire user experience. The above follows Criterion A of the IB Design Cycle.



After the above research is conducted, the findings will be used to create an app promoting existing sustainable and eco-friendly stores in Hong Kong. A wire-frame mockup of the app will first be created to ensure clear flow and cohesiveness between all pages, before a final prototype will be created using the information collected. The prototype will be tested against Don Norman’s framework with the same user group from the questionnaire user trial of the Instagram interface, following Criteria B and C (Figure 5).

## 2.1 Secondary Research Analysis

After his book was published, Don Norman’s principles were the first and most used framework for user experience design. However, with time, numerous authors and designers have come out with their own published frameworks, which they state are crucial in an interface. Below, I sorted through frameworks from five different sources to see if their principles aligned with Don Norman’s. The matched ones were written in each column, and others were written below.

Source 1: [The 7 principles of UX design \(99designs Team, 2020\)](#)

Source 2: [The 5 Key UX Design Principles You Need to Know \(Grass, 2021\)](#)

Source 3: [5 Core Principles of UX Design \(Hughes, 2019\)](#)

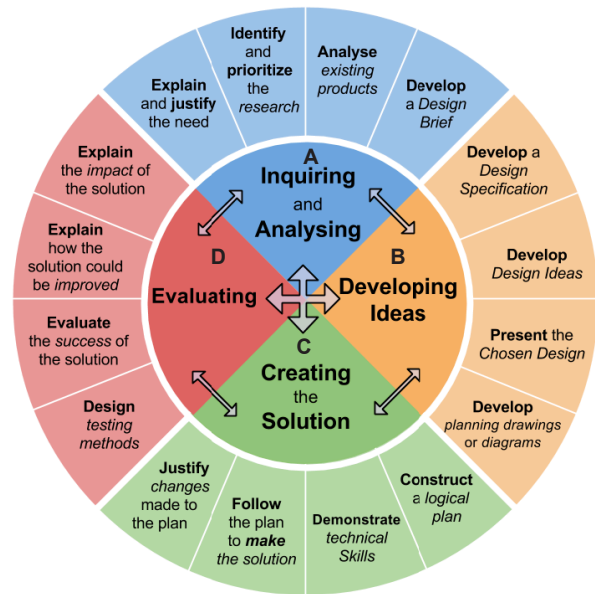


Figure 5. IB Design Cycle (MYP Design, 2015)

Source 4: [7 fundamental UX design principles all designers should know \(UX Design Institute, 2022\)](#)

Source 5: [5 main principles of interactive design you can’t leave out \(BüttonPublish, 2018\)](#)

Visibility	Feedback	Affordance	Mapping	Constraints	Consistency
Hierarchy	Usability testing	User in control	Context is key	Accessibility	Consistency
Hierarchy	Confirmation	User Control	Navigation	Accessibility	Consistency
Relevance	Feedback	Usability	Context	Accessibility	Familiarity
Hierarchy		User control	Prevision	Accessibility	Consistency
		Usability			Consistency
		Usability			Learning
Non-included:					
Focus on the user					
User-centricity					

As seen above, the majority of principles from the five sources are in line with Don Norman’s principles, as many of the terms have overlapping definitions or refer to similar concepts. The two I could not group were “focus on the user” and “user-centricity” as they are more general and refer to the definition of the user experience itself. Although the five sources may not encompass all new principles for user experience design, I can conclude they significantly align with Don Norman’s principles, proving that they are still a credible framework for designing the user experience.

Multiple case studies were used to understand the frameworks and principles used to analyze existing interfaces. I found that in the three case studies used, all specification points were similar to those of Don Norman, similar to the five sources above. One specific case study utilized Don Norman’s six principles to analyze and develop their application (Sheila, 2018). The app, named Qlue, is an Indonesian social media app that allows users to report criminal activity to local police. The government first issued a questionnaire

concerning Don Norman’s design principle, finding that citizens believed the app did not meet the principles of constraint and consistency, due to the shape and color of the buttons being inconsistent and being able to access error pages.

The app’s interface was revised based on the responses. Another round of questionnaires was issued, showing that more than double the respondents agreed that the app reached the two principles. Therefore, the research above supports that Don Norman’s principles are still relevant and continue to play a significant role in user experience design today.

## 2.2 Primary Research Analysis: Small Sample User Trial Questionnaire on Instagram Interface

A survey was created asking respondents to review the Instagram interface using Don Norman’s principles as a specification. Each respondent was asked to explore the Instagram interface for 10 minutes before completing the survey. A total of 50 responses were collected from a range of Grade 6-12 students in Hong Kong (Refer to Appendix A for the complete questionnaire).

The first part of the questionnaire consisted of six questions, each addressing one of Don Norman’s principles.

The responses show that the majority of respondents agree all functions were easily visible; that the interface provides feedback when interacted with; that all

functions had the attribute of affordance; that elements had clear functions; no invalid areas were accessible; and that the app has a consistent appearance.

Hence, the responses above show that the Instagram interface should provide a positive user experience, as the majority of respondents agreed that it matches all of Don Norman’s principles.

100% of respondents agreed that the six principles had cohesively covered the entire user experience of the Instagram interface, further supporting that Don Norman’s principles are a suitable framework.

## 2.3 Usability Test: User Trial Product Analysis

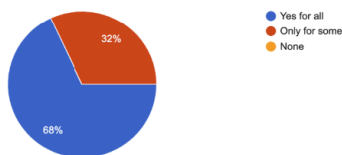
The following shows a product analysis to evaluate the positives and negatives of three existing interfaces using Don Norman’s principles as a specification. This allowed me to identify areas and acted as evidence for areas to carry forward into my designs as well as which parts to avoid.

The interfaces analyzed were chosen based on their relevance to my application: Instagram was chosen as it is a popular social media platform with common features to the sharing page I will implement; OpenRice has a database of restaurants across Hong Kong and is a search tool to find, review and share experiences; NatureHub is a platform with a similar purpose but is based in the US.

Question 1. Are all main functions visible or easy to find through the menus?

**Visibility:** Visibility refers to functions that can be visually seen, all functions should be visible and easily accessible to show users what functions can be performed.

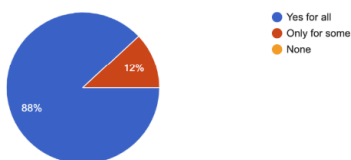
50 responses



Question 3. Do you know the functions of a menu or button without any explanation needed?

**Affordance:** Affordance refers to an attribute of an object that allows people to know how to use it.

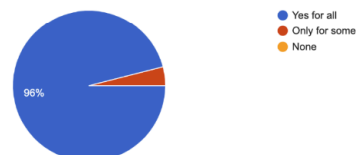
50 responses



Question 4. Is it clear how each menu or button results in different functions?

**Mapping:** Mapping is the relationship between controls and their effect, and making it clear to the user which outcome each action will result in.

50 responses



Question 7. The user experience refers to the entire process and experience of using a product, by considering the usability, accessibility, and interactions between the user and product. The goal of UX design is to give users a positive and satisfying experience after using the interface.

Did the above questions cohesively cover the entire user experience of the Instagram interface?

50 responses

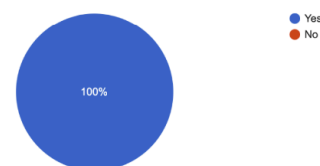
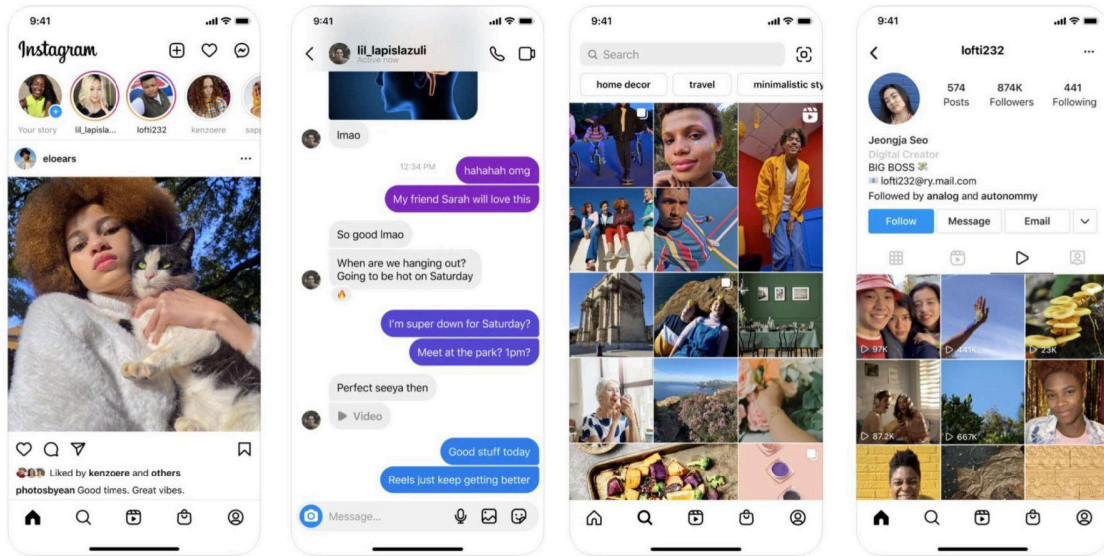


Figure 6. Data from most important questions on survey

## Interface 1: Instagram - Social Media App



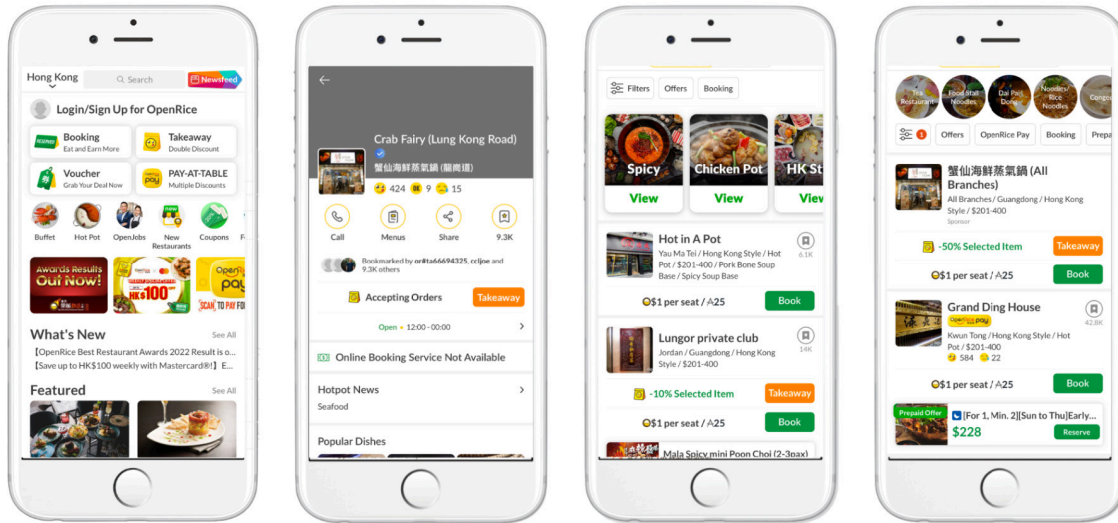
(Instagram, 2020)

Instagram is a photo and video social networking software, allowing users to upload media that can be edited and shared with their following.

Principle	Score	Justification
Visibility	4/5	<ul style="list-style-type: none"> <li>All functions are easily visible or accessible</li> <li>The five main features for viewing content are placed on a tab bar at the bottom of the screen</li> <li>Feed, search function, reels, shopping, and the user's own profile</li> </ul>
Feedback	5/5	<ul style="list-style-type: none"> <li>Feedback is given for every function</li> </ul>
Affordance	4.5/5	<ul style="list-style-type: none"> <li>Icons and labels are used throughout the application</li> <li>Communicates to the user the function of each button or icon</li> <li>Other features are hidden in the settings pages, and are easy to reach by following the labels</li> </ul>
Mapping	5/5	
Constraints	5/5	<ul style="list-style-type: none"> <li>No invalid areas or functions accessible</li> </ul>
Consistency	5/5	<ul style="list-style-type: none"> <li>Consistent design throughout</li> <li>Main pages of the application following a white and grey colour theme with blue accent</li> <li>Sense of organization and cleanliness</li> <li>Similar functions also have similar appearance to prevent confusion to the user</li> </ul>

In general, Instagram's interface is relatively user-friendly, straightforward to use, and follows all of Don Norman's principles of design. The only disadvantage is it may be difficult to find less-used features as they are hidden and need to be accessed through multiple pages.

## Interface 2: OpenRice - Food and Restaurant Guide



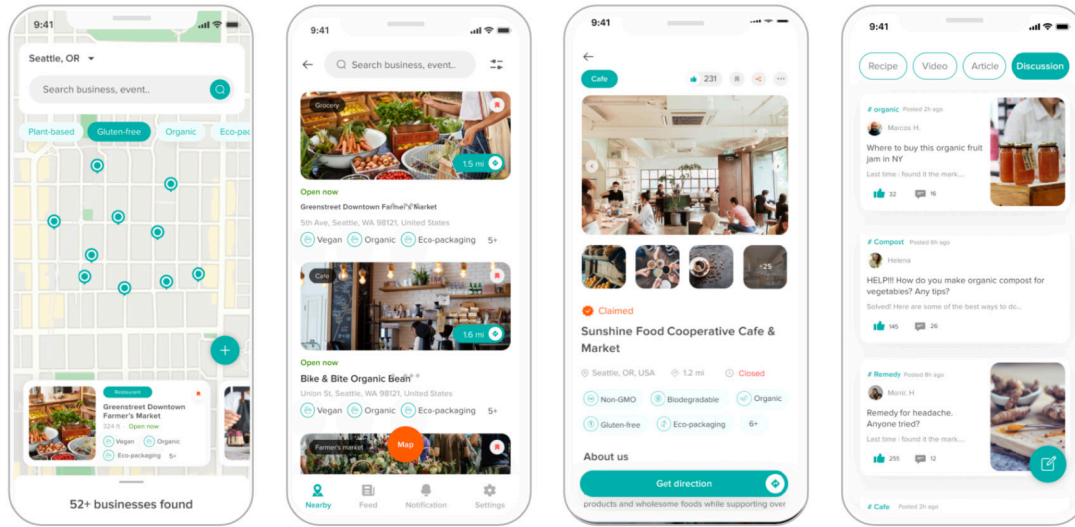
OpenRice, 2022)

OpenRice is a popular dining guide service available in Hong Kong and across various Asian regions, providing users with comprehensive dining information, restaurant reviews, and ratings (OpenRice, 2022).

Principle	Score	Justification
Visibility	4/5	<ul style="list-style-type: none"> <li>OpenRice has a tab bar similar to the one on the Instagram interface</li> <li>Showing the four main pages of the application and the pay button</li> <li>All functions are easily accessible from the tab bar or pages; however, they are relatively crowded on the home page</li> </ul>
Feedback	5/5	<ul style="list-style-type: none"> <li>Feedback is given for every function</li> </ul>
Affordance	4.5/5	<ul style="list-style-type: none"> <li>Some objects have unclear functions</li> </ul>
Mapping	5/5	<ul style="list-style-type: none"> <li>For example, some of the text that does not look like a button actually opens to another page</li> <li>This may make it complicated or unclear how to access some pages, or users may not be aware specific functions exist</li> </ul>
Constraints	5/5	<ul style="list-style-type: none"> <li>No invalid areas or functions accessible</li> </ul>
Consistency	5/5	<ul style="list-style-type: none"> <li>The same fonts, colors, and shapes are used</li> <li>Features a range of images and icons that are all created in different styles, making their appearance less organized and professional</li> <li>Similar elements are still used to perform similar operations</li> </ul>

In summary, although OpenRice's interface is not difficult to use, some functions or parts of the UI are unclear, particularly within visibility, affordance, mapping, and consistency. The home page of the interface first needs to be less crowded, so specific functions are easier to find, and designers need to ensure it is clear whether different texts act as buttons or if they have other functions. Finally, the use of images and the style of icons need to be kept consistent throughout different categories to make its appearance more organized and cohesive.

### Interface 3: NatureHub - Platform promoting health and sustainability



(NatureHub, 2022)

NatureHub is a US-based platform and brand that encourages citizens to live sustainable and healthy lifestyles. The application aims to match environmentally conscious consumers with ethical, green, local businesses, inspiring resources, and like-minded communities (NatureHub, 2022). The application's purpose is similar to the app I will prototype for Hong Kong.

Principle	Score	Justification
Visibility	4/5	<ul style="list-style-type: none"> <li>All functions on the are clearly visible</li> <li>Tab bar similar to the two other platforms analyzed</li> </ul>
Feedback	5/5	<ul style="list-style-type: none"> <li>All features and controls on the app have clear effects</li> <li>Feedback is provided whenever any function is activated</li> <li>Communicates to the user the function of each button or icon</li> </ul>
Affordance	4.5/5	
Mapping	5/5	
Constraints	5/5	<ul style="list-style-type: none"> <li>Majority of the invalid areas are restricted</li> <li>Some possible invalid actions are makeable</li> </ul>
Consistency	5/5	<ul style="list-style-type: none"> <li>The same fonts, colors, and shapes are used</li> <li>Similar elements are still used to perform similar operations</li> </ul>

In general, the NatureHub interface follows Don Norman's principles of design, and provides a good user experience. The application is simple to use and all of its available functions are clear and easy to find. The only disadvantage is some invalid actions can be performed, such as saving the same store or restaurants multiple times. However, this may be since the platform is relatively new and hence these bugs have yet to be fixed.

### 3. Research Conclusion

Through both the secondary and primary research conducted above, it can be seen that Don Norman's principles of design are a successful framework in determining the success of the design of a user interface, and are crucial in shaping the user experience.

Although not all sources in the secondary research were specific to the principles chosen in this investigation, similar methodologies and conclusions were found in all journals used and justified Don Norman's framework. Despite limitations in sample size and research methods, the primary research and product analysis further supported the framework. Hence, I will continue using Don Norman's principles to create a specification and use them as considerations for my design.

### 4. Design Specification

Based on the primary and secondary findings in the research conducted, a short specification was created based on Don Norman's principles to frame the design of my application, and assist me in shaping a better user experience.

This specification will be used as a rubric for receiving feedback and evaluating the finished product at a later stage, similar to the method used in Criteria B and D of the IB Design Cycle.

Don Norman's Principle	Specification (By Priority)	Justification
1. Visibility	1.1 Crucial functions must be displayed on a tab bar 1.2 All functions must be accessible within five interactions 1.3 All functions on a page must either be immediately visible, or accessible by scroll bars or buttons	All elements must be visible so all the available functions of the interface are known to the user. Making more important elements more visible will make them stand out to users.
2. Feedback	2.1 Every function on the interface must provide either visual or auditory feedback 2.2 Every function must serve a purpose in benefiting the user experience	Demonstrates to the user what action was taken and what was accomplished with their action; lack of feedback may result in the user thinking they did an invalid action.
3. Affordance	3.1 Must follow attributes of common elements in user interface design 3.2 All interactive elements such as buttons or links must be differentiated from normal text	Users need to immediately or be quickly able to learn how to interact and use the different elements on an interface for it to function.
4. Mapping	4.1 Controls must have visual elements (either image or text) that closely resemble or describes what they affect	Users must know which controls affect which part of the interface, to create a smoother user experience and create clarity for the user.
5. Constraints	5.1 No invalid areas should be accessible on the interface 5.2 No invalid actions should be able to be performed on the interface	Limits the range of possible interactions the user can make to prevent them from misusing the interface, it will guide the user to the appropriate following action.
6. Consistency	6.1 The interface should have a set theme of colours, fonts and shapes kept consistent throughout 6.2 The appearance of elements with similar functions or repeating elements must be kept constant	Keeping elements constant throughout the interface will help to create a smoother, stable and more efficient user experience, eliminating any possible confusion for the user.

## 5. Designing a User-Centered App for Sustainability

### 5.1 Basic Flowchart

A flowchart was first created to map out the different functions of the product and clarify the user experience, as referenced in the design process of the interfaces and studies previously analyzed.

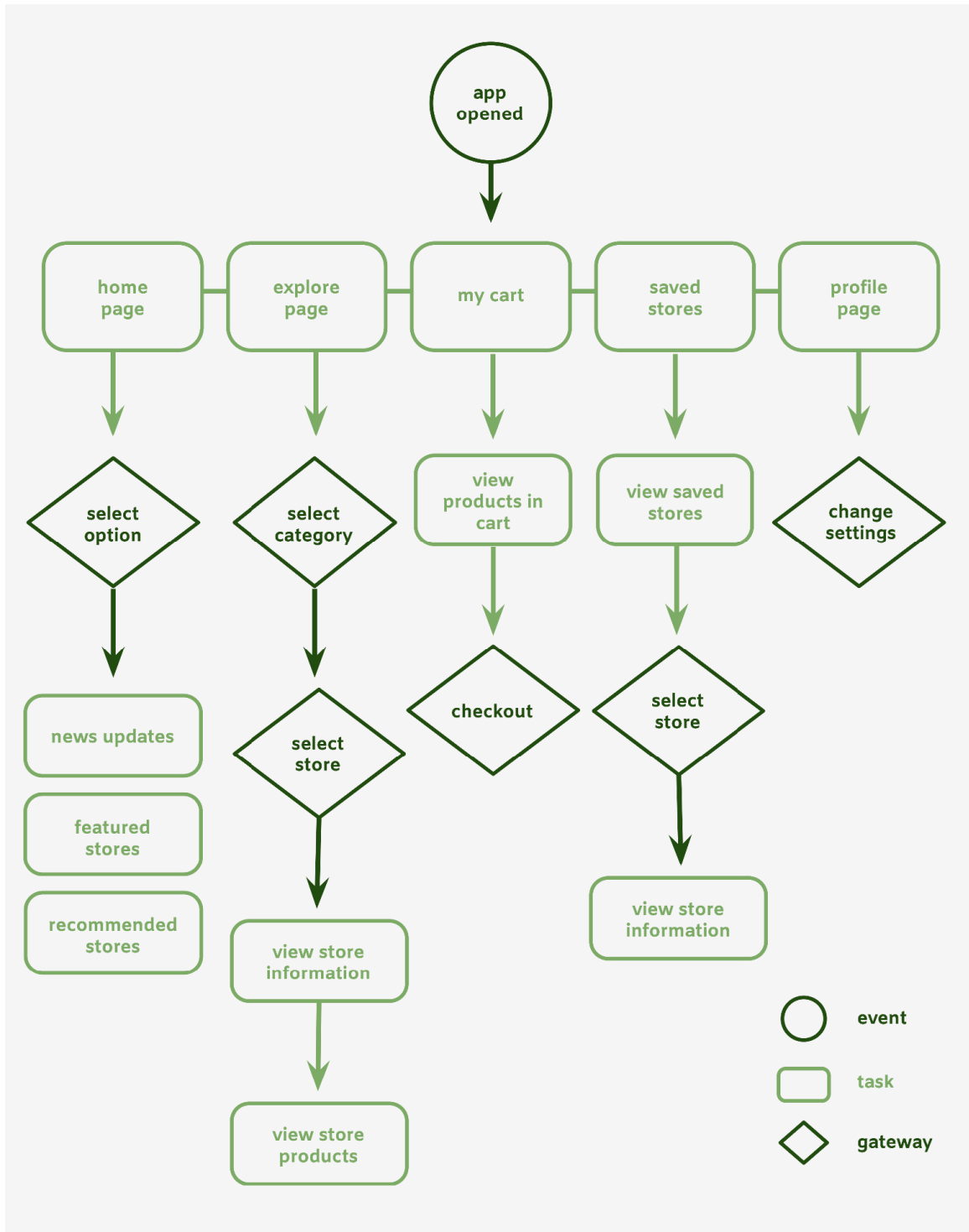


Figure 7. Flowchart mapping all functions on the final product

## 5.2 User Scenario and User Personas

A storyboard of a possible user scenario (Figure 8) and user personas (Figure 9) were first created to plan out the possible pages of the app, how the app would be used and who would use the app.

### User Scenario

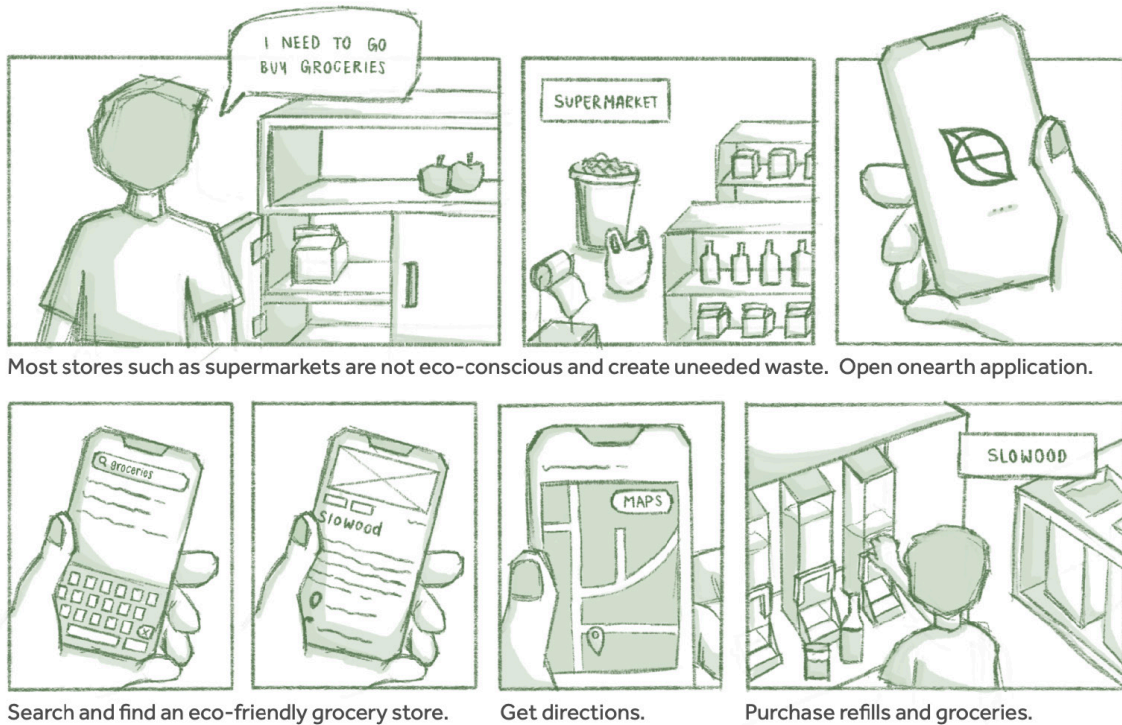


Figure 8. Possible user scenario of user using the app interface

### User Personas

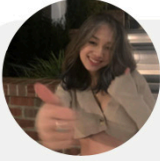

	<p><b>Isabelle Cheung</b> 17 years old student</p> <ul style="list-style-type: none"> <li>• Learnt about emissions in school</li> <li>• Currently not tracking carbon footprint</li> </ul> <p>"I want to start making changes in my buying habits, but I'm not sure where to start and what sustainable alternatives exist."</p>		<p><b>Sandy Sun</b> 34 years old teacher / mother</p> <ul style="list-style-type: none"> <li>• Sustainability advocate</li> <li>• Aware of her carbon footprint</li> </ul> <p>"I try my best to reduce my carbon footprint, however I am not aware of the stores and resources available in Hong Kong."</p>
---	--	--	---

Figure 9. User personas for potential users of the app interface



### 5.3 Wireframe Design

A wireframe of the final prototype was made to map out the paths between pages and flow of the app to create a better user experience.

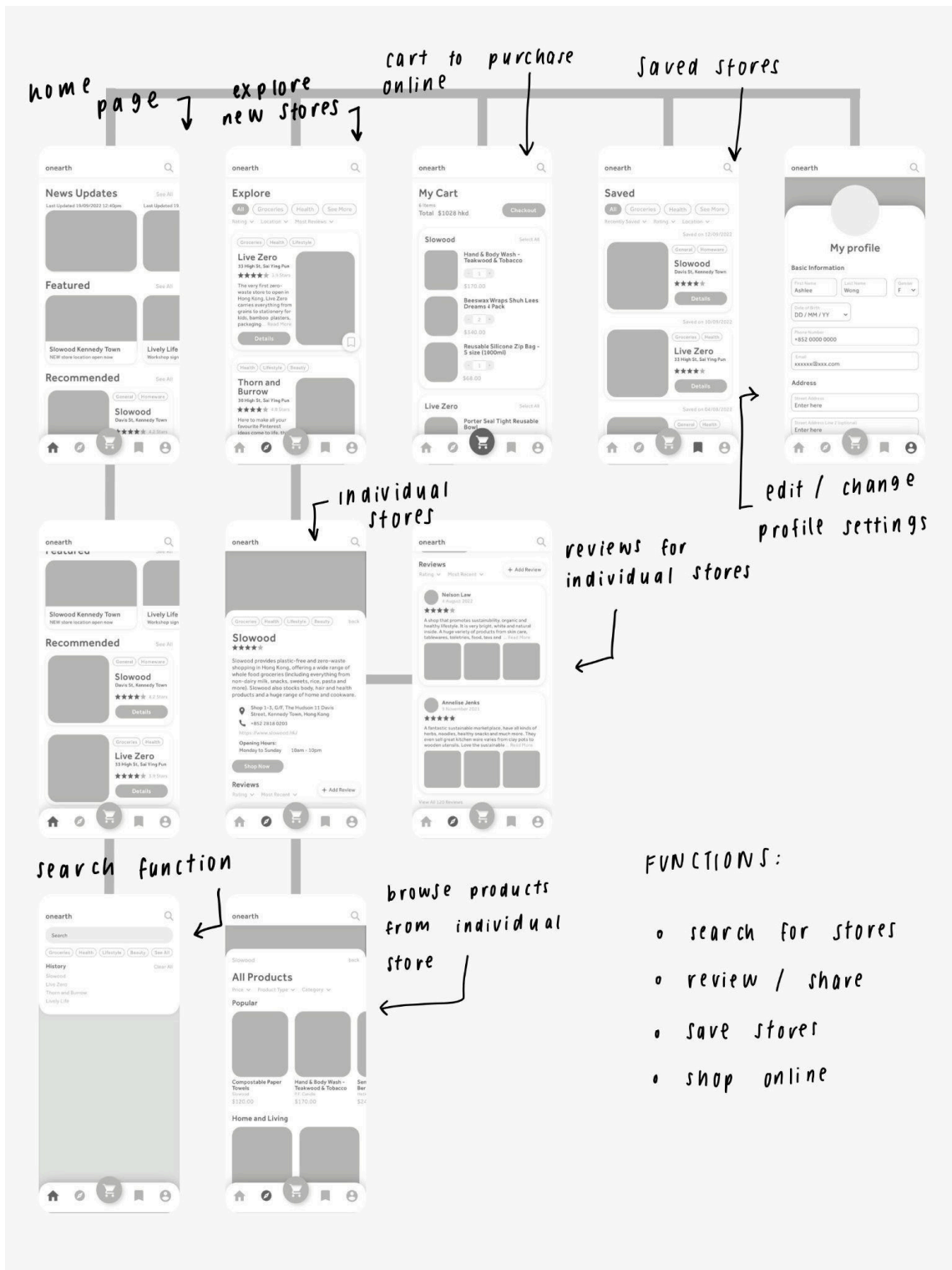


Figure 10. Wireframe design of all pages in the final product

## 5.4 Prototype Mock-up

The interface was then created following the wireframe by substituting in suitable brand colours, images and text to best reflect the purpose of the app, as seen below.

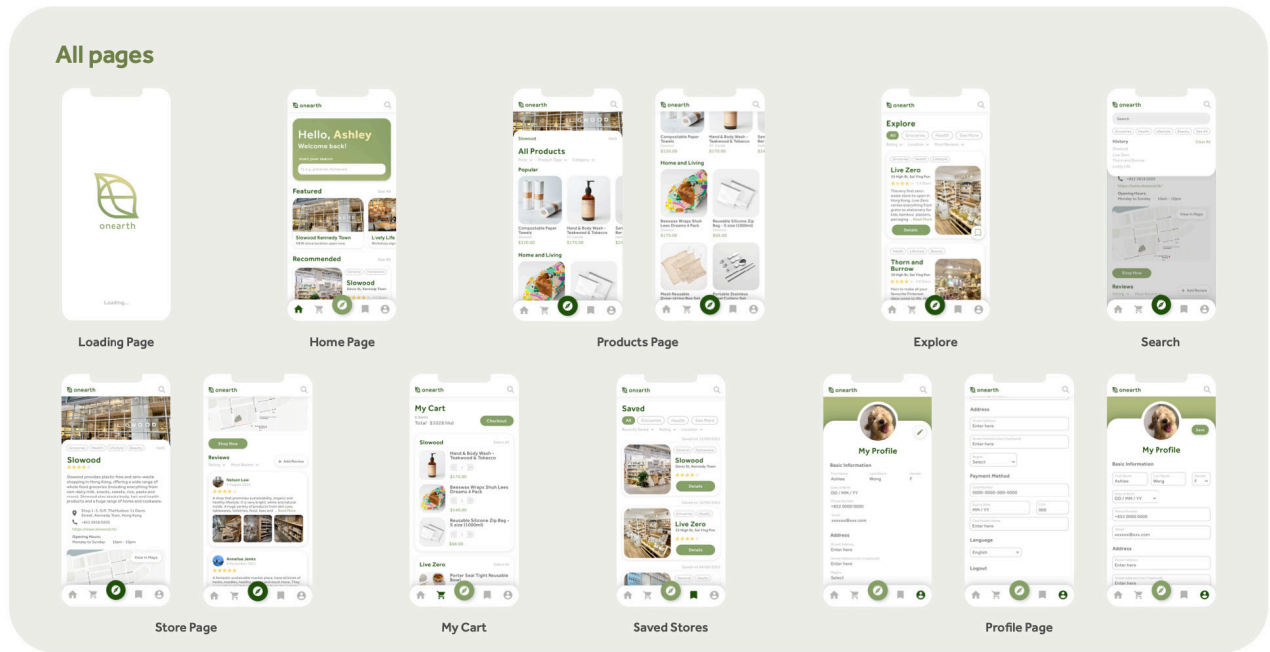


Figure 11. Final design of all pages on interface

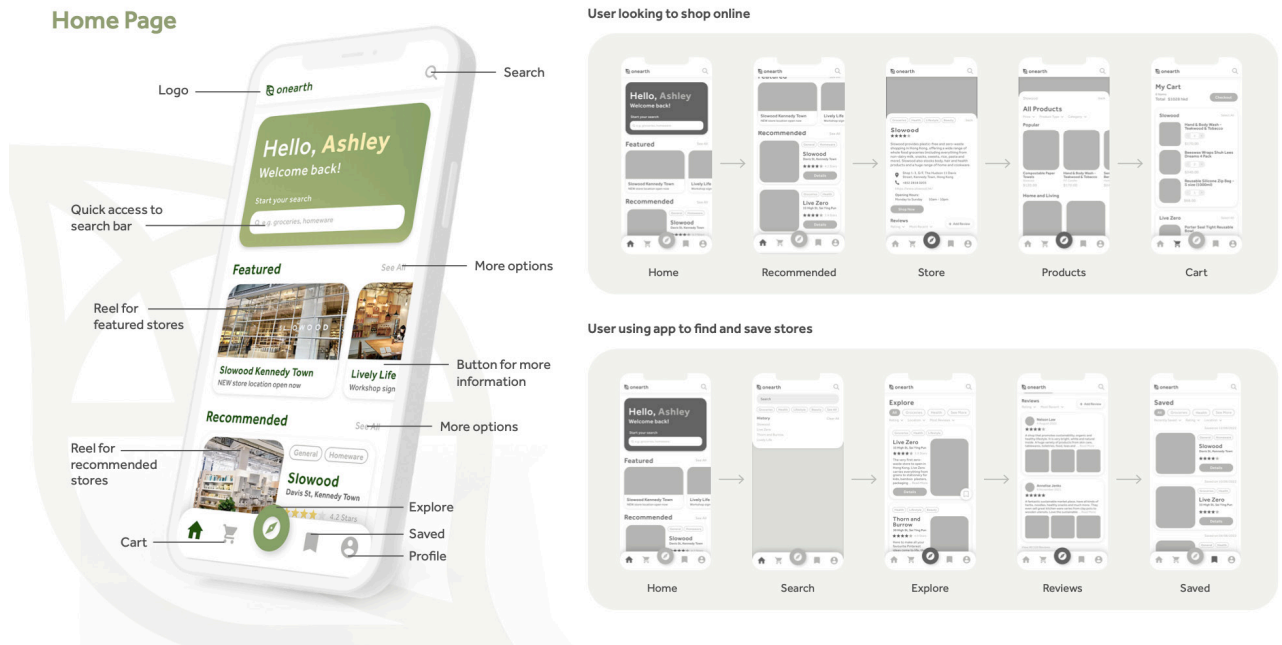


Figure 12. Functions on home page of interface and additional user scenarios

## 5.5 Working Prototype

Using the interfaces created above, a working prototype of the app was produced, allowing users to complete basic navigation of the interface.

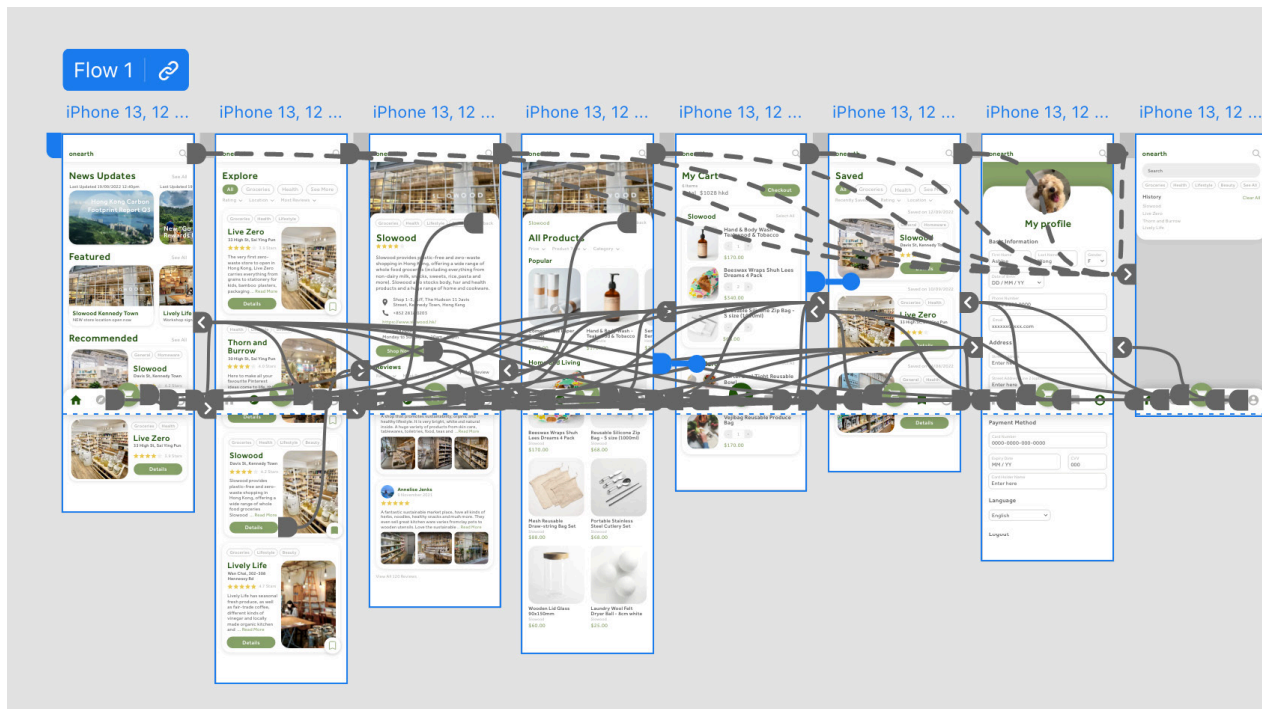


Figure 13. Working prototype created in Adobe XD

The link to this prototype was given to the members of the user group for the Instagram User Trial Questionnaire, including 50 users from a range of Grade 6-12 students in Hong Kong. The users were asked to follow the same process: spend 10 minutes exploring the interface and its functions before filling out the survey. (Refer to Appendix B for the complete questionnaire and responses).

The responses successfully allowed for the interpretation of whether utilizing Don Norman's principles were significant in shaping the user experience. However the sample size is limited, and the prototype is yet to be finalized.

## 6. Results and Data Analysis

The first question on the questionnaire (optional) asked the users for a short answer on what they believed the purpose of the product was. From the 16 responses received, it could be seen that most users believed the app was made to promote consumption at eco-friendly stores. Other users also suggested that it was to inform users about the environmental impact in Hong Kong, which would be considered the app's secondary purpose,

thus showing that the App's purpose is communicated through the interface clearly.

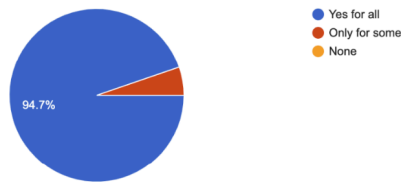
The next part of the questionnaire consisted of the same six questions as the initial questionnaire, each addressing one of Don Norman's principles. As seen in Figure 14, the responses above show that the final App interface should provide a positive user experience, as the majority of respondents agreed that it matches all of Don Norman's principles.

In the second last question respondents were given the definition of the user experience and asked if they thought that the user experience was fully accounted for in the design of the final product. 94.7% of respondents agreed that the six principles had cohesively covered the entire user experience of the Instagram interface, showing that the majority of users thought that the design successfully creates a positive user experience.

The final question of the questionnaire (optional) asked users if there was any additional feedback they would like to give regarding the App. Through the four responses received, it can be seen that several users found the functions on the tab bar to be unclear as there were no descriptions available, and they could only find

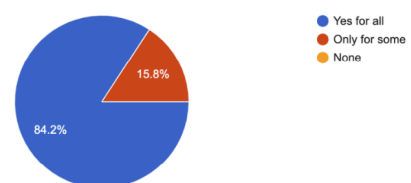
Question 2. Are all main functions visible or easy to find through the menus?

50 responses



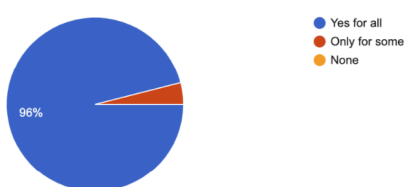
Question 4. Do you know the functions of a menu or button without any explanation needed?

50 responses



Question 7. Does the app have a consistent appearance throughout, are all elements constant?

50 responses



Question 5. Is it clear how each menu or button results in different functions

50 responses

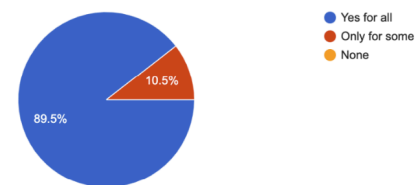


Figure 14. Data from most important questions on feedback survey

out what each page encompassed through trial and error. This would have negatively impacted the principle of affordance.

The test is valuable as it provides clear insight to answering the research question, as it can be concluded that Don Norman's principles significantly shaped the user experience. The App was successful in encompassing all of his principles.

However, one major limitation of this test is it was restricted to a testing group of 50, all part of a similar demographic. As the majority of students were from my school, this largely excludes the opinions of other students in Hong Kong, and may have impacted the data collected. For further research a wider range and number of users could be included in the testing.

## Conclusion

Through investigating the question "To what extent have Don Norman's principles of design been significant in shaping the user experience, and how can they be utilized in designing a user-centered app interface for sustainability?", it can be concluded that Don Norman's principles of design serve as a crucial framework in interface design. These principles allowed me to create my app interface addressing the urgent issue of carbon emissions in Hong Kong, with functions to locate and purchase from eco-friendly stores. The app was prototyped so users could navigate between functions, and allowed me to collect feedback on the user experience, which to a greater extent, was positive.

This investigation addresses the application and significance of Don Norman's principles in shaping the user experience. Compiling case studies of other interfaces and creating an App interface following his principles answers the initial problem and questions, showing that his principles are of great use in user experience design. Through promoting sustainable stores in Hong Kong and providing users with an alternative to shop more sustainably, the application also contributes to the initially stated problem of carbon emission goals in Hong Kong.

The major limitations of this report are the limited access to current statistics on sustainable stores in Hong Kong, and the quality and quantity of feedback from users. There are currently very few published statistics about the number of eco-friendly stores in Hong Kong and the environmental impact of the increased consumption at these stores.

For further investigation, a wider range of users outside of students can be used, as the issue of environmental impact in Hong Kong is one that applies to all citizens, and even others globally. With more resources, additional forms of testing the prototype based on Don Norman's principles can also be completed to better understand its significance.

## References

- Babich, N. "Interaction Design vs UX: What's the Difference? | Adobe XD Ideas." *Adobe Xd Ideas*, 16 Oct. 2019, [xd.adobe.com/ideas/principles/human-computer-interaction/what-is-interaction-design/](https://xd.adobe.com/ideas/principles/human-computer-interaction/what-is-interaction-design/). Accessed 23 May 2022.
- BüttonPublish. "5 Main Principles of Interactive Design You Can't Leave Out." *BüttonPublish*, 26 Mar.2018, [buttonpublish.com/blog/5-main-principles-interactive-design/](https://buttonpublish.com/blog/5-main-principles-interactive-design/). Accessed 23 Aug. 2022.
- Dzera, L. "UI vs. UX Design: What's the Difference? - Lisa Dzera - Medium." *Medium*, Medium, 19 Oct. 2017, [medium.com/@lisadzera/ui-vs-ux-design-whats-the-difference-69aac99940f4](https://medium.com/@lisadzera/ui-vs-ux-design-whats-the-difference-69aac99940f4). Accessed 23 May 2022.
- Edpresso Team. "What Are Norman's Design Principles?" *Educative: Interactive Courses for Software Developers*, Educative, 6 Mar. 2020, [www.educative.io/edpresso/what-are-normans-design-principles](https://www.educative.io/edpresso/what-are-normans-design-principles). Accessed 23 May 2022.
- Enginess. "The 6 Principles of Design, a La Donald Norman | Enginess Insights." *Enginess.io*, 3 Nov. 2014, <https://www.enginess.io/insights/6-principles-design-la-donald-norman>. Accessed 23 May 2022.
- GovHK (2020) GOVHK: Global Environment. <https://www.gov.hk/en/residents/environment/global/>. Accessed 30 Jun 2022.
- GovHK, 2021. Hong Kong's Climate Action Plan 2050.[pdf], [https://www.epd.gov.hk/epd/english/news\\_events/current\\_issue/current\\_issue.html](https://www.epd.gov.hk/epd/english/news_events/current_issue/current_issue.html). Accessed 23 Aug 2022.
- Grass, J. "These Are the Top UX Design Principles You Need to Know." *CareerFoundry*, 5 Aug.2021, [careerfoundry.com/en/blog/ux-design/5-key-principles-for-new-ux-designers/](https://careerfoundry.com/en/blog/ux-design/5-key-principles-for-new-ux-designers/). Accessed 23 Aug. 2022.
- Hughes, J. "What Is UX? Plus 5 Core Principles of UX Design for Websites." *ThemeIsle Blog*, ThemeIsle Blog, 21 Aug. 2019, [themeisle.com/blog/what-is-ux/](https://themeisle.com/blog/what-is-ux/). Accessed 23 Aug. 2022.
- "Instagram." *Instagram.com*, 2020, [www.instagram.com/](https://www.instagram.com/). Accessed 24 Aug. 2022.
- Interaction Design Foundation - IxDF. (2016, June 5). What is User Centered Design?. Interaction Design Foundation - IxDF. <https://www.interaction-design.org/literature/topics/user-centered-design>. Accessed 23 May 2022.
- Kwiatk, K. "UX Principles: Constraints, Discoverability, Feedback, and More." *Zivtech*, 11 Mar. 2019, [www.zivtech.com/blog/ux-principles-constraints-discoverability-feedback-and-more](https://www.zivtech.com/blog/ux-principles-constraints-discoverability-feedback-and-more). Accessed 23 May 2022.
- Ma, Y. "Hong Kong: Adoption of Sustainable Practices in Shopping 2022 | Statista." *Statista*, Statista, 2022, [www.statista.com/statistics/1321028/hong-kong-sustainable-practices-adoption-in-shopping/](https://www.statista.com/statistics/1321028/hong-kong-sustainable-practices-adoption-in-shopping/). Accessed 12 Sept. 2022.
- MYP Design. "Design Cycle | MYP IB." *MYP Design: Ed Tech*, 2015, [www.designmyp.com/myp-design-cycle](https://www.designmyp.com/myp-design-cycle). Accessed 22 Nov. 2022.
- NatureHub. "NatureHub - Healthy Lifestyles Community - about Us." *Naturehub.com*, 2022,[naturehub.com/about-us](https://naturehub.com/about-us). Accessed 25 Aug. 2022.
- Novensa, S. & Mungana, W, 2018. Analysis and Development of Interface Design on DKI Jakarta & Tangerang'S Qlue Application based on Don Norman's 6 Design Principles. *International Journal of New Media Technology*, 5, pp.1-7. 10.31937/ijnmt.v5i1.809.
- OpenRice. "Hong Kong Restaurants Guide Hong Kong Restaurant | OpenRice Hong Kong." OpenRice Hong Kong, 2022, [www.openrice.com/en/hongkong](https://www.openrice.com/en/hongkong). Accessed 25 Aug. 2022.
- Prisma Network. "10 Digital Skills to Master in 2021: UX-Design." *Prisma-Network.eu*, Prisma Network, 16 Feb. 2021, [prisma-network.eu/our-work/10\\_digital\\_skills\\_to\\_master\\_in\\_2021\\_UX-Design\\_](https://prisma-network.eu/our-work/10_digital_skills_to_master_in_2021_UX-Design_). Accessed 22 Nov.2022.
- Reid, D. 2019. "The World Is Our Interface – the Evolution of UI Design." Toptal Design Blog, Toptal, <https://www.toptal.com/designers/ui/touch-the-world-is-our-interface>. Accessed 23 May 2022.
- Rekhi, S. "Don Norman's Principles of Interaction Design - Sachin Rekhi - Medium." *Medium*, Medium, 23 Jan. 2017,[medium.com/@sachinrekhi/don-normans-principles-of-interaction-design-51025a2c0f33](https://medium.com/@sachinrekhi/don-normans-principles-of-interaction-design-51025a2c0f33). Accessed 23 May 2022.
- Service Design Sydney. "Donald Norman's Design Principles for Usability." *UX Design Sydney*, UX Design Sydney, 10 May 2017,[datacloud.design/2017/05/10/donald-normans-design-principles-for-usability/](https://datacloud.design/2017/05/10/donald-normans-design-principles-for-usability/). Accessed 23 May 2022.
- Sharma, R. "Understanding the World of Digital Design: UX, UI, IA, and IxD." *TechGenies*, 8 June 2021, [techgenies.com/understanding-the-world-of-digital-design-ux-ui-ia-and-ixd-explained/](https://techgenies.com/understanding-the-world-of-digital-design-ux-ui-ia-and-ixd-explained/). Accessed 23 May 2022.
- Thackara, J., 2001. "Why Is Interaction Design Important?" <https://thackara.com/notopic/why-is-interaction-design-important/>. Accessed 21 May 2022.
- United Nations. "THE 17 GOALS | Sustainable Development." *Un.org*, 2022, [sdgs.un.org/goals](https://sdgs.un.org/goals). Accessed 12 Sept. 2022.
- UX Booth. "Where UX Comes from | UX Booth." *Uxbooth.com*, 2013, [www.uxbooth.com/articles/where-ux-comes-from/](https://www.uxbooth.com/articles/where-ux-comes-from/). Accessed 23 May 2022.
- UX Design Institute. "7 Fundamental UX Design Principles All Designers Should Know - UX Design Institute." *UX Design Institute*, 22 June 2022, [www.uxdesigninstitute.com/blog/ux-design-principles/](https://www.uxdesigninstitute.com/blog/ux-design-principles/). Accessed 23 Aug. 2022.
- 99designs Team. "The 7 Principles of UX Design—and How to Use Them." *99designs*, 7 Aug. 2020, [99designs.com/blog/web-digital/ux-design-principles/](https://99designs.com/blog/web-digital/ux-design-principles/). Accessed 23 Aug. 2022.

**Full article as submitted to the IB,  
including Appendices**



---

# The Effect of Framing Information on Decision-Making about Vaccines

Ava Osann

---

## Introduction

Every country faces vaccine hesitancy which refers to a “delay in acceptance or refusal of vaccination despite the availability of vaccination services” (MacDonald, 2015). Reasons for vaccine hesitancy include a lack of confidence in the government, misinformation, and a preference for alternative medicine (FPM, 2020). Health programs aim to address underlying issues that lead to vaccine hesitancy, but they have various levels of effectiveness depending on how the information is presented. This leads to the question “to what extent is negative framing of information more effective than positive on the decision to vaccinate?”.

My research question is highly relevant due to vaccine hesitancy becoming more pronounced in recent years during the COVID-19 pandemic. A study conducted in 2021 showed that 22% of 1000 Americans identify as “anti-vax” (Clark, 2021), and at the moment 2.8 billion people have not been vaccinated against COVID-19 despite some of them having access to the vaccine (Penn, 2022). This raises the question of why people are deciding not to vaccinate, and perhaps part of this answer lies in the way information is framed.

Framing of information refers to what is made salient. For example, positive framing could be emphasizing the benefit of getting vaccinated which may have a different effect than if a negative frame is used by emphasizing the threat of not vaccinating. This is known as the “framing effect”, proposed by Amos Tversky and Daniel Kahneman in 1981, which postulates that decisions, such as the decision to get vaccinated, are affected by how the information is framed rather than the information itself.

This research question falls into the category of cognitive psychology because I will be examining how the framing bias, which is a cognitive bias, affects decision-making. Beginning by defining key ideas, cognition is “all forms of knowing and awareness, such as problem-solving” (APA, 2022). Decision-making is a process

that involves thinking and deciding between options. According to the dual processing model, thinking occurs in either system one: intuitive and fast, or system two: analytical and deliberate (Djulgovic *et al.*, 2012). Usually, people use system one thinking which allows for cognitive biases, for example, the framing bias, to influence decisions such as the decision to vaccinate.

The framing bias becomes even more important when considering that globally the average time spent on social media is 2 hours and 27 minutes, where information can be dramatized and misconstrued to sensationalize information and real-world issues (Dixon, 2022). Social media is also an echo chamber that enforces these cognitive biases through the algorithm that specifically shows users what they agree with. With the wide range of information available through social media, it is important to be aware of how information is being framed to confirm an idea.

I predict that negative framing of information will have a greater impact than positive framing for the following three reasons. Firstly, the participant must be aware of the disease’s severity to be motivated to get vaccinated as shown by Weinstein (2000) and supported by the Health Belief model. Secondly, people tend to be more responsive to negative information than positive information. This is known as the negativity bias, which is shown in Betsch and Sachse (2012). Thirdly, denying all risks of vaccination can decrease participants’ trust and subsequently their intention to get vaccinated, thus acknowledging threat is important in increasing vaccination intentions. This is shown by Schwarzer and Fuchs (1996) and is supported by Betsch *et al.* (2010)’s findings.

I predict framing benefit as salient will be less effective because, firstly, while benefit framing is seen in Meyerowitz and Chaiken (1987) to give participants a better attitude towards vaccinations, only participants in the negative frame show retention of information and consistent intention to vaccinate. Secondly, while

positive framing is shown in Ferguson and Gallagher (2007) to be most effective in high-risk situations, the study does not investigate the long-term effect which is previously shown to be where negative frames are most effective.

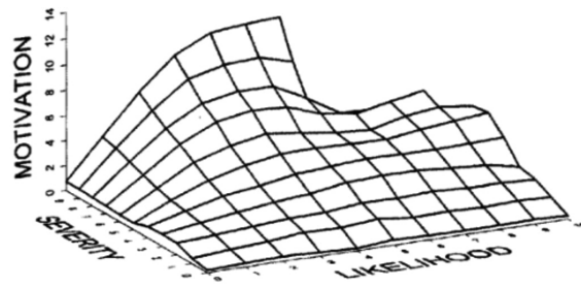
Lastly, positively framing getting vaccinated by emphasizing the personal benefit can have varying levels of effectiveness depending on what is made salient. This is supported by Betsch, Böhm, and Korn (2013) who investigated the effects of making personal or social benefits salient. Thus, I expect negative framing to be more effective than positive framing when aiming to influence people's decision to vaccinate.

## 1. Negative Framing

I predict that negative framing will have a greater impact on the decision to vaccinate as shown by the Health Belief Model (HBM) and the negativity bias. The HBM, developed in the 1950s by Schwartz and Fuchs, postulates that a person must believe that the illness has a personal threat to accept preventative measures such as vaccines (Boskey, 2022). Furthermore, the negativity bias refers to how people tend to have a stronger response to negative information than positive (Frothingham, 2019). To investigate this further, I will first discuss the requirement of severity to motivate action. Next, I will explore negativity bias and the tendency to respond to negative information. Finally, I will look at the need for acknowledgment of risk in getting vaccinated.

Firstly, Weinstein (2000) demonstrated that by making the severity of the disease known, participants are more likely to get vaccinated. Researchers investigated the relationship between two threat attributes: severity and likelihood by first constructing a list of 201 events of varying likelihood and severity. Participants were then asked to rate them in terms of how likely they were to happen, the severity of the event, and how likely they were to perform protective health behaviors such as getting vaccinated.

The results showed that motivation to prevent the event was nonexistent when the likelihood or severity was zero (see figure 1 for graph). The graph shows that as long as the disease is perceived as having some severity, there will be motivation to act which is not seen for likelihood. Thereby showing that people were significantly more responsive to severity than likelihood. In other studies severity of the disease would most likely be used as the negative frame thus, when the patient is unaware of the severity of the disease they will have no motivation to act, showing that the severity of the disease is driving the decision to vaccinate.



**Figure 1.** Graph demonstrating the relationship between likelihood, severity, and motivation (Weinstein *et al.*, (2000))

This study, therefore, corroborates the HBM in showing that the personal threat of the disease (i.e using a negative frame to emphasize the personal threat of not getting vaccinated) is necessary for the patient to feel motivated to get vaccinated.

While Weinstein (2000) provides convincing data in support of severity being a requirement for motivation, the sample size is small (12) which decreases its generalizability as well as the study's internal and external validity. However, the study's results are still significant and are supported by the HBM which means that the results are relatively reliable. This study also uses intention to represent behavior which may allow for some discrepancies but is still a relevant predictor for behavior.

Betsch and Sachse (2012) investigated the effect of negativity bias on the perceived threat. They define perceived threat as probability and severity, similar to the variables used in Weinstein (2000). In the experiment, information was presented on a blank white website, then participants were asked to imagine that they were the parent of an infant and had been recommended to vaccinate the infant against a fabricated illness. They were told that the illness could lead to serious consequences including death, and they were unsure whether the vaccination would have negative effects.

Betsch and Sachse (2012) showed that when participants were shown strong denials of risk, their intention to vaccine increased but messages indicating that there was no risk (i.e using a completely positive frame) resulted in an increase in the perceived risk of vaccinating and a decrease in intention to vaccinate. This study also extends the negativity bias by showing that people don't trust messages that imply there is no risk and are more trustful of messages that indicate some risk. This demonstrates that information about vaccinations cannot be framed only in a beneficial frame by emphasizing that vaccinations have no risks. Connecting these results to Weinstein (2000)'s results, programs that make the severity of not getting vaccinated clear and don't

deny all risks in getting vaccinated will perform better in increasing intention to vaccinate when compared to programs that employ a positive frame by only emphasizing the benefits of getting vaccinated.

Betsch and Sachse (2012) also found that this effect occurred independently of how many denials of risk were presented, their attitude towards vaccination, and participant involvement but the credibility of the source moderated the effects of the frame. This does not diminish the effects of negative frames on decisions to vaccinate but does imply that providers need to understand their audience and adjust the strength of the negative frame accordingly. Betsch and Sachse (2012)'s experiment is seen to be replicable because follow-up experiments replicated the results found in their first experiment. Betsch and Sasche (2012) recruited participants through a previous experiment thus the sample represents participants who use the internet more. Yet, this does not decrease the external validity because the results are being generalized to people who use the internet.

Secondly, negative frames have a deeper and longer-lasting effect on the decision to vaccinate. This is shown by Betsch *et al.* (2010) who investigated the effect of vaccine-critical websites on the perceived risks of getting vaccinated. They did this by comparing the perception of risk and intention to vaccinate between a control group, who accessed a government website, and a group that accessed a vaccine-critical website (negative frame). The control website was from the German Federal Ministry of Health, which aimed to have a neutral stance (no frame). Participants were told that conventional/unconventional practitioners (depending on their medical preference) stated that getting/not getting vaccinated lead to considerable risk (depending on which group the participant was in). Then they were given 5-10 minutes to read either the control website or the critical website to find evidence for their given assumption.

Betsch *et al.* (2010) found that participants who viewed the vaccine critical website showed a decrease in intention to vaccinate and an increase in the perceived threat of the vaccine because they used negative frames to make the threat of vaccinating salient. Even when participants who read vaccine-critical websites then read the neutral website, their intention to vaccinate did not increase, only participants who exclusively viewed the control website had an increase in intention to vaccinate. Thus it seems that not only does negative framing used to emphasize the threat of getting vaccinated greatly decrease the intention to vaccinate but also has lasting effects. From these results, making the threat of either

getting or not getting vaccinated using a negative frame seems to be the greatest predictor of change in the decision to vaccinate. The more significant result of this experiment is showing the lasting effects of negative framing on the decision to vaccinate. This study also found that while the vividness and emotive quality of the message did affect the participants' response to the frame, they were only moderators.

Betsch *et al.* (2010) also showed that negative framing is especially effective when the person has less knowledge about the vaccination. The study sample consists of people who are interested in science as participants were recruited through a volunteer link on a website about medicine and science therefore even participants considered "less experienced" with the topic of vaccination most likely still understood the topic. Thus showing negative framing can still affect well-educated individuals but is even more effective on patients who have less experience with the topic of vaccination. However, Betsch *et al.* (2010)'s use of opportunity sampling decreases the generalizability of the experiment as well as the internal and external validity. A significant finding of this experiment is that negative framing has more of an effect because of the negativity bias, which has significant research to support, thus Betsch *et al.* (2010) is supported by other research as well.

The culmination of results from the above studies shows that using negative framing by emphasizing the personal threat of not getting vaccinated is a key part of decision-making regarding vaccination. Threat seems to be required in different stages of understanding the vaccine. First, in understanding the disease, the participants must know that there is a level of personal threat, otherwise, they will not have the motivation to act. Secondly in understanding the vaccine itself, providers cannot use a fully positive frame if they are attempting to increase vaccination intention. Providers also need to use negative framing if they want the frame to have long-term effects. Thus, the above studies provide evidence in support of negative framing having more of an effect on the decision to vaccinate.

## 2. Positive Framing

In the above-discussed studies, the personal benefit does not seem to be a required basis for decision making which questions how much of an effect positive framing would have on vaccine intentions. To investigate this further, I will first discuss how a positive frame can give the participant a better attitude towards vaccinations but does not have lasting effects. Next, I will explore how the benefit frame affects decision-making, but only in



specific instances. Finally, I will investigate the different effects that benefit framing can have depending on what part of the benefit is made salient.

Firstly, Meyerowitz and Chaiken (1987) show that positive framing gives participants a better attitude towards Breast Self Evaluations (BSE) but negative framing is the only frame that resulted in the behavior actually being performed. Participants were given a pamphlet on BSE that was either framed in terms of loss (negative frame), gains (positive frame), or neutral (no frame). After reading they indicated their BSE intentions. After four months, participants were recontacted to investigate their behavioral changes and general attitude towards BSE.

Results showed that participants who were given information positively framed recalled more things to gain by doing the BSE. Participants in the loss condition expressed no heightened intention to BSE. However, after the 4-month period, participants in the negative frame condition were the only group that did not have a significant decrease in intention to perform BSE. Connecting these results to vaccination intentions, it seems that patients may not have a significant increase in intention to vaccinate immediately after reading the threat-framed information, but over time, threat-framed information will have a longer-lasting effect.

Meyerowitz and Chaiken (1987) investigates the framing effect in relation to breast cancer, which means that the predictive validity is not as high in terms of getting vaccinated because these two medical issues are different by nature. The sample of Meyerowitz and Chaiken (1987) is also composed of college-level females which questions how well the results can be generalized to the larger population. Despite this, the study provides evidence for the negative framing having long-term effects which is supported by Betsch *et al.* (2010) and the negativity effect. This study also investigates the actual behavior of doing BSE instead of intention which is a more reliable indicator of how the negative frame has affected participants' decisions to vaccinate.

Secondly, positive framing was shown to have a limited effect on the decision to vaccinate by Ferguson and Gallagher (2007). In this study, 200 undergraduate students were randomly assigned to one of four conditions. The two variables tested were: frame valence (positive or negative), and method (attribute or goal). Participants were assigned to one of the four conditions and given a pamphlet accordingly. For example, participants in the negative attribute control were given pamphlets with attributes that were framed negatively (see table 1 for examples of the four ways information was framed).

### 3. Comparison of Positive and Negative Framing

Firstly, Weinstein (2000) and the HBM both postulate that there is a requirement for the personal threat of the disease to be made clear in order for the vaccination to be taken. This then should mean that when presenting information, the patients have to be made aware that if they got the disease it would be severe, this therefore would logically mean that negative framing would be used to explain what would happen if they got the disease. Furthermore, when explaining the process of getting the vaccination, participants must also be made aware of the possible side effects, otherwise, their perceived risk of getting the vaccination will increase, most likely also lowering their intention to vaccinate. This means that information about getting the vaccine must also be framed negatively, this does not mean that the language used must be vivid, but rather that the risks of getting the vaccine must be made clear and that information cannot only be framed positively otherwise the patient will not trust the message.

An additional point in support of the argument for negative framing having a more influential effect is that people seem to be more reactive to negative information than positive. This is shown by Betsch *et al.* (2010), who demonstrated the lasting effects that negative framing can have. This was also corroborated by Meyerowitz and Chaiken (1987) where it can be seen that negative

	Negative frame	Positive frame
Attribute	The jab is not effective for 10% to 30% of cases.	The flu jab is effective in preventing the development of the flu virus in 70-90% of cases.
Goal	By not getting vaccinated you fail to take advantage of the best method of defense against the flu.	By going and getting the flu jab you take advantage of the best method of defense against the flu.

**Table 1.** Examples of negative frames (attribute and goal) and positive frames (attribute and goal) (Ferguson and Gallagher, 2007)

framing has a longer impact when compared to positive framing despite initially showing no significant impact of negative framing. This is a significant point to consider when looking at research that seems to be in support of positive framing because they do not look at the long-term effects which are where negative framing is seen to have the biggest impact. For example, Ferguson and Gallagher (2007) showed that positive attributes were most effective in increasing intention to vaccinate in high-risk situations, but they did not investigate this effect over time. This raises a question about whether negative frames would have longer lasting effects as compared to benefit framing over time as was seen by Meyerowitz and Chaiken (1987) and Betsch *et al.* (2010).

Furthermore, Betsch, Böhm, and Korn (2013)'s investigation of the difference in using a positive frame to emphasize the personal or social benefit of many people getting vaccinated resulted in either no change or decreased intention to vaccinate. This is significant because it shows that the effectiveness of positive framing is further limited to the discussion of the vaccine itself, which as previously shown through other studies seems to be more effectively discussed through a negative frame. Thus these studies, while showing the usefulness of positive framing in some instances, fail to show positive framing as more effective than negative framing.

## Conclusion

From the above discussion, negative framing of information is to a great extent more effective than positive framing in affecting the decision to vaccinate. There are instances where positive framing is more effective, but looking at the evidence holistically, negative framing has a greater effect than positive framing in a wider variety of instances.

These studies and findings significance have real-life applications in politics, education, and commercials but more specifically in medical programs that aim to increase vaccination intentions. The findings can also be applied to many other programs aimed to increase other preventative medical behaviors. There is, however, the requirement for these programs to fully understand their audience for the negative framing to have maximum effectiveness. For example, it is important to understand their audience's trust in the program, and adjust the strength of language used accordingly. These findings are also significant for people while on social media.

Ultimately, the decision to vaccinate is based on many things. One of the major factors as previously shown is the type of frame used because when the information is consistent in content but the framing changes, negative framing is shown to affect the decision to vaccinate to the greatest extent.

## References

- APA. (2022). *APA Dictionary of Psychology*. Apa.org. <https://dictionary.apa.org/>
- Betsch, C., & Sachse, K. (2013). Debunking vaccination myths: Strong risk negations can increase perceived vaccination risks. *Health Psychology, 32*(2), 146–155. <https://doi.org/10.1037/a0027387>
- Betsch, C., Böhm, R., & Korn, L. (2013). Inviting free-riders or appealing to prosocial behavior? Game-theoretical reflections on communicating herd immunity in vaccine advocacy. *Health Psychology, 32*(9), 978–985. <https://doi.org/10.1037/a0031590>
- Betsch, C., Renkewitz, F., Betsch, T., & Ulshöfer, C. (2010). The influence of vaccine-critical websites on perceiving vaccination risks. *Journal of health psychology, 15*(3), 446–455. <https://doi.org/10.1177/1359105309353647>
- Boskey, E. (2022). *What Is the Health Belief Model?* Verywell Mind. <https://www.verywellmind.com/health-belief-model-3132721>
- Clark, Caitlin. (2021) *Social Identity within the Anti-Vaccine Movement*. Texas A&M Today, [today.tamu.edu/2021/06/04/social-identity-within-the-anti-vaccine-movement/](http://today.tamu.edu/2021/06/04/social-identity-within-the-anti-vaccine-movement/).
- Dixon, S. (2022). *Global daily social media usage 2022 | Statista*. Statista; Statista. <https://www.statista.com/statistics/433871/daily-social-media-usage-worldwide/>
- Djulgovic, B., Hozo, I., Beckstead, J., Tsalatsanis, A., & Pauker, S. G. (2012). Dual processing model of medical decision-making. *BMC Medical Informatics and Decision Making, 12*(1). <https://doi.org/10.1186/1472-6947-12-94>
- Ferguson, E., & Gallagher, L. (2007). Message framing with respect to decisions about vaccination: The roles of frame valence, frame method, and perceived risk. *British Journal of Psychology, 98*(4), 667–680. <https://doi.org/10.1348/000712607x190692>
- FPM. (2020). *Four reasons for COVID-19 vaccine hesitancy among health care workers, and ways to counter them*. Aafp.org. [https://www.aafp.org/pubs/fpm/blogs/inpractice/entry/countering\\_vaccine\\_hesitancy.html](https://www.aafp.org/pubs/fpm/blogs/inpractice/entry/countering_vaccine_hesitancy.html)
- Frothingham, S. (2019). *What Is Negativity Bias, and How Does It Affect You?* Healthline; Healthline Media. <https://www.healthline.com/health/negativity-bias#:~:text=We%20humans%20have%20a%20tendency,experiences%20are%20insignificant%20or%20inconsequential.>
- MacDonald, N. E. (2015). Vaccine hesitancy: Definition, scope and determinants. *Vaccine, 33*(34), 4161–4164. <https://doi.org/10.1016/j.vaccine.2015.04.036>
- Meyerowitz, B. E., & Chaiken, S. (1987). The effect of message framing on breast self-examination attitudes, intentions, and behavior. *Journal of Personality and Social Psychology, 52*(3), 500–510. <https://doi.org/10.1037/0022-3514.52.3.500>
- Penn, M. (2022). *A Renewed Call to Close the Global Vaccine Gap*. Duke Global Health Institute. <https://globalhealth.duke.edu/news/renewed-call-close-global-vaccine-gap>
- Tversky, A., & Kahneman, D. (1981). The framing of decisions and the psychology of choice. *Science, 211*(4481), 453–458. <https://doi.org/10.1126/science.7455683>
- Weinstein, N. D. (2000). Perceived probability, perceived severity, and health-protective behavior. *Health Psychology, 19*(1), 65–74. <https://doi.org/10.1037/0278-6133.19.1.65>



**Artist:** John Chan

**Title:** *Rhythm of the Gai See*

**Medium:** Fine liner, ink marker, 58 x 45 cm

**Description:** This piece combines my love for Hong Kong with my favorite pastime. I have always loved doodling weird and mesmerizing patterns, and after being inspired by Chuck Close, who paints realistic subjects using different types of patterns, I decided to do the same, using different thickness and depth of lines and patterns to recreate the business of Wan Chai, not only expressing my love for Hong Kong, but bringing me one step closer to the development of my style.



The Independent Schools Foundation Academy  
1 Kong Sin Wan Road, Pokfulam, Hong Kong  
Tel +852 2202 2000  
Fax +852 2202 2099  
Email [enquiry@isf.edu.hk](mailto:enquiry@isf.edu.hk)

